

https://dspace.org/

The treatment of brewery wastewater using carbon nanotubes synthesized from carbon dioxide carbon source

Simate, Geoffrey Simate

2013-02-13
http://hdl.handle.net/10539/12417

Downloaded from a DSpace repository. https://dspace.org/

THE TREATMENT OF BREWERY WASTEWATER USING CARBON NANOTUBES SYNTHESIZED FROM CARBON DIOXIDE CARBON SOURCE

Geoffrey Simate Simate

A thesis submitted to the Faculty of Engineering and the Built Environment, University of the Witwatersrand, Johannesburg, in fulfillment of the requirements for the degree of Doctor of Philosophy.

Johannesburg, 2012

DECLARATION

I declare that this thesis is my own unaided work. It is being submitted for the degree of Doctor of Philosophy to the University of the Witwatersrand, Johannesburg. It has not been submitted before for any degree or examination to any other University.



Geoffrey Simate Simate

31st day of July 2012

ABSTRACT

The brewing industry is considered to be among the economically strategic industries in most nations since it creates large scale employment opportunities and generates revenue to governments through different forms of taxations. However, the brewing industry faces a serious water consumption and pollution problem. This is because during beer production large volumes of clean water are consumed; consequently large quantities of wastewater contaminated with high concentrations of pollutants are generated. It is estimated that for every litre of beer produced, close to ten litres of fresh water is used. Recently, the complete treatment of brewery wastewater for reuse and disposal has become particularly important due to increasingly scarce water resources, ever increasing wastewater disposal costs, and stricter discharge regulations that have lowered permissible contaminant levels in waste streams. Currently, a good number of brewery wastewater treatment methods are either in operation, being piloted or under evaluation. Each method has its uses, advantages and disadvantages, and the removal of contaminants using these technologies can be complex and costly. Therefore, it is imperative that new and cheaper technologies are developed for the treatment of brewery wastewater. With the advent of carbon nanomaterials, the aim of this study was to access the suitability of using carbon nanotubes (CNTs) as heterogeneous coagulants and/or flocculants in the treatment of brewery wastewater. In addition, CNTs were also evaluated as adsorptive filter media in granular filtration.

Using already existing chemical vapour deposition (CVD) techniques, CNTs used in this research were synthesized from carbon dioxide (CO_2). The CO_2 was used in the production of CNTs because compared to the most widely used carbon precursors such as graphite, methane, acetylene, ethanol, ethylene, and coal-derived hydrocarbons, CO_2 is cheaper with relatively high carbon yield content. In addition, the proposed technique could be scaled-up in future so that it contributes to the efforts

of utilising CO_2 in the control of its impact on global warming. The results showed that in the synthesis of CNTs from CO_2, temperature plays an important role. The results showed that when the temperature was lower than 750°C or above 840°C, there were no CNTs formed. The optimum growth temperature was about 800°C. The influence of CO_2 concentration and flow rate were also studied. Very high concentration and flow rates negatively affected the CNT growth rates.

Subsequently, a series of experiments were conducted in which the efficiencies of pristine and hydrochloric acid functionalised CNTs were compared with the efficiency of ferric chloride in a coagulation/flocculation process. Both pristine and functionalised CNTs demonstrated the ability to coagulate colloidal particles in the brewery wastewater. Overall, ferric chloride was found to be a more effective coagulant than both the pristine and functionalised CNTs. In granular filtration, the treatment scheme in which CNTs were added to both the coagulation/flocculation tanks and the filter bed was found to be the best option for the treatment of brewery wastewater. This treatment scheme removed 96.0% of chemical oxygen demand (COD) and residual turbidity of only 5 NTU remained in the effluent. In its guidelines, World Health Organisation (WHO) recommends turbidity should be maintained at less than 5 NTU, but if water is disinfected, it would be better to aim for values of less than 1 NTU.

To summarise, this research has demonstrated new applications of CNTs - heterogeneous coagulation and/or flocculation of colloidal particles, and as a granular filter media. The study has also highlighted the potential human health effects of CNTs with respect to drinking water such as cancer, granulomas, inflammation and fibrosis, etc.

PREFACE

The work presented in this thesis was conducted in the School of Chemical and Metallurgical Engineering, University of the Witwatersrand, Johannesburg. Several articles as indicated in the list of publications have been published on this work, or contain elements thereof. The papers were extensively and independently reviewed by various scientists who are experts in their fields. The articles are readily available online. These published articles which are based on the objectives of this study can be summarised as follows; **Paper I** gives a brief overview of the brewing process and also discusses in detail several brewery wastewater treatment processes. The hypothesis behind this research is also contained in **Paper I**. **Paper II** is a review of literature that describes the production of carbon nanotubes (CNTs) from carbon dioxide (CO_2). Subsequently, **Paper III** which is centred on **Objective I** of this study discusses the effects of various critical factors that were monitored during the production of CNTs from CO_2 in a 'modified' swirled floating catalytic chemical vapour deposition (SFCCVD) reactor. **Paper IV** focuses on the results of the heterogeneous coagulation and flocculation of brewery wastewater. It compares the effectiveness of using CNTs to ferric chloride which is a traditional water treatment chemical. The results of the assessment of CNTs as adsorptive granular media are contained in **Paper V**. The concerns of human health effects of residual CNTs in drinking water are critically reviewed and compared to traditional water treatment chemicals in **Paper VI**.

LIST OF PUBLICATIONS

I. **Simate, G. S..,** Cluett, J., Iyuke, S. E., Musapatika, E. T., Ndlovu, S., Walubita, L. F., Alvarez, A. E., 2011.The treatment of brewery wastewater for reuse: State of the art. *Desalination* 273 (2-3), 235-247.

II. **Simate, G. S**., Iyuke, S.E., Ndlovu, S., Yah, C., Walubita, L. F., 2010. The production of carbon nanotubes from carbon dioxide: Challenges and opportunities. *Journal of Natural Gas Chemistry* 19 (5), 453-460.

III. **Simate, G. S**., Iyuke, S. E., Heydenrych, M., Ndlovu, S., Moothi, K., 2012. The production of carbon nanotubes from carbon dioxide in a 'modified' swirled floating catalytic chemical vapour deposition reactor. *Carbon*. [Submitted for Publication].

IV. **Simate, G. S**., Iyuke, S. E., Ndlovu, S., Heydenrych, M., 2012. The heterogeneous coagulation and flocculation of brewery wastewater using carbon nanotubes. *Water Research* 46 (4), 1185-1197.

V. **Simate, G. S**., Iyuke, S. E., Ndlovu, S., Heydenrych, M., 2012. The treatment of brewery wastewater for reuse: Integration of coagulation/flocculation and sedimentation with carbon nanotubes 'sandwiched' in a granular filter bed. [Submitted for Patent Registration].

VI. **Simate, G. S**., Iyuke, S. E., Ndlovu, S., Heydenrych, M., Walubita, L. F., 2012. Human health effects of residual carbon nanotubes and traditional water treatment chemicals in drinking water. *Environment International* 39, 38-49.

DEDICATION

Dedicated to my mother Bo ma-Mwiya Mukatimui Mashela, and my wife plus children for their everlasting love.

Ni itumezi shaa. Koozo!

ACKNOWLEDGEMENTS

"...No man is an island, entire of himself...'' (John Donne, 1572-1631). In executing this work, I encountered a lot of obstacles, but triumphed all the way; mostly through the assistance of others. This is the reality; life is never easy.

I wish to thank Professor Sunny Esayegbemu Iyuke, one of the leading researchers in carbon nanotube synthesis and applications, for his invaluable supervision of my research. I am also very grateful to my co-supervisors Professor Sehliselo Ndlovu and Professor Mike Heydenrych for all their efforts throughout my studies.

Special thanks are due to Dr. Lubinda F. Walubita (Texas A&M University System), for his excellent scientific critical analysis and review of this thesis and many of the published papers from this research. Sincere thanks are also extended to Professor Mjumo Mzyece (Tshwane University of Technology) for professionally reviewing this thesis. I appreciate Dr. Clarence S. Yah's efforts for running the statistical program. I also wish to acknowledge all the co-authors of various papers for their input. I convey my heartfelt appreciation to Mr. Wayne Costopoulos of the School of Civil and Environmental Engineering, University of the Witwatersrand for fabricating the laboratory scale water treatment plant used in this research. Mrs Thelma Booysen is also acknowledged for the chemical analysis of all brewery wastewater samples.

I wish to thank and acknowledge the love of my family – Namakau (my wife) and my babies – for their moral understanding and unparalleled support during the period of my studies. Thanks guys; I love you!!

This research work would not have been completed without the financial support of the University of Witwatersrand University Staff Bursary Scheme. This financial support is dully acknowledged and greatly appreciated. South African Breweries Limited is appreciated for generously providing the wastewater used in this research.

TABLE OF CONTENTS

Declaration ii
Abstract iii
Preface v
List of publications vi
Dedication vii
Acknowledgements viii
Table of contents ix
List of figures xv
List of tables xviii
List of acronyms, abbreviations and symbols xix

CHAPTERS

1. INTRODUCTION 1
1.1 Introduction 2
1.2 Research Problem 4
1.3 Aim and Objectives 5
1.4 Research Methodology 6
1.4.1 Literature review 6
1.4.2 Experimental design and materials selection 6
1.4.3 Laboratory testing and data analysis 7
1.4.4 Human health analysis 7
1.4.5 Conclusions and recommendations 7
1.5 Thesis Layout 7
1.6 Summary 9

References 9

2. LITERATURE REVIEW 13

2.1 General Introduction 14

2.2 Brewing Process 15

2.2.1 Malting 15

2.2.2 Mashing 16

2.2.3 Wort processing, hop addition, and kettle boiling 16

2.2.4 Fermentation 18

2.2.5 Maturation and conditioning 18

2.2.6 Finishing 19

2.3 Brewery Wastewater Treatment 19

2.3.1 Coagulation and flocculation processes 20

2.3.2 Mechanisms of coagulation 20

2.3.3 Flocculation process modelling 27

2.3.4 Types of coagulants 28

2.4 Carbon Nanotubes 34

2.4.1 The synthesis of carbon nanotubes 35

2.4.2 Bonds and structures of the carbon nanotubes 37

2.4.3 Chemistry of carbon nanotubes …… 42

2.4.4 Applications of carbon nanotubes in water treatment 47

2.5 Summary 50

References 51

3. EXPERIMENTAL MATERIALS AND METHODS 62

3.1 Introduction 63

3.2 Experimental Materials 63

3.2.1 Raw wastewater 63

3.2.2 Ferric chloride 63

3.2.3 Carbon nanotubes 63

3.3 Experimental Methods 64

3.3.1 Synthesis, purification and functionalisation of carbon nanotubes 64

3.3.2 Jar tests 67

3.3.3 Semi-continuous laboratory-scale water treatment plant 69

3.3.4 Experimental design 72

3.4 Analytical Techniques 73

3.4.1 Raw water and treated water quality 73

3.4.2 Characterisation of carbon nanotubes 78

3.5 Data Analysis 91

3.6 Summary 92

References 92

4. SYNTHESIS OF CARBON NANOTUBES FROM CARBON DIOXIDE 99

4.1 Introduction 100

4.2 Results and Discussion 101

4.2.1 Identification of carbon nanotubes 101

4.2.2 Effect of the concentration of carbon dioxide 103

4.2.3 Effect of the volumetric flow rate of carbon dioxide 104

4.2.4 Effect of reactor temperature 106
4.3 Summary and Conclusions 108
References 109

5. EVALUATION OF CARBON NANOTUBES AS HETEROGENEOUS COAGULANTS/FLOCCULANTS FOR BREWERY WASTEWATER TREATMENT 114
5.1 Introduction 115
5.2 Results and Discussion 116
5.2.1 Characterisation of carbon nanotubes 116
5.2.2 Comparison of carbon nanotubes and ferric chloride 124
5.2.3 Effect of pH 128
5.2.4 Effect of dosage 133
5.2.5 Mixture of carbon nanotubes and ferric chloride 134
5.2.6 Mechanisms of heterogeneous coagulation 136
5.2.7 Adsorption isotherm models 137
5.3 Challenges and Future Prospects 142
5.4 Summary and Conclusions 144
References 145

6. TREATMENT OF BREWERY WASTEWATER THROUGH A SEMI-CONTINUOUS LABORATORY SCALE WATER TREATMENT PLANT .. 151
6.1 Introduction 152
6.2 Results and Discussion 152
6.2.1 Determination of the optimum dose of ferric chloride coagulant 153

6.2.2 Determination of the optimum loading rate 153
6.2.3 Comparison of different modes of filtration 157
6.2.4 Effects of carbon nanotubes 164
6.2.5 Backwashing studies 169
6.2.6 Determination of entrained carbon nanotubes in the filtrate 172
6.3 Summary of Results 174
6.4 Summary and Conclusions 175
References 176

7. COMPARISON OF HUMAN HEALTH EFFECTS OF CARBON NANOTUBES WITH TRADITIONAL WATER TREATMENT CHEMICALS . 179
7.1 Introduction 180
7.2 Discussion of Literature Reviewed 180
7.2.1 Human health effects of residual carbon nanotubes 180
7.2.2 Human health effects of residual traditional water treatment chemicals .. 188
7.3 Summary and Conclusions 194
References 196

8. CONCLUSIONS AND RECOMMENDATIONS 204
8.1 Conclusions 205
8.1.1 Introduction 205
8.1.2 Synthesis of carbon nanotubes from carbon dioxide 205
8.1.3 Evaluation of carbon nanotubes as heterogeneous coagulants/flocculants for brewery wastewater 207

8.1.4 The treatment of brewery wastewater in a semi-continuous laboratory scale water treatment plant 208

8.1.5 Comparison of human health effects of residual carbon nanotubes with traditional water treatment chemicals in drinking water 209

8.1.6 Potential application in industry 210

8.2 Recommendations 211

8.2.1 Use of water-dispersible carbon nanotubes 211

8.2.2 Extension of monitoring parameters 211

8.2.3 Functionalisation of carbon nanotubes 212

8.2.4 Economic analysis of using carbon nanotubes 212

APPENDICES 213

Appendix A Abstracts of published/submitted papers 214

Appendix B Data for Chapter 4 221

Appendix C Data for Chapter 5 223

Appendix D Data for Chapter 6 229

Appendix E Statistical validation of equipment and reproducibility of experimental data 245

Appendix F Derivation of the simple kinetic model for the production of carbon nanotubes from carbon dioxide 253

LIST OF FIGURES

Figure 1.1 Thesis layout 8
Figure 2.1 The brewing process 17
Figure 2.2 Two ways to visualize the double layer 22
Figure 2.3 Illustration of sp hybridization and resulting structure 38
Figure 2.4 Illustration of sp^2 hybridization and resulting structure 38
Figure 2.5 Illustration of sp^3 hybridization and resulting structure 39
Figure 2.6 Bonding in carbon structures 39
Figure 2.7 sp^3 and sp^2 hybridisation scheme in C-C structure 40
Figure 2.8 Schematic diagram of an individual layer of graphene sheet 41
Figure 2.9 Common methods for chemical functionalisation of carbon nanotubes ... 45
Figure 2.10 Models of non-covalent functionalisation 46
Figure 3.1 Swirled floating catalyst chemical vapour deposition reactor with inserted quartz wool 65
Figure 3.2 The flocculator and jar test experimental set up 67
Figure 3.3 The filtration setup of treated brewery wastewater 68
Figure 3.4 The semi-continuous laboratory scale water treatment plant 69
Figure 3.5 Arrangement of the filter media 70
Figure 3.6 Thermogravimetric analyser 79
Figure 3.7 Fourier transform infrared absorption spectroscopy 85
Figure 3.8 Electrostatic potential near a negatively charged spherical particle 88
Figure 3.9 Zetasizer Nanoseries Nano ZS 89
Figure 4.1 TEM image of CNTs produced at 800°C 101
Figure 4.2 Raman spectrum of CNTs produced at 800°C 102
Figure 4.3 Effect of concentration of CO_2 on the production rate of CNTs at 800°C ... 104
Figure 4.4 Effect of volumetric flow rate of CO_2 on the production rate of CNTs at 800°C 105

Figure 4.5 Effect of temperature on the production rate of CNTs at 400 ml/min carbon dioxide 107
Figure 5.1 TGA of pristine and purified CNTs in oxygen atmosphere 117
Figure 5.2 Raman spectra of pristine and acid functionalised CNTs 118
Figure 5.3 FT-IR spectra of pristine and acid functionalised CNTs 120
Figure 5.4 Mass titration results for acid functionalised CNTs 123
Figure 5.5 Comparison of CNTs and ferric chloride on removal of turbidity 125
Figure 5.6 Electron micrographs showing colloidal materials on CNTs after coagulation/flocculation 127
Figure 5.7 Zeta potential of pristine and acid functionalised CNTs 129
Figure 5.8 Effect of pH on turbidity and COD reduction 132
Figure 5.9 Effect of CNT dosage on turbidity and COD removal 134
Figure 5.10 Effect of a mixture of CNTs and ferric chloride on turbidity 135
Figure 5.11 Electrokinetic zeta potential of brewery wastewater as a function of CNT dosage 137
Figure 5.12 Langmuir isotherm plot for COD adsorption onto hydrochloric acid functionalised CNTs 140
Figure 5.13 Freundlich isotherm plot for COD adsorption onto hydrochloric acid functionalised CNTs 141
Figure 6.1 Head loss development under various hydraulic loading rates 155
Figure 6.2 Diagram of a granular filter pore showing particles to be filtered 155
Figure 6.3 The evolution of outlet hydraulic loading rates over time 156
Figure 6.4 Head loss development under various modes of filtration 158
Figure 6.5 Effect of the mode of filtration on removal of turbidity 160
Figure 6.6 Mechanisms of filtration 161
Figure 6.7 Effect of the mode of filtration on removal of COD 163
Figure 6.8 Head loss development under various treatment schemes with CNTs 165
Figure 6.9 Turbidity removal under various treatment schemes with CNTs 166
Figure 6.10 COD removal under various treatment schemes with CNTs 168

Figure 6.11 Head loss development in backwashed and un-backwashed conventional filtration..... 170
Figure 6.12 Turbidity removal in backwashed and un-backwashed conventional filtration..... 171
Figure 6.13 COD removal in backwashed and un-backwashed conventional filtration 171
Figure 6.14 Optical density at 600 nm as a function of the concentration of CNTs. 173
Figure 7.1 Summary of particles translocation across the gastrointestinal tract..... 182

LIST OF TABLES

Table 2.1 Common chemical coagulants used in the treatment of drinking water 29
Table 3.1 Principle characteristics of the filter media..... 71
Table 3.2 Experimental design..... 72
Table 3.3 Water quality characteristics of the brewery wastewater..... 73
Table 5.1 The amount of functional groups on the surfaces of pristine and acid functionalised CNTs..... 121
Table 5.2 Physicochemical properties of CNTs..... 123
Table 5.3 Isotherm parameters for the adsorption of COD by functionalised CNTs 141
Table 6.1 Summary of results of different treatment schemes 175
Table 7.1 Some common traditional chemicals recommended for use in the treatment of drinking water..... 188
Table 7.2 Chlorination by-products and their health effects..... 191
Table 7.3 Summary of human health effects of various water treatment chemicals 195

LIST OF ACRONYMS, ABBREVIATIONS AND SYMBOLS

AD ..... Alzheimer's disease
ANOVA ..... Analysis of Variance
BET equation ..... Brunauer, Emmett and Teller equation
C ..... Carbon
CBPs ..... Chlorination by-products
CO_2 ..... Carbon dioxide
CO ..... Carbon monoxide
COD ..... Chemical oxygen demand
CNTs ..... Carbon nanotubes
CVD ..... Chemical vapour deposition
DBPs ..... Disinfection by-products
DNA ..... Deoxyribonucleic acid
EDL ..... Electrical double layer
EM ..... Electron microscopy
ENMs ..... Engineered nanomaterials
FT-IR ..... Fourier transform infrared
FTU ..... Formazin turbidity unit
GAC ..... Granulated activated carbon
H_2 ..... Hydrogen
ICC ..... Indian Childhood Cirrhosis
ICT ..... Idiopathic Chronic Toxicosis
IEP ..... Isoelectric point
MWCNTs ..... Multi-walled carbon nanotubes
NOM ..... Natural organic matter
NTU ..... Nephelometry turbidity unit
O_2 ..... Oxygen
PAC ..... Powdered activated carbon

PD.....Parkinson's disease

PZC .....Point of zero charge

PVC..... Polyvinyl chloride

$scCO_2$ .....Super-critical carbon dioxide

SEM .....Scanning electron microscopy

Semi-continuous LSWTP .....Semi-continuous laboratory scale water treatment plant

SFCCVD .....Swirled floating catalyst CVD

SHE ..... Standard hydrogen electrode

SWCNTs .....Single-walled carbon nanotubes

TEM ..... Transmission electron microscopy

TGA ..... Thermogravimetric analysis

UASB .....up-flow anaerobic sludge blanket

UHP..... Ultra high purity

WHO .....World Health Organisation

ζ..... Zeta potential

CHAPTER ONE

INTRODUCTION

"The distinction between past, present and future is only an illusion, however persistent".

- Albert Einstein

1.1 Introduction

Though the brewing industry is faced by a number of problems, their most critical concerns are water usage – its quality and scarcity - and the subsequent wastewater generated. The industry requires the use of large volumes of clean water in its beer production. The main water consuming areas of a typical brewery are brewhouse, cellars, packaging and general water use (van der Merve and Friend, 2002). Specifically, of the water consumed, about two-thirds is used in the process and the rest in the cleaning operations (Fillaudeau et al., 2006). As revealed in literature survey of Simate et al. (2011), it is estimated that about 3-10 litres of water is required to produce 1 litre of beer. As a result, a large quantity of wastewater is produced. Consequently, water and wastewater management in breweries remains a critical practical problem (Fillaudeau et al., 2006).

The ever increasing need for clean, but scarce water in the brewing industry has continued to motivate the need to find alternative sources of water. One alternative that requires attention is wastewater reclamation and reuse. Wastewater reclamation and reuse has been an important option since industrialisation and urbanisation accelerated pollution in water environment, making it a limited resource for production activities (Seo et al., 1996). When properly treated and recycled, wastewater can be an alternative water source which can reduce the demand for fresh water. Recycled wastewater can reduce stress on the environment as well (Abdessemed et al., 2000). However, the removal of contaminants from wastewater remains a big challenge. Simate et al. (2011) have shown that a good number of brewery wastewater treatment methods are either in operation, being piloted or under evaluation. These treatment processes are selective depending on the purpose of water and the water quality required (Seo et al., 1996), and wastewater characteristics (Chuang et al., 2005). Furthermore, each method has its advantages and

disadvantages, and the removal of contaminants using these technologies can be complex and costly (Renault at al., 2009).

However, in recent times, coagulation and flocculation have remained the most widely used processes for water and wastewater treatment (Simate at al., 2012a); mainly for removal of colloidal material, which cause colour and turbidity (Amuda and Alade, 2006). Though particles in the colloidal size range possess certain properties that prevent agglomeration (Peavy et al., 1985; Crawford and Margolies, 1988), coagulants and flocculants reduce the electric charges on colloidal surfaces, allowing the colloidal particles to agglomerate into flocs (Crawford and Margolies, 1988; Drinan, 2001). Subsequently, the larger particles are removed by solids removal processes such as sedimentation, flotation and filtration (Simate at al., 2011). Therefore, coagulation and flocculation are the two key steps which often determine finished water quality (Zeta-Meter Inc., 1993).

Despite the existence of a wide range of coagulating and flocculating chemicals, most of the current traditional coagulants and flocculants such as aluminum and ferric salts have several disadvantages which include already known human health effects. For example, residual aluminium salts in treated water may cause Alzheimer's disease (McLachlan, 1995; Ndabigengesere and Narasiah, 1998; Simate et al., 2012b). Therefore, the need to use alternative coagulant and /or flocculants is taken as a priority in the water and wastewater treatment industry.

Interestingly, the ‘rediscovery’ of carbon nanotubes (CNTs) (Monthioux and Kuznetsov, 2006) by Iijima (Iijima, 1991) has come at an opportune time, so to say. Simplistically, CNTs can be described as sheets of graphite that have been rolled into tubes (Baddour and Briens, 2005). Owing to their unique structural, mechanical, and electronic properties, CNTs possess great potential in a large variety of applications. Of particular interest in this study is their exceptional adsorption capability property

as described by Simate et al. (2012a). They have shown extraordinary adsorption capabilities and high adsorption efficiencies for various organic pollutants (Lu et al., 2005; Goering and Burghaus, 2007; Lu and Su, 2007; Li et al., 2007) and inorganic pollutants such as fluoride (Li et al., 2003a). The CNTs have also been found to be superior sorbents for heavy metals (Li et al., 2003b; Li et al., 2006; Li et al., 2007), and have been used in the separation and pre-concentration of various metal ions (Liang et al., 2004; Yuan et al., 2011). They are particularly attractive as sorbents because, on the basis of mass, they have larger surface areas than bulk particles, and they can be functionalised with various chemical groups to increase their affinity towards target compounds (Savage and Diallo, 2005). Furthermore, CNTs are small in size, hollow and have layered structures (Wu, 2007) which are important attributes for adsorption.

1.2 Research Problem

A review of the literature has shown that although CNTs have been proven to possess good potential as superior adsorbents for removing many kinds of organic and inorganic pollutants, and heavy metals from aqueous solutions, no published work is available regarding their application as heterogeneous coagulants and/or flocculants (Simate et al., 2011; Simate et al., 2012a). Furthermore, despite the brewery industry being a large consumer of groundwater in most countries, the use of CNTs for brewery wastewater treatment has not been explored. However, it can be theorised that if CNTs can adsorb on separate colloidal particles, then the particles can be drawn together; a phenomenon known as bridging flocculation (Everett, 1988; Swenson et al., 1998). Furthermore, the adsorption of CNTs onto colloidal particle surfaces can also result in charge neutralisation. Once the surface charge has been neutralised, the ionic cloud dissipates and the electrostatic potential disappears resulting in a near zero net charge so that the contact among colloidal particles occurs freely. The control of surface charges or, in other words, the control of zeta potential

of the CNTs is needed to effect adsorption. Furthermore, the adsorptive capabilities and the relatively large surface area per unit volume of CNTs are expected to enhance particulate matter adhesion in granular filtration. These are the conceptual (fundamental) theories upon which this study is based; consequently, various questions that need to be addressed arise and include the following:

(a) Would CNTs, therefore, feasibly be used as coagulants and /or flocculants, or as adsorptive granular filter media?
(b) What are the advantages and limitations of using CNTs as coagulants and/or flocculants?
(c) What are the human health effects of using CNTs as coagulants and/or flocculants or as adsorptive granular filter media compared to existing methods and techniques?

1.3 Aim and Objectives

The aim of this research is to synthesize, treat, and characterize CNTs synthesized from carbon dioxide (CO_2), and subsequently use CNTs in the treatment of brewery wastewater.

The specific objectives of the study are:-

I. To synthesize CNTs from CO_2 using existing chemical vapour deposition (CVD) techniques.
II. To evaluate the feasibility of using CNTs in the treatment of brewery wastewater, by comparing their coagulation/flocculation capacities with traditionally used water treatment chemicals.
III. To assess the possibility of using CNTs as adsorptive filter media in granular filtration.

IV. To use available literature and give a qualitative comparison of the human health impact (if any) of residual CNTs with traditional water treatment chemicals.

1.4 Research Methodology

The research methodology for this study involved the following major tasks: review of the existing literature; experimental design and materials selection; laboratory testing; laboratory test data analysis; a review of the human health effects of CNTs and traditional water treatment chemicals in water treatment; conclusions and recommendations. These tasks are briefly discussed in the subsequent text.

1.4.1 Literature review

Literature review was conducted, (1) to discuss the brewing process, (2) to review the principles of coagulation and flocculation processes, (2) to discuss the methods of preparing CNTs, (3) to discuss the surface chemistry of CNTs with particular focus on functionalisation methodologies.

The information from literature review also served as the basis for formulating the experimental design programme which included materials selection.

1.4.2 Experimental design and materials selection

The CNTs produced solely from CO_2 as carbon source were used throughout these test works. Ferric chloride was used for comparative studies. Two main quality determinants were used to determine the effectiveness of CNTs as coagulants, i.e., turbidity and chemical oxygen demand (COD).

1.4.3 Laboratory testing and data analysis

In line with the study's experimental design, a series of laboratory tests under various conditions were carried out to test each quality determinant chosen. Output data from these laboratory tests were used for determining the effectiveness of CNTs as coagulants/flocculants and/or as granular filter media.

1.4.4 Human health analysis

The human health aspect of CNTs is not well understood. It is believed that when CNTs are used in the treatment of water there is a possibility that they may gain access into the body and pose serious toxicological problems. This sub-section, therefore, compares in detail the risk aspects of residual CNTs with traditional water treatment chemicals in drinking water.

1.4.5 Conclusions and recommendations

When the data analysis and a review of the human health aspects of CNTs were complete, the results were synthesised to draw conclusions and recommendations. The conclusions include the significant findings of the production of CNTs from carbon dioxide, the coagulation/flocculation studies and/ or granular filter media studies as well as the human health effects of the CNTs. The recommendations in turn highlight the general applicability and validity aspects of the use of CNTs as coagulants and/or granular filter media and their limitations.

1.5 Thesis Layout

As shown in Figure 1.1, this thesis consists of eight Chapters including this chapter (Chapter One) that provides the motivation for the research, the problem statement,

and the overall objectives of this study. At the end of each Chapter, a summary of the important points and findings is provided.

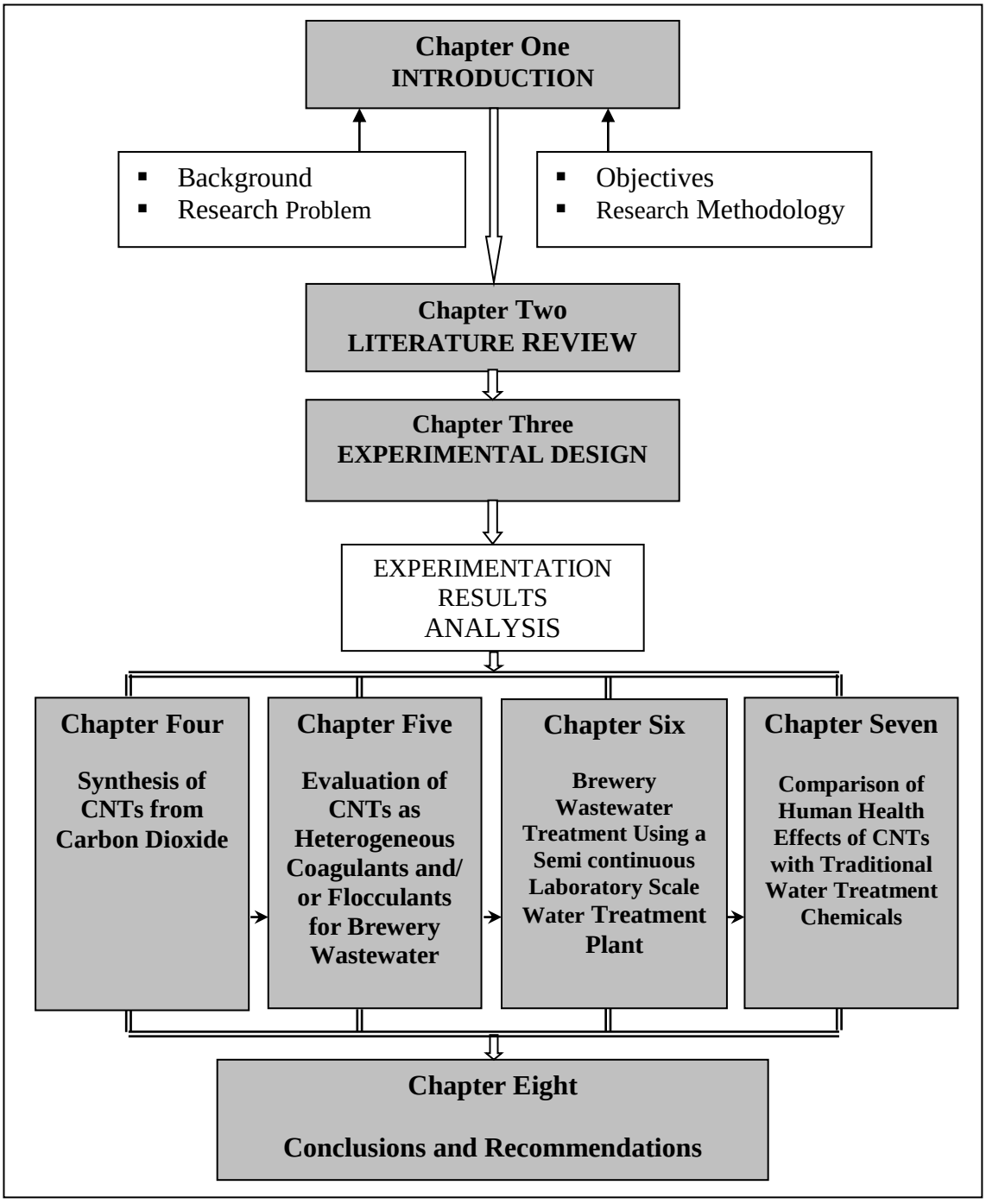


Figure 1.1. Thesis layout.

Chapter Two is the literature review, which includes an overview of the processes of coagulation and flocculation; the production, properties and applications of CNTs in water treatment processes. Chapter Three (experimental design) describes the materials and methods used in the study. The subsequent chapters (Chapter Four through Six) describe the laboratory tests, findings and conclusions. Chapter Seven is a review of the toxicity and the human health risk aspects of residual CNTs and some traditional water treatment chemicals in drinking water. The thesis concludes in Chapter Eight with a summary of the findings and recommendations. The appendices section comprises abstracts of all the published/submitted papers, and also includes detailed laboratory test results and other important data.

1.6 Summary

In this introductory chapter, the background, problem statement, and study objectives were discussed. The research methodology was then briefly described, followed by the dissertation layout.

References

Abdessemed, D., Nezzal, G., Aim, R. B., 2000. Coagulation-adsorption-ultrafiltration for wastewater treatment and reuse. *Desalination* 131, 307-314.

Amuda, O. S., Alade, A., 2006. Coagulation/flocculation process in the treatment of abattoir wastewater. *Desalination* 196, 22-31.

Baddour, C. E., Briens, C., 2005. Carbon nanotube synthesis: a review. *International Journal of Chemical Reactor Engineering* 3, R3.

Chuang, S.H., Chang, T.C., You, S.J., Ouyang, C.F., 2005. Evaluation of wastewater reclamation processes in a high-tech industrial park. *Desalination* 175, 143-152.

Crawford, H. B., Margolies, R. T., 1988. The NALCO water handbook. McGraw-Hill Book Company, New York.

Drinan,J. E., 2001. Water and wastewater treatment: A guide for the nonengineering Professional. CRC Press, New York.

Everett, D. H., 1988. Basic principles of colloid science. Royal Society of Chemistry, London.

Fillaudeau, L., Blanpain-Avet, P., Daufin, G., 2006.Water, wastewater and waste management in brewing industries. *Journal of Cleaner Production* 14, 463-471.

Goering, J., Burghaus, U., 2007. Adsorption kinetics of thiophene on single-walled carbon nanotubes (CCNTs).*Chemical Physics Letters* 447, 121-126.

Iijima, S., 1991.Helical microtubules of graphitic carbon. *Nature* 354, 56-58.

Li, Y-H., Wang, S., Zhang, X., Wei, J., Xu, C., Luan, Z., Wu, D., 2003(a).Adsorption of fluoride from water by aligned carbon nanotubes. *Materials Research Bulletin* 38 (3), 469-476

Li, Y-H., Ding, J., Luan, Z., Di, Z., Zhu, Y., Xu, C, Wu, D., Wei, B., 2003(b). Competitive adsorption of Pb^{2+}, Cu^{2+} and Cd^{2+} ions from aqueous solutions by multiwalled carbon nanotubes. *Carbon* 41, 278-2792.

Li, Y-H., Zhu, Y., Zhao, Y., Wu, D., Luan, Z., 2006. Different morphologies of carbon nanotubes effect on the lead removal from aqueous solutions. *Diamond and Related Materials* 15, 90-94.

Li, Y-H., Zhao, Y. M., Hu, W. B., Ahmad, I., Zhu, Y. Q., Peng, J. X., Luan, Z. K., 2007. Carbon nanotubes – the promising adsorbent in wastewater treatment. *Journal of Physics: Conference Series* 61, 698-702.

Liang, P., Liu, Y., Guo, L., Zeng, J., Lu, H.B., 2004. Multiwalled carbon nanotubes as solid-phase extraction adsorbent for the preconcentration of trace metal ions and their determination by inductively coupled plasma atomic emission spectrometry. *Journal of Analytical Atomic Spectrometry* 19, 1489-1492.

Lu, C., Chung, Y-L., Chang, K-F., 2005.Adsorption of trihalomethanes from water with carbon nanotubes. *Water Research* 39, 1183-1189.

Lu, C., Su, F., 2007.Adsorption of natural organic matter by carbon nanotubes. *Separation and Purification Technology* 58, 113-121.

McLachlan, D.R.C.,1995. Aluminum and the risk for Alzheimer's disease. *Environmetrics* 6, 233-275.

Monthioux, M., Kuznetsov, V. L., 2006. Who should be given the credit for the discovery of carbon nanotubes? *Carbon* 44, 1621-1623.

Ndabigengesere, A., Narasiah, K. S., 1998. Quality of water treated by coagulation using Moringa oleifera seeds. *Water Research* 32, 781-791.

Peavy, H. S., Rowe, D. R., Tchobanoglous, G., 1985. Environmental Engineering. McGraw-Hill, Inc., New York.

Renault, F., Sancey, B., Badot, P.M., Crini, G., 2009. Chitosan for coagulation/flocculation processes - an eco-friendly approach. *European Polymer Journal* 45, 1337-1348.

Savage, N., Diallo, M. S., 2005. Nanomaterials and water purification: Opportunities and challenges. *Journal of Nanoparticle Research* 7, 331-342.

Seo, G. T., Suzuki, Y., Ohgaki, S., 1996.Biological powdered activated carbon (BPAC) microfiltration for wastewater reclamation and reuse. *Desalination* 106, 39-45.

Simate, G. S., Cluett, J., Iyuke, S. E., Musapatika, E. T., Ndlovu, S., Walubita, L. F., Alvarez, A. E., 2011.The treatment of brewery wastewater for reuse: State of the art. *Desalination* 273 (2-3), 235-247.

Simate, G. S., Iyuke, S. E., Ndlovu, S., Heydenrych, M., 2012a. The heterogeneous coagulation and flocculation of brewery wastewater using carbon nanotubes. *Water Research* 46 (4), 1185-1197

Simate, G. S., Iyuke, S. E., Ndlovu, S., Heydenrych, M., Walubita, L. F., 2012b. Human health effects of residual carbon nanotubes and traditional water treatment chemicals in drinking water. *Environment International* 39, 38-49.

Swenson, J., Smalley, M. V., Hatharasinghe, H. M. L., 1998. Mechanism and strength of polymer bridging flocculation. *Physical Review Letters* 81 (26), 5840-5843.

van der Merwe, A., Friend, J.F.C., 2002. Water management at a malted barley brewery. *Water SA* 28 (3), 313-318.

Wu, C. H., 2007. Adsorption of reactive dye onto carbon nanotubes: Equilibrium, kinetics and thermodynamics. *Journal of Hazardous Materials* 144, 93-100.

Yuan, C. G., Zhang, Y., Wang, S., Chang, A., 2011. Separation and preconcentration of palladium using modified multi-walled carbon nanotubes without chelating agent. *Microchim Acta* 173, 361-367.

Zeta-Meter Inc., 1993. Everything you need to know about coagulation and flocculation-guide. Zeta-Meter Inc., Virginia.

CHAPTER TWO

LITERATURE REVIEW

"*If I rest, I rust*".

- Martin Luther

2.1 General Introduction

Beer is one of the oldest alcoholic beverages known to man (Wyatt, 1900; Arnold, 1911; Hornsey, 2003), and the art and craft of beer-making can be traced back almost 5000 years, as documented by excavations undertaken in many parts of the world (Phiarais and Arendt, 2008). Because of this extremely long history, brewing is considered as a typical example of traditional or old biotechnology (Linko et al., 1998). However, over the years, the brewing industry has evolved to include new technical, biochemical, microbiological and genetic inventions (Linko et al., 1998). Despite all the progress and innovations, the brewing industry is still facing challenging times, particularly, due to water scarcity, water quality requirements and enormous volumes of brewery wastewater generated. Therefore, it has become imperative to manage and reduce water usage at breweries. One eminent solution to the 'water stress' is wastewater reclamation and reuse. Consequently, a lot of research works devoted to devising new technologies and integration of conventional processes for brewery wastewater treatment, reclamation and reuse as shown by Simate et al. (2011) have received attention more than ever before.

With the above background, the objectives of this literature review are, (1) to discuss the brewing process, (2) to review different methods of treating brewery wastewater including the principles of coagulation and flocculation, (2) to discuss the methods of preparing CNTs, (3) to discuss the key properties of CNTs which include the surface chemistry, focusing on functional groups which may interact with a range of particles (i.e., organic and inorganic pollutants, and heavy metals) present in aqueous solutions, and (4) to relate the surface chemistry of CNTs to their use in the neutralisation of particle surface charges, and reduction of the electrical double layer.

2.2 Brewing Process

The brewing industry employs a number of batch-type operations in processing raw materials to the final beer product (van der Merve and Friend, 2002). However, the two most important processes in beer production are the degradation of starch to sugar during mashing followed by the fermentation of these sugars to form alcohol and CO_2 (Phiarais and Arendt, 2008). In its simplest form, the brewing process involves five main steps as illustrated in Figure 2.1 (Harrison, 2009).

Simplified descriptions of the stage by stage chemistry of the brewing process are summarised in the sub-sections below:-

2.2.1 Malting

The cereals from which beer is ultimately derived require first to be converted into a substrate which can be metabolized by yeast. This conversion is achieved by malting (Dalgliesh, 1979). To produce malted barley, barley grains are first steeped in 10-15°C aerated water and then germinated at 15-20°C for 3-7 days (Harrison, 2009). Germination is then stopped by heating ('kilning') before much actual breakdown occurs and before significant seedling growth takes place (Dalgliesh, 1979). The main objective of malting is to produce an ample supply of enzymes that degrade starch, proteins, and other components of grain (Harrison, 2009). The subsequent enzymatic changes provide fermentable sugars from starch and substances needed to support yeast growth (e.g., amino acids and fatty acids) from the other substrates. Malt also is a major contributor to the final color and body characteristics of the finished beer. For example, dark beers are made using darker, more flavourable malt while less roasted malt is used to brew paler beers.

2.2.2 Mashing

The malted barley is first crushed to form very coarse flour (i.e., grist) in the grit mill (Phiarais and Arendt, 2008) so as to expose the starchy endosperm of the grain, thus making the carbohydrates more available (Harrison, 2009). During the mashing step, most of the non-soluble, un-fermentable carbohydrates and proteins are hydrolysed into soluble fermentable materials by the enzymes present in the malt (Harrison, 2009). The breaking down of the macromolecular food reserves of the grain to small molecules is necessary because brewing yeasts cannot in general metabolize anything larger than a trisaccharide (Dalgliesh, 1979). To accomplish this, the ground malt is mixed with water and placed into a mash tun. To enhance α-amylase action during the initial mashing period, the temperature of the mixture is maintained between 40 and 50°C. After a period of time, the temperature of the mix is increased to 65-70°C to enhance β-amylase activity. Within a few hours, the process is complete, and the temperature is increased to at least 75°C to inactivate the enzymes.

After the naturally occurring and any added enzymes are inactivated, the solids settle out, leaving the wort. The soluble extract in the wort is separated from the insoluble 'spent grains' (grain husk) in the lauter tun (Phiarais and Arendt, 2008). Furthermore water is sprayed from the top of the tank onto the mash to increase extract. The insoluble 'spent grains' are either discarded or sold as animal feed (Cook, 2011).

2.2.3 Wort processing, hop addition, and kettle boiling

After the wort has been separated from the insoluble 'spent grains', the wort is transferred into a heating tank, called the brew kettle, in which hops are added to the wort before the mixture is boiled (Dalgliesh, 1979; Harrison, 2009) for 1-2 hrs (Harrison, 2009). This halts enzyme action, sterilizes the wort, coagulates some proteins and imparts distinctive flavors and aromas to the wort from the hops

(Phiarais and Arendt, 2008; Harrison, 2009). After boiling, the wort is then separated from the spent hops and precipitated particles (i.e., trub) in the whirlpool, cooled rapidly and aerated, and placed into a fermentation vessel. Cooling and aeration of the wort produce an ideal medium for yeast fermentation (Phiarais and Arendt, 2008). The spent hops may be used as fertilizer.

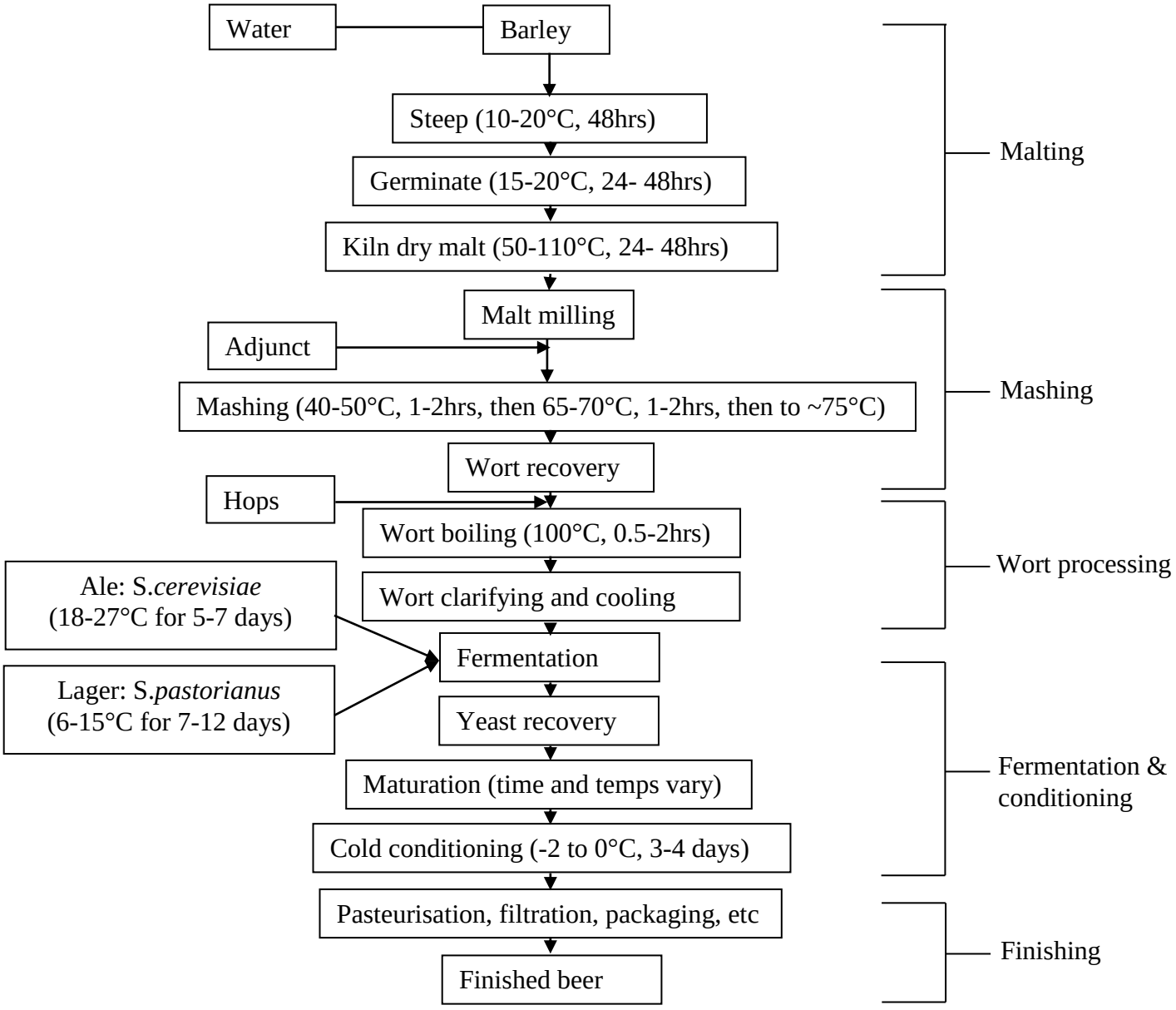


Figure 2.1.The brewing process (Harrison, 2009).

2.2.4 Fermentation

The wort is fermented, first, by inoculating it with brewers' yeast. The inoculation step is also called other names, such as pitching and seeding (Harrison, 2009). The strain of yeast used depends on what type of beer is desired. Lagers are produced using bottom-fermenting yeasts in the range of 6-15°C and takes 2-7 days, where the yeasts tend to flocculate and settle to the bottom of the fermentation vat (Harrison, 2009). On the other hand, ales are produced using top-fermenting yeasts at temperatures of 6-15°C for 5-7 days, where yeasts tend to form small clumps of cells that are carried to the top of the fermenting liquid and adsorbed to bubbles of carbon dioxide (Harrison, 2009). These yeasts have traditionally been referred to as *Saccharomyces pastorianus* and *Saccharomyces cerevisiae* for bottom-fermenting and top-fermenting, respectively (Harrison, 2009). During fermentation, the yeast converts the carbohydrates present to produce alcohol, carbon dioxide, and contribute some additional flavour and aroma constituents (Phiarais and Arendt, 2008; Harrison, 2009).

2.2.5 Maturation and conditioning

At the end of fermentation, the 'green beer' is separated from the sediment and transferred to wooden (e.g., oak) or glass-lined steel tanks. In traditional brewing, maturation of the beer occurs during storage at 0-2°C for several weeks. Lagers are normally aged for slightly longer periods of time than ales. This step allows the beer to develop its final flavor, color, and body characteristics. Many brewers include a short conditioning period after fermentation. Conditioning can be done at temperatures of approximately -1°C for at least 3 days. Consequently, clarification occurs to some extent as the yeasts, unstable proteins, and other suspended solids precipitate.

2.2.6 Finishing

Finally, the beer is packaged in cans, bottles, barrels, and kegs, usually after it has been sterile-filtrated or pasteurized (Phiarais and Arendt, 2008) to increase the shelf life of beer, particularly canned or bottled beer (Harrison, 2009).

2.3 Brewery Wastewater Treatment

As noted above, the brewing industry employs a number of batch-type operations in processing raw materials to the final beer product. In the process, a large quantity of water is used for the production of beer itself, as well as for washing, cleaning and sterilizing of various units after each batch is completed (van der Merve and Friend, 2002). Therefore, large amount of brewery wastewater is generated. It is generally estimated that for every litre of beer produced about 3-10 litres of water are used (Simate et al., 2011). As stated by Simate et al. (2012a), the resulting brewery wastewater contains significant amount of toxic chemicals which may pose serious risk to human beings, the environment, and aquatic life if not properly treated prior to consumption or disposal. As a result, the treatment and safe disposal of brewery wastewaters has become an important aspect in the running of breweries. Simate et al. (2011) gives a spectrum of different techniques that are used in the treatment of brewery wastewater.

In this section of the thesis, the focus will be on coagulation and flocculation processes. Over the years, coagulation and flocculation have remained the widely used methods for solid-liquid separation in water and wastewater pretreatment. Hence coagulation and flocculation are considered as the two key steps which often determine finished water quality (Zeta-Meter Inc., 1993).

2.3.1 Coagulation and flocculation processes

Coagulation and flocculation processes are an important part of water and wastewater treatment, and are considered as consisting of three sequential steps, i.e., coagulant formation, colloid/particle destabilisation, and inter-particle collisions and aggregation (Jiang and Graham, 1996; Jiang and Graham, 1998). Coagulant formation and particle destabilisation occur in rapid mixing tanks whilst inter-particle collisions occur in slow mixing flocculation tanks (Amirthrajah and O'Melia, 1990; Jiang and Graham, 1998). Coagulation or destabilisation of a colloidal suspension results in joining of minute particles. On the other hand, flocculation results in formation of larger structures that settle fast and that are more resistant to break-up into smaller particles in turbulent and high-shear zones. Subsequently, the larger particles are removed by solids removal processes. Depending on the solids separation processes, significant different coagulation regimes might be required (Newcombe and Dixon, 2006). For example, (1) sedimentation requires particles that are large and dense enough to settle, (2) dissolved air flotation requires particles that are hydrophobic enough to attach to non-polar air bubbles, (3) rapid filtration (direct filtration operation) requires chemically destabilised particles that will stick to the filter media plus previously attached particles, and (4) membrane filtration requires particles large enough to be rejected by the pores of the membrane.

2.3.2 Mechanisms of coagulation

In water treatment plants, chemical coagulation is usually accomplished by the addition of trivalent metallic salts such as aluminium sulphate ($Al_2(SO_4)_3$) or ferric chloride ($FeCl_3$). Four mechanisms are believed to occur during coagulation, i.e., double or ionic layer compression, adsorption and charge neutralisation, entrapment in a flocculent mass, and adsorption and inter-particle bridging (Peavy et al., 1985; Zeta-Meter Inc., 1993).

In the sub-sections that follow, each of these mechanisms is discussed separately, but the solution to any specific coagulation-flocculation problem will almost always involve the simultaneous use of more than one of these.

Double or ionic layer compression

Particles in aqueous solutions usually carry a charge on their surface (Fitzpatrick and Gregory, 2003; Tripathyand Ranjan De, 2006), which lead to stabilisation of the suspension (Tripathyand Ranjan De, 2006). Irrespective of the origin of the surface charge, it must be associated with an appropriate number of oppositely charged ions (counter-ions) in solution, so that overall the system has no net charge (Fitzpatrick and Gregory, 2003). Here, the double layer model (Figure 2.2) is used to visualize the ionic environment in the vicinity of a charged colloid and explain how electrical repulsive forces occur.

In explaining the double layer model, it is important to first consider the effect of the colloid on the counter-ions (Zeta-Meter Inc., 1993).

(1) Initially, attraction from the negative colloid causes some of the positive ions to form a firmly attached layer around the surface of the colloid. This layer of counter-ions is known as the Stern layer.
(2) Any additional positive ions will still be attracted by the negative colloid, but would also be repelled by the positive Stern layer as well as by other nearby positive ions that are also trying to approach the colloid. The positive ions diffuse away or are driven away from the surface, resulting in a diffuse layer of counter-ions. This diffuse layer of positive ions has a high concentration near the colloid but gradually decreases with distance until it reaches equilibrium with the normal counter-ion concentration in solution.

(3) The formation of the electrical double layer (EDL) occurs via attraction of oppositely charged counter ions by the primary surface charge and then a diffusion of the counter ions away from the surface. In other words, the attached counter-ions in the Stern layer and the charged atmosphere in the diffuse layer are referred to as the double layer.

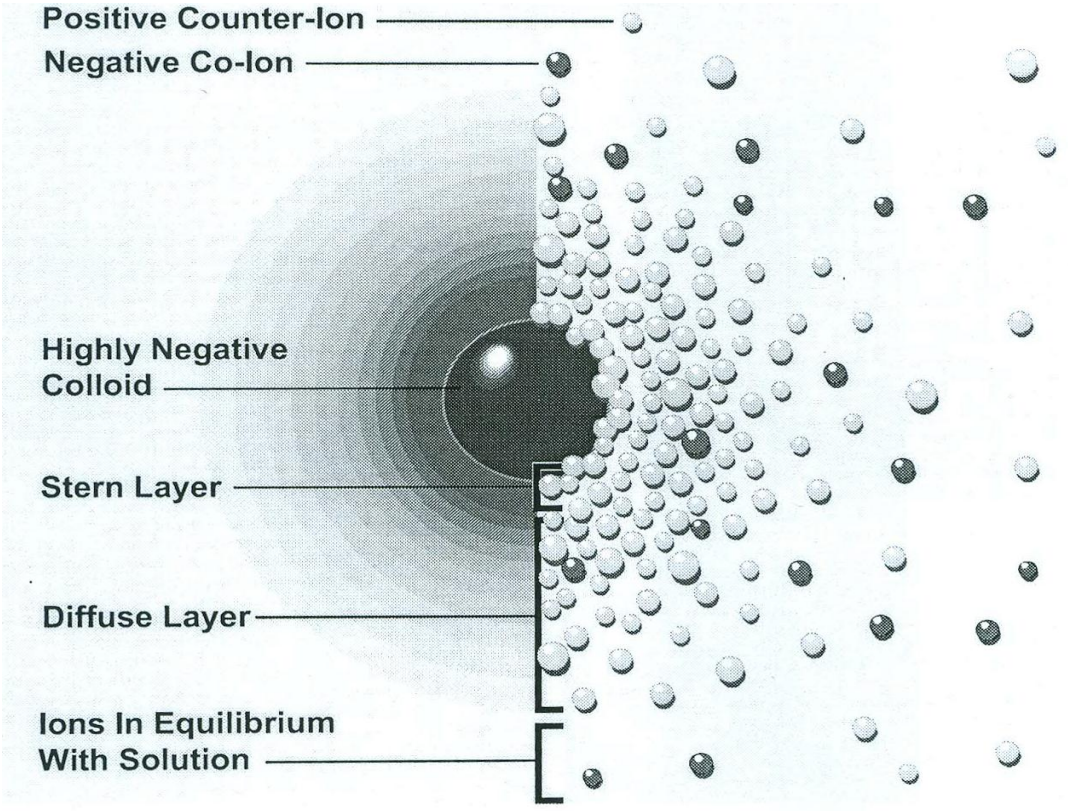


Figure 2.2.Two ways to visualize the double layer. The left view shows the change in charge density around the colloid. The right shows the distribution of positive and negative ions around the charged colloid (Zeta-Meter Inc., 1993).

When two charged particles approach each other their diffuse layers overlap and this leads to repulsion or attraction depending on the signs of charge (Fitzpatrick and

Gregory, 2003; Somasundaran and Runkana, 2003). If there is significant repulsion between particles, then they will not be able to come into close contact and aggregation will be prevented (Fitzpatrick and Gregory, 2003). Such particles are said to be *colloidally stable*, in the sense that they remain dispersed over long times. Therefore, in order to promote coagulation, it is necessary to reduce electrical repulsion between particles (Fitzpatrick and Gregory, 2003). This is achieved by the reduction of the thickness of the double layer or what is termed double layer compression. Double layer compression is achieved by adding large quantities of indifferent electrolyte (charged ions with no specific attraction for colloid primary surface) to the system (Zeta-Meter Inc., 1993), thus increasing the ionic strength of solution. High concentration of positive ions in the solution results in correspondingly high concentrations of the counter-ion in the diffuse layer. Therefore, the volume of the diffuse layer necessary to maintain electroneutrality is lowered and consequently the thickness of the diffuse layer is reduced (Weber, 1972). If this layer is sufficiently compressed by high ionic concentration, then the van der Waals force will be predominant across the entire area of influence, so that no energy barriers will exist and the net force will be attractive (Peavy et al., 1985). In other words, high ionic strength induces the collapse of the double layer and hence lowers the Stern potential, resulting in particles being close to each other for the van der Waals force to dominate (Han, 2002).

In summary, adding indifferent electrolyte increases the ionic strength of solution which has the effect of compressing the electrical double layer. As the counter-ions are pushed closer to the surface the repulsion forces becomes easier to negate by van der Waals forces.

It is important, however, to note that salting out just compresses the colloid's sphere of influence and does not necessarily reduce its charge (Zeta-Meter Inc., 1993). In general, double layer compression is not a practical coagulation technique for water

treatment, but it can have application in industrial wastewater treatment if waste streams with divalent or trivalent counter-ions happen to be available (Zeta-Meter Inc., 1993

Adsorption and charge neutralisation

Charge neutralisation involves adsorption of a positively charged coagulant on the surface of the colloid (Zeta-Meter Inc., 1993). This charged surface coating neutralises the negative charge of the colloid, resulting in a near zero net charge (Zeta-Meter Inc., 1993). For example, the ionisation of alum in water produces aluminium cations (Al^{3+}) which reacts immediately with water to form a variety of aquometallic ions and hydrogen as shown in equations below (Peavy et al., 1985).

$$Al^{3+} + H_2O \rightarrow AlOH^{2+} + H^+ \quad (2.1)$$

$$Al^{3+} + 2H_2O \rightarrow Al(OH_2)^+ + 2H^+ \quad (2.2)$$

$$7Al^{3+} + 17H_2O \rightarrow Al_7(OH)_{17}{}^{4+} + 17H^+ \quad (2.3)$$

…….

…….

$$Al^{3+} + 3H_2O \rightarrow Al(OH)_3 + 3H^+ \quad (2.n)$$

The aquometallic ions thus formed become part of the ionic cloud surrounding the colloid and, because they have great affinity for surfaces, are adsorbed on the surface of the colloid where they neutralise the surface charge. Once the surface charge has been neutralised, the ionic cloud dissipates and the electrostatic potential disappears so that the contact amongst colloidal particles occurs freely. This is a different mechanism from a double layer compression.

In summary, if charged counter-ions have a specific affinity for the surface of the colloid (not merely electrostatic attraction) then adsorption of the counter-ion will

reduce the primary charge of the colloid. Subsequently, this will reduce the net potential at any particular distance thus making the attraction forces more effective.

Enmeshment in a precipitate

If certain metal salts (e.g., aluminium or iron) are added to water in sufficient amounts, rapid formation of precipitates will occur. The colloidal particles themselves can serve as nuclei for the formation of the precipitate or the colloidal particles can be enmeshed in these precipitates as they settle (Packham, 1965;Lai, 1975). The removal of colloids in this manner is termed as 'sweep coagulation' since colloidal particles are 'swept out' of water by an amorphous precipitate (Duan and Gregory, 2003; Ye et al., 2007). Sweep flocculation generally gives considerably improved particle removal than when particles are just destabilised by charge neutralisation; partly because of the increased solids concentration which greatly improve the rate of aggregation (Duan and Gregory, 2003).

According to the 'sweep flocculation' model, the incorporation of colloids into precipitate follows two pathways: one is the heterogeneous nucleation involving charge neutralization and subsequent growth of precipitate at low pH values, and the other is homogeneous nucleation involving precipitation and subsequent particle aggregation at high pH values (Ye et al., 2007). Furthermore, in this type of mechanism, because the colloidal particles can serve as nuclei for formation of precipitate, the rate of precipitation increases with the increasing concentration of the colloidal particles to be removed. This result is an inverse relationship between the optimum coagulant dose and the concentration of material to be removed, i.e., the greater the amount of colloidal material in the water, the lower the amount of metal coagulant required to accomplish its removal (Packham, 1965; Weber, 1972; Lai, 1975). Thus, the 'sweep flocculation' mechanism significantly minimizes the cost of wastewater treatment when the concentration of colloidal particles.

Adsorption and inter-particle bridging

Inorganic primary coagulants and organic polyelectrolytes both have the capability of bridging (Zeta-Meter Inc., 1993). The bridging mechanism occurs when a coagulant forms threads or fibres which attach to several colloids, capturing and binding them together (Zeta-Meter Inc., 1993). Attachment may result from the columbic attraction if the coagulant and particle are of opposite charges or from ion exchange, hydrogen bonding and van der Waals forces if they are of similar charges (Jin, 2005). For example, to be effective in destabilization, a polymer molecule must contain chemical groups which can interact with sites on the surface of the colloidal particle (Weber, 1972; Mishra and Bajpai, 2005; Kalia and Avérous, 2011). When the polymer molecule comes into contact with the colloidal particle, some of these groups adsorb at the particle surface, leaving the remainder of the molecule extending out into the solution (Mishra et al., 2006). If a second molecule with some vacant adsorption sites contacts these extended segments, attachment can occur, thus forming a particle-polymer-particle complex in which the polymer serves as a bridge (Mishra et al., 2006). If a second particle with vacant adsorption sites is not available, the extended segments of the polymer may eventually adsorb on other sites on the original particle, so that the polymer is no longer capable of serving as a bridge (Mishra et al., 2006).

Bridging is often used in conjunction with charge neutralisation to grow fast settling and/ or shear resistant flocs (Zeta-Meter Inc., 1993). For example, alum or a low molecular weight cationic polymer is first added under rapid mixing conditions to lower the charge and allow microflocs to form. Then a slight amount of high molecular weight polymer, often an anionic, can be added to bridge between the microflocs. The fact that the bridging polymer is negatively charged is not significant because the small colloids have already been captured as microflocs.

Overdosing is possible in bridging mechanism. Basically the polymer covers the surface of the colloids without bridging to another colloid.

2.3.3 Flocculation process modelling

The mathematical description of the flocculation process is based on the classic population balance model (PBM) introduced by Smoluchowski to describe the pure coagulation case (Smoluchowski, 1916, 1917). It must be noted that, in the literature, the modelling of the flocculation process is broadly approached by many authors. Therefore, for simplification, this sub-section only summarizes a literature review article written by Thomas et al. (1999) as described below.

The mathematical representation of flocculation, i.e., the process whereby destabilized suspended particles are aggregated, has conventionally been based on considering the process as two discrete steps: transport and attachment. The transport step, leading to the collision of two particles, is achieved by virtue of local variations in fluid/particle velocities arising through, (1) the random thermal "Brownian" motion of the particles (perikinetic flocculation), (2) imposed velocity gradients from mixing (orthokinetic flocculation), and (3) differences in the settling velocities of individual particles (differential sedimentation). Attachment is then contingent upon a number of short range forces largely pertaining to the nature of the surfaces themselves.

The two precepts are most succinctly expressed mathematically as a rate of successful collision between particles of size i and j:

$$\text{rate of flocculation} = \alpha\, \beta(i, j) n_i n_j \qquad (2.5)$$

where α is the collision efficiency, β (i, j) is the collision frequency between particles of size i and j, and n_i, n_j are the particle concentrations for particles of size i and j, respectively.

The collision frequency, β, is a function of the mode of flocculation, i.e., perikinetic, orthokinetic or differential sedimentation. The collision efficiency, α (taking values from 0 to 1), is a function of the degree of particle destabilisation: the greater the degree of destabilisation, the greater the value of α. Thus, in effect, β is a measure of the transport efficiency leading to collisions, whilst α represents the percentage of those collisions leading to attachment.

Nearly all flocculation models are based upon this one fundamental equation. The values of the parameters α and β are dependent upon a large number of factors ranging from the nature of the particles to the method of destabilization, and the prevailing flow regime during flocculation. Much of the research in flocculation modeling has been directed at establishing equations and specific values for these two parameters. It is important, however, not to forget the importance of the terms n_i and n_j in the equation, as the overall rate always increases with particle concentration.
The interpretation of α and β given above implies that the two parameters are independent of one another.

2.3.4 Types of coagulants

The materials used as flocculating agents can be classified broadly into two categories, i.e., inorganic coagulants and polymeric coagulants (Tripathyand Ranjan De, 2006). The polymeric materials are further classified into natural and synthetic; the synthetic materials may be cationic, anionic or nonionic (Tripathyand Ranjan De, 2006; Bolto and Gregory, 2007). Furthermore, a new class of polymeric flocculants

have also been developed which are synthesized from natural and synthetic polymers (Tripathyand Ranjan De, 2006). Table 2.1 lists the most commonly used coagulants.

Table 2.1. Common chemical coagulants used in the treatment of drinking water (Pizzi, 2010).

Common name	Chemical formula	Comments
Aluminium sulphate	$Al_2(SO_4)_3.14H_2O$	Most common coagulant. Often used with cationic polymers
Ferric chloride	$FeCl_3.6H_2O$	May be more effective than alum in some applications
Ferric sulphate	$Fe_2(SO_4)_3$	Often used with lime softening
Ferrous sulphate	$FeSO_4.7H_2O$	Less pH depended than alum
Sodium aluminate	$Na_2Al_2O_4$	Used with alum to improve coagulation
Sodium silicate	$Na_2O.(SO_4)x$	x can range from 0.5-4.0; ingredient of activated silica coagulant aids
Aluminium polymers	-	Include polyaluminium chloride and polyaluminum sulphate
Cationic polymers	-	Synthetic polyelectrolytes; large molecules

Inorganic coagulants

The use of inorganic metal salts for coagulation/flocculation is very well-established in the field of water treatment (Jiang and Graham, 1998). The various inorganic metal salts used in coagulation/flocculation depend on the characteristics of the water being treated (Tripathyand Ranjan De, 2006). Nevertheless, the commonly used metal coagulants are mostly based upon the hydrolysable salts of aluminium and iron (Jiang and Graham, 1998; Tripathyand Ranjan De, 2006). Fundamental studies of coagulation chemistry indicate that a range of hydrolysed aluminium or iron species, but not aluminium or iron salt itself are responsible for the removal of suspended particles and colloidal impurities from water (Jiang and Graham, 1998). The addition of Al^{3+} in the form of alum (or ferric iron in the form of ferric salts) at concentrations less than the solubility limit for the metal hydroxide, results in the formation of the metal hydroxide that adsorbs onto particles causing destabilisation by charge neutralisation (Mihelcicet al., 1999). Addition of Al^{3+}or Fe^{3+}salts at concentrations

greater than the solubility limit of the metal hydroxide will result in formation of the hydroxide precipitate. In this situation, charge neutralisation and enmeshment in the precipitate both contribute to coagulation (Mihelcicet al., 1999). Furthermore, hydrogen ions liberated by the addition of alum or ferric salt will react with the water's natural alkalinity (Equation 2.6),

$$Al_2(SO_4)_3.14H_2O + 3Ca(HCO_3)_2 \rightarrow 2Al(OH)_3\downarrow + 3CaSO_4 + 14H_2O + 6CO_2 \qquad (2.6)$$

The formed precipitate (e.g., $Al(OH)_3$) is charged at certain pHs, and when the precipitate is positively charged, it will neutralise the negatively charged particles (Mihelcicet al., 1999).

However, it has been observed that the addition of these inorganic coagulants to water and the subsequent chemical reactions that occur tend to destroy alkalinity and lower the pH (Leiw, 2006) as shown above. This is unfortunate since the coagulation/flocculation process works best in the pH range from about 5.5 to 8.5 (Dobias, 1993). As a result, lime, soda ash or some other substance must be added to maintain the optimum pH range (Mihelcicet al., 1999).

Aluminium compounds: Principal aluminium compounds that are commercially available for suspended solids removal are dry and liquid alum (Tripathyand Ranjan De, 2006). Alum, which has a chemical formula $Al_2(SO_4)_3.14H_2O$, is the most common coagulant used in water treatment (Tripathyand Ranjan De, 2006). Alum is an effective flocculant at pH range 4.0 and 7.0 in which the tetravalent aluminium hydroxo complex ($Al_8(OH)_{20}^{4+}$) is dominant (Narkis and Rebhun, 1977). Another aluminium compound in use which is much more alkaline than alum is sodium aluminate while other compounds include activated alum which contains 9% sodium silicate, and black alum which contains activated carbon (Tripathyand Ranjan De, 2006).

Despite several advantages, aluminium coagulants have also some disadvantages. The residual in the treated water leads to Alzheimer's disease (Simate et al., 2012b), and a very large sludge volume is generated (Liew et al., 2006). The toxic sludge must be converted into stabilized product to prevent heavy metals from leaking into the environment (Kurniawan et al., 2006). Furthermore, as mentioned above, aluminium coagulants are only effective within a small pH range of 4.0 to 7.0 (Narkis and Rebhun, 1977).

Iron compounds: The iron salts most commonly used as coagulants include ferric sulfate, ferric chloride and ferrous sulfate (Tripathyand Ranjan De, 2006). The coagulants have lower pH and are much more corrosive than aluminium coagulants due to lower pK_a values for Fe^{3+}, oxidising power of Fe^{3+}, and the catalytic effect of chloride at the low pH of ferric coagulants (Simate et al., 2012a). Furthermore, the iron compounds often present difficulties in dissolving, and their use may result in high soluble iron concentration in process effluents (Tripathyand Ranjan De, 2006).In spite of these disadvantages, compared to other coagulants such as alum, iron based coagulants are more effective over a wider pH range of 4-11, and that the ferric hydroxide floc is heavier than alum, thus improving its settling characteristics (Simate et al., 2012a). In addition, the cost of iron compounds may often be less than that of alum (Tripathyand Ranjan De, 2006).

Polymeric inorganic coagulants: Polymeric compounds with species of iron (Fe^{3+}) and aluminium (Al^{3+}) which include polyaluminium chloride, aluminium chlorohydrate and polyaluminium chlorohydrate, have been developed and used as coagulants. Polymeric inorganic coagulants have numerous advantages compared to alum (Jiang and Graham, 1998; Gebbie, 2001; Nozaic et al., 2001; Gregory, 2006). Some of these advantages include, (1) a lower level of alkalinity is consumed, (2) smaller doses are required, (3) less sludge is produced, (4) less levels of aluminium in the treated water are achieved, and (4) they have ability to work efficiently at lower

temperatures. In general, the superior performance of polymeric inorganic coagulants is due to the presence of a range of preformed polymeric species having both high cationic charge and medium to high molecular weight (Jiang and Graham, 1998; Gregory, 2006), and their strong adsorption on negatively charged surfaces (Gregory, 2006).

Polymeric coagulants

Organic polymers, both natural and synthetic can adsorb on a wide range of surfaces and have a great effect on particle interactions, and hence on colloid stability (Gregory, 2006). Polymers may give enhanced stability, for instance by steric stabilisation, or may promote aggregation of particles by a 'bridging' mechanism (Gregory, 2006), as discussed in sub-section 2.3.2. Polymeric materials used as flocculants are mostly water soluble linear polymers of very high molecular weights (Tripathyand Ranjan De, 2006). To be effective in destabilization, a polymer molecule must contain chemical groups which can interact with sites on the surface of the colloidal particle (Weber, 1972). Polymers may be nonionic, anionic or cationic, and if there are ionic groups, then they are known as polyelectrolytes (Tripathyand Ranjan De, 2006; Bolto and Gregory, 2007; Gregory, 2006). By far the most important are those based on polyarcylamide, which can be produced with very high molecular weights (20 million or more) (Gregory, 2006).

Cationic polyelectrolytes: Cationic polyelectrolytes are polymers that produce positively charged ions when dissolved in water (Pizzi, 2010). There are many varieties of cationic polymers available (Bolto and Gregory, 2007), but can be divided into three categories: ammonium (including amines), sulfonium and phosphonium quaternaries (Tripathyand Ranjan De, 2006). The cationic polyelectrolytes can be used as primary coagulants or coagulant aids (Edzwald et al., 1987). They are widely used because the suspended and colloidal solids found in

water are generally negatively charged. Some advantages of using cationic polyelectrolytes are (Narkis and Rebhun, 1977): (1) the amount of coagulant used can be reduced, (2) floc particles settle better, (3) sensitivity to pH is reduced, and (4) the flocculation of living organisms e.g. bacteria and algae is improved

Anionic polyelectrolytes: These are polymers that produce negatively charged ions when dissolved in water (Scholz, 2006; Pizzi, 2010). They are used to remove positively charged solids present in the raw water and are used primarily with inorganic or organic coagulants (Scholz, 2006). It is often observed that the most economical treatment is obtained with an anionic polymer, even though the solid particles in the water are also negatively charged. Such observations cannot be explained by electrostatic model (Weber, 1972). Anionic polyelectrolytes produce larger flocs and are not materially affected by pH, alkalinity, hardness or turbidity.

Nonionic polyelectrolytes: These polyelectrolytes have a balanced or neutral charge (Pizzi, 2010). However, for the purpose of classifying as flocculants, a polymer is considered nonionic if less than 1% of the monomer units are charged (Tripathyand Ranjan De, 2006). Upon dissolving, they release both positively and negatively charged ions, and they primarily function as flocculants by the bridging mechanisms (Tripathyand Ranjan De, 2006). Hence, they must be of high or very high molecular weight for practical applications (Tripathyand Ranjan De, 2006). They are aids to primary coagulation and are added in larger doses than cationic or anionic polyelectrolytes (Pizzi, 2010). They are also less expensive than cationic and anionic polyelectrolytes. Polyacrylamide is the most prominent member of this class followed by poly(ethylene oxide (Tripathyand Ranjan De, 2006).

2.4 Carbon Nanotubes

Sub-section 2.3.4 reviewed in detail various chemicals that are used in the coagulation and flocculation processes. However, the majority of these chemicals have been found to have several disadvantages. The human health effects of inorganic coagulants with respect to the residual chemicals that remain during the treatment of wastewaters were thoroughly reviewed by Simate et al. (2012b). For example, residual aluminium salts in treated water may cause Alzheimer's disease; and increased levels of iron in the body above the World Health Organisation (WHO) limit levels can increase the risk of a variety of diseases including cancer, vascular diseases, and neurological disorder conditions (Simate et al., 2012b). With regards to polymeric coagulants, there is greater sensitivity to incorrect dosage, with turbidity and natural organics removal less efficient in some instances (Nozaic et al., 2001; Bolto and Gregory, 2007). Higher costs have also been witnessed in some situations (Bolto and Gregory, 2007). In addition, little full scale data is available compared to in organic coagulants. More importantly, environmental and human health effects are the other main concerns (Nozaic et al., 2001; Bolto and Gregory, 2007).

As a result of these disadvantages and many others already mentioned in some parts of sub-section 2.3.4, the search to find alternative coagulants and/or flocculants is eminent. Fortunately, the advent of nanotechnology has brought a lot of hope, and actually nanotechnology for water purification has been identified as a high priority area for most research institutions and national governments (Simate et al., 2012b). Nanotechnology can be defined as the science and engineering involved in the design, synthesis, characterization and application of materials and devices whose smallest functional organization in at least one dimension is on the nanometer scale (one-billionth of a meter) (Sahoo et al., 2007). Amongst the nanomaterials that are used in the water treatment, CNTs which have dimensions ranging from 1-100 nm have been the focus of considerable study because of their adsorption properties (Upadhyayula

et al., 2009; Simate et al., 2012a). Therefore, this section discusses the production of these carbon nanomaterials; their structures and bonding; the chemistry of CNTs; and ends by reviewing some of their applications in water treatment.

2.4.1 The synthesis of carbon nanotubes

The production of CNTs in terms of the type and quality (for example) is controlled by several factors including carbon source and type of reactor (Iyuke and Simate, 2011). Various methods have been developed for the production of these materials (Dresselhaus et al., 2001; Agboola et al., 2007; Simate et al., 2010; Iyuke and Simate, 2011), but the three very useful and widespread methodologies include arc discharge, laser ablation, and chemical vapour deposition (CVD) (Robertson, 2004; Agboola et al., 2007).

A systematic study of the various production parameters of these methods and their influence on the growth of nanotubes is paramount in enhancing the quantity and quality of nanotubes that are produced (Journet and Bernier, 1998). However, two key requirements revealed in these methods are, (i) a heat source to achieve the desired operating temperature, and (ii) a carbon source (Iyuke and Simate, 2011). In the arc discharge, CNTs are produced from carbon vapour generated by an electric arc discharge between two graphite electrodes (with or without catalysts), under an inert gas atmosphere (Journet et al., 1997; Lee et al., 2002; Agboola et al., 2007). In the laser ablation, a piece of graphite target is vapourised by laser irradiation under an inert atmosphere (Journet and Bernier, 1998; Paradise and Goswami, 2007). As for the technique of CVD, it involves the use of an energy source such as plasma, a resistive or inductive heater, or furnace to transfer energy to a gas phase carbon source (Meyyappan, 2005). In other words, in a CVD, precursor gases (often diluted in carrier gases) are delivered into the reaction chamber at an appropriate temperature. As the gases pass over or come into contact with a heated substrate, they

react or decompose forming a solid phase which is deposited onto the substrate. In these methods, the type of nanotube that is produced depends strongly upon the presence or absence of catalysts; multi-walled carbon nanotubes (MWCNTs) are most commonly produced via non-catalytic means, whereas single-walled carbon nanotubes (SWCNTs) are usually the dominant products under catalytic growth conditions (Bernholc et al., 1998).

As would be expected, some of these methods are more effective than others (Iyuke and Simate, 2011) such that, at the moment, the only promising process for the production of CNTs on a reasonably large-scale is the CVD methodology (Coleman, 2008). Therefore, this study will only use the CVD methodology (or variations thereof) in the synthesis of nanotubes.

As mentioned above carbon source is another key requirement for the production of CNTs. The commonly used carbon sources include carbon monoxide (Nasibulin, 2003) and hydrocarbon feed stocks such as methane (Wei et al., 2005), acetylene (Afolabi et al., 2007), ethylene (Yuan et al., 2001), and n-hexane (Lyu et al., 2004). However, though the pyrolysis of hydrocarbon precursors for synthesizing CNTs is very useful and is used widely, there are some disadvantages associated with these methods. Most hydrocarbons used in these methods are hazardous chemicals, and for most cases, the pyrolysis temperatures are around 1000°C, which are impractical for large scale industrial production (Qian et al., 2006). One approach to tackling this problem is by the use of CO_2 which is a cheap, non-toxic, low-energy, and abundant molecule on the earth (Qian et al., 2006). The CO_2 is easily formed by the oxidation of organic molecules during combustion or respiration. Furthermore, CO_2 can be acquired from natural reservoirs or recovered as a by-product of industrial chemical processes, so, no new production of CO_2 is necessary and there will be no addition to greenhouse gases (Young et al., 2000).

Therefore, more recently, CO_2 has also been used in the synthesis of CNTs (Xu and Huang, 2007; Maphutha, 2009; Moothi, 2009; Simate et al., 2010). Hence, this study adopted the use of CO_2 in the production of CNTs.

2.4.2 Bonds and structures of the carbon nanotubes

Carbon hybridisation

Natural carbon exists in two isotopic forms, ^{12}C and ^{13}C. The nucleus of the abundant isotope of carbon, ^{12}C, is composed of six protons and six neutrons. Neutral carbon atom is tetravalent and has a total of six electrons with four of them occupying the outer orbit. The electronic configuration of the carbon atom at fundamental state is $1s^2 2s^2 2p_x^1 2p_y^1 2p_z^0$. It has four electrons in its outer valence shell with the ground state electronic configuration of $2s22p^2$ (Terrones, 2003). However, this does not explain several bonds of carbon structures.

According to organic chemistry, one of the two 2s electrons is promoted to $2p_z$ orbital. So the electronic wave functions for the four weakly bound electrons can mix with each other, thereby changing the occupation of the 2s and 2p orbitals, since the energy difference between the lower 2s and the upper 2p levels is low compared to the binding energy in the chemical bonds. This mixing of atomic orbitals is called *hybridization*. In carbon, three possible hybridizations occur: sp, sp^2 and sp^3 (Dresselhaus et al., 2001).

In the sp hybridization, there is linear combination of 2s orbital and one of the three 2p orbitals, $2p_x$ for example. From these two atomic orbitals, two equivalent orbitals are formed, called *hybridized orbitals* and, are expressed by linear combinations of $|2s\rangle$ and $|2p_x\rangle$ as illustrated in Figure 2.3, and denoted $|2p_a\rangle$ and $|2p_b\rangle$.

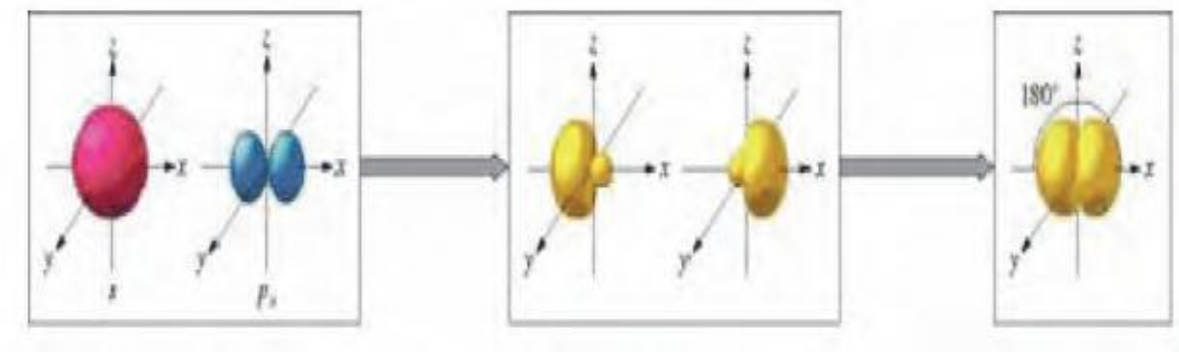


Figure 2.3. Illustration of sp hybridization and resulting structure.

In the sp^2 hybridization, three atomic orbitals are involved. The 2s and two of 2p orbitals, for example $2p_x$ and $2p_y$, are mixed. The three obtained *hybridized orbitals* are in the same plane and form three σ bonds in molecules. The resulting structure is planar. The hybrid atomic orbitals obtained have large amplitude in the directions of the three nearest neighbouring atoms. These three directions are denoted by a trigonal bonding, as shown in Figure 2.4.

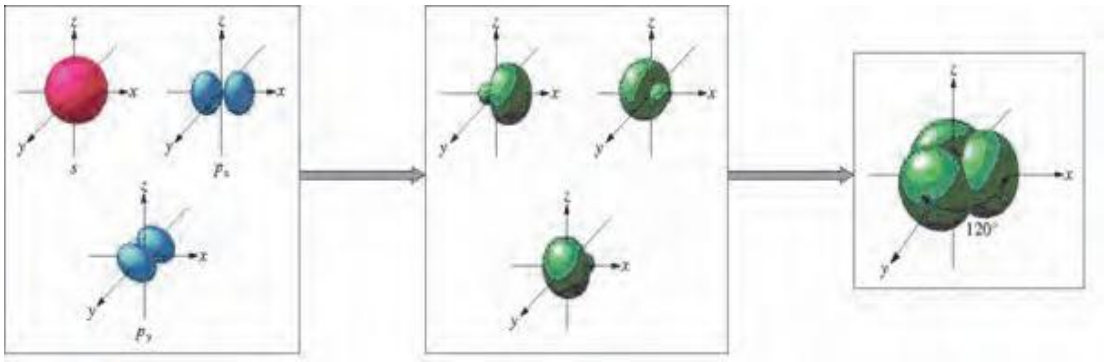


Figure 2.4. Illustration of sp^2 hybridization and resulting structure.

In the sp^3 hybridization, the 2s orbital and the three 2p orbitals are mixed. Theerefore, carbon atom provides sp^3 hybridization through its tetragonal bonding to four nearest neighbouring atoms which have the maximum spatial magnitude from each other as

graphically presented in Figure 2.5. The four directions of tetrahedral bonds from the carbon can be selected as (1,1,1), (-1,-1,1), (-1,1,-1) and (1,-1,1).

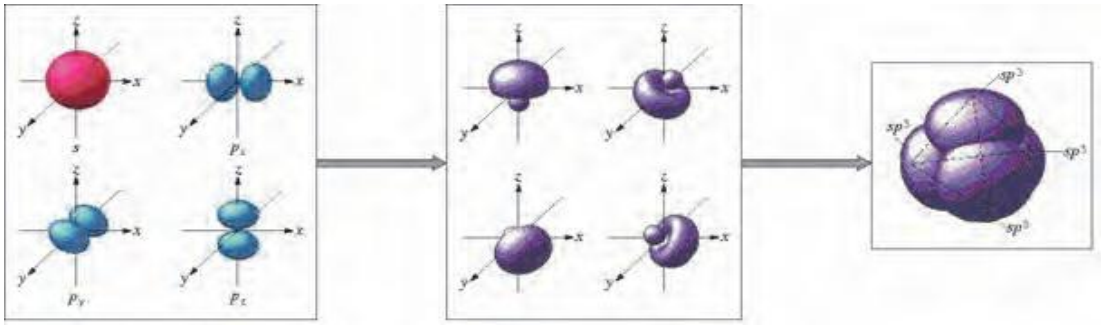
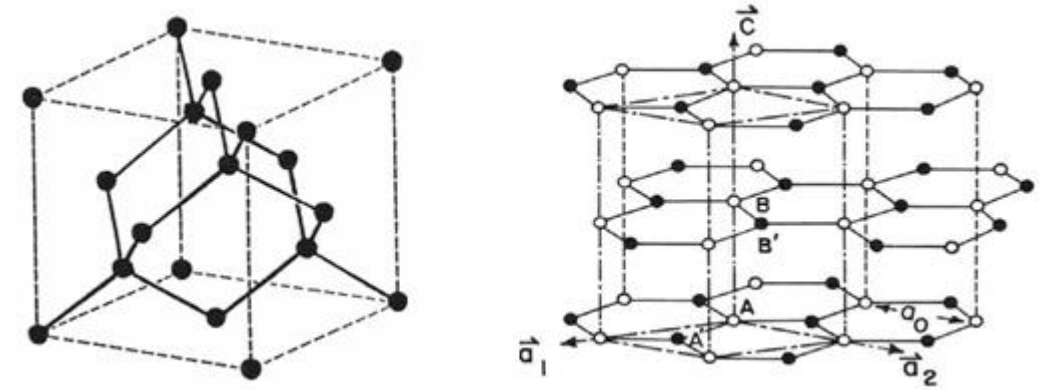


Figure 2.5. Illustration of sp^3 hybridization and resulting structure.

Bonds of the carbon nanotubes

Diamond and graphite are the two natural crystalline forms of pure carbon with sp^3 and sp^2 hybridizations, respectively (Terrones, 2003). In diamond, carbon atoms exhibit sp^3 hybridization (C-C sp^3 bond length ~1.56 Å), in which four bonds are directed toward the corners of a regular tetrahedron (Terrones, 2003) as shown in Figure 2.6. The resulting three-dimensional network is extremely rigid.



(a) (b)

Figure 2.6. Bonding in carbon structures. (a) is the tetrahedrally bonded diamond structure, and (b) is the trigonally bonded graphite structure (Dresselhaus et al., 1996; 2001).

In graphite, sp^2 hybridization occurs (C-C sp^2 bond length ~ 1.42Å), in which each atom is connected evenly to three carbon atoms at 120° in the xy plane (Figure 2.6) and a weak π-bond due to the p_z orbital is present in the z-axis (Terrones, 2003). Unlike the sp^3 hybridized diamond structure, in which all electrons are localized in the sp^3 framework, the free electrons in the p_z orbital of the graphite lattice are delocalized and move within the lattice framework (Terrones, 2003). Consequently, graphite is able to conduct electricity while diamond behaves as an insulator (Terrones, 2003). The sp^3 and sp^2 hybridization scheme in the C–C structure is depicted by Figure 2.7.

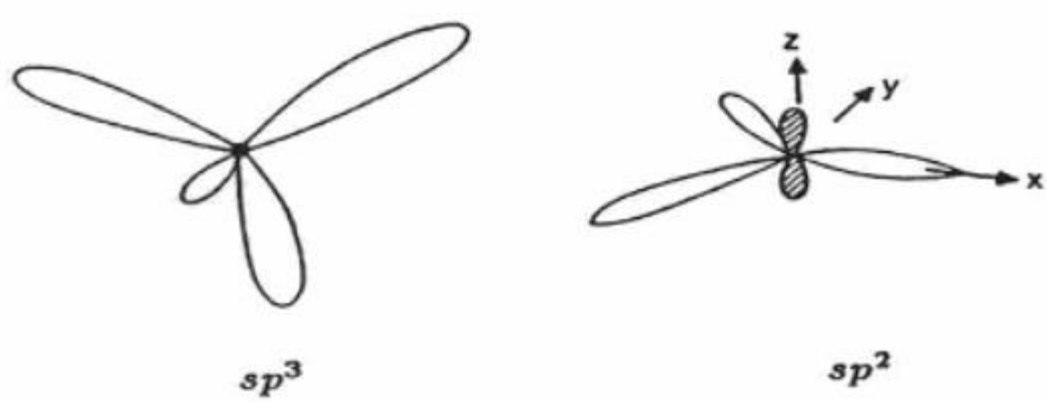


Figure 2.7. sp^3 and sp^2 hybridisation scheme in C-C structure (Dresselhaus et al., 1996; 2001).

On the other hand, CNTs are cylindrical molecules composed of dominant sp^2 hybridization of the carbon atoms, and a small amount of sp^3 hybridized carbon atoms at defects formed during preparation of the tubes. Therefore, CNTs have two types of bonds. Along the cylinder wall the in-plane σ-bonds form the hexagonal network. The out-of-plane π-bonds are responsible for the weak van der Waals interaction between the layers in multi-walled CNTs (MWCNTs), and between MWCNTs or single walled CNTs (SWCNTs) in the bundles. But, curvature produces a local strain in the π-ring systems (Ouyang et al., 2002).

Structures of carbon nanotubes

The CNTs consist of honeycomb structures of graphene sheets rolled up into cylinders (Figure 2.8) with diameter of a few nanometers (< 100 nm), but length of many micron or even centimeters (Dai, 2002a; Tasis et al., 2006). There are typically two forms of CNTs according to the number of rolled up graphene layers that form the tube, i.e., SWCNT and MWCNT. A SWCNT is a graphene sheet rolled-over into a cylinder with typical diameter of the order of 1.2-1.4 nm in magnitude (Journet and Bernier, 1998), while a MWCNT consists of concentric cylinders with an interlayer spacing of about 0.34 nm (3.4Å) and a diameter typically of the order of 10-20 nm in magnitude (Dai, 2002a).

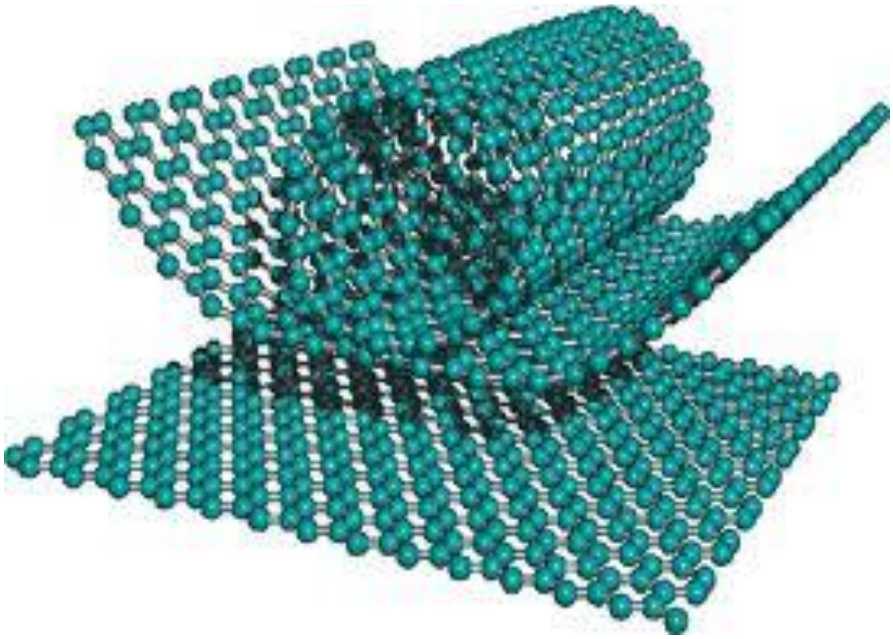


Figure 2.8. Schematic diagram of an individual layer of graphene sheet; and how it could be rolled in order to form a carbon nanotube (Endo et al., 2006).

In addition, there are two models which can be used to describe the structures of MWCNT. In the Russian doll model, a certain number of SWCNT with growing diameters on the order of nanometers and lengths on the order of micrometers are

arranged in concentric cylinders (Wu et al., 2009). In the parachute model, a single graphite sheet is rolled around itself with several turns, similar to a parachute or rolled paper (Shah, 2008).

The nanotubes are typically bound together by strong van der Waals interaction forces and form tight bundles (Dai, 2002a). Due to strong intertube van der Waals interactions, CNTs lack solubility and are difficult to manipulate in any solvent (Liu, 2008).

2.4.3 Chemistry of carbon nanotubes

The chemistry of CNTs is an area of nanotechnology which is continuously producing advanced and novel materials because of intensive research (Tasis et al., 2006; He et al., 2009). Therefore, this sub-section gives an overview of the chemistry of CNTs.

Oxidation and surface charges of carbon nanotubes

The surface chemistry of carbon materials is basically determined by the acidic and basic character of their surface, and can be changed by treating them with oxidising agents either in the gas phase or in solution (Moreno-Castilla, et al., 2000). Generally, the main aim of oxidation of a carbon surface is to obtain a more hydrophilic surface with a relatively large number of oxygen-containing groups which may behave as acid or bases, and possess ion exchange properties (Shim et al., 2001). Oxygen containing acids, including HNO_3, $HNO_3 + H_2SO_4$, $HClO_4$, $H_2SO_4 + K_2Cr_2O_7$, $H_2SO_4 + KMnO_4$ remain as the main class of oxidants that have been reported in literature, though several other oxidants (e.g., OsO_4, H_2O_2) have also been used (Lin et al., 2003). The degree of oxidation depends strongly on the nature of the oxidant and

reaction conditions. More interestingly, SWCNT and MWCNT behave differently towards the oxidation reactions (Lin et al., 2003).

The groups introduced by oxidation of CNTs using strong acids (e.g., carboxyls, lactones, phenols, ketones, quinons, alcohols and ethers) occur predominantly at the more reactive (open) end or defect sides of single-walled and multiwalled CNTs, rather than on their side walls (Yang et al., 2007). In other words, CNT walls are not reactive, but their fullerene-like tips are known to be more reactive (Lin et al., 2003). The CNT walls are unreactive due to the seamless arrangement of hexagon rings with no dangling bonds (Lin et al., 2003).

Functionalisation of oxidised carbon nanotubes

It is well known that the as-produced CNTs are insoluble in all organic solvents and aqueous solutions (Tasis at al., 2006) due to strong inter-tube van der Waals and π-π interactions (Liu, 2008). In other words, CNTs readily bundle together and it is very difficult to dissolve or disperse them in solution. This lack of solubility and the difficulty of manipulation in any solvent have led to many limitations to the use of CNTs (Matarrendona, 2003; Tasis at al., 2006). The successful incorporation of CNTs into practical materials relies on the capability of breaking up the bundles into individual nanotubes and keeping them in homogeneous and stable suspensions (Matarrendona, 2003). Therefore, CNTs have to be functionalised in order to obtain the optimal performance in various applications. Nevertheless, as discussed in sub-section 2.4.4, CNTs' lack of dispersion and solubility may be advantageous in their application in water treatment.

Indeed, CNTs can undergo various chemical reactions that make them more soluble so that they can be integrated into inorganic, organic and biological systems (Tasis at al., 2006). Particularly, the oxidatively introduced carboxylic groups are useful for

anchoring functional moieties, through either ionic or covalent linkage (Liu, 2008). For example, dissolution of CNTs in organic solvents requires the introduction of a hydrophobic substituent onto the carboxylic groups (Liu, 2008). Major approaches in this regard include amidation or esterification (Liu, 2008). Functionalisation is, therefore, an important aspect of the chemistry of CNTs (Dai, 2002b). In fact, functionalisation permits easy manipulation of CNTs for use in diverse technological fields (Rai et al., 2007).

The main approaches for the functionalisation or modification of the CNT structures can be grouped into three categories (Tasis et al., 2006): (1) the covalent attachment of chemical groups through reactions onto the π-conjugated skeleton of CNT, (2) the non-covalent adsorption or wrapping of various functional molecules, and (3) the endohedral filling of their inner empty cavities.

Covalent approaches. The covalent reaction of CNTs with polymers is essential because the long polymer chains help to dissolve the tubes into a wide range of solvents even at low degree of functionalisation (Tasis et al., 2006). Two main methodologies exist for the covalent attachment of polymeric substances onto the surfaces of CNTs (Liu, 2005; Tasis et al., 2006), i.e., 'grafting to' and 'grafting from' methods. The 'grafting to' method begins with the synthesis of a polymer of a specific molecular weight followed by end group transformation. Subsequently, this polymer chain is attached to the graphitic surface of CNTs. In other words 'grafting to' method means that the readymade polymers with reactive end groups reacted with the functional groups on the nanotube surfaces, i.e., it is the reaction between the surface groups of nanotubes and readymade polymers (Liu, 2005). The 'grafting from' is based on the covalent immobilization of the polymer precursor on the surface of the nanotubes and subsequent propagation of the polymerization in the presence of monomeric species (Tasis et al., 2006; Wu et al., 2011). In other words 'grafting from' method means the reactive groups are covalently attached to the nanotube

surface and then the polymers graft from the reactive groups, i.e., it is the reaction between the reactive groups on the surface of the nanotubes and monomers (Liu, 2005). Figure 2.9 shows different forms of chemical functionalisation processes.

It is noted, however, that covalent sidewall functionalisation of nanotubes from sp^2 to sp^3 structure is both difficult and undesirable because of the loss of conjugation (Dai, 2002b). In addition, the covalent attachment of functional groups to the surface of nanotubes might introduce defects on the walls of the perfect structure of the nanotubes thus lowering the strength of the reinforcing component (Liu, 2005).

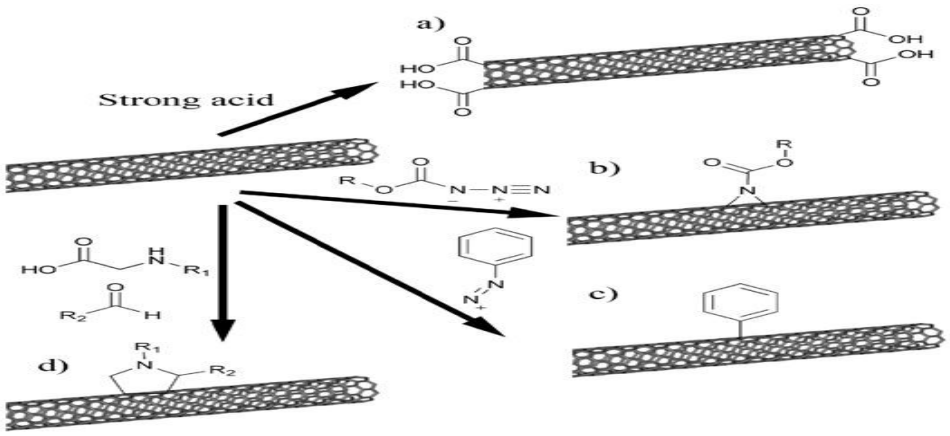
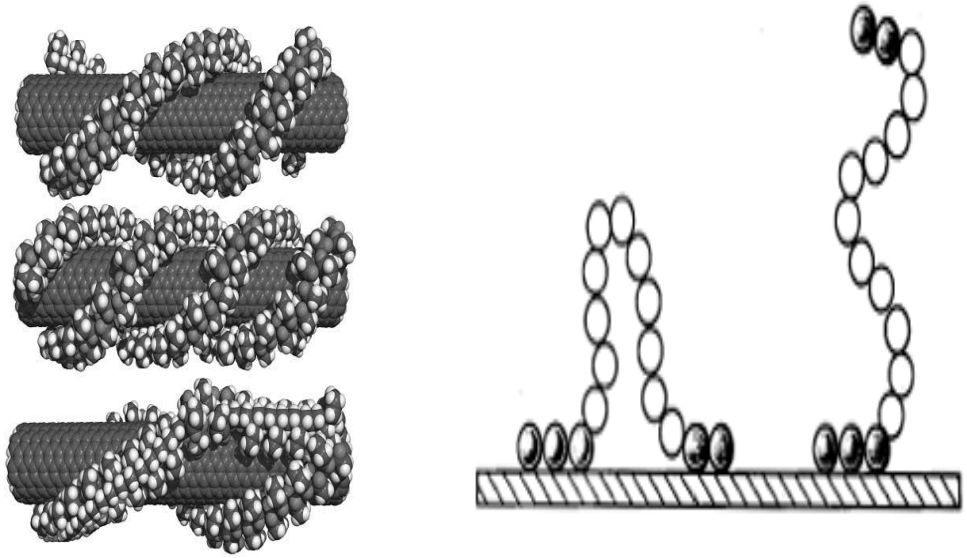


Figure 2.9. Common methods for chemical functionalisation of carbon nanotubes. (a) oxidation by strong acids, (b) nitrene cycloaddition, (c) arylation using diazonium salts, and (d) 1,3-dipolar cycloadditions (Yang et al., 2007).

Non-covalent approaches. Non-covalent sidewall functionalization of CNTs is based on weak interactions e.g., hydrogen bonding, π-π stacking, electrostatic forces, van der Waals forces and hydrophobic interactions (Trojanowicz, 2006), and it is controlled by thermodynamics (O'Connell et al., 2001; Liu, 2005; Tasis et al., 2006). In this method polymer chains are wrapped, or small molecules or biochemically active molecules are attached onto the sidewall of CNTs (Trojanowicz, 2006). The

solubility of CNTs in a solvent depends on the type and concentration of the molecules adsorbed on the tube surface (Liu, 2008). Figure 2.10 shows polymer wrapping and polymer adsorption models.



(a) (b)

Figure 2.10. Models of non-covalent functionalisation. (a) Polymer wrapping (O'Connell et al., 2001), and (b) Polymer attachment or adsorption (Dai et al., 2003).

Non-covalent functionalisation of CNTs is particularly attractive because it offers the possibility of attaching chemical handles without affecting the electronic networks of the tubes (Tasis et al., 2006), thus their mechanical properties should not change (Goyanes et al., 2007). Electronic properties and sp^3 structures are useful for various post-functionalisation applications (Dai, 200b). The other two advantages are its simple preparation procedure and, it is applicable to as-produced full-length CNTs (Liu, 2008).The disadvantage of non-covalent attachment is that the forces between the wrapping molecule and the nanotube might be weak, thus as a filler in a composite the efficiency of the load transfer might be low (Liu, 2005; Goyanes et al., 2007).

Endohedral filling. Open ended CNTs provide internal cavities that are capable of accommodating molecules of suitable sizes (Tasis et al., 2006). In this regard, of particular interest to researchers is the use of CNTs in nanofluidisc applications (Werder et al., 2001; Tasis et al., 2006). Nanofluidics is the study of fluid (gas, liquid) flow around and inside nanoscale systems (Werder et al., 2001). Nanofluidics is envisioned as a key technology for designing engineering devices for biological applications, such as biomedical devices (e.g., nanoexplorers, cell manipulators, etc.) in which the dominant biomolecular transport process is carried out by natural and forced convection (Werder et al., 2001; Tasis et al., 2006). Other applications include the usage of CNT as nanopipets, as sieves for DNA sequencing applications, and (in arrays of CNTs) as acoustic sensors in the form of artificial stereocilia (Werder et al., 2001; Tasis et al., 2006).

It has been predicted that any liquid having a surface tension below approximately 180 mNm^{-1} should be able to wet the inner cavity of tubes through an open end in atmospheric pressure (Dujardin et al., 1994; Tasis et al., 2006), whereas in the case of high surface tension, a highly pressurized liquid must be used to force it to enter inside the cavity (Tasis et al., 2006). This limit implies that typical pure metals will not be drawn into the inner cavity of nanotubes through capillarity, whereas water and organic solvents will (Dujardin et al., 1994).

2.4.4 Applications of carbon nanotubes in water treatment

In recent years, there has been a rapid increase in interest in the use of nanoparticles including CNTs in wastewater treatment. Simate et al. (2011) and Simate et al. (2012a) discussed some of the important applications of CNTs with respect to water treatment. Indeed, recent advances suggest that many of the recent problems involving water quality could be solved or greatly ameliorated by using

nanomaterials such as CNTs (Savage and Diallo, 2005). In fact, the CNTs have been used successfully as nano-sorbents and as nano-filters (Upadhyayula et al., 2009).

Sorbents are widely used as separation media in water purification to remove inorganic and organic pollutants from contaminated water due to their simplicity and cost effectiveness (Li et al., 2003a). The CNTs have shown exceptional adsorption capabilities and high adsorption efficiencies for various organic pollutants (Lu et al., 2005; Goering and Burghaus, 2007; Lu and Su, 2007; Li et al., 2007) and inorganic pollutants such as fluoride (Li et al., 2003b). The CNTs have also been found to be superior sorbents for heavy metals (Li et al., 2003a; Li et al., 2006; Li et al., 2007), and have been used in the separation and pre-concentration of various metal ions (Liang et al., 2004; Yuan et al., 2011). They are particularly attractive as sorbents because, (1) on the basis of mass, they have larger surface areas than bulk particles, (2) have well developed internal pore structures, and (3) they can be functionalised with various chemical groups to increase their affinity towards target compounds (Savage and Diallo, 2005; Pyrzyńska and Bystrzejewski, 2010). Furthermore, CNTs are small in size, hollow and have layered structures (Wu, 2007).

As for their application as nano-filters, CNTs can be uniformly aligned to form membranes with nanoscale pores that are able to filter out contaminants (Meridian Institute, 2006). The success of CNTs as membranes for nano-filters is based on their unique properties which include high surface areas, and good mechanical and thermal stability (Srivastava et al., 2004). Despite having smaller pores, CNTs have high permeability with comparable flow rates to conventional methods thus, less pressure is required to pump water through the filter, possibly due to smooth CNT interiors (Risbud, 2006). The main advantage of this is reduced costs through energy savings (Risbud, 2006). The nano-filters can also be easily cleaned by back washing compared to conventional methods (Biliuti, 2010). In addition, their nano-scale pores make these filters more selective than other filtration technologies (Meridian Institute,

2006). For example, Srivastava et al. (2004) efficiently carried out filtration of heavier hydrocarbon species from hydrocarboneceous oil, and were able to remove *Escherichia coli* and nanometer-sized poliovirus from drinking water using CNT nano-filters.

In addition, an interesting development has been reported; Lee and Baik (2010) synthesized a membrane filter possessing both super-hydrophobicity and superoleophilicity from vertically-aligned multi-walled CNTs on a stainless steel mesh for the separation of oil and water. Both super-hydrophobicity and superoleophilicity could be obtained due to the dual-scale structure, needle-like nano-tube geometry on the mesh with micro-scale pores, combined with the low surface energy. The nano-tube filter could separate diesel and water layers, and even surfactant-stabilised emulsions. The successful phase separation of the high viscosity lubricating oil and water emulsions was also carried out (Lee and Baik, 2010; Lee et al., 2011). The separation mechanism can be readily expanded to a variety of different hydrophobic and oleophilic liquids such as brewery wastewater.

Nanomesh is another device where CNTs are used in the water industry. Nanomesh is composed of CNTs that are bound together and placed on a flexible, porous substrate (filter media) (Meridian Institute, 2006). During the assembly of the filtration system, nanomesh gets rolled out as a paper, and is then wrapped around one of two types of supporting spindles (activated carbon, or plastic), depending on which device is being made (Cooper et al., 2005; Parker and Appelbaum, 2010). Functionalised versions of nanomesh can remove organic contaminants such as pesticides and herbicides, as well as inorganic contaminants such as heavy metals, fertilizers, industrial effluents, and others (Cooper et al., 2005; Meridian Institute, 2006). The filter media can also be coated with an antibacterial agent to prevent bio-film formation (Cooper et al., 2005; Meridian Institute, 2006).

As discussed by Simate et al. (2011) and Simate et al. (2012a) (including sub-section 2.4.3 of this thesis), CNTs lack dispersion and solubility properties. Nevertheless, this may be advantageous in their application in water treatment. If CNTs escape whilst in use, they can easily be recovered using separation processes such as membrane filtration, ultracentrifugation, flocculation and sedimentation (Simate et al., 2012b), thus residual CNTs that may pose risk to human health are minimized or completely prevented. Furthermore, converting CNTs to complete water soluble form is not recommended since it poses practical difficulties of using them as adsorbent media (Upadhyayula et al., 2009). Nevertheless, dispersivity of CNTs is important because the benefit of water soluble CNTs can be exploited in the fabrication of CNT composite membranes (Upadhyayula et al., 2009). On the other hand, semi dispersible and partially hydrophobic CNTs exhibit greater affinity towards bacteria than both completely dispersed or weakly dispersed CNTs (Upadhyayula et al., 2009).

2.5 Summary

This Chapter discussed different stages that are involved in the brewing process which subsequently lead to the generation of enormous amount of wastewater. The suitability of brewery wastewater for reuse is dependent on an effective wastewater treatment mechanism. In particular, this Chapter discussed the coagulation and flocculation processes because of their widespread usage, and they are also considered as the two key steps which often determine water quality. Though there is a vast amount of coagulation and flocculation materials, the suitability of most of them is rather questionable in most instances. For example, there are human health risks associated with residual chemicals that remain in drinking water after the treatment process. Clearly, this means the need to find alternative coagulants and flocculants is eminent. Subsequently, the CNTs were discussed as nanomaterials that may substitute the traditional coagulants and flocculants because of their adsorption

properties. These nanomaterials are evaluated as heterogeneous coagulants and /or flocculants, and as adsorptive granular filter media in Chapters five and six, respectively.

References

Afolabi, A. S., Abdulkareem, A. S., Iyuke, S. E., 2007. Synthesis of carbon nanotubes and nanoballs by swirled floating catalyst chemical vapour deposition method. *Journalof Experimental Nanoscience* 2 (4), 269-277.

Agboola, A. E., Pike, R. W., Hertwig, T. A., Lou, H. H., 2007. Conceptual design of carbon nanotube processes. *Clean Technologies and Environmental Policy* 9, 289-311.

Amirtharajah, A., O'Melia, C. R., 1990. Coagulation processes: destabilization, mixing, and flocculation. In: Pontius, F. W. (Editor), Water Quality and Treatment. McGraw-Hill, New York, pp. 269-365.

Arnold, J.P., 1911. Origin and history of beer and brewing. Alumni Association of the Wahl - Henius Institute of Fermentology, Chicago.

Bernholc, J., Brabec, C., Buongiorno, N. M., Maiti, A., Roland, C., Yakobson, B. I., 1998.Theory of growth and mechanical properties of nanotubes. *Applied Physics* A 67, 39-46.

Biliuti, S., 2010. Nano filters for pure water. Available at http://news.softpedia.com /news/Nanofilters-For-Pure-Water-149548.shtml. [Accessed: January 2012]

Bolto, B., Gregory, J., 2007. Organic polyelectrolytes in water treatment. *Water Research* 41, 2301-2324.

Coleman, K. S., 2008. Nanotubes. *Annual Reports on the Progress of Chemistry, Section A: Inorganic Chemistry* 104, 379-393.

Cook, D., 2011. Brewers' grains: opportunities abound. In: Brewers' Guardian, Advantage Publishing Ltd, London, November/December 2011, pp. 60-63.

Cooper, C. H., Cummings, A., Starostin, M., Honsinger, C., 2005. Nanomesh article and method of using the same for purifying fluids. United States Patent Application 20050263456, December 1, 2005.

Dai, H., 2002a. Carbon nanotubes: opportunities and challenges. *Surface Science* 500, 218-241.

Dai, H., 2002b. Carbon nanotubes: synthesis, integration, and properties. *Accounts of Chemical Research* 35 (12), 1035-1044.

Dai, L., He, P., Li, S., 2003. Functionalized surfaces based on polymers and carbon nanotubes for some biomedical and optoelectronic applications. *Nanotechnology* 14, 1081-1097.

Dalgliesh, C. E., 1979.Biochemistry and brewing. *Trends in Biochemical Sciences* 4 (5), N102-N104.

Dobiáš, B., 1993. Coagulation and flocculation: Theory and Applications. Marcel Dekker, New York.

Dresselhaus, M.S., Dresselhaus, G., Eklund, P.C., 1996. Science of Fullerenes and Carbon Nanotubes. Academy Press, London.

Dresselhaus, M. S., Dresselhaus, G, Avouris, P., 2001. Carbon nanotubes: Synthesis, Structure, Properties and Applications, Topics in Applied Physics, volume 80. Springer-Verlag, Berlin.

Duan, J., Gregory, J., 2003. Coagulation by hydrolysing metal salts. *Advances in Colloid and Interface Science* 100-102, 475-502.

Dujardin, E., Ebbesen, T. W., Hiura, H., and Tanigaki, K., 1994. Capillarity and wetting of carbon nanotubes. *Science* 265, 1850-1852

Endo, M., Hayashi, T., Kim, Y. A., 2006.Large-scale production of carbon nanotubes and their applications. *Pure and Applied Chemistry* 78 (9), 1703-1713.

Fitzpatrick, C. S., Gregory, J., 2003.Coagulation and filtration. In: Mara, D., Horan, N. (Editors), The Handbook of Water and Wastewater Microbiology, Third Edition. Elsevier, London, pp. 633-655.

Gebbie, P., 2001. Using polyaluminium coagulants in water treatment.64th Annual Water Industry Engineers and Operators' Conference, Melbourne, pp. 39-47.

Goering, J., Burghaus, U., 2007. Adsorption kinetics of thiophene on single-walled carbon nanotubes (CNTs). *Chemical Physics Letters* 447, 121-126.

Goyanes, S., Rubiolo, G. R., Salazar, A., Jimeno, A., Corcuera, M. A., Mondragon, I., 2007. Carboxylation treatment of multiwalled carbon nanotubes monitored by infrared and ultraviolet spectroscopies and scanning probe microscopy. *Diamond and Related Materials* 16, 412-417.

Gregory, J., 2006. Particles in Water: Properties and Processes. CRC Press, Boca Raton.

Han, K. N., 2002. Fundamentals of Aqueous Metallurgy. Society for Mining, Metallurgy, and Exploration Inc, Colorado.

Harrison, M. A., 2009. Beer/brewing.In: Schaechter, M. (Editor), Encyclopedia of Microbiology,Third Edition. Elsevier, Oxford, pp. 23-33.

He, N., Chen, Y., Bai, ,J., Wang, J., Blau, W. J., Zhu, J., 2009. Preparation and Optical Limiting Properties of Multiwalled Carbon Nanotubes with π-Conjugated Metal-Free Phthalocyanine Moieties. *Journal of Physical Chemistry* C 113, 13029-13035.

Hornsey, J.S., 2003. A History of Beer and Brewing. The Royal Society of Chemistry, Cambridge.

Iyuke, S. E., Simate, G. S., 2011. Synthesis of carbon nanomaterials in a swirled floating catalytic chemical vapour deposition reactor for continuous and large scale production. In: Naraghi. M. (Editor), Carbon Nanotubes – Growth and Applications. In-Tech, Rijeka, pp. 35-58.

Jiang, J-Q., Graham, N. J. D., 1998.Pre-polymerised inorganic coagulants and phosphorus removal by coagulation – A review. *Water SA* 24 (3), 237-244.

Journet, C., Maser, W. K., Bernier, P., Loiseau, A., Lamy de la Chapelle, M., Lefrant, S.,Denlard, P., Lee, R., Fischer, J. E., 1997.Large-scale production of single-walledcarbon nanotubes by the electric arc discharge. *Nature* 388, 756-758.

Journet, C., Bernier, P., 1998. Production of carbon nanotubes. *Applied Physics* A 67, 1-9.

Kalia, S., Avérous, L. (Editors), 2011. Biopolymers: biomedical and environmental applications. John Wiley and Sons Inc., New Jersey.

Kinoshita, K., 1988. Carbon: Electrochemical and Physicochemical Properties. Wiley, New York.

Kurniawan, T.A., Lo, W. H., Chan, G.Y.S., 2006. Degradation of recalcitrant compounds from stabilized landfill leachate using a combination of ozone-GAC adsorption treatment. *Journal of Hazardous Materials* B137, 433–455.

Lai, R. J., 1975. Physical aspects of mixing in coagulation control. PhD Thesis, University of Florida, USA.

Lee, S. J., Baik, H. K., Yoo, J., Han, J. H., 2002. Large scale synthesis of carbon nanotubes by plasma rotating arc discharge technique. *Diamond and Related Materials* 11, 914-917.

Lee, C., Baik, S., 2010. Vertically-aligned carbon nano-tube membrane filters with superhydrophobicity and superoleophilicity. *Carbon* 48 (8), 2192 - 2197.

Lee, C. H., Johnson, N., Drelich, J., Yap, Y. K., 2011. The performance of superhydrophobicity and superoleophilicity carbon nanotube meshes in water-oil filtration. *Carbon* 49, 669 - 676.

Li, Y-H., Ding, J., Luan, Z., Di, Z., Zhu, Y., Xu, C, Wu, D., Wei, B., 2003a. Competitive adsorption of Pb^{2+}, Cu^{2+} and Cd^{2+} ions from aqueous solutions by multiwalled carbon nanotubes. *Carbon* 41, 278-2792.

Li, Y-H., Wang, S., Zhang, X., Wei, J., Xu, C., Luan, Z., Wu, D., 2003b. Adsorption of fluoride from water by aligned carbon nanotubes. *Materials Research Bulletin* 38 (3), 469-476.

Li, Y-H., Zhao, Y. M., Hu, W. B., Ahmad, I., Zhu, Y. Q., Peng, J. X., Luan, Z. K., 2007. Carbon nanotubes – the promising adsorbent in wastewater treatment. *Journal of Physics: Conference Series* 61, 698-702.

Liang, P., Liu, Y., Guo, L., Zeng, J., Lu, H.B., 2004. Multiwalled carbon nanotubes as solid-phase extraction adsorbent for the preconcentration of trace metal ions and their determination by inductively coupled plasma atomic emission spectrometry. *Journal of Analytical Atomic Spectrometry* 19, 1489-1492.

Liew, A. G., Noor, M. J. M. M., Muyibi, S. A., Fungara, A. M. S., Muhammed, T. A., Iyuke, S. E., 2006. Surface water clarification using M. oleifera seeds. *International Journal of Environmental Studies* 63(2), 211-219.

Lin, T., Bajpai, V., Ji, T., Dai, L., 2003.Chemistry of carbon nanotubes. *Australian Journal of Chemistry* 56, 635-651.

Lin, J., 2005. Use of a high resolution photographic technique for studying coagulation/flocculation in water treatment. MSc Dissertation, University of Saskatchewan, Canada.

Linko, M., Haikara, A., Ritala, A., Penttilä, M., 1998.Recent advances in the malting and brewing industry. *Journal of Biotechnology* 65, 85-98.

Liu, P., 2005. Modifications of carbon nanotubes with polymers. *European Polymer Journal* 41, 2693-2703.

Liu, R., 2008. The functionalisation of carbon nanotubes. PhD Thesis, University of New South Wales, Australia.

Lu, C., Chung, Y-L., Chang, K-F., 2005. Adsorption of trihalomethanes from water with carbon nanotubes. *Water Research* 39, 1183-1189.

Lu, C., Su, F., 2007. Adsorption of natural organic matter by carbon nanotubes. *Separation and Purification Technology* 58, 113-121.

Lyu, S. C., Liu, B. C., Lee, S. H., Park, C. Y., Kang, H. K., Yang, C. W., Lee, C. J., 2004. Large-Scale Synthesis of High-Quality Double-Walled Carbon Nanotubes by Catalytic Decomposition of n-Hexane. *Journal of Physical Chemistry* B 108, 2192-2194.

Maphutha, S. K., 2009. Thermodynamic study of carbon nanotube production from greenhouse gases during syngas synthesis. MSc Dissertation, University of the Witwatersrand, Johannesburg, South Africa.

Matarredona, O., Rhoads, H., Li, Z., Harwell, J. H., Balzano, L., Resasco, D. E., 2003. Dispersion of single-walled carbon nanotubes in aqueous solutions of the anionic surfactant NaDDBS. *Journal of Physical Chemistry* B 107, 13357-13367.

Meridian Institute, 2006. Overview and comparison of conventional treatment technologies and nano-based treatment technologies – water. Available at http://www.merid.org/nano/watertechpaper. [Accessed: January 2012]

Meyyappan, M., 2005. Growth: CVD and PECVD. In: Meyyappan, M. (Editor), Carbon Nanotubes: Science and Applications. CRC Press, Boca Raton.

Mihelcic, J. R., 1999. Fundamentals of environmental engineering. John Wiley and Sons, Inc., New York.

Mishra, A., Bajpai, M., 2005. Flocculation behaviour of model textile wastewater treated with a food grade polysaccharide. *Journal of Hazardous Materials* B118, 213-217.

Mishra, A., Bajpai, M., Pandey, S., 2006. Removal of dyes by biodegradable flocculants: a lab scale investigation. *Separation Science and Technology* 41, 583-593.

Mishra, A., Bajpai, M., Pandey, S., 2006. Removal of dyes by biodegradable flocculants: a lab scale investigation. *Separation Science and Technology* 41, 583-593.

Moothi, K., 2009. Carbon nanotube production from greenhouse gases during syngas synthesis. MSc Dissertation, University of theWitwatersrand, Johannesburg, South Africa.

Moreno-Castilla, C., López-Ramón, M. V., Carrasco-Marín, F., 2000.Changes in surface chemistry of activated carbon by wet oxidation. *Carbon* 38, 1995-2001.

Narkis, N., Rebhun, M., 1977.Stoichiometric relationship between humic and fulvic acids and flocculants. *Water Technology*, June, 325-328.

Nasibulin, A. G., Moisala, A., Brown, D. P., Kauppinen, E.I., 2003. Carbon nanotubes and onions from carbon monoxide using Ni(acac)2 and Cu(acac)2 as catalyst precursors. *Carbon* 41, 2711-2724.

Newcombe, G., Dixon, D., 2006. Interface Science in Drinking Water Treatment: Theory and Applications, volume 10. Academic Press, London.

Nozaic, D. J., Freese, S. D., Thompson, P., 2001. Longterm experience in the use of polymeric coagulants at Umgeni water. *Water Science and Technology: Water Supply* 1 (1), 43-50.

O'Connell, M. J., Boul, P., Ericson, L. M., Huffman, C., Wang, Y., Haroz, E., Kuper, C., Tour, J., Ausman, K. D., Smalley, R. E., 2001. Reversible water-solubilisation of single-walled carbon nanotubes by polymers wrapping. *Chemical Physics Letters* 342, 265-271.

Ouyang, M., Huang, J-L., Lieber, C.M., 2002. Scanning tunneling microscopy studies of the one-dimensional electronic properties of single-walled carbon nanotubes. *Annual Review of Physical Chemistry* 53, 201-220.

Packham, R.F., 1965. Some studies of the coagulation of dispersed clays with hydrolyzing salts. *Journal of Colloid Science* 20, 81-92.

Paradise, M., Goswami, T., 2007. Carbon nanotubes – Production and industrial Applications. Materials and Design 28, 1477-1489.

Parker, R., Appelbaum, R. P., 2010. Multi-walled carbon nanotubes in water filtration systems: From new material innovation to new product innovation. Available at http://nanopolicy.gatech.edu/wp-content/uploads/2011/04/MWCNTs_Waterfilters-Innovations_FINAL.pdf. [Accessed: January 2012]

Peavy, H. S., Rowe, D. R., Tchobanoglous, G., 1985. Environmental Engineering. McGraw-Hill, Inc., New York.

Phiarais, B. P. N., Arendt, E. K., 2008. Malting and brewing with gluten-free cereals. *Gluten-Free Cereal Products and Beverages*, 347-372.

Pizzi, N. G., 2010. Principles and practices of water supply – water treatment, 4th Edition. American Water Works Association, Denver.

Pyrzyńska, K., Bystrzejewski, M., 2010. Comparative study of heavy metal ions sorption onto activated carbon, carbon nanotubes, and carbon-encapsulated magnetic nanoparticles. *Colloids and Surfaces A: Physicochemical and Engineering Aspects* 362, 102-109.

Qian, W., Wei, L., Cao, F., Chen, Q., Qian, W., 2006. Low temperature synthesis of carbon nanospheres by reducing supercritical carbon dioxide with bimetallic lithium and potassium. *Carbon* 44 (7), 1298-1352.

Rai, P K., Parra-Vasquez, A. N. G., Chattopadhyay, J., Pinnick, R. A., Liang, F., Sadana, A. K., Hauge, R. H., Billups, W. E., Pasqual, M., 2007. Dispersions of functionalized single-walled carbon nanotubes in strong acids: solubility and rheology. *Journal of Nanoscience and Nanotechnology* 7 (10), 3378-3385.

Risbud, A., 2006. Cheap drinking water from the ocean. Technology Review, MIT. Available at http://www.technologyreview.com/Nanotech/16977/. [Accessed: January 2012]

Robertson, J., 2004. Realistic applications of CNTs. *Materials Today* 7 (10), 46-52.

Sahoo, S. K., Parveen, S., Panda, J. J., 2007. The present and future of nanotechnology in human health care. *Nanomedicine: Nanotechnology, Biology, and Medicine* 3, 20-31.

Savage, N., Diallo, M. S., 2005. Nanomaterials and water purification: Opportunities and challenges. *Journal of Nanoparticle Research* 7, 331-342.

Scholz, M., 2006. Wetland systems to control urban runoff, 1st Edition. Elsevier, Amsterdam.

Shah, H. M., 2008. Dispersion of narrow diameter carbon nanotubes for optical characterization. MSc Dissertation, University of Louisville, USA.

Shim, J-W., Park, S-J., Ryu, S-K., 2001.Effect of modification with HNO_3 and NaOH on metal adsorption by pitch-based activated carbon fibres. *Carbon* 39, 1635-1642.

Simate, G. S., Iyuke, S. E., Ndlovu, S., Yah, C., Walubita, L. F., 2010. The production of carbon nanotubes from carbon dioxide: Challenges and opportunities. *Journal of Natural Gas Chemistry* 19 (5), 453-460.

Simate, G. S.., Cluett, J., Iyuke, S. E., Musapatika, E. T., Ndlovu, S., Walubita, L. F., Alvarez, A. E., 2011.The treatment of brewery wastewater for reuse: State of the art. *Desalination* 273 (2-3), 235-247.

Simate, G. S., Iyuke, S. E., Ndlovu, S., Heydenrych, M., 2012a. The heterogeneous coagulation and flocculation of brewery wastewater using carbon nanotubes. *Water Research* 46 (4), 1185-1197.

Simate, G. S., Iyuke, S. E., Ndlovu, S., Heydenrych, M., Walubita, L. F., 2012b. Human health effects of residual carbon nanotubes and traditional water treatment chemicals in drinking water. *Environment International* 39, 38-49.

Smoluchowski M., 1916. Drei vortrage uber diffusion brownsche molecularbewegung und koagulation vor kolloidteilchen. *Physick Zeitschrift* 17, 557-571.

Smoluchowski, M., 1917.Versuch einer mathematischen theorie der koagulationskinetik kolloider lösungen. *Zeitschrift für Physikalische Chemie* 92 (2), 129-168.

Somasundaran, P., Runkana, V., 2003. Modeling flocculation of colloidal mineral suspensions using population balances. *International Journal of Mineral Processing* 72, 33-55.

Srivastava, A., Srivastava, O. N., Talapatra, S., Vajtai, R., Ajayan, P. M., 2004. Carbon nanotube filters. *Nature Materials* 3 (9), 610-614.

Tasis, D., Tagmatarchis, N., Bianco, A., Prato, M., 2006.Chemistry of carbon nanotubes. *Chemical Reviews* 106 (3), 1105-1136.

Terrones, M., 2003. Science and technology of the twenty-first Century: Synthesis, properties and applications of carbon nanotubes. *Annual Review of Materials Research* 33, 419-509.

Thomas, D. N., Judd, S. J., Fawcett, N., 1999. Flocculation modeling: A review. *Water Research* 33 (7), 1579-1592.

Tripathy, T., Ranjan De, B., 2006. Flocculation: A new way to treat the waste water. *Journal of Physical Sciences* 10, 93-127.

Trojanowicz, M., 2006. Analytical applications of carbon nanotubes: a review. *Trends in Analytical Chemistry* 25 (5), 480-489.

Upadhyayula, V. K. K., Deng, S., Mitchell, M. C., Smith, G. B., 2009. Application of carbon nanotube technology for removal of contaminants in drinking water: a review. *Science of the Total Environment* 408, 1-13.

van der Merwe, A., Friend, J.F.C., 2002. Water management at a malted barley brewery. *Water SA* 28 (3), 313-318.

Weber, W. J., 1972. Physicochemical processes for water quality control. John Wiley and Sons Inc., New York.

Wei, R., Li, F., Ju, Y., 2005. Preparation of Carbon Nanotubes from Methane on Ni/Cu/Al Catalyst. *Journal of Natural Gas Chemistry* 14, 173-176.

Werder, T., Walther, J. H., Jaffe, R. L., Halicioglu, T., Noca, F., Koumoutsako, P., 2001. Molecular dynamics simulation of contact angles of water droplets in carbon nanotubes. *Nano Letters* 1 (12), 697-702.

Wu, G. T., Wang, C. S., Zhang, X. B., Yang, H. S., Qi, Z. F., He, P. M., Li, W. Z., 1999. Structure and lithium insertion properties of carbon nanotubes. *Journal of The Electrochemical Society* 146 (5), 1696-1701.

Wu, X., Chen, X., Wang, J., Liu, J., Fan, Z., Chen, X., Chen, J., 2011. Functionalization of multiwalled carbon nanotubes with thermotropic liquid-crystalline polymer and thermal properties of composites. I*ndustrial and Engineering Chemistry Research*. 50, 891-897.

Wyatt, F., 1900.The influence of science in modern beer brewing. *Journal of the Franklin Institute* 150 (3), 190-214.

Xu, X.J., Huang, S. M., 2007. Carbon dioxide as a carbon source for synthesis of carbon nanotubes by chemical vapour deposition. *Materials Letters* 61, 4235-4237

Yang, W., Thordarson, P., Gooding, J. J., Ringer, S. P., Braet, F., 2007.Carbon nanotubes for biological and biomedical applications. *Nanotechnology* 18, 1-12.

Yuan, L., Saito, K., Hu, W., Chen, Z., 2001. Ethylene flame synthesis of well-aligned multi-walled carbon nanotubes. *Chemical Physics Letters* 346, 23-28.

Yuan, C. G., Zhang, Y., Wang, S., Chang, A., 2011. Separation and preconcentration of palladium using modified multi-walled carbon nanotubes without chelating agent. *Microchim Acta* 173, 361-367.

Ye, C., Wang, D., Shi, B., Yu, J., Qu, J., Edwards, M., Tang, H., 2007. Alkalinity effect of coagulation with polyaluminum chlorides: Role of electrostatic patch. *Colloids and Surfaces A: Physicochemical and Engineering Aspects* 294, 163-173.

Young, J. L., DeSimone, J. M., 2000. Frontiers in green chemistry utilising carbon dioxide for polymer synthesis and applications. *Pure and Applied Chemistry* 72 (7), 1357-1363.

Zeta-Meter Inc., 1993. Everything you need to know about coagulation and flocculation-guide. Zeta-Meter Inc., Virginia.

CHAPTER THREE

EXPERIMENTAL MATERIALS AND METHODS

"*Work is the greatest thing in the world, so we should always save some of it for tomorrow*".

-Don Herald

3.1 Introduction

This chapter discusses the preparation of the materials as well as the experimental and analytical methods employed in the study. Data analysis is also discussed. A summary is subsequently provided to wrap-up the chapter.

3.2 Experimental Materials

3.2.1 Raw wastewater

The brewery waste water used in this study was obtained from the outlet of the up-flow anaerobic sludge blanket (UASB) reactor at the wastewater treatment plant of the South African Breweries Limited plant in Alrode, South Africa. The collected wastewater was allowed to settle for 24 hours, and the supernatant was carefully collected and preserved at 4°C in a refrigerator for use in subsequent test works.

3.2.2 Ferric chloride

Ferric chloride used in this study was obtained from Merck, South Africa (unless stated otherwise). Ferric chloride was chosen amongst other inorganic coagulants such as alum because it is effective over a wider pH range of 4-11, and that the ferric hydroxide floc is heavier than alum, thus improving its settling characteristics (Simate et al., 2012a).

3.2.3 Carbon nanotubes

The MWCNTs used in this study were produced locally by the CVD method as described in sub-section 3.3. 1.

3.3 Experimental Methods

This section presents in detail, the description of equipment and the experimental methodologies used.

3.3.1 Synthesis, purification and functionalisation of carbon nanotubes

Catalyst preparation

The CNTs were synthesized from CO_2 following the method similar to that by Xu and Huang (2007). The catalyst used was 10% iron on calcium carbonate support. Calcium carbonate was chosen from amongst other supports because of the good quality, high yield and high purity materials obtained from using it as a support (Mhlanga, 2009). The catalyst was prepared by the modified wet impregnation technique as described by See and Harris (2008). The calcium carbonate supported catalyst, containing 10% mass fraction of iron was prepared by mixing a calculated amount of iron nitrate, and citric acid in approximately 1:1 molar ratio into deionized water. Ammonia solution was added in drops until a neutral pH was reached. After 6 hrs, a reddish brown solution with no precipitate was obtained. A calculated amount of calcium carbonate was then stirred into this solution to form dry slurry, which was then left overnight. Thereafter, the resulting powder was calcined at 500°C between 6 and 12 hrs in a muffle furnace so as to decompose the nitrates from the catalyst (Li et al., 2009).

Equipment

The CNTs were synthesised from CO_2 in a 'modified' swirled floating catalyst CVD reactor (SFCCVD). The picture of modified SFCCVD reactor is shown in Figure 3.1. This 'modified' SFCCVD reactor consists of a vertical quartz or silica tube inside a

furnace. The upper end of the reactor is connected to a condenser that leads to two delivery cyclones where the CNTs produced are collected. Feed materials including carrier gases are uniformly mixed with the aid of a swirled coiled mixer to give optimum interaction. The flow of gases into the SFCCVD reactor is aided by a system of valves and rotameters (Yah et al., 2011a).

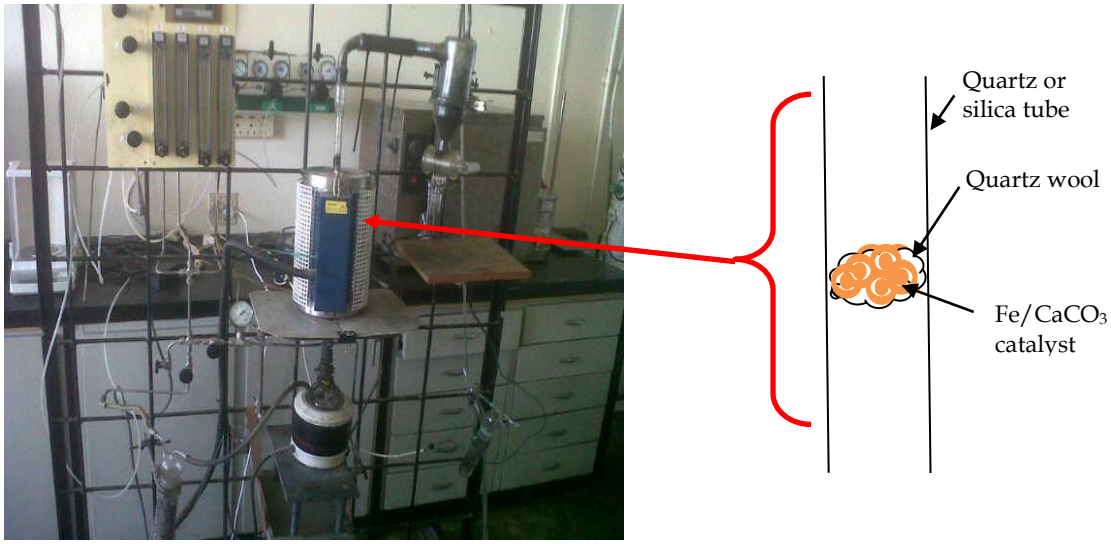


Figure 3.1.Swirled floating catalyst chemical vapour deposition reactor with inserted quartz wool (Iyuke, 2007; Iyuke and Simate, 2011).

Procedure

Approximately 10 g of calcium carbonate supported catalyst, containing 10% mass fraction of iron was placed on quartz wool and was located within a vertical silica tube that was later heated by an electric furnace (Figure 3.1). Once the equipment was setup, all the connections were sealed with high vacuum grease to ensure that there were no gas leaks (Yah et al., 2011b). Thereafter, the reactor was purged with argon so as to remove oxygen that could oxidise the formed CNTs. Ultra high purity (UHP) grade gases as supplied by AFROX Ltd (South Africa) were used in this study. The reaction gas consisted of a mixture of CO_2 (99.99% minimum purity) and hydrogen

(95.5% minimum purity). Experiments were conducted at temperatures ranging from 740-850°C.

Carbon nanotubes purification

The crude pristine CNTs produced were purified by treating them with 10% nitric acid by gentle vortexing for 2½ hours at 120°C (Yah et al., 2011a). The lower acid concentration was to remove the impurities, but prevent the CNTs from being oxidised (Simate et al., 2012a). The products were filtered, washed repeatedly with deionised water until a pH of 7 was reached, and were dried at 80°C in a hot air oven overnight (Yah et al., 2011a).

Carbon nanotubes functionalisation

The functionalisation of carbon materials is used to obtain a more hydrophilic surface structure with relatively large number of oxygen containing surface groups (Li et al., 2002). These oxygen-containing groups behave as acids or bases, which possess ion exchange properties and improve the dispersibility of CNTs in liquids such as water (Li et al., 2002), i.e., the dissociation of the surface functional groups facilitates the dispersion by creating a negative or positive charge or providing hydrophilic sites on a hydrophobic surface (Boehm, 1994). Furthermore, the introduction of functional groups on the surface of CNTs provides several chemical sites for adsorption of colloidal particles from wastewater. As stated earlier, the adsorption of colloidal particles can lead to bridging flocculation and neutralisation of charges on the particles, thus facilitating agglomeration.

As stated by Simate et al. (2012a), the CNTs were functionalised by soaking 100 g of purified CNTs in concentrated hydrochloric acid overnight, and then filtered. Hydrochloric acid was chosen as it has been found to be effective in driving the zeta

potential of carbon material in the positive direction (Suzuki and Chihara, 1988). The filtered CNTs were rinsed with deionised water until the pH of 7 was reached. After this step the CNTs were ready for use in some test works.

3.3.2 Jar tests

The heterogeneous coagulation and flocculation potential of CNTs were evaluated using the standard jar tests (Figure 3.2). To compare the coagulation/flocculation capability of CNTs, ferric chloride was used. For each jar test, the procedure followed is as given below.

Initially, a stock suspension of 1000 mg/L of CNTs was prepared by adding 100 mg of CNTs to 100-mL of distilled water and mixed over a magnetic stirrer at 500 rpm. The stock suspension was continuously mixed during the duration of the experiments. Similarly, a stock solution of ferric chloride was also prepared.

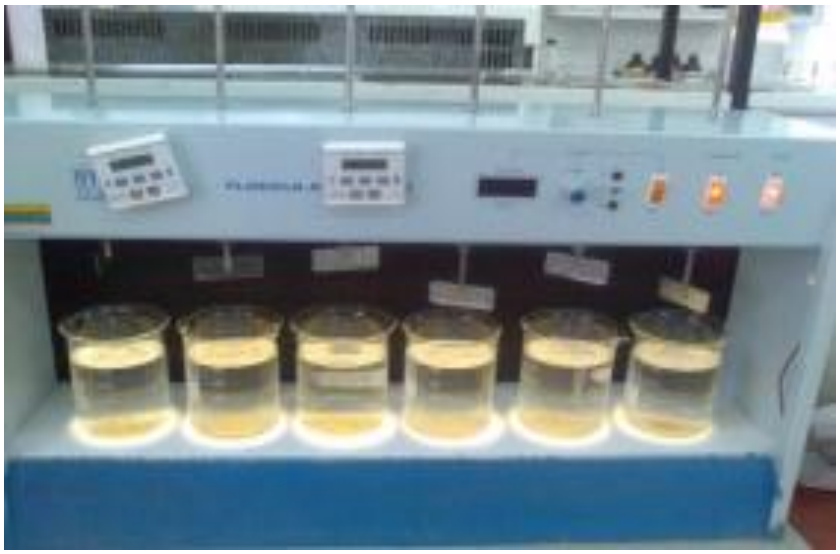


Figure 3.2. The flocculator (Stuart Scientific Flocculator SW1) and jar test experimental set up.

In a typical experiment, exactly 100-mL of brewery waste water was measured into each jar test beaker. The pH was adjusted accordingly using 0.1N HCl or 0.1N NaOH before addition of the coagulant. The stirrer speed was then set to the predetermined 'flash mix' value of 150 rpm, and the brewery wastewater was then spiked with small volumes of stock suspension or stock solution of either CNTs or ferric chloride, respectively, near the vortex to achieve predetermined concentrations of CNTs or ferric chloride. After the predetermined 'flash mix' duration of 3 minutes, the mixing speed was reduced to the predetermined flocculation or 'slow mix' of 60 rpm for a period of 20 minutes. After this period, the stirrer was withdrawn and the floc was allowed to settle for 30 minutes. However, since no flocs were visible due to poor dispersivity of CNTs, the treated water was filtered through a Whatman # 1 filter paper (as shown in Figure 3.3) and the parameters (turbidity and COD) of the filtered water were measured as an indication of coagulation (Nozaic et al., 2001). The parameters analysed were turbidity and chemical oxygen demand (COD).



Figure 3.3. The filtration setup of treated brewery wastewater.

3.3.3 Semi-continuous laboratory-scale water treatment plant

Equipment

The paraphernalia in Figure 3.4 illustrates the setup of the semi-continuous laboratory-scale water treatment plant (semi-continuous LSWTP) which was used to evaluate the use of CNTs as adsorptive granular filter media (i.e., **Objective III**). In addition, the experiment also helped to assess the integration of coagulation/flocculation and sedimentation with CNTs adsorption in a granular filter bed. The semi-continuous LSWTP consists of the raw water tank, coagulant dosing tank, coagulation tank, flocculation and high rate settling tank as a combined unit, rapid sand filter, and treated water tank.

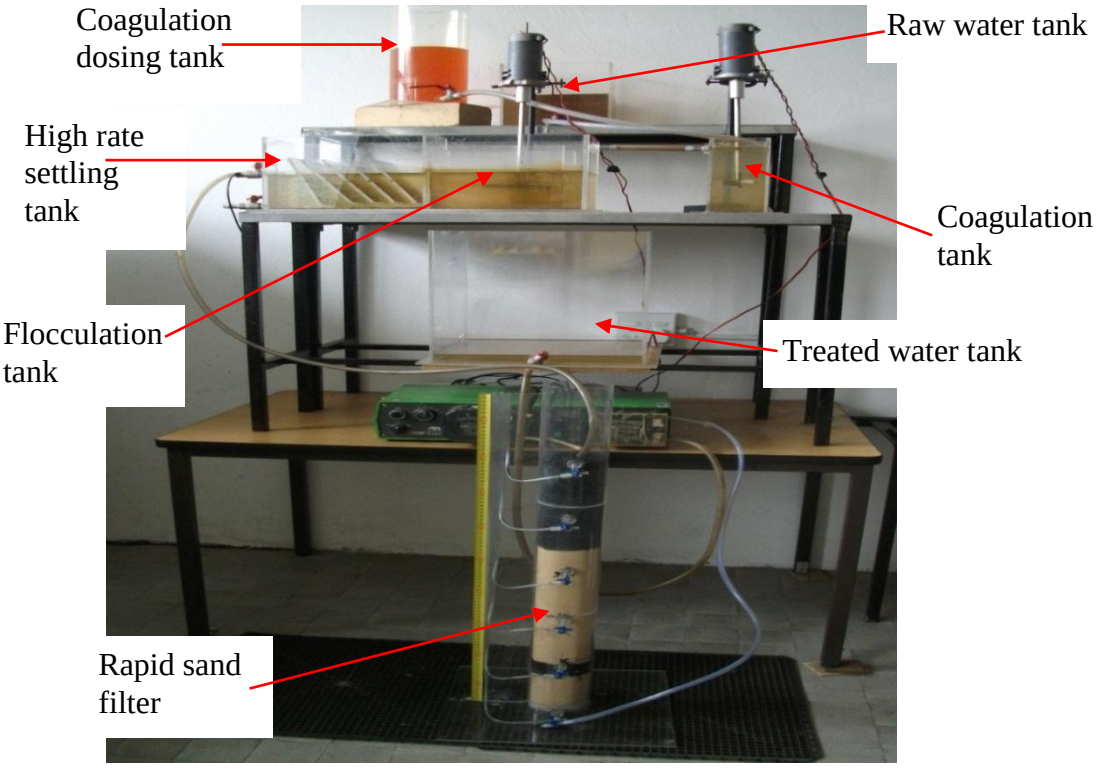


Figure 3.4. The semi-continuous laboratory-scale water treatment plant.

Filter configuration

The filter column was made using a transparent polyvinyl chloride (PVC) pipe with an internal diameter of 9 cm and a total height of 95 cm. The column consisted of six sampling and pressure points. In order to avoid wall effect discrepancies that could lead to inaccurate measurements of the filtrate quality, the sampling ports were inserted 4.5 cm inside the column (Aronino et al., 2009). Furthermore, to avoid head loss surges, the sampling ports were kept constantly open to permit rapid dripping (Gitis et al., 2005).

Granular media

Initially, the granular media was selected and arranged as follows (Figure 3.5): - The lighter anthracite was placed on denser sand, and sintered plastic beads under-drain supported the media. The depth of the anthracite bed was approximately 25 cm with sufficient sand to give a combined depth of 75 cm.

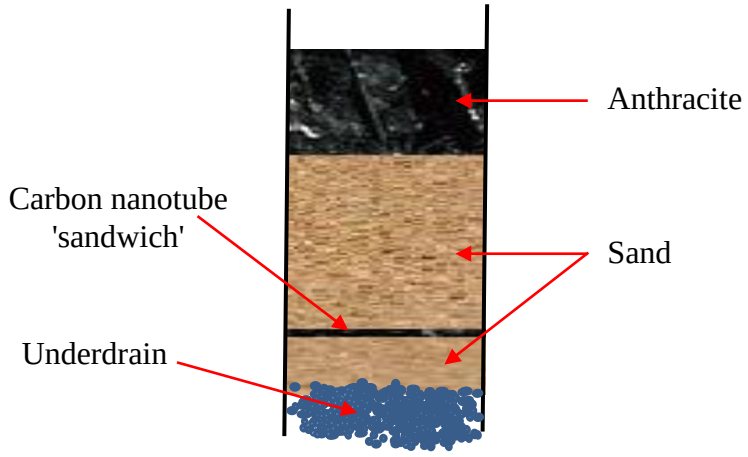


Figure 3.5. Arrangment of the filter media.

Due to the low quantity and high cost of producing CNTs; the CNTs were installed within the filter bed. The ‘sandwich’ bed used a 10 mm layer of CNTs installed 35

cm below the sand surface. Before the media was loaded into the filter column, it was washed with distilled water to remove any contaminants and dried overnight in an oven.

Table 3.1 shows the effective sizes (sieve size through which 10% of the filter media passes), uniformity coefficient (ratio of sieve sizes through which 60% pass and through which 10% pass) and other principle characteristics of the filter media excluding CNTs. In Table 3.1, voidage (or porosity) which is a measure of the void spaces (i.e., empty spaces) is calculated as, voidage = 100 x (particle specific density-bulk density)/particle specific density. It represents a fraction of the volume of voids over the total volume.

Table 3.1. Principle characteristics of the filter media.

Media	Diameter (mm)	Effective size (mm)	Uniformity coefficient	Specific gravity	Bulk density (g/cm^3)	Sphericity (sphere = 1.0)	Porosity (pore volume/filter volume)
Anthracite	1.4-2.8	1.5	1.4	1.40-1.45	0.73	0.70	0.50
Sand	0.6-1.18	0.75	1.5	2.55-2.65	1.56	0.85	0.40

Operational procedure

Typical operations of the semi-continuous LSWTP consisted of the followings: - The raw water flowed by gravity to the coagulant tank and was controlled by a valve. Addition of a coagulant from the dosing tank to the coagulant tank was controlled by a valve. In the coagulant tank, the raw water was mixed with the coagulant by mechanical agitation with a stirrer. Thereafter, the water flowed to the first compartment of the flocculation and settling unit where slow mixing took place. This mixing caused the collision and enmeshment of particulates into flocs and consequently, settled in the second compartment. This second compartment has inclined plates to enhance settling (Liew et al., 2006). The water from the settling unit

flowed to the rapid sand filter (mixture of anthracite coal, sand and carbon nanotubes).

Backwashing

Several criteria exist that necessitates backwashing (see section 3.5), but in this study the need for backwashing was determined by using a fixed time interval criteria, i.e., after 24 hours of operation. The filter was backwashed for 2 minutes with air followed by 15 minutes with water at high pressure. The media was then tapped down to the specified elevations after backwashing was completed (AWWA, 1992; Williams et al., 2007).

3.3.4 Experimental design

Table 3.2 is a summary of the design of the experiments carried out in this study indicating test conditions, materials and/or samples tested, and the number of replicates in each experimental test in this study.

Table 3.2. Experimental design.

Test type	Test conditions	Material/Samples tested	Replicates
Synthesis of carbon nanotubes	-temperature -flow rate -weight	-reactor -gases -CNTs	4
Heterogeneous coagulation and flocculation	-pH -COD -weight -volume	-brewery wastewater -ferric chloride - CNTs	4
Lab-scale water treatment plant	-pH -COD -weight -volume	-brewery wastewater -ferric chloride - CNTs -quartz sand -anthracite coal	4

3.4 Analytical Techniques

This section describes the analytical techniques that were used in characterizing, (1) raw water and treated water quality, and (2) pristine and functionalised CNTs.

3.4.1 Raw water and treated water quality

The quality of raw water is one of the fundamental variables in water treatment. The parameters that define the quality of water can be categorised as physical, chemical and biological (Peavy et al., 1985). Physical parameters define those characteristics of water that respond to the senses of sight, touch, taste, or smell. Suspended solids, turbidity, colour, taste, odour, and temperature fall into this category. On the other hand, total dissolved solids, alkalinity, fluorides, hardness, metals, organics, and nutrients are chemical parameters of concern in water quality management.

An understanding of how the variables affect water chemistry is necessary to achieve the treatment goals. Therefore, if the above variables are reviewed prior to embarking on the coagulant and flocculant selection process, a considerable amount of time and needless effort can be saved.

The majority of analytical methods listed in this sub-section follow the standard methods for the examination of water and wastewater (Clescrei et al., 1998). Table 3.3 is a summary of the water quality characteristics of the brewery wastewater used in this study.

Table 3.3. Water quality characteristics of the brewery wastewater.

Parameter	Mean	Standard deviation	Range
pH	8.3	0.2	7.9-8.7
Alkalinity (mg $CaCO_3$/L)	21.8	3	19.7-25.2
Turbidity (NTU)	85	6	79-94
COD (mg/L)	597.3	50	454-673
Conductivity (mS/cm)	3.12	0.12	2.44-4.71
Zeta potential (mV)	-38	0.8	-53-(-19)

Turbidity

Turbidity is a measure of the extent to which light is either absorbed or scattered by suspended materials in water. Because absorption and scattering are influenced by both size and surface characteristics of the suspended material, turbidity is not a direct quantitative measurement of suspended solids (Peavy et al., 1985). Most turbidity in water comes from the erosion of colloidal material such as clay, silt, rock fragments, and metal oxides from the soil. Soaps, detergents, and emulsifying agents produce stable colloids that result in turbidity. Microorganisms may also contribute to turbidity.

Measurements. Turbidity is measured using a turbidity meter. It is measured photometrically by determining the percentage of light of a given intensity that is either absorbed or scattered. In the absorption mode, a photometer measures the light intensity on the side of the vial opposite the light source, while in the scattering mode a photometer measures the light intensity at a 90° angle from the light source. Most turbidity meters today work on scattering principle; however, turbidity caused by the dark substances that absorb rather than scatter light should be measured by the absorption technique. Turbidity meter readings are expressed as formazin turbidity units (FTU). The term nephelometry turbidity unit (NTU) is often used to indicate that the test was run according to the scattering principle.

In this study the Hatch 2100N turbidimeter was used following the scattering principle with NTU as unit of measure. The reproducibility of the experimental data by the Hatch 2100N turbidimeter was statistically validated at 99% confidence level (Appendix E).

pH and redox potential

The pH is an important parameter because it affects the efficiency of the flocculant. The inorganic based flocculants are pH sensitive such that they may or may not perform well in the alkaline or acidic region. For example, aluminium sulphate ($Al_2(SO_4)_3$), the most common coagulant in water purification, is most effective between pH ranges of 5.0-7.5; ferric chloride is effective down to 4.5; ferrous sulphate is effective only above 9.5 (Peavy et al., 1985). Furthermore, redox potential can also be used as an indicator for flocculation (Fasemore, 2004). The significance of redox potential measurements when using inorganic coagulants is as follows: as the concentration of hydronium ions (H_3O^+) increases or the concentration of hydroxide ions (OH^-) decreases, the measured potential will increase. Since flocculation involves the formation of hydroxide precipitate, it would lead to the removal of hydroxide ions from solution and an increase in redox potential. Large quantities of hydroxide removed in form of precipitates lead to effective flocculation (sweep flocculation) and thus turbidity is reduced.

Measurements. The pH and redox potentials of the water were measured using the 744 pH meter Metrohm. The redox potential readings were obtained using the Ag/AgCl/3M KCl reference electrode and subsequently converted to the standard hydrogen electrode (SHE) by adding 210 mV (Friis et al., 1998). The measurements were standardised with Metrohm buffer solutions at pH = 4 and 7. The measurement of the pH of treated (or untreated) water was done by decanting it into a beaker and the pH probe was inserted to read off the measurement on the digital screen of the meter. The same pH meter was also used to determine the redox potential of the water which is a measure of the reducing or oxidising ability of water. A negative reading on the digital display indicates an oxidising potential of water, while a positive number display indicates a reducing potential of water. After use the electrode was washed with distilled water and then dried. The electrode was then stored in 3M KCl

solution to prevent desiccation. The pH meter was statistically validated for accuracy at 99% confidence level (Appendix E).

Conductivity

Conductivity is a measure of electrical conductance of water or the mineral content of water. It gives a qualitative measure of the total dissolved solids in water, though only ionised substances contribute to the specific conductance (Peavy et al., 1985). It is important to measure conductivity of water in order to know the likelihood of the water becoming corrosive (Kemmer, 1988).

Measurements. Conductivity was measured in milli Siemens per centimeter (mS/cm) using inoLab Cond 720 meter together with the TetraCon 325 probe.

Alkalinity

Alkalinity is defined as the quantity of ions in water that will react to neutralise hydrogen ions, i.e., it is a measure of the ability of water to neutralise acids. The most common constituents of alkalinity are bicarbonate (HCO_3^-), carbonate (CO_3^{2-}), and hydroxide (OH^-). These compounds result from the dissolution of mineral substances in the soil, CO_2 in the atmosphere, and as products of microbial decomposition of organic material. The relative quantities of alkalinity are pH dependent.

Measurements. Alkalinity measurements are made by titrating the water with an acid and determining the hydrogen equivalent. Alkalinity is then expressed as mg/L of $CaCO_3$. Hydrogen ions from the acid react with the alkali according to the following equations:

$$H^+ + OH^- \rightarrow H_2O \quad (3.1)$$

$$CO_3^{2-} + H^+ \rightarrow HCO_3^- \quad (3.2)$$

$$HCO_3^- + H^+ \rightarrow H_2CO_3 \quad (3.3)$$

The amount of acid required to titrate a sample to pH 4.5 is equivalent to the total alkalinity of the water. If 0.02N H_2SO_4 is used in the titration, then 1 mL of the acid will neutralise 1 mg of alkalinity as $CaCO_3$ (Peavyet al., 1985).

Equation 3.4 shows the formula for calculating the total alkalinity of the water,

$$\text{Total alkalinity in mg/L as } CaCO_3 = \frac{\text{mL of 0.02N } H_2SO_4 \text{ x 1000 mL/L}}{\text{mL of sample}} \quad (3.4)$$

If the volume of 0.02N H_2SO_4 required to reach pH 8.3 end point is known, the species alkalinity can also be determined (Peavy et al., 1985). Because all of the hydroxide and one-half of the carbonate have been neutralised at pH 8.3, the acid required to lower the pH from 8.3 to 4.5 must measure the other one-half of the carbonate, plus all of the original bicarbonate. If P is the amount of acid required to reach pH 8.3 and M is the total amount of acid required to reach 4.5, the following generalisation concerning the forms of alkalinity can be made:

(1) if P = M, all alkalinity is OH^-,
(2) if P = M/2, all alkalinity is CO_3^{2-},
(3) IF P = 0 (i.e., initial pH is below 8.3, all alkalinity is HCO_3^-,
(4) If P < M/2, predominant species are CO_3^{2-} and HCO_3^-,
(5) If P > M/2, predominant species are OH^- and CO_3^{2-}.

Chemical oxygen demand

The extent to which the organic material in water consumes dissolved oxygen is known as chemical oxygen demand (COD). The COD (with units in mg O_2/L) is used as a quick indicator of the presence of organic pollutants in water. A high COD value indicates that there is a high demand of oxygen thus high organic pollutants present.

In the brewery industry, COD is the most important parameter that is required to be in smaller quantities if the water has to be recycled and it needs to be measured at all times (Simate et al., 2011).

Measurements. The procedure followed is as described by Mihelcic (1999). In the test, a sample is added to a 250 mL flask. Also added to the flask is silver sulphate catalyst that ensures complete oxidation of the organic matter; a strong acid (H_2SO_4), dichromate ($Cr_2O_7^{2-}$, a strong oxidizing agent); and mercury sulphate in order to provide Hg^{2+} ions that complexes chloride ions, Cl^-. Chloride ions interfere with the test because it can be oxidised to Cl^0 by dichromate as well as by organic matter. However, the complexed form of Cl^- is not oxidised. Thus, if uncomplexed Cl^- ions are allowed to be oxidized to Cl^0, it will result in higher COD values if not accounted for. The sample and all the reagents are combined and the sample is refluxed for 3 hrs. The concentration of unconsumed yellow hexavalent chromium (or the produced green trivalent chromium) was determined photometrically in a Shimadzu UV-1601 spectrophotometer using a 600 nm wavelength.

From the spectrophotometer reading, the amount of hexavalent chromium reduced to trivalent chromium was determined and this value was related to the amount of organic matter that was oxidized. The reproducibility of the experimental data by the Shimadzu UV-1601 spectrophotometer was statistically validated at 99% confidence level (Appendix E).

3.4.2 Characterisation of carbon nanotubes

A complete characterisation of a CNT sample implies determining, (1) the mass fraction of the sample, (2) their geometric and physical characteristics, and (3) their surface chemical characteristics. This sub-section discusses the tools and methods employed in order to achieve the above mentioned tasks.

Determination of carbon content

Thermogravimetry measurements are carried out using thermogravimetric analysis (TGA) to determine the carbon content of the sample. In this method, the information is primarily derived from the change in weight, which then is indirectly related to the reactivity or oxidation. However, since these methods do not distinguish between the reactants and products, they can be affected by factors other than the true carbon oxidation. For example, the weight of the residual catalyst, its oxidation products, and the adsorption/desorption of other species can bias the results. Consequently, the oxidation of nanotubes should really be studied based on product formation, rather than weight loss (Brukh and Mitra, 2007). For the purpose of this study, though, the TGA was used because of simplicity. The TGA was performed with a TG 209 F1 Libra thermogravimetric analyser (Figure 3.6).



Figure 3.6. Thermogravimetric analyser (TG 209 F1 Libra TGA).

Prior to the analysis the sample was weighed on a balance and then placed in a crucible which was later suspended on the balance of the TGA apparatus. The

temperature was then ramped linearly from about 30°C to 750°C at a rate of 10°C/min. The temperature of the sample was monitored by a PC and the loss in weight of the sample was expressed on a percentage basis.

Determination of the surface area and pore volume of carbon nanotubes

The specific surface area of the CNTs was calculated using the equation developed by Brunauer, Emmett and Teller - the BET equation. The BET equation was developed based on the Langmuir adsorption model and is given in Equations 3.5 and 3.6 (Han, 2002).

$$V = \frac{V_m c P}{(P_0 - P)\left[1 + (c-1)\frac{P}{P_0}\right]} \quad (3.5)$$

or

$$\frac{P}{V(P_0 - P)} = \frac{1}{V_m c} + \frac{c-1}{V_m c}\frac{P}{P_0} \quad (3.6)$$

In Equations 3.5 and 3.6, P is the partial pressure of nitrogen gas; P_0 is the saturated pressure at a given temperature; V is the volume of the gas adsorbed at P (or relative pressure P/P_0); V_m is the volume of the gas adsorbed when all the active sites are covered; and c is a dimensionless constant for the particular gas-solid system (Han, 2002).

From Equation 3.6, a plot of $\frac{P}{V(P_0 - P)}$ versus $\frac{P}{P_0}$ is used to calculate V_m and c as follows: The slope of the generated line, $S = (c-1)/(V_m c)$; and the intercept, $I=1/V_m c$.

From these values, $V_m = 1/(S+I)$ and $c = (I+S)/I$ are calculated. When V_m is known and since A_m (cross-sectional area of adsorbed gas) is 15.8 x 10^{-16} cm^2 for nitrogen, the specific surface area of the solid (e.g., CNTs), S_g, can be calculated (Han, 2002):

$$S_g = \frac{V_m N_{Avog} A_m}{22.4 \text{ x } 10^3 W} (cm^2/g) \quad (3.7)$$

In Equation 3.7, N_{Avog} is the Avogadro's number and W is the weight of the solid used in the measurement.

The measurements on the CNTs were done via the isothermal adsorption/desorption of N_2 in a Tristar 3000 surface area and porosity analyser (Micromeritics instrument). After degassing, the sample material was placed in a vacuum chamber at a constant and very low temperature of liquid nitrogen (-195.6°C). Controlled doses of nitrogen were introduced and the gas adsorbed (or the gas was withdrawn and desorbed) so as to generate adsorption (or desorption) isotherms, and then the specific surface area was determined as described above.

The specific adsorption pore volume of the CNTs was determined from the desorption isotherms using the procedure described by Barrett et al. (1951).

Determination of structural characteristics of carbon nanotubes

This sub-section describes the application of various techniques so as to determine the structural characteristics of CNTs. These techniques include the transmission electron microscopy (TEM), the scanning electron microscopy (SEM), and the Raman spectroscopy.

Electron Microscopy (EM) such as TEM or SEM is a specialised field of science that employs the electron microscope as a tool and uses a beam of electrons to form an image of a specimen (Stadtländer, 2007). In contrast to light microscopy (LM) which uses visible light as a source of illumination and optical (glass) lenses to magnify specimens in the range between approximately 10 to 1,000 times their original size, EM is operated in the vacuum and focuses the electron beam and magnifies images with the help of electromagnetic lenses (Stadtländer, 2007). The electron microscope takes advantage of the much shorter wavelength of the electron (e.g., $\lambda = 0.005$ nm at an accelerating voltage of 50 kV) when compared to the wavelengths of visible light ($\lambda = 400$ nm to 700 nm) (Stadtländer, 2007).

(1) Transmission electron microscopy (TEM, JEOL JEM-4010) was used to depict the morphological and qualitative characteristics of the CNTs including tube dimensions (e.g., diameter and length) and level of aggregation. In TEM images, metal nanoparticles are easily recognised by dark spots, usually covered by graphitic structures (Martinez et al., 2003). Graphitic particles appear like coiled or layered globules, and amorphous carbon constitutes disordered aggregates surrounding the CNTs (Martinez et al., 2003). The TEM has the advantage over SEM in that structures of the specimen can be viewed at higher magnifications (Stadtländer, 2007).

To prepare the samples for TEM analysis, a trace amount of the CNT sample which is usually in powder form and black in colour, was ultrasonically vibrated in ethanol until it was well dispersed and formed a suspension in the solvent. A drop of this suspension was spread on a 300 mesh copper grid (coated with lacey carbon thin film) and allowed to dry. After drying the grid was loaded into the instrument for the TEM measurements.

(2) The scanning electron microscopy (SEM, Hitachi S-4300) was used to generate micrographs for comparing the surface morphologies of CNTs after the coagulation/flocculation process. The SEM technique provides a large depth of field, which means, the area of the sample that can be viewed in focus at the same time is actually quite large (Stadtländer, 2007). The SEM has also the advantage that the range of magnification is relatively wide allowing the investigator to easily focus in on an area of interest on a specimen that was initially scanned at a lower magnification (Stadtländer, 2007). Furthermore, the three-dimensional appearing images may be more appealing to the human eye than the two-dimensional images obtained with a TEM (Stadtländer, 2007).

A sample for the SEM was prepared by placing a few particles of the CNT powder on top of aluminum stub holder using wet pasty graphite as mounting media and was left for about 24 hours to dry. The sample was then placed into the SEM chamber with the aid of a sample exchange rod. The SEM images were taken under specific magnifications using working distance of either 39 or 48 mm and 15 keV voltage.

(3) Raman spectroscopy (Renishaw micro-Raman 2000) using the standard 514.5 nm line of an argon ion laser was used to provide the structural characteristics of the CNTs and an indication of the degree of crystallinity. The operation can also be used to determine whether the nanoparticles produced are single-walled or multi-walled or double-walled CNTs (Costa et al., 2008). The CNTs usually have four main characteristic bands in Raman spectra, (1) the G-mode, in the region of 1500-1600 cm^{-1} (Korneva, 2008; Osswald et al., 2007), (2) the D-mode, which appears from 1100-1500 cm^{-1}, (Potgieter-Vermaak et al., 2011), (3) the radial breathing mode (RBM) in the region of 100-400 cm^{-1} (Korneva, 2008; Osswald et al., 2007), and (4) the D'-mode at ~ 1615 cm^{-1} (Korneva, 2008; Osswald et al., 2007).

The G-band originates from the tangential in-plane stretching vibrations of the carbon–carbon bonds within the graphene sheets (Osswald, 2007). The RBM mode is a radial breathing mode; it is characteristic only for single-walled nanotubes. In most cases, multi-walled nanotubes do not show this signal, but show the D'-band, which is assigned to the in-plane vibrations of graphite. The D-band is a double resonance mode and appears when nanotubes have structural defects or amorphous carbon on the walls. The ratio of the D-band intensity to the G-band intensity, $R = I_D/I_G$, usually serves as a measurement of the disordered sites on CNTs walls, serving as the indicator of the level of the covalent functionalisation of the CNTs. In other words, the structural quality of a CNT sample can be measured by the ratio I_D/I_G between the intensities of peaks D and G (Mhlanga, 2009). The higher the ratio, the more disordered carbon is present in a sample. The D'-mode also serves to show the disorder and defects of graphitic walls (Korneva, 2008; Osswald et al., 2007).

For the Raman spectroscopy analysis, CNTs were dispersed in ethanol and one drop of the dispersion was placed on a degreased silicon wafer or glass slide and air-dried before measurements were taken.

Identification of surface functional groups

The existence or absence of functional groups on the surface of the CNTs was identified using the Fourier transform infrared (FT-IR) absorption spectrometer shown in Figure 3.7.

The FT-IR spectroscopy method is based on the principle of infrared spectroscopy. Infrared spectrum measures the quantity of radiation absorbed versus its frequency. When CNTs are submitted to an infrared radiation, the difference of charge state between carbon atoms induces the formation of an electric dipole; the appearance of these dipoles generates signals that are detected (Osorio et al., 2008). Atoms involved

in stretch and bending vibrations usually determine the frequencies of absorption (Osorio et al., 2008).



Figure 3.7. Fourier transform infrared absorption spectroscopy (Bruker Tensor 27).

Thus, an infrared spectrum represents a fingerprint of a sample with absorption peaks which correspond to the frequencies of vibrations between the bonds of the atoms making up the material (TNC, 2001). Since each different material is a unique combination of atoms, no two compounds can produce the exact same infrared spectrum (TNC, 2001). Therefore, infrared spectroscopy results in a positive identification (qualitative analysis) of every different kind of material. In addition, the size of the peaks in the spectrum is a direct indication of the amount of material present (TNC, 2001). The FT-IR has been successfully applied for nanomaterial characterisation (Baudot et al., 2010).

For the FT-IR measurements, the nanotube material was first ultrasonicated in ethanol. Several drops of the solution were then deposited from solution onto ZnSe

substrates. The solvent from each drop was allowed to evaporate before the next drop was added. The spectral resolution for the IR measurements was 4 cm^{-1}.

Determination of amounts of surface acidic/basic groups

The Boehm's titration method (Boehm, 1966; Boehm, 1994) was used to quantitatively evaluate the attached functional groups on the surfaces of CNT after functionalisation. As described by Simate et al. (2012a), the procedure included the following typical steps: (1) One hundred milligrams of the CNT was placed in a 100 mL flask containing 50 mL of 0.1M NaOH and 0.1M HCl solutions. All the solutions were supplemented with 0.1M NaCl so as to maintain a desirable conductivity (Lin et al., 2001). (2) The flask was sealed and shaken for 48 hours, and then filtered through a 0.45μm Nylon fibre filter and 10 mL of each filtrate was pipetted. (3) The excess acid and base was titrated with 0.1M NaOH and 0.1M HCl, respectively, to a pH value of 7.0. (4) The concentration of acidic sites was determined from the amount of NaOH that reacted with the CNTs; while the concentration of the basic sites was determined from the amount of HCl that reacted with the CNTs.

Determination of the pH of the point of zero charge

Important properties of solid/liquid systems are influenced by the electric charges on the particle surface. As mentioned in sub-section 2.2.2, when immersed in an electrolyte solution, a charged particle will be surrounded by ions of opposite sign (counterions) so that, in overall the system has no net charge. The surface charge depends greatly on the pH of the solution, with positive values at low pH and negative values at high pH. There is a characteristic pH value at which the surface charge is zero, corresponding to equal number of positive and negative surface groups. This pH value required to give zero net surface charge is designated the point of zero charge (pzc) or isoelectric point (IEP).

The pH of the pzc was determined using the procedure of mass titration (Noh and Schwarz, 1988; Noh and Schwarz, 1990). This method was chosen because of its accuracy, and that the widely used acid/base titration method has limited success for carbons (Noh and Schwarz, 1990).

To measure the pzc of the CNT samples, three different solution pH were prepared using 0.1M HNO_3 and 0.1M NaOH (e.g., pH = 3, 6, 11). The 0.1M $NaNO_3$was used as background electrolyte. For each initial pH, six containers were filled with 100 mL of solution, and different amounts of CNT samples were added (e.g., 0.05%, 0.1%, 0.5%, 1%, 5%, and 10% by weight/volume of solution) followed by magnetic stirring. The equilibrium pH was measured after 24 hrs. Subsequently, the graphs of equilibrium pH (y-axis) after 24 hrs as a function of mass fraction of carbon in solution (x-axis) were plotted for each initial pH. A plateau is obtained in this plot of pH versus mass fraction. The average value of the three asymptotic pH values (i.e., asymptote to x-axis) is taken as the pH of the pzc (Simate et al., 2012a).

Determination of surface charges

As already discussed in sub-section 2.2.2, the particles in a colloidal suspension or emulsion usually carry an electrical charge. Several methods have been developed for measuring the particle charge, but one of the most effective method, a process called electrophoresis, is to apply an electric field to the suspension and to measure how fast the particles move as a result. The bigger the charge they carry, the faster the particles will move.

In such an experiment not all of the particle charge is usually observed because the electric field pulls the particle in one direction while it is also being pulled by the counter-ions in the opposite direction. Some of the counter-ions will move with the

particle (e.g., those within the Stern layer) so the measured charge will be a net charge.

The electrostatic potential near the particle surface is shown in Figure 3.8. It changes very quickly (and linearly) from its value at the surface through the first layer of counter-ions and then changes more or less exponentially through the diffuse layer. In Figure 3.8, the junction between the bound charges and the diffuse layer is marked by the broken line. The surface, which separates the bound charge from the diffuse charge around the particle, marks where the solution and the particle move in opposite directions when an external field is applied. It is called the surface of shear or the slip surface. The electrostatic potential on that surface is called the zeta potential and it is that potential which is measured, when one measures the velocity of the particles in a direct current electric field.

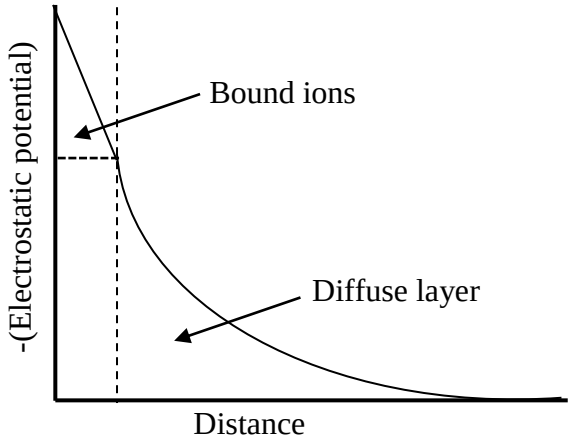


Figure 3.8.Electrostatic potential near a negatively charged spherical particle.

Thus, the zeta potential is a function of the surface charge which develops when any material is placed in a liquid. It is a very good index of the magnitude of the electrostatic repulsive interaction between particles. Generally, the higher the absolute value of the zeta potential, the more stable the system will be.

Measurements. The zeta potential on the CNT samples was measured as a function of pH using the Zetasizer Nanoseries Nano ZS (Malvern Instruments) which is shown in Figure 3.9. With the zeta potential measured as a function of pH, pzc of the CNT samples may be determined (Pillay et al., 2009). Zeta potential was measured four times per sample and an average zeta potential value was used. The reproducibility of the experimental data by the Zetasizer Nanoseries Nano ZS was statistically validated at 99% confidence level (Appendix E).



Figure 3.9. Zetasizer Nanoseries Nano ZS (Malvern Instruments).

Determination of dispersion stability of carbon nanotubes

The CNTs tend to cohere in aqueous solutions due to their high energy and lack of chemical affinity for the dispersing chemicals (Lee et al., 2007). This lack of dispersion (or solubility) of CNTs in either water or organic solvents has been a limitation for the practical application of these unique materials (Matarredona, 2003; Tasis, 2006). Nevertheless, as discussed in sub-section 2.4.4, the lack of dispersion of CNTs is advantageous in water treatment. This is because in the insoluble state, CNTs can easily be retained and separated from treated water using separation

processes such as membrane filtration and ultracentrifugation, thus preventing the human health risks arising from drinking water contaminated with CNTs (Simate et al., 2012b).

The two methods that may be used to establish the dispersion (or solubility) of CNTs are outlined below.

Method 1. The tests for the dispersion (or solubility) of CNTs used in this study were prepared at room temperature by gently mixing 5 mg of CNTs in 100 mL of water with a magnetic stirrer (no sonication) for 24 hrs. This was followed by centrifugation at 3400 rpm for 25 minutes (Matarredona, 2003). The concentration of the CNTs in the supernatant was quantified by the UV-visible absorption spectrophotometer at a wavelength of 600 nm (Vuković, 2009), and using the specific extinction coefficient (ε) of CNTs at 600 nm, ε_{600} = 26.05 cm^2/mg, in the Beer-Lambert law (Bahr et al., 2001) which states that,

$$A = \varepsilon bc \qquad (3.8)$$

where A is the absorbance (formerly the 'optical density'), ε is the absorption coefficient (formerly, and still widely, the 'extinction coefficient'), b is the path length, and c is the concentration of absorbing species (Atkins, 1994).

The UV-visible absorption was chosen amongst other methods because it is rapid and versatile (Green, 2010).

Method 2. Water samples of different pHs were prepared by using 0.1M HNO_3 and 0.1M NaOH. Approximately 5 mg of CNTs was then added to 100 mL of water samples of different initial pHs followed by magnetic stirring for 24 hours. To quantitatively examine the solubility (or dispersion) of the CNTs in an aqueous

solution, zeta potential of the solution was measured as a function of initial pH (Shieh et al., 2010). The Zetasizer Nanoseries Nano ZS (Malvern Instruments) shown in Figure 3.8 was used for measuring the zeta potentials of solutions.

3.5 Data Analysis

The data collected were analysed using different analytical techniques as described in the previous sections and sub-sections of this chapter. The data was used to develop relationships between output variables (e.g., residual turbidity of wastewater, residual COD of wastewater, weight of CNT produced, etc) and the parameters tested (e.g., pH of wastewater, temperature of reactor, dosage of coagulant, etc). These relationships and the observed results are discussed in the subsequent chapters of this thesis.

Some of the experimental data in Chapters 5 and 6 were statistically analysed using STATAS 12.1 software (StataCorp LP, College Station, Texas 77845 USA). The statistical significance of the experimental results was analysed by the analysis of variance (ANOVA) using Fisher's *F*-test and Student's *t*-test. The significance level (α) was 0.05 (i.e., 95% confidence level), and the hypotheses for ANOVA are as follows:

(1) The null hypothesis states that 'all means of the sample population are equal'
H_0: $\mu_1 = \mu_2 = \ldots = \mu_k$
(2) The alternative hypothesis states that 'at least one of the means of the sample polulation differs from all of the other'
H_A: Not $\mu_1 = \mu_2 = \ldots = \mu_k$ or the means are not all equal

In addition to the coefficient of regression, the isotherm models were also evaluated by an error function (F_{error}), which compared the differences in the mount of

adsorbate uptaken by the adsorbent using the models to the actual uptake measured experimentally (Arenas et al., 2007). The reproducibility of the experimental data by various equipment (e.g., pH meter, spectrophotometer, turbidimeter, and zetasizer) was statistically validated at significance level (α) of 0.01 (Appendix E). Error bars were also deplayed to represent the degree of uncertainty in experiemental data.

3.6 Summary

This chapter presented and discussed the materials and methods used in the study. In particular, the focus of the chapter was on the following activities that constitutes the laboratory testing aspect of the study:

- Collection and preparation of brewery wastewater.
- Synthesis and functionalisation of CNTs.
- Characterisation of both the brewery wastewater samples and the CNTs.
- Experimental procedures.
- Data analysis and interpretation.

References

American Water Works Association (AWWA) and American Society of Civil Engineers (ASCE), 1998. Water Treatment Plant Design. McGraw-Hill, New York.

Atkins, P. W., 1994. Physical Chemistry. 5th Edition. Oxford University Press, Oxford.

Arenas, L. T., Lima, E. C., dos Santos, A. A., Vaghetti, J. C. P., Costa, T. M. H., Benvenutti, E. V., 2007. Use of statistical design of experiments to evaluate the sorption capacity of 1,4-diazoniabicycle (2.2.2) octane/silica chloride for

Cr (VI) adsorption. *Colloids and Surfaces* A: *Physicochemical and Engineering Aspects* 297, 240-248.

Aronino, R., Dlugy, C., Arkhangelsky, E., Shandolov, S., Oron, G., Brenner, A., Gitis, V., 2009. Removal of viruses from surface water and secondary effluents by sand filtration. *Water Research* 43, 87-96.

Berrett, E.P., Joyner, L.G., Halenda, P.P., 1951. The determination of pore volume and area distributions in porous substances. I. computations from nitrogen isotherms. *Journal of American Chemical Society* 73, 373-380.

Bahr, J. L., Mickelson, E. T., Bronikowski, M. J., Smalley, R. E., Tour, J. M., 2001. Dissolution of small diameter single-wall carbon nanotubes in organic solvents? *Chemical Communications* 2, 193-194.

Baudot, C., Tan, C. M., Kong, J. C., 2010. FTIR spectroscopy as a tool for nano-material characterization. *Infrared Physics and Technology*, 53 434-438.

Boehm , H.P., 1966. Chemical identification of surface groups. In: Eley, D.D., Pines, H., Weisz, P. B. (Editors), Advances in Catalysis 16. Academic Press, New York, pp. 179-287.

Boehm, H. P, 1994. Some aspects of the surface chemistry of carbon blacks and other carbons. *Carbon* 32 (5), 759-769.

Brukh, R., Mitra, S., 2007.Kinetics of carbon nanotube oxidation. *Journal of Materials Chemistry* 17, 619-623.

Clesceri, L. S., Greenberg, A. E., Eaton, A. D., 1998 (Editors).Standard Methods for the examination of water and wastewater, 20th edition. American Public Health Association, Washington DC.

Costa, S., Borowiak-Palen, E., Krusyñska, M., Bachmatiuk, A., Kaleńczuk, R.J., 2008. Characterisation of carbon nanotubes by Raman spectroscopy. *Materials Science* – Poland 26 (2), 433-441.

Fasemore, O. A., 2004. The flocculation of paint wastewater using inorganic salts. MSc Dissertation, University of the Witwatersrand, Johannesburg, South Africa.

Friis, E. P., Andersen, J. E. T., Madsen, L. L.., Bonander, N., Møiler, P., Ulstrup, J., 1998. Dynamics of Pseudomonas aeruginosaazurin and its Cys3Ser mutant at single-crystal gold surfaces investigated by cyclic voltammetry and atomic force microscopy. *Electrochimica Acta* 43 (9), 1114-1122.

Gitis, V., Freger, V., Haugth, R. C., Clark, R. M., 2005. Removal of cryptosporidium parvum oocysts by rapid sand filtration with ballasted flocculation-filtration and intermediate downwashes. *Acta Hydrochimica et Hydrobiologica* 33 (4), 355-364.

Green, M. J., 2010. Analysis and measurement of carbon nanotube dispersions: nanodispersion versus macrodispersion. *Polymer International* 59, 1319-1322.

Han, K. N., 2002. Fundamentals of Aqueous Metallurgy. Society for Mining, Metallurgy, and Exploration Inc, Colorado.

Iyuke, S. E., 2007. A process for production of carbon nanotubes. International application published under the Patent Cooperation Treaty (PCT), World Intellectual Property Organisation, International Bureau, WO 2007/026213 A1.

Iyuke, S. E., Simate, G. S., 2011. Synthesis of carbon nanomaterials in a swirled floating catalytic chemical vapour deposition reactor for continuous and large scale production, In: Naraghi. M. (Editor), Carbon Nanotubes – Growth and Applications. In-Tech, Rijeka, pp. 35-58.

Kemmer, F.M., 1988 (Editor). The Nalco Water Handbook, 2nd edition. McGraw-Hill, New York.

Korneva, S., 2008. Functionalisation of carbon nanotubes. PhD Thesis, Drexel University, USA.

Lee, J., Kim, M., Hong, C. K., Shim, S. E., 2007. Measurement of the dispersion stability of pristine and surface-modified multiwalled carbon nanotubes in various nonpolar and polar solvents. *Measurement Science and Technology* 18, 3707-3712.

Li, Y. H., Xu, C., Wei, B., Zhang, X., Zheng, M., Wu, D., Ajayan, P. M., 2002. Self-organized ribbons of aligned carbon nanotubes. *Chemistry of Materials* 14, 483-485.

Li, Z., Dervishi, E., Xu, Y., Saini, V., Mahmood, M., Oshin, O.D., Biris, A. R., Biris, A. S., 2009. Carbon nanotube growth on calcium carbonate supported molybdenum-transition bimetal catalysts. *Catalysis Letters* 131, 356-363.

Liew, A. G., Noor, M. J. M. M., Muyibi, S. A., Fugara, A. M. S., Muhammed, T. A., Iyuke, S. E., 2006. Surface water clarification using M. oleifera seeds. *International Journal of Environmental Studies* 63 (2), 211-219.

Lin, C-F., Liu, S-H., Hao, O. J., 2001. Effect of functional groups of humic substances on UF performance. *Water Research* 35 (10), 2395-2402.

Martinez, M.T., Callejas, M. A., Benito, A. M., Cochet, M., Seeger, T., Ansón, A., Schreiber, J., Gordon, C., Marhic, C., Chauvet, O., Fierro, J. L. G., Maser, W. K., 2003. Sensitivity of single wall carbon nanotubes to oxidative processing: structural modification, intercalation and functionalisation. *Carbon* 41, 2247-2256.

Matarredona, O., Rhoads, H., Li, Z., Harwell, J. H., Balzano, L., Resasco, D. E., 2003. Dispersion of single-walled carbon nanotubes in aqueous solutions of the anionic surfactant NaDDBS. *Journal of Physical Chemistry* B 107, 13357-13367.

Mhlanga, S. D., 2009. Synthesis and study of carbon nanotubes and carbon spheres. PhD Thesis, University of the Witwatersrand, Johannesburg, South Africa.

Mihelcic, J. R., 1999. Fundamentals of Environmental Engineering. John Wiley & Sons Inc., Hoboken.

Morrison, R. T., Boyd, R. N., 1992. Organic Chemistry. Prentice-Hall, Inc., New Jersey.

Noh, J. S., Schwarz., 1988. Estimation of the point of zero charge of simple oxides by mass titration. *Journal of Colloid and Interface Science* 130 (1), 157-164.

Noh, J. S., Schwarz., 1990. Effect of HNO_3 treatment on the surface acidity of activated carbon. *Carbon* 28 (5), 675-682.

Nozaic, D.J., Freese, S.D., Thompson, P., 2001.Long terme xperience in the use of polymeric coagulants at Umgeni water. *Water Science and Technology* 1 (1), 45-50.

Osswald, S., Havel, M., Gogotsi, Y., 2007. Monitoring oxidation of multiwalled carbon nanotubes by Raman spectroscopy. *Journal of Raman Spectroscopy* 38, 728-736.

Osorio, A. G., Silveira, I. C. L., Bueno, V. L., Bergmann, C. P., 2008. H_2SO_4/HNO_3/HCl -functionalization and its effect on dispersion of carbon nanotubes in aqueous media. *Applied Surface Science* 255, 2485-2489.

Peavy, H. S., Rowe, D. R., Tchobanoglous, G., 1985. Environmental Engineering. McGraw-Hill Inc., New York.

Pillay, K., Cukrowska, E. M., Coville, N. J., 2009. Multi-walled carbon nanotubes as adsorbents for the removal of parts per billion levels of hexavalent chromium from aqueous solution. *Journal of Hazardous Materials* 166, 1067-1075.

Potgieter-Vermaak, S., Maledi, N., Wagner, N., van Heerden, J. H. P., van Grieken, R., Potgieter, J. H., 2011. Raman spectroscopy for the analysis of coal: a review. *Journal of Raman Spectroscopy* 42, 123-129.

See, C. H., Harris, A. T., 2008. $CaCO_3$ supported Co-Fe catalyst for carbon nanotube synthesis in fluidised bed reactors. *American Institute of Chemical Engineers* 54(3), 657-664.

Shieh, Y. T., Wu, H. M., Twu, Y. K., Chung, Y. C., 2010. An investigation on dispersion of carbon nanotubes in chitosan aqueous solutions. *Colloid and Polymer Science* 288, 377-385.

Simate, G. S., Iyuke, S. E., Ndlovu, S., Yah, C. S., Walubita, L.F., 2010. The production of carbon nanotubes from carbon dioxide: challenges and opportunities. *Journal of Natural Gas Chemistry* 19 (5), 453-460.

Simate, G. S.., Cluett, J., Iyuke, S. E., Musapatika, E. T., Ndlovu, S., Walubita, L. F., Alvarez, A. E., 2011.The treatment of brewery wastewater for reuse: State of the art. *Desalination* 273 (2-3), 235-247.

Simate, G. S., Iyuke, S. E., Ndlovu, S., Heydenrych, M., 2012a. The heterogeneous coagulation and flocculation of brewery wastewater using carbon nanotubes. *Water Research* 46 (4), 1185-1197.

Simate, G. S., Iyuke, S. E., Ndlovu, S., Heydenrych, M., Walubita, L. F., 2012b. Human health effects of residual carbon nanotubes and traditional water treatment chemicals in drinking water. *Environment International* 39 (1), 38-49.

Stadtländer C. T. K. H, 2007. Scanning electron microscopy and transmission electron microscopy of mollicutes: challenges and opportunities. In: Mendez,-Vilas, A., Diaz, J. (Editors), Modern Research and Educational Topics in Microscopy, Series 2. Formatex, Badajoz, pp.122-131.

Suzuki, M., Chihara, K., 1988. Heterogeneous coagulation of organic colloid and powdered activated carbon. *Water Research* 22 (5), 627-633.

Tasis, D., Tagmatarchis, N., Bianco, A., Prato, M., 2006.Chemistry of carbon nanotubes. *Chemical Reviews* 106 (3), 1105-1136.

Thermo Nicolet Corporation (TNC), 2001. Introduction to fourier transform infrared spectrometry. Thermo Nicolet Corporation, Madison.

Vuković, G., Marinković, A., Obradović, M., Radmilović, V., Colić, M., Aleksić, R., Uskoković, P. S., 2009. Synthesis, characterisation and cytotoxicity of surface amino-functionalised water-dispersible multi-walled carbon nanotubes. *Applied Surface Science* 255, 8067-8075.

Williams, G. J., Sheikh, B., Holden, R. B., Kouretas, T. J., Nelson, K. L.., 2007. The impact of increased loading rate on granular media, rapid depth filtration of wastewater. *Water Research* 41, 4535-4545.

Xu, X-J., Huang, S-M., 2007. Carbon dioxide as a carbon source for synthesis of carbon nanotubes by chemical vapour deposition. *Materials Letters* 61, 4235-4237

Yah, C.S., Iyuke, S.E., Simate, G.S., Unuabonah, E.I., Bathgate, G., Matthews, G., Cluett, J.D., 2011a. Continuous synthesis of multi-walled carbon nanotubes from xylene using the swirled floating catalyst chemical vapour deposition technique. *Journal of Materials Research* 26 (5), 640-644.

Yah, C.S., Simate, G.S., Moothi, K., Maphutha, S. K., Iyuke, S.E., 2011b. Synthesis of large carbon nanotubes from ferrocene: The chemical vapour deposition technique. *Trends in Applied Sciences Research* 6 (11), 1270-1279.

CHAPTER FOUR

SYNTHESIS OF CARBON NANOTUBES FROM CARBON DIOXIDE

"*Gloom and despondency have never defeated adversity. Trying times need courage and resilience. Our strength as a people is not tested during the best of times. We should never become despondent because the weather is bad nor should we turn triumphalist because the sun shines".*

- Thabo Mbeki (Former President of South Africa)

4.1 Introduction

Until recently, the synthesis of CNTs from CO_2 was mainly through the use of supercritical CO_2 ($scCO_2$) in autoclaves or sealed quartz tubes (Motiei et al., 2001; Lou et al., 2003; Zheng et al., 2005; Lou et al., 2006). However, the use of $scCO_2$ requires abnormally high pressure (Simate et al., 2010). For example, the pressure is autogenic depending on the amount of reactants added and reaction temperature (Qian et al., 2006), therefore, proper equipment that can withstand pressures up to 10 kbar is required (Simate et al., 2010). Several other studies also showed that CNTs can be synthesized by passing CO_2 over oxygen deficient ferrites in a furnace (Khedr and Farghali, 2005; Khedr et al., 2006, 2007, 2008). However, the use of metal bearing ferrites has been limited to the conditions where reduction of the catalyst is possible. Furthermore, these catalysts are used while fresh to avoid reoxidation (Simate et al., 2010). The use of freshly reduced catalysts together with the need for an inert environment during their synthesis requires a proper control of the process parameters (Simate et al., 2010).

In the recent past, the use of a CVD reactor for synthesizing CNTs from CO_2 was introduced (Xu and Hung, 2007; Maphutha, 2009; Moothi, 2009). In a CVD, precursor gases (often diluted in carrier gases) are delivered into the reaction chamber at an appropriate temperature. As the gases pass over or come into contact with a heated substrate, they react or decompose forming a solid phase which is deposited onto the substrate. However, other types of CVDs do not use any form of substrates for the synthesis of CNTs. As stated in sub-section 2.4.1, CVD is the only promising methodology for the synthesis of CNTs on a reasonably large-scale. What is now needed is to study the effect of parameters that affect the synthesis of CNTs from CO_2. This would help to understand and optimise the large scale synthesis of CNTs from CO_2.

Therefore, the study of the effect of reactor temperature as well as the concentration and flow rate of CO_2 is the focus of this Chapter. References should also be made to Appendix F.

The details of the equipment, experimental setup and procedures followed during the synthesis of CNTs are outlined in sub-section 3.3.1. Some of the analytical techniques outlined in sub-section 3.4.2 were used to characterise the CNTs synthesized.

4.2 Results and Discussion

Once CNTs have been synthesized it is important that they are identified as such. Therefore, sub-section 4.2.1 discusses this aspect. The results of the factors that govern the general synthesis of CNTs are discussed in the subsequent sub-sections.

4.2.1 Identification of carbon nanotubes

The morphologies of the synthesized CNTs were observed from TEM images as shown in Figure 4.1. The TEM image in Figure 4.1 show hollow structures with inner diameters and length of several nanometers which confirm the presence of CNTs. In fact, these are the characteristic physical features of CNTs as observed by other researchers (Afolabi et al., 2007).

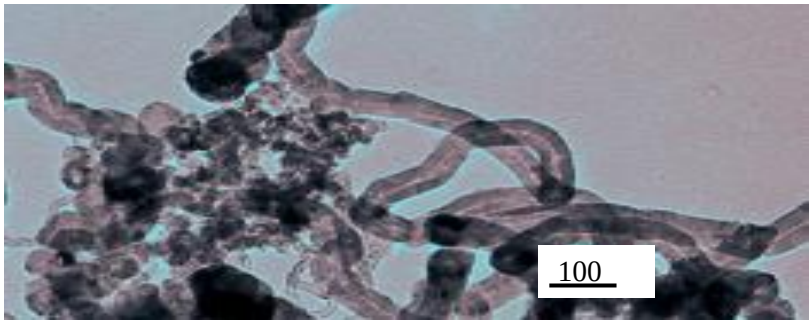


Figure 4.1. TEM image of CNTs produced at 800°C.

Figure 4.2 shows the Raman spectra of the CNTs. As discussed in sub-section 3.4.2, the basis of most studies involving the Raman spectra revolves around the assignment of the G-band (graphitic, ~1580 cm^{-1}) to crystalline graphite and any other bands, called D-bands (disorder, varies from 1100 to 1500 cm^{-1}) to any type of structural disorder in the graphitic structure (Potgieter-Vermaak et al., 2011). However, the other band that is characteristic only for SWCNTs called radial breathing mode (RBM) lies in the region of 100-400 cm^{-1} (Korneva, 2008; Osswald et al., 2007).

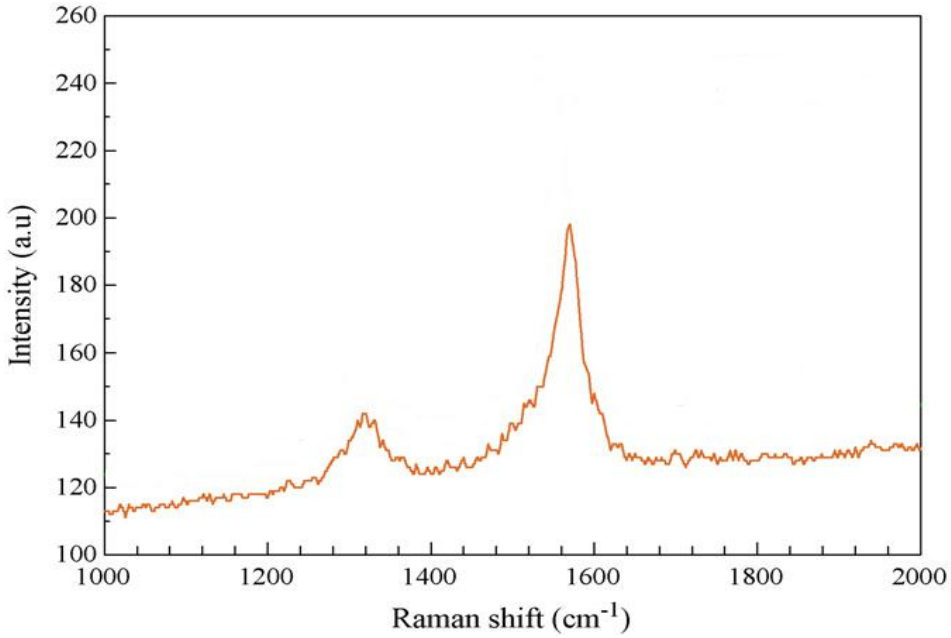


Figure 4.2. Raman spectrum of CNTs produced at 800°C.

Figure 4.2 shows two significant peaks at 1358 cm^{-1} and 1582 cm^{-1}, representing the D-band and G-band, respectively. As stated already, the G-band represents the graphitisation degree of the nanotube structure while the D-band describes the degree of structural defects; including amorphous (non-graphitic) carbon adhered on the nanotube structure (Patole et al., 2008; Lee et al., 2010). The absence of the RBM in the Raman spectra implies that the CNTs produced were multi-walled.

The I_D/I_G ratio, which shows the relative intensity of the D- and G-bands of a Raman spectrum (Lee et al., 2010), was found to be 0.71. The I_D/I_G ratio reveals the degree of disorder in the graphite sheets and it can be used as a measure of the degree of graphitisation and crystallinity of the as-produced CNTs (Tsoufis et al., 2007; Lee et al., 2010). In other words, the extent of carbon-containing defects can be evaluated by the intensity ratio of D- and G-bands (I_D/I_G) (Lu and Su, 2007). In this study, the relatively small value of the I_D/I_G ratio of 0.71 suggests that the as-produced CNTs exhibit a remarkable crystallinity. This implies that the raw CNTs have smoother carbon surfaces and less structural defects. The higher purity of CNTs produced from CO_2 as compared to those produced from gaseous hydrocarbons has also been reported by Xu and Huang (2007).

4.2.2 Effect of the concentration of carbon dioxide

For the figure discussed in this sub-section, reference should be made to the experimental data in Appendix B (Table B2). The results are an average of the runs conducted under similar experimental conditions.

The experimental production rates of CNTs at different concentrations of CO_2 at a temperature of 800°C are shown in Figure 4.3. The temperature of 800°C was chosen because it had the highest CNT production rate as shown in Figure 4.5.

From Figure 4.3, it can be seen that initially the production of CNTs increased with the concentration of CO_2 up to a concentration of about 5000 ppm. Thereafter, as seen from the figure, the gradient of the plot reduced with an increase in CO_2 concentration. This means that the rate of production per unit quantity of CO_2 reduced. This trend was also observed from other similar studies by other researchers (Andrews et al., 1999; Liu et al., 2002; Abbaslou et al., 2010), thus supporting the results of this study. These studies also found that as carbon concentration of the

carbon source increases, the CNT yield decreases significantly. It was deduced from these results that at higher carbon concentrations, the rate of formation of adsorbed surface carbon exceeds the diffusion rate leading to formation of monolayer or multiple layers of carbon on the catalyst particles (Abbaslou et al., 2010). This phenomenon stops further surface reactions resulting in the confinement of catalyst (Abbaslou et al., 2010). In the case of lower carbon concentration in the gas phase, the rate of formation of adsorbed surface carbon is lower than or equal to the rate of diffusion and precipitation of carbon in the form of CNTs, resulting in continuous production process (Abbaslou et al., 2010).

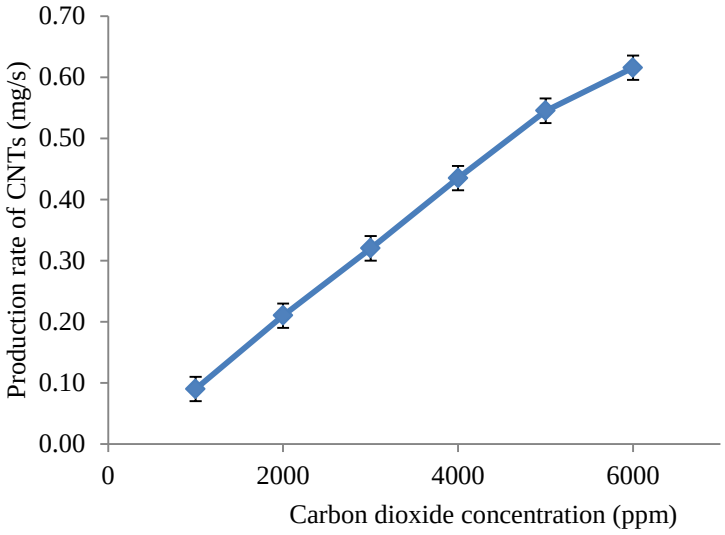


Figure 4.3. Effect of concentration of CO_2 on the production rate of CNTs at 800°C.

4.2.3 Effect of the volumetric flow rate of carbon dioxide

For the figure discussed in this sub-section, reference should be made to the experimental data in Appendix B (Table B3). The results are an average of the runs conducted under similar experimental conditions.

Figure 4.4 shows the effect of the volumetric flow rate of CO_2 on CNT production rate, for a reactor temperature of 800°C after a reaction time of 45 minutes. It can be seen from Figure 4.4 that initially an increase in flow rate increased the rate of CNT production. However, at higher flow rates the rate of production of CNT reduced. This is because a higher volumetric flow rate reduces the residence time for the reaction, leading to the production of lower number of carbon atoms during the reaction.

These results agree with the findings by Singh et al. (2003) and Toussi et al. (2011). They found that higher flow rate of the carbon source led to the production of fewer CNTs. In contrast, Vallés et al. (2009) found that higher carbon feed stock supply rates led to increased CNTs yields.

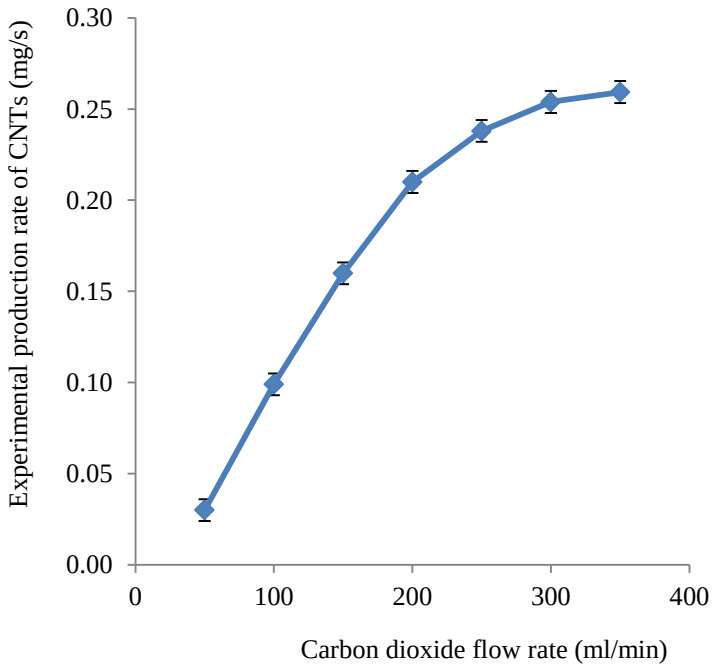


Figure 4.4. Effect of volumetric flow rate of CO_2 on the production rate of CNTs at 800°C.

4.2.4 Effect of reactor temperature

For the figure discussed in this sub-section, reference should be made to the experimental data in Appendix B (Table B1). The results are an average of the runs conducted under similar experimental conditions.

Temperature is a very important parameter that affects both the decomposition of CO_2 (Equation 4.1) and the disproportionation of CO (Equation 4.2). The effect of temperature on the CNT production rate is shown in Figure 4.5.

$$2CO_2 \rightarrow 2CO + O_2 \quad (4.1)$$

$$2CO \rightarrow C + CO_2 \quad (4.2)$$

Figure 4.5 shows that the production of CNT only occurs between 750-840°C. Initially, the rate of production increased with an increase in temperature up to about 800°C, and then, it reduced drastically. An increase in temperature in the first region implies that there was enough heat to effect the decomposition of CO_2 leading to the formation of CNTs from the CO disproportionation reaction. However, at higher temperatures the production rates of CNTs reduced until it finally ceased at approximately 850°C. These results may be explained from CO_2 decomposition, Boudouard reaction requirements, and the kinetics of carbon diffusion as discussed below.

The CO disproportionation reaction (Equation 4.2) has two main limitations, namely: (1) at lower temperatures the reaction is limited kinetically, and (2) at higher temperatures it is limited thermodynamically (Nasibulin et al., 2006). In fact, previous studies have shown that kinetic and thermodynamic factors limit the effective CO disproportionation reaction to a temperature range of 520-800°C at atmospheric pressure (Moisala et al., 2003); and equilibrium favours the right side at

temperatures below 700°C (Boehm, 1973). The observations by Moisala et al. (2003) and Boehm (1973) agree with the findings of this study which showed an increase in CNT production for temperatures lower than about 800°C. However, attainment of equilibrium is possible only in the presence of catalysts, mainly iron, cobalt, and nickel. Even then, temperatures in excess of 400°C are needed for measurable reaction rates, with maximum rates observed around 550°C (Boehm, 1973). Furthermore, previous studies have also shown that although the conversion of CO may be fast at low temperatures, the CNT yield is very low (Chen et al., 1997). This is because plenty of carbon that form on the catalyst surface is not able to be transferred away in time due to the relatively low rate of carbon diffusion in the bulk of the metal catalyst particles at low temperatures, and thus, block the active catalyst surface leading to a decrease in activity (Chen et al., 1997).

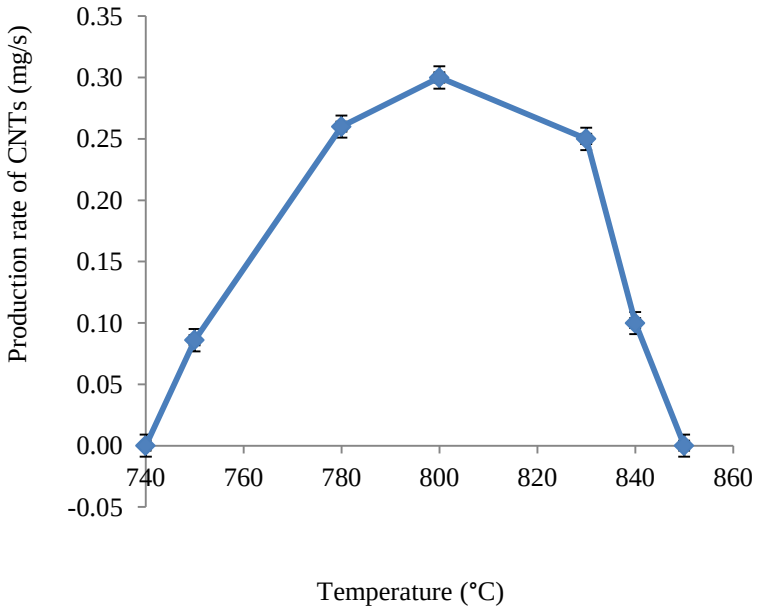


Figure 4.5. Effect of temperature on the production rate of carbon nanotubes at 400 ml/min carbon dioxide.

In summary, CO_2 decomposition is an endothermic reaction with CO formation being favoured at high temperatures. By contrast, CO disproportionation is an exothermic reaction, such that both the CO conversion and carbon formation decline as the reaction temperature is increased. In addition, at high temperatures, CO_2 as a mild oxidising agent can react with the graphitic layers of the CNTs, leading to the erosion of CNTs and thus, a low yield is achieved (Tsang et al., 1993). No oxidation reactions for CNTs occur at low temperatures (Lou et al., 2005).

Since the Boudouard reaction is an exothermic reaction limited by equilibrium at the high temperatures needed to activate CO on the catalyst, it has been found that high CO pressures are needed in order to counter the effect of temperature and drive the reaction in the forward direction (Nikolaev et al., 1999; Resasco et al., 2002; Nasibulin et al., 2006). Therefore, high pressure results in both the enhancement of the reaction rate due to an increase in the amount of reagent and in the widening of the temperature range for CNT production (Nasibulin et al., 2006).

4.3 Summary and Conclusions

It was seen from the study that in the synthesis of CNTs from CO_2, temperature plays an important role. The results showed that when the temperature was below 750°C or above 840°C, there were no CNTs formed. The optimum growth temperature was about 800°C. The influence of CO_2 concentration and flow rate were also studied. Very high concentration and flow rates negatively affected the CNT production rates.

The next Chapter focuses on evaluating the feasibility of using CNTs in the treatment of brewery wastewater, by comparing their coagulation/flocculation capacities with traditionally used ferric chloride.

References

Abbaslou, R. M. M., Soltan, J., Dalai, A. K.., 2010. The effects of carbon concentration in the precursor gas on the quality and quantity of carbon nanotubes synthesized by CVD method. *Applied Catalysis A: General* 372, 147-152.

Andrews, R., Jacques, D., Rao, A.M., Derbyshire, F., Qian, D., Fan, X., Dickey, E.C., Chen, J.,1999. Continuous production of aligned carbon nanotubes: a step closer to commercial realisation. *Chemical Physics Letters* 303, 467-474

Afolabi, A. S., Abdulkareem, A. S., Iyuke, S. E., 2007. Synthesis of carbon nanotubes and nanoballs by swirled floating catalyst chemical vapour deposition method. *Journal of Experimental Nanoscience* 2 (4), 269-277.

Boehm, H. P., 1973 Carbon from carbon monoxide disproportionation on nickel and iron catalysts: Morphological studies and possible growth mechanisms. *Carbon* 11 (6), 583-586.

Chen, P., Zhang, H. B., Lin, G. D., Hong, Q., Tsai, K. R., 1997. Growth of carbon nanotubes by catalytic decomposition of CH4 or CO on a Ni-MgO catalyst. *Carbon* 35 (10-11), 1495-1501.

Iijima, S., 1991. Helical microtubules of graphitic carbon. *Nature* 354, 56-58.

Khedr, M. H., Farghali, A. A., 2005. Microstructure, kinetics and mechanisms of CO_2 catalytic decomposition over freshly reduced nano-crystallite $CuFe_2O_4$ at 400-600°C. *Applied Catalysis* B*: Environmental* 61, 219-226.

Khedr, M. H., Omar, A. A., Abdel-Moaty, S. A., 2006. Reduction of carbon dioxide into carbon by freshly reduced $CoFe_2O_4$ nanoparticles. *Materials Science and Engineering* A 432, 26-33.

Khedr, M. H., Bahgat, M., Nasr, M. I., Sedeek, E. K., 2007. CO_2 decomposition over freshly reduced nanocrystalline Fe_2O_3. *Colloids and Surfaces* A*: Physicochemical and Engineering Aspects* 302, 517-524.

Khedr, M. H., Abdel Halim, K. S., Zaki, A. H., 2008. CO_2 decomposition over freshly reduced nano-crystallite $Cu_{0.5}Zn_{0.5}Fe_2O_4$. *Journal of Analytical and Applied Pyrolysis* 81, 272-277.

Korneva, S., 2008. Functionalisation of carbon nanotubes. PhD, Drexel University, USA.

Lee, K., Yeoh, W., Chai, S., Ichikawa, S., Mohamed, A. R., 2010. Optimisation of carbon nanotubes synthesis via methane decomposition over alumina-based catalyst. *Fullerenes, Nanotubes, and Carbon Nanostructures* 18, 273 – 284.

Liu, X. Y., Huang, B. C., Coville, N. J.., 2002. The influence of synthesis parameters on the production of multiwalled carbon nanotubes by the ferrocene catalyzed pyrolysis of toluene. *Fullerenes, Nanotubes and Carbon Nanostructures* 10 (4), 339-352.

Lou, Z., Chen, Q., Wang, W., Zhang, Y., 2003. Synthesis of carbon nanotubes by reduction of carbon dioxide with metallic lithium. *Carbon* 41, 3063-3074.

Lou, Z., Chen, C., Chen, C., Gao, J., 2005. Formation of variously shaped carbon nanotubes in carbon dioxide-alkali metal (Li, Na) system. *Carbon* 43, 1084-1114.

Lou, Z., Chen, C., Huang, H., Zhao, D., 2006. Fabrication of Y-junction carbon nanotubes by reduction of carbon dioxide with sodium borohydride. *Diamond and Related Materials* 15, 1540-1543

Lu C., Su, F., 2007. Adsorption of natural organic matter by carbon nanotubes. *Separation and Purification Technology* 58, 113-121.

Maphutha, S. K., 2009. Thermodynamic study of carbon nanotube production from greenhouse gases during syngas synthesis. Dissertation, University of the Witwatersrand, Johannesburg, South Africa.

Moisala A., Nasibulin A.G., Kauppinen E.I., 2003. The role of metal nanoparticles in the catalytic production of singlewalled carbon nanotubes – A review. *Journal of Physics: Condensed Matter* 15(42), S3011-S3035.

Moisala, A., Nasibulin, A. G., Brown, D. P., Jiang, H., Khriachtchev, L., Kauppinen, E. I., 2006. Single-walled carbon nanotube synthesis using ferrocene and iron pentacarbonyl in a laminar flow reactor. *Chemical Engineering Scie*nce. 61, 4393-4402.

Moothi, K., 2009. Carbon nanotube production from greenhouse gases during syngas synthesis. MSc Dissertation, University of the Witwatersrand, Johannesburg, South Africa.

Motiei, M., Hacohen, Y. R., Calderon-Moreno, J., Gedanken, A., 2001. Preparing carbon nanotubes and nested fullerenes from supercritical CO_2 by a chemical reaction. *Journal of the American Chemical Societ*y 123, 8624-8625.

Nasibulin, A. G., Moisala, A., Brown, D. P., Kauppinen, E.I., 2003. Carbon nanotubes and onions from carbon monoxide using Ni(acac)2 and Cu(acac)2 as catalyst precursors. *Carbon* 41, 2711-2724.

Nasibulin, A. G., Queipo, P., Shandakov, S. D., Brown, D. P., Jiang, H., Pikhitsa, P. V., Tolochko, O. V., Kauppinen. E. I., 2006. Studies on mechanism of single-walled carbon nanotube formation. *Journal of Nanoscience and Nanotechnology* 6, 1233-1246.

Nikolaev, P., Bronikowski, M. J., Bradley, R. K., Rohmund, F., Colbert, D. T., Smith, K. A., Smalley, R. E., 1999. Gas-phase catalytic growth of single-walled carbon nanotubes from carbon monoxide. *Chemical Physics Letters* 313, 91-97.

Osswald, S., M. Havel and Y. Gogotsi, 2007. Monitoring oxidation of multiwalled carbon nanotubes by Raman spectroscopy. *Journal of Raman Spectroscopy* 38, 728-736.

Patole, S. P., Alegaonkar, P. S., Lee, J. H., Yoo, J. B., 2008. Water-assisted synthesis of carbon nanotubes: acetylene partial pressure and height control. *Europhysics Letters* 81, 1-6.

Potgieter-Vermaak, S., Maledi, N., Wagner, N., van Heerden, J. H. P., van Grieken, R., Potgieter, J. H., 2011. Raman spectroscopy for the analysis of coal: a review. *Journal of Raman Spectroscopy* 42, 123-129.

Qian, W., Wei, L., Cao, F., Chen, Q., Qian, W., 2006. Low temperature synthesis of carbon nanospheres by reducing supercritical carbon dioxide with bimetallic lithium and potassium. *Carbon* 44, 1298-1352.

Resasco, D.E., Alvarez, W.E., Pompeo, F., Balzano, L., Herrera, J.E., Kitiyanan, B., Borgna, A., 2002. A scalable process for production of single-walled carbon nanotubes (SWNTs) by catalytic disproportionation of CO on a solid catalyst. *Journal of Nanoparticle Research* 4, 131-136.

Simate, G. S., Iyuke, S.E., Ndlovu, S., Yah, C., Walubita, L. F., 2010. The production of carbon nanotubes from carbon dioxide: Challenges and opportunities. *Journal of Natural Gas Chemistry* 19 (5), 453-460.

Singh, C., Shaffer, M. S. P., Windle, A. H., 2003. Production of controlled architectures of aligned carbon nanotubes by an injection chemical vapour deposition method. *Carbon*, 41 (2), 359-368.

Toussi, S. M., A. Fakhru'l-Razi, A. L. Chuah and A. R. Suraya, 2011. Optimisation of synthesis conditions for carbon nanotubes by catalytic vapour deposition (CCVD). *Materials Science and Engineering* 17, 012003.

Tsang, S. C., Harris, P. J. F., Green, M. L .H., 1993. Thinning and opening of carbon nanotubes by oxidation using carbon dioxide. *Nature* 362 (6420), 520-522.

Tsoufis, T., Xidas, P., Jankovic, L., Gournis, D., Saranti, A., Bakas, T., Karakassides, M. A., 2007. Catalytic production of carbon nanotubes over Fe-Ni bimetallic catalysts supported on MgO. *Diamond and Related Materials* 16(1), 155 -160.

Vallés, C., Pérez-Mendoza, M., Maser, W. K., Martínez, M. T., Alvarez, L., Sauvajol, J. L., Benito, A. M., 2009. Effects of partial and total methane flows on the yield and structural characteristics of MWCNTs produced by CVD. *Carbon* 47, 998-1004.

Xu, X.J., Huang, S. M., 2007. Carbon dioxide as a carbon source for synthesis of carbon nanotubes by chemical vapour deposition. *Materials Letters* 61, 4235-4237.

Zheng, L. Y., Zhao, L .X., Wan, Y. Z., Wang, Y. L., Xiong, W. H.,2005. Three dimensionally braided carbon fabric-reinforced nylon composites prepared by in situ polymerization. *Carbon* 43 (5), 1084-1087.

CHAPTER FIVE

EVALUATION OF CARBON NANOTUBES AS HETEROGENEOUS COAGULANTS/FLOCCULANTS FOR BREWERY WASTEWATER TREATMENT

"*Intellectuals solve problems; geniuses prevent them*".

- Albert Einstein

5.1 Introduction

Currently, a good number of brewery wastewater treatment methods are either in operation, being piloted or under evaluation (Simate et al., 2011). These treatment processes are selective depending on various factors including the following: the purpose of water and its quality requirements (Seo et al., 1996), wastewater characteristics (Chuang et al., 2005), etc. However, over the years, coagulation and flocculation have remained the widely used methods for water and wastewater pretreatment. These physicochemical processes are commonly used for the removal of colloidal material, which cause colour and turbidity (Amuda and Alade, 2006). Often, the terms coagulation and flocculation are used synonymously despite an existing subtle difference between the two (Tripathy and Ranjan De, 2006). In water and wastewater treatment, coagulation implies the step where particles are destabilised by a coagulant. On the other hand, the subsequent process in which larger aggregates (flocs) are formed by the action of shear is known as flocculation (Gregory, 2006). After small particles have formed larger aggregates, colloidal material can then be removed more easily by physical separation processes such as sedimentation, flotation, and filtration (Simate et al., 2011).

At present the coagulants used for water and wastewater treatment are predominantly inorganic salts of iron and aluminium as already discussed in sub-section 2.3.4. However, the current traditional coagulants and flocculants have several disadvantages. One of the major concerns is that the chemicals used result in a net increase in the dissolved constituents associated with the added metal coagulants in the final wastewater (Barrera-Díaz et al., 2009). Since high concentrations of residual traditional coagulants/flocculants in water may have severe adverse implications including human health effects, environmentally friendly coagulants will present an interesting alternative for the treatment and purification of wastewaters. Therefore, it

is imperative that new technologies are developed for the treatment of brewery wastewater.

In this study, the phenomenon of heterogeneous coagulation and flocculation was applied. Since the colloidal particles found in brewery wastewater are negatively charged (see Table 3.3), positively charged CNTs or basic type CNTs would be suitable for heterogeneous coagulation with the colloidal particles in the wastewater. Therefore, this Chapter presents the results of a study carried out to investigate whether CNTs can be used as heterogeneous coagulants and /or flocculants in the pretreatment of brewery wastewater. These results endeavour to answer questions raised in **Objective II.**

The details of the equipment, experimental setup and procedures followed in the heterogeneous coagulation and flocculation of brewery wastewater are described in sub-section 3.3.2. The analytical techniques outlined in sub-section 3.4.1 were used to analyse the quality of raw and treated water samples. The CNTs were characterized as described in sub-section 3.4.2.

5.2 Results and Discussion

5.2.1 Characterisation of carbon nanotubes

The TEM results of pristine CNTs are already reported in sub-section 4.3.1. Therefore, this sub-section only reports the results of the TGA, Raman spectroscopy, and the FTIR.

The TGA analysis carried out on pristine and purified CNTs in oxygen atmosphere to monitor the weight loss and thermal stability of the CNTs is shown in Figure 5.1. It is evident from Figure 5.1 that both CNT samples are considerably stable and show a

little weight loss below 500°C. From this figure, it is found that the initial oxidation temperature was at around 580°C and this occurred mainly due to the presence of amorphous carbon in the CNTs mixture (Ramesh et al., 2006). Figure 5.1 also shows that gasification of both samples ends at about 600°C at which 2.81% and 1.22% remaining weight was observed for pristine and acid treated CNT samples, respectively. This shows that the purity or carbon content of CNTs increases slightly from 97.19% to 98.78% after acid treatment.

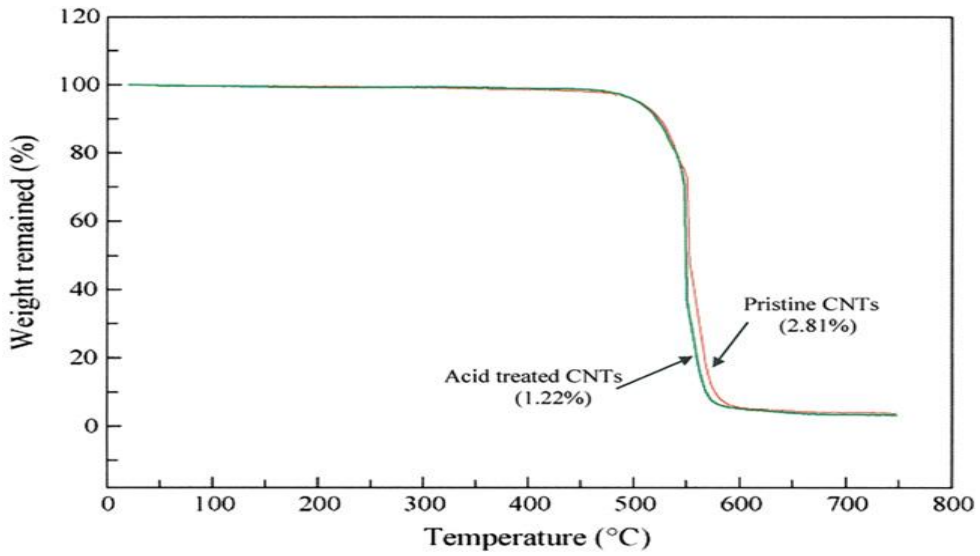


Figure 5.1. TGA of pristine and purified CNTs in oxygen atmosphere.

However, the following should be noted when using the TGA data. The information from TGA is primarily derived from the change in weight, which then is indirectly related to reactivity or oxidation (Brukh and Mitra, 2007). Since it does not distinguished between the reactants and the products, it can be affected by factors other than true amorphous carbon (Brukh and Mitra, 2007). For example, the weight of the residual catalyst, its oxidation, and the adsorption/desorption of other species can bias the results. Consequently, the oxidation of amorphous carbon should really

be studied based on product formation, rather than weight loss. However, such a study is not reported in this thesis.

The Raman spectra of both the pristine and acid functionalised CNT samples excited with the 514.5 nm laser line are shown in Figure 5.2.

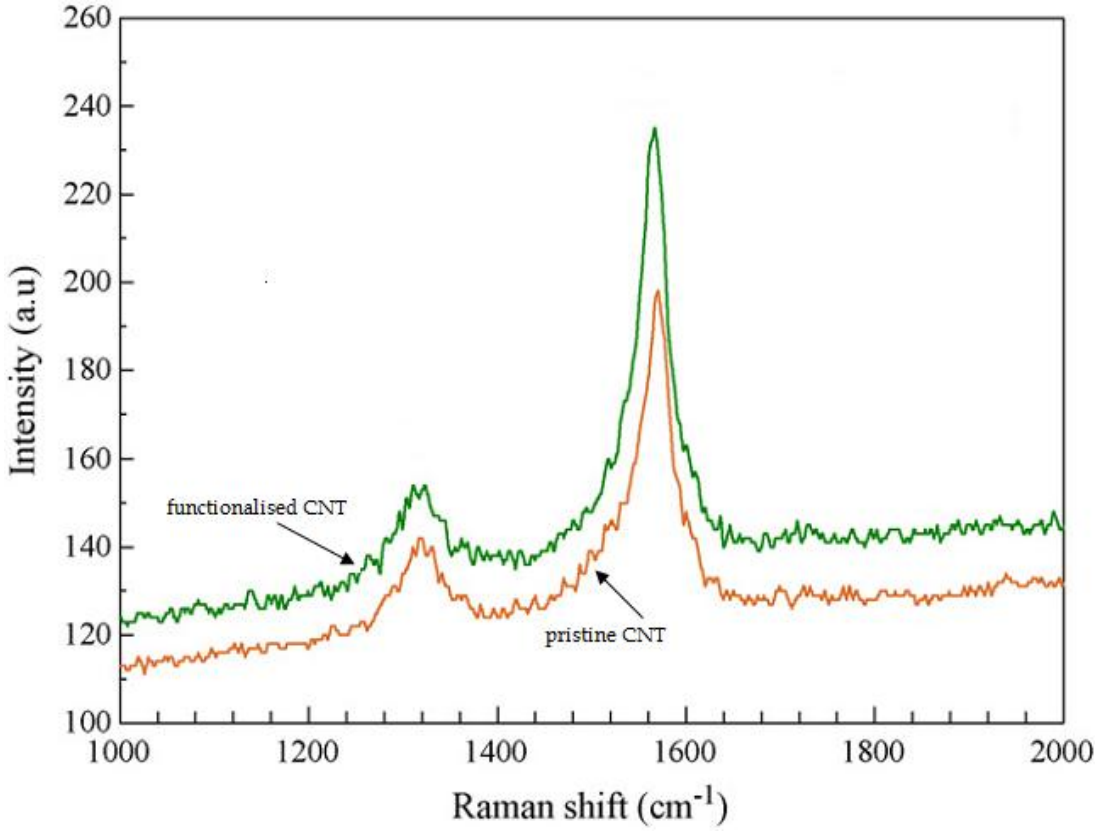


Figure 5.2. Raman spectra of pristine and acid functionalised CNTs.

As can be seen from these spectra, the two characteristic peaks of CNTs, named the D band at 1358 cm^{-1} and the G band at 1582 cm^{-1}, approximately, are easily identified. When oxidation (or functionalisation) of nanotubes was performed, these characteristic peaks can still be identified, proving that the acid treatment did not damage the structure of the CNTs. The Raman intensity of hydrochloric acid

functionalised CNTs is higher than that of pristine CNTs. When comparing the values of the ratio I_D/I_G for acid functionalized (0.76) and pristine (0.71) CNT samples, it is observed that after functionalisation, the ratio increased. This is expected because the functionalisation of CNTs breaks some of its bonds and induces chemical groups that can be interpreted as defects on the structure (Osorio et al., 2008; Su et al., 2010). In other words, there was an increase in the relative intensity of the disorder mode attributed to an increased number of sp^3-hybridized carbons in the nanotube framework (Bahr and Tour, 2001). In the absence of quantitative methods, an increase in values of the ratio I_D/I_G can actually be taken as a crude measure of the degree of functionalisation (Jorio et al., 2003; Graupner, 2007; Singh et al., 2009).

The infrared spectra of the pristine and acid functionalised CNT samples are shown in Figure 5.3. It can be seen from the figure that the infrared spectrum of pristine CNT samples has very low infrared absorption intensities, thus it shows no significant peaks. This is because the high symmetry present on pristine CNTs generates very weak infrared signals due to the weak difference of charge state between carbon atoms (Osorio et al., 2008). The weak difference of charge state leads to very small induced electric dipole, providing a silent spectrum (Osorio et al., 2008).

As expected, it can be seen from Figure 5.3 that a number of infrared peaks are present in the infrared spectra for acid functionalised CNT samples. Therefore, the FT-IR spectrum is in good agreement with results showed on Raman spectrometry (Figure 5.2). The presence of functional groups confirmed with FT-IR spectrum agrees with the higher ratio I_D/I_G, proving the addition of functional groups on the nanotubes.

Figure 5.3 shows peaks at 1300-1750 cm^{-1}, around 2300 cm^{-1} and 3400-4000 cm^{-1}. The 1300-1750 cm^{-1} range can be mainly attributed to acidic groups like carboxylic acids (–COOH) and phenolic acids (O–H) (Li et al., 2002; Lu and Su, 2007). In

particular, the peaks at 1310 and 1710 cm^{-1} may be attributed to acidic groups such as lactone or basic groups such as ketones, chromene and pyrones (Montes-Moran et al., 2004; Naseh et al., 2009). In addition, the signature of carbonyl (>C=O) appears at around 1750 cm^{-1} (Li et al., 2002). The 3400-4000 cm^{-1} range can be primarily related to hydroxyl groups (–OH) (Li et al., 2002; Lu and Su, 2007).

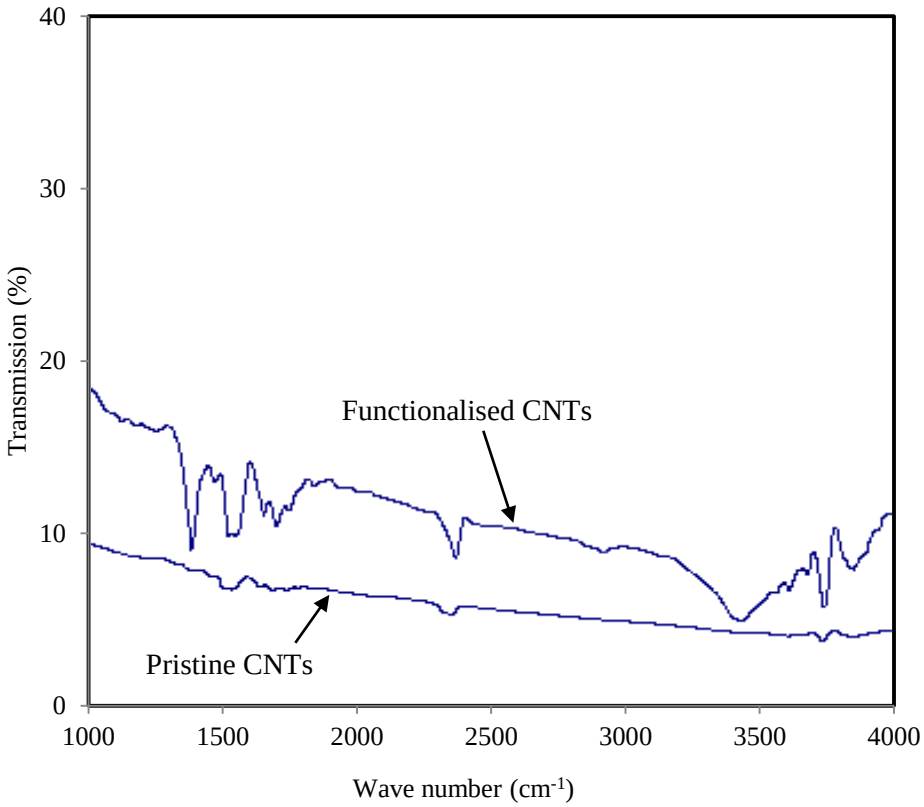


Figure 5.3. FT-IR spectra of pristine and acid functionalised CNTs.

As mentioned in sub-sections 2.4.3 and 3.3.1 the functionalisation of CNTs provides several chemical sites for adsorption of colloidal particles from wastewater, and that the adsorption of colloidal particles can lead to bridging flocculation and neutralisation of charges on the particles, thus facilitating agglomeration.

However, assessing the nature of adsorption exclusively by the presence of specific functional groups is rather complex. In the case of flocculating negatively charged colloidal particles, the adsorption process might be due to the presence of basic groups such as carbonyl and hydroxyl groups. Considering the fact that the point of zero charge for acid functionalised CNTs (see discussion below) was 7.3, it means that the functional groups were weakly acidic or more basic in nature, e.g., carbonyl groups or hydroxyl. The carbonyl group is moderately polar indicating the presence of a slight negative charge on the oxygen (δ^-) and a slight positive charge (δ^+) on the carbon of the C=O double bond. However, the sites responsible for the adsorption process might not be exclusively due to the basic groups, other sites on the CNTs can also contribute to the adsorption process and even physical adsorption is also possible.

The Boehman's method (or the depletion technique) was used to qualitatively determine the surface concentrations of the acidic and basic sites on the CNTs in Table 5.1 (Boehm, 1966; Boehm, 1994). The procedure has already been described in sub-section 3.4.2. The quantity of functional groups in Table 5.1 is in good agreement with the FT-IR spectra. There is only trace amounts of functional groups present on pristine CNTs compared to acid functionalised CNTs.

Table 5.1 The amount of functional groups on the surfaces of pristine and acid functionalised CNTs.

CNT	Concentration of acidic sites (mmol/g)	Concentration of basic sites (mmol/g)
Pristine	0.120	0.216
Functionalised	2.751	4.310

From Table 5.1, it is seen that hydrochloric acid functionalised CNTs contain more basic functional groups than acidic functional groups. Therefore, the hydrochloric acid functionalised CNTs can exhibit considerable anion exchange capabilities, i.e., it can effectively function as a cationic coagulant in water and wastewater treatment. In

other words, the basic sites would be responsible for adsorbing anions from aqueous solutions (Pereira et al., 2003; Lu and Su, 2007). On the other hand, the acidic sites would be responsible for adsorbing cations (Pereira et al., 2003; Lu and Su, 2007).

The phenomena of basicity as applied to adsorption are described in Equations 5.1 to 5.3 (Leon et al., 1992).

$$S_B + H^+ \rightleftharpoons HS_B^+ \quad (5.1)$$

$$\text{-COH} + H^+ \rightleftharpoons C^+ + H_2O \quad (5.2)$$

$$\text{-COH} + H^+ \rightleftharpoons COH_2^+ \quad (5.3)$$

where S_B is an alkaline substrate.

In Equations (5.2) and (5.3), the basic properties are implicitly restricted to hydroxyl type groups or at most, extended to include other oxygen functional groups as well (Leon et al., 1992). These expressions are useful to understand the phenomena of adsorption in practice.

Though the particle size distribution of the CNTs was not done, the specific surface area and pore volume of the two CNT samples were determined and are presented in Table 5.2. From Table 5.2, it can be seen that both the specific surface area and pore volume are higher for hydrochloric acid functionalised CNTs than the pristine CNTs. Since the CNTs tend to form long bundles stabilised by numerous π-π interaction between the tubes (Naseh et al., 2009), the inclusion of functional groups on the surface of nanotubes generates repulsion force, which leads to de-bundling of nanotubes and, therefore, causes surface area increases (Naseh et al., 2009; Rurlle et al., 2007).

Table 5.2. Physicochemical properties of CNTs.

Property	Pristine	Hydrochloric acid functionalised
Surface area (m^2/g)	499	601
Pore volume (cm^3/g)	0.64	0.93

The pH value at which the zeta potential (ζ) equals to zero is called the point of zero charge (PZC) or the isoelectric point (IEP). It is used to assess the adsorbent surface charge qualitatively. At pH < PZC, the surface of the adsorbent is positively charged and is accessible to anions; at pH = PZC, the surface is neutral; and at pH > PZC, the surface is negatively charged and will repel the anions. The mass titration results for hydrochloric acid functionalised CNTs are shown in Figure 5.4. For the discussion of Figure 5.4, reference should also be made to the experimental data in Appendix C (Table C1). The results in Table C1 are an average of the runs conducted under similar experimental conditions.

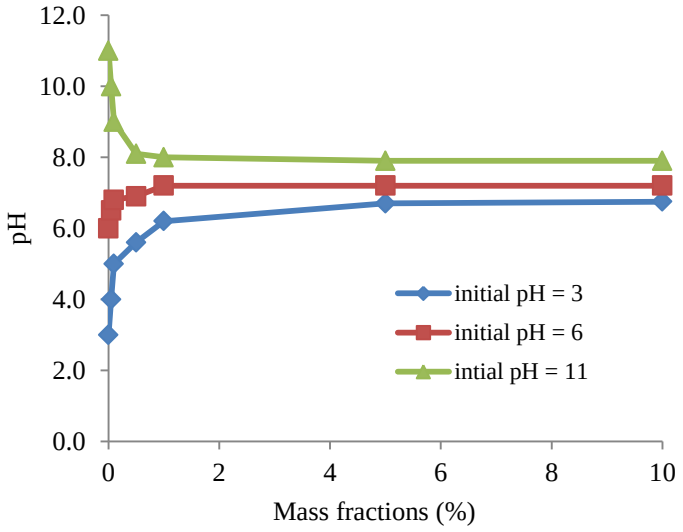


Figure 5.4. Mass titration results for acid functionalised CNTs.

As can be seen from Figure 5.4, a plateau is obtained in this plot of pH versus mass fraction. By taking the average value of the three asymptotic pH values (i.e.,

asymptotes to x-axis), the pH of the PZC for functionalised CNTs was found to be 7.3. Therefore, it is obvious that the hydrochloric acid functionalised CNTs were basic in nature. This indicates that very little acidic functional groups such as carboxylic groups have been added on the surface of CNTs. This concurs well with the amount of acidity compared to basicity of the functionalised CNTs shown in Table 5.1, i.e., there are more basic groups than acidic groups.

With the PZC of 7.3, it makes the hydrochloric acid functionalised CNTs more appropriate for the heterogeneous coagulation of brewery wastewater, which has a zeta potential of -38mV (see Table 3.3). With a negative zeta potential brewery wastewater is considered to be having predominantly negatively charged colloidal particles.

5.2.2 Comparison of carbon nanotubes and ferric chloride

The suitability of using CNTs as heterogeneous coagulants and/or flocculants in the treatment of brewery wastewater was compared with ferric chloride. As mentioned earlier (sub-section 3.2.2), ferric chloride was chosen amongst other inorganic coagulants such as alum because it is effective over a wider pH range of 4-11, and that the ferric hydroxide floc is heavier than alum, thus improving its settling characteristics (Ebeling et al., 2003). The initial evaluation of the coagulation process in jar tests (sub-section 3.3.2) was determined by analysis of turbidity as it has been used as a measure of water quality for many years. In fact, the turbidity of raw water is the targeted substance that is removed during coagulation-sedimentation treatment (Anadurai et al., 2004), and that turbidity is an important parameter for checking the efficiency of coagulation (Cheng et al., 2005). Turbidity is a principal physical characteristic of water, which is an expression of the optical property that causes light to be scattered and absorbed by particles and molecules rather than transmitted in straight lines through a water sample. In simple terms, turbidity is the cloudiness of

water. The higher the turbidity, the harder it is to see through the water. It is caused by suspended matter or impurities that interfere with the clarity of the water. These impurities may include clay, silt, finely divided inorganic and organic matter, soluble coloured organic compounds, plankton, and other microscopic organisms.

Figure 5.5 shows a comparison of the effectiveness of CNTs and ferric chloride in removing turbidity from brewery wastewater. For the discussion of Figure 5.5, reference should also be made to the experimental data in Appendix C (Table C2). The results in Table C2 are an average of the runs conducted under similar experimental conditions.

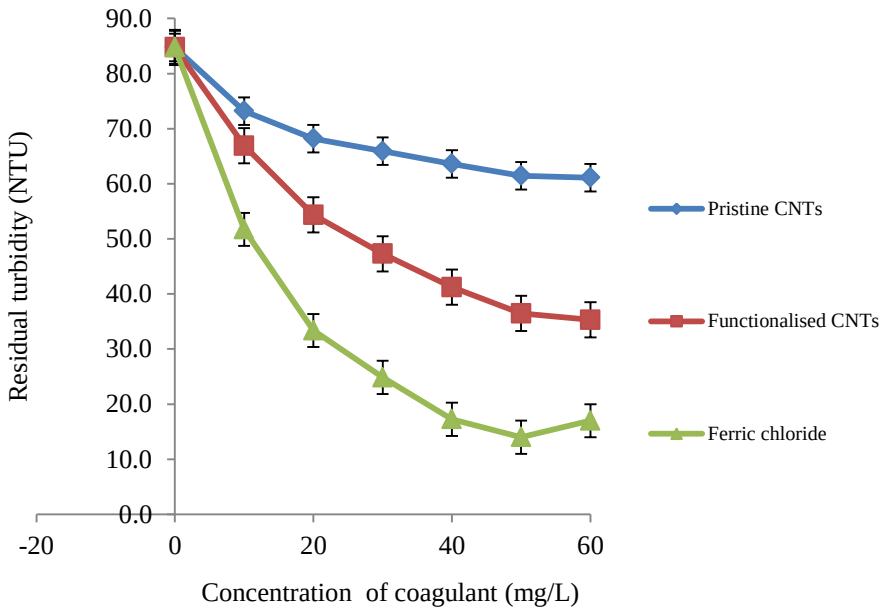


Figure 5.5. Comparison of CNTs and ferric chloride on removal of turbidity. P-value = 0.0126 at the significance level of 0.05.

An overview of the figure shows that all the three coagulants are able to remove turbidity to a certain extent. However, ferric chloride was found to display higher

efficiency than CNTs for the coagulation/flocculation of colloidal matter in brewery wastewater. This may be attributed to the fact that several flocculation mechanisms may have been simultaneously involved when ferric chloride is used, i.e., (1) adsorption/ charge neutralisation, and (2) sweep-floc coagulation (or enmeshment). Sweep-floc coagulation is significant and is more likely to have predominated because ferric chloride doses used in this investigation may have significantly exceeded the solubility limit. In sweep-floc coagulation, metal hydroxide precipitates promote coagulation by increasing the interparticle collision rate and enmeshing suspended particles (Childress et al., 1999). As for CNTs, the most probable mechanisms are (1) adsorption/charge neutralisation, and (2) adsorption and interparticle bridging. These are not likely to have a high impact for CNTs. For example, adsorption and interparticle bridging is likely to be insignificant because CNTs do not form several long chains. Furthermore, the charge density may not have been as high as that for ferric ions for effective charge neutralisation to occur.

One interesting observation to note is that hydrochloric acid functionalised CNTs performed better than pristine CNTs. This is a good confirmation that hydrochloric acid functionalised CNTs indeed possessed basic (or positively charged) functional groups as shown in Table 5.1. Nevertheless, the results suggest that the colloids were, to a certain degree, destabilised by pristine CNTs and as a result were forced to agglomerate, hence the considerable reduction in turbidity. These results indicate that though pristine CNTs were found not to possess significant peaks (Figure 5.3), they were partially oxidised due to high temperatures during their production. Furthermore, it is also noted that basic surface oxides are always present on carbon surfaces, and that oxidised carbons always contain basic sites (Boehm, 1994). Therefore, these basic surface groups could have contributed to the coagulation of colloidal particles from brewery wastewater.

In addition to the results shown in Figure 5.5, it is seen from the ANOVA (Table C2) that at the significance level of 0.05, a *p*-value of 0.0126 was obtained. This shows

that the differences in the results of at least two coagulants were statistically significant. These ANOVA results imply that at least two types of coagulants studied performed differently. This is in agreement with the results shown in Figure 5.5.

Figure 5.6 shows SEM images which compare the surface morphologies of pristine and hydrochloric acid functionalised CNTs after the coagulation/flocculation tests. It can be seen from the figure that hydrochloric acid functionalised CNTs are intensely covered by colloidal matter compared to pristine CNTs. This is in agreement with Figure 5.5, which sho
ws that hydrochloric acid functionalised CNTs perform better than pristine CNTs.

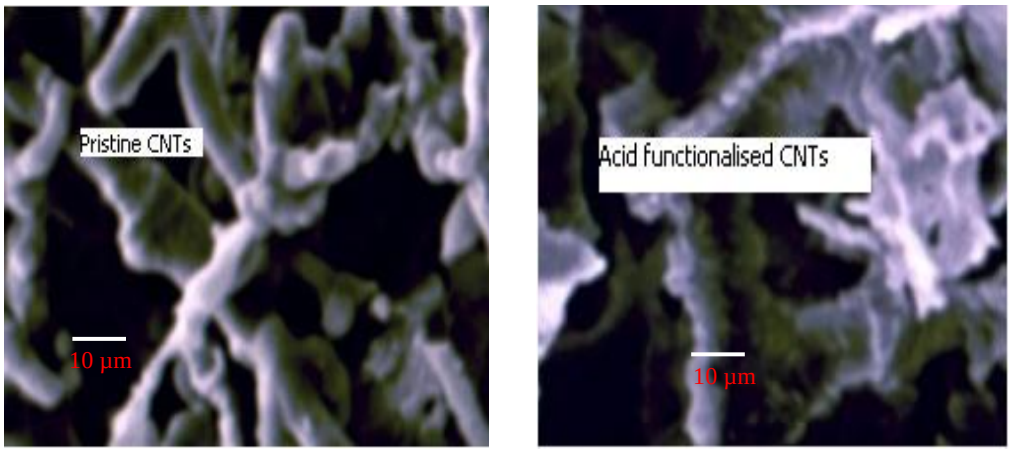


Figure 5.6. Electron micrographs showing colloidal materials on CNTs after coagulation/flocculation.

Since these results have certainly established that hydrochloric acid functionalised CNTs can act as heterogeneous coagulants, a series of tests that followed were conducted with hydrochloric acid functionalised CNTs only (unless stated otherwise). Furthermore, the study involved the expansion of coagulation objectives from turbidity removal only to include COD removal as well. As mentioned in sub-section 3.4.1, in the brewery industry, COD is the most important parameter for recycling water or is required to be measured at all times.

5.2.3. Effect of pH

The pH of the solution is an important parameter and, therefore, plays a preponderant role in the coagulation and flocculation processes. It affects both the surface charge density of the colloid and the action of the coagulant (e.g., degree of ionization, charge density, speciation, etc). For example, the colloidal particles possess positive charges at low pH and negative charges at high pH. Furthermore, pH is an important factor that affects the dissociation of functional groups contained on CNTs (Kuo and Lin, 2009).

Variation of the zeta potential

Zeta potential is defined as the potential at the boundary of the hydrodynamic shear plane of a charged particle (Lin et al., 2003). This parameter is particularly important in that it relates to the degree of repulsion or attraction a suspended particle in a liquid has with other particles or with charged surfaces. In addition, it is the magnitude of the zeta potential that determines the extent of interaction between colloids and other surfaces. This means that high zeta potential values provide greater colloidal stability (by way of increased electrostatic repulsion between charged surfaces). As alluded to earlier, the point at which the zeta potential switches its sign from negative to positive is called the PZC (or IEP), and it is in this area that the colloidal particles possess the lowest stability, and hence the greater chance of aggregation or deposition (Rodriguez-Santiago et al., 2008).

The zeta potential of charged particles is influenced not only by the surface charge on the particle, but also by the environmental conditions in which the particles are suspended (e.g., pH, conductivity, temperature, ion concentration, etc). Therefore, in this study, pH (at a fixed temperature of 25°C) was chosen as the main tool to vary

the zeta potential of CNTs. The zeta potential of pristine and hydrochloric acid functionalised CNT samples at various pHs are shown in Figure 5.7.

For the discussion of Figure 5.7, reference should also be made to the experimental data in Appendix C (Table C3). The results in Table C3 are an average of the runs conducted under similar experimental conditions.

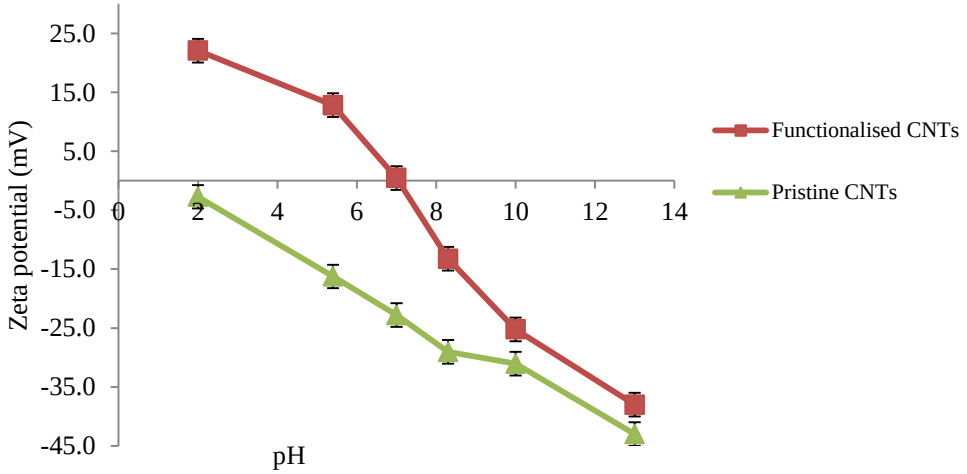


Figure 5.7. Zeta potential of pristine and acid functionalised CNTs. P-value = 0.0044 at the significance level of 0.05.

As can be seen from Figure 5.7, the zeta potential of both the pristine and hydrochloric acid functionalised CNT samples decrease with an increase in pH. The figure confirms the results of Figure 5.4 where the PZC for hydrochloric acid functionalised CNT samples occurs at a pH of about 7.3, whereas, the zeta potential of pristine CNT samples was negative throughout the pH studied, and no PZC value was observed. Indeed, as can be seen from Table C3, the results of the one tail Student's t-test of p = 0.0044 shows that the differences in the zeta potential for hydrochloric acid functionalised CNT samples and pristine CNT samples are statistically significant at significance level of 0.05. The hydrochloric acid

functionalised CNT samples have positive zeta potentials at pHs < 7.3, which indicates that they are positively charged and negative zeta potential at pHs > 7.3, implying that they are negatively charged. These results show that at pH < PZC, there will be electrostatic interactions between the positively charged CNTs and the negatively charged colloidal particles in the brewery wastewater. The electrostatic interactions can facilitate adsorption and charge neutralisation of the colloidal particles leading to the coagulation and flocculation of the colloidal particles.

Dispersion efficacy of carbon nanotubes

The results of the CNT dispersion tests are very important in this study because they help to establish whether treated water would have significant amount of residual CNTs dispersed (or dissolved) in it or not.

The potential stability of the dispersion system can be deduced from the absolute magnitude of the zeta potential (MIL, 2004; Shieh et al., 2010). In fact, the commonest way to establish the stability of colloidal dispersions is by determining the magnitude of zeta potential (Mandzy et al., 2005). Therefore, in this study, the stability of the dispersion of CNTs in aqueous solution was determined by monitoring the zeta potential.

The results are analysed in accordance with the Derjaguin, Landau, Verwey and Overbeek theory (DLVO theory) (Derjaguin and Landau, 1941; Verwey and Overbeek, 1948). Basically, if all the particles in dispersion have a large negative or a large positive zeta potential, then they will tend to repel each other, and thus there will be no tendency for the particles to stick together (MIL, 2004; Shieh et al., 2010). In other words, a higher absolute zeta potential leads to enhanced electrostatic repulsion (Heister et al., 2010). On the other hand, if the absolute zeta potential of the particles is low, then there will be no force to prevent the particles from coming

together and coagulating (Shieh et al., 2010; MIL, 2004). The general dividing line between stable and unstable dispersions is generally taken at either +30 or −30 mV (Shieh et al., 2010; Raj and Lewis, 2011; MIL, 2004). Particles with zeta potentials more positive than +30 mV or more negative than −30 mV are normally considered stable (Shieh et al., 2010; Raj and Lewis, 2011; MIL, 2004). Particles with zeta potential between −30 and +30 mV are considered unstable and will precipitate sooner or later depending on the density of the particles (Shieh et al., 2010).

The most important factor that affects zeta potential is pH (MIL, 2004), therefore, zeta potential of the CNTs was measured as a function of pH following the procedure described in sub-section 3.4.2. As already stated above, the changes in zeta potential of pristine and hydrochloric acid functionalised CNTs at various pHs are shown in Figure 5.7. As can be seen from the figure, the zeta potential of both types of CNTs fall between -30 mV and +30 mV for pHs below 10. This means that below the pH of 10 the CNTs cannot form a stable dispersion. Above the pH of 10, the zeta potential is more negative than -30 mV thus the CNTs are likely to form a stable dispersion.

In this study, for effective heterogeneous coagulation and flocculation of brewery wastewater, the pH of the hydrochloric acid functionalised CNTs is supposed to be below 7.3; the PZC. As already discussed, at pHs below 10 the CNTs do not form a stable dispersion. This is advantageous because there will be no residual CNTs dispersed in the treated brewery wastewater. In fact, unlike soluble CNTs, the insoluble CNTs can easily be retained and separated from treated water using low cost, but effective separation processes such as membrane filtration and ultracentrifugation, thus preventing the apparent human health risks of residual CNTs in treated water (Simate et al., 2012b).

Variation of turbidity and chemical oxygen demand

The effect of initial pH on turbidity and COD removal is shown in Figure 5.8. For the discussion of Figure 5.8, reference should also be made to the experimental data in Appendix C (Table C4). The results in Table C4 are an average of the runs conducted under similar experimental conditions. Figure 5.8 shows that turbidity removal is pH dependent. Turbidity removal by hydrochloric acid functionalised CNTs decreases with an increase in pH, and vice-versa. The dependence of turbidity removal on pH is due to the dependence of the surface charge of hydrochloric acid functionalised CNTs on pH values that have been shown by the zeta potential values in Figure 5.7.

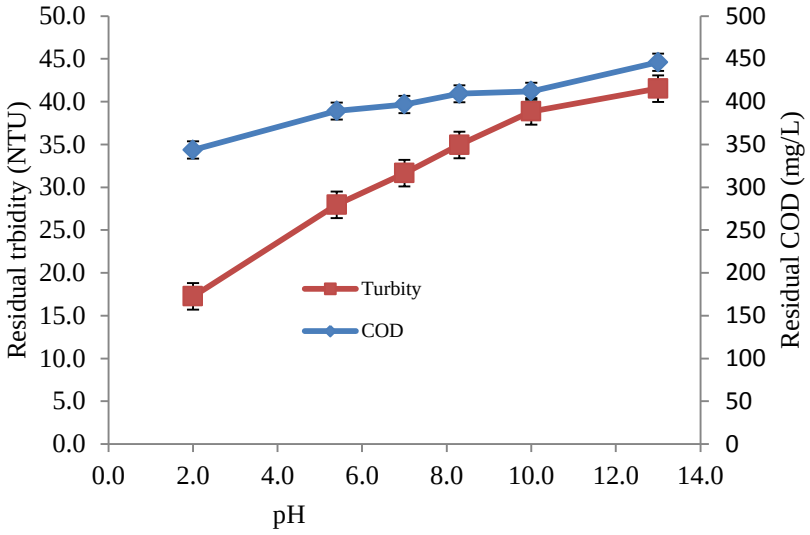


Figure 5.8. Effect of pH on turbidity and COD reduction.

At pH < PZC, the H^+ ions adsorb onto the surface of CNTs rendering the surface charges of hydrochloric acid functionalised CNTs to be positive. Therefore, coulombic attractions can take place between the positively charged acidified CNTs and the negatively changed colloidal particles. At higher pH, the surface charges of CNTs become more negative because of the deposition of more OH^- on the CNT

surface, thus increasing electrostatic repulsion between the negatively charged colloidal particles. Therefore, the turbidity removal decreases at pH > PZC due to the negatively charged hydrochloric acid functionalised CNTs.

A similar trend to turbidity removal (see Figure 5.8) was also observed for the COD removal, i.e., removal decreases with an increase in the pH value and vice-versa.

5.2.4. Effect of dosage

To investigate the effect of dosage, 100 mL of brewery wastewater was mixed with different doses of hydrochloric acid functionalised CNTs, while keeping other parameters as constants. The results of the effect of varying the dosage on turbidity and COD removal are shown in Figure 5.9. For the discussion of Figure 5.9, reference should also be made to the experimental data in Appendix C (Table C5). The results in Table C5 are an average of the runs conducted under similar experimental conditions.

Figure 5.9 shows that there is a significant reduction in turbidity and COD up to dosages of about 40-50 mg/L. Beyond this value, the rate of turbidity and COD removal is small. This is in contrast to the fact that with more CNTs, more charged sites are available for uptake of colloidal particles from the brewery wastewater. A possible explanation is that increased amounts of CNTs beyond a certain level may favour competitive CNT-CNT associations at the expense of CNT-colloidal particle interactions. These results imply that the mechanisms of coagulation by CNTs may be similar to those by polymers. This is because low dosages of polymers have been found to achieve a fast and efficient removal of colloids as observed by Roussy et al. (2004) and Assaad et al. (2007).

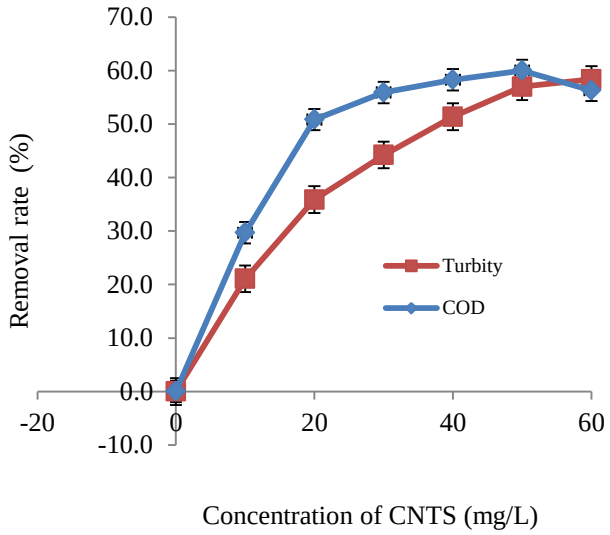


Figure 5.9. Effect of CNT dosage on turbidity and COD removal.

However, since the turbidity and COD decreased consistently as the dosage of hydrochloric acid functionalised CNTs increased, it would be expected that charge neutralisation played a key role in the heterogeneous coagulation of colloidal particles.

5.2.5. Mixture of carbon nanotubes and ferric chloride

The overall degree of turbidity (or COD) removal by hydrochloric acid functionalised CNTs was not sufficiently high compared to ferric chloride (Figure 5.5). In order to explore the coagulation efficiency further, hydrochloric acid functionalised CNTs were used in conjunction with ferric chloride. Therefore, synergic effect of a mixture of hydrochloric acid functionalised CNTs and ferric chloride was investigated. The results of this evaluation are shown in Figure 5.10.

For the discussion of Figure 5.10, reference should also be made to the experimental data in Appendix C (Table C2 and Table C6). The results in Table C2 and Table C6 are an average of the runs conducted under similar experimental conditions.

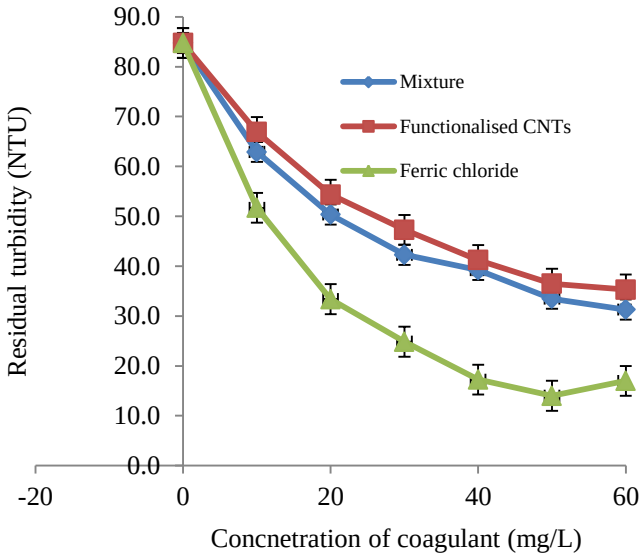


Figure 5.10. Effect of a mixture of CNTs and ferric chloride on turbidity; ferric chloride in mixture = 2 mg/L; pH = 6.5. P-value = 0.0013 at the significance level of 0.05.

It can be seen from Figure 5.10 that the turbidity removal only improved slightly at all dosages of CNTs. Therefore, it is difficult to distinguish the contribution of a mixture of hydrochloric acid functionalised CNTs and ferric chloride from the results presented in Figure 5.10. However, the results may be explained as follows: (1) the flocculation capability of ferric chloride was suppressed by the adsorption of ferric ions onto some 'negative sites' of CNTs, and (2) the presence of repulsive effects between positively charged ferric ions and CNTs.

Nevertheless, the value of the test statistic (t = 4.9609) and its p-value (0.0013) as shown in Table C6 at a significance level of 0.05 indicate that there is an

overwhelming eveidence to infer that a mixture of functionalised CNTs and ferric chloride is better on average than hydrochloric acid functionalised CNTs alone. It is, therefore, expected that at high dosages of ferric chloride in the mixture, lower residual turbidity would be observed.

5.2.6. Mechanisms of heterogeneous coagulation

This sub-section discusses the mechanisms by which the heterogeneous coagulation of colloidal particles is occurring. The knowledge of the mechanism is paramount for understanding the design, operation and control of the separation processes at industrial scale. To better understand the coagulation and flocculation mechanism, in this study, it was essential to study the evolution of zeta potential of the flocculated colloidal particles as a function of CNT dosage. Prior to the test work, the pH of the brewery wastewater was adjusted to 6.5 at which the colloidal particles were still moderately negatively charged (-25.5mV) and the CNTs were positively charged.

The evolution of zeta potential of brewery wastewater as a function of CNT dosages is shown in Figure 5.11. For the discussion of Figure 5.11, reference should also be made to the experimental data in Appendix C (Table C7). The results in Table C7 are an average of the runs conducted under similar experimental conditions.

It can be seen from Figure 5.11 that the magnitude of the negative zeta potential decreases with an increase in the dosage of CNTs. In other words, there is an increase in zeta potential with an increase in CNT dosage, and that the increased zeta potential remained positive. The increase in zeta potential by CNTs was high enough to make coagulation by charge neutralisation.

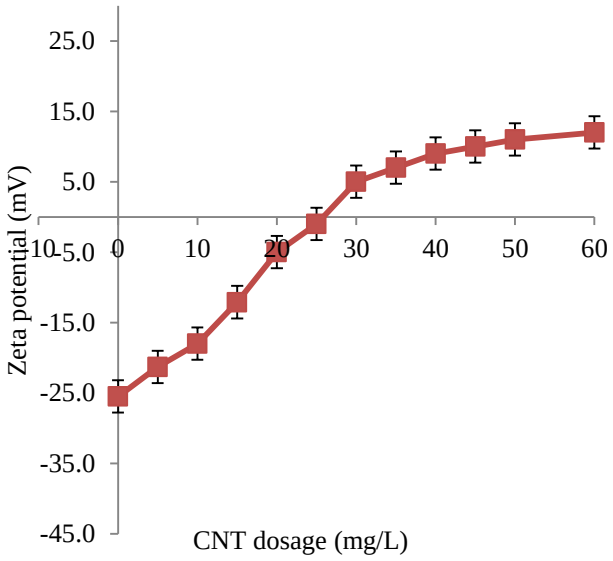


Figure 5.11. Electrokinetic zeta potential of brewery wastewater as a function of CNT dosage.

Charge neutralisation is caused by the reduction in the electric double layer repulsion between particles due to adsorption of coagulants on oppositely charged particles (Zhou and Franks, 2006). Therefore, these results show that the heterogeneous coagulation of colloidal particles by hydrochloric acid functionalised CNTs in brewery wastewater occurs by the mechanisms of charge neutralisation. These results are in agreement with the deduction in sub-section 5.2.4 about the heterogeneous coagulation mechanism; turbidity and COD removal increased with an increase in dosage. From Figure 5.11 it can be seen that the isoelectric point was reached at ~25 mg/L of the CNTs.

5.2.7. Adsorption isotherm models

In sub-section 5.2.6, it was shown that charge neutralisation is the main mechanism governing the coagulation of brewery wastewater using hydrochloric acid

functionalised CNTs. However, prior to charge neutralisation, coagulants adsorb on oppositely charged colloidal particles (Zhou and Franks, 2006). This sub-section discusses the interaction mode and mechanism of adsorption reactions in the coagulation process.

Two widely used isotherm models of Freundlich and Langmuir were applied to the adsorption of the colloidal particles onto the hydrochloric acid functionalised CNTs (or vice-vesa) in the coagulation process in this study. An adsorption isotherm relates the concentration of the adsorbing particles in the liquid phase to the concentration in the adsorbent phase at a given temperature (Toor and Jin, 2012).

For determining the adsorption isotherms, the COD was chosen as a study parameter because its unit of mg/L was more convenient. Therefore, in this study, the adsorption isotherms are the equilibrium relationships between the concentrations of the adsorbed COD and COD in solution at a given temperature. Approximately 50 mg of hydrochloric acid functionalised CNTs were added to 100 mL of brewery wastewater. The solutions with initial concentration range of COD of 600-400 mg/L were prepared by proper dilutions from the stock brewery wastewater solutions. As can be seen from Table 3.3, the COD concentration range was chosen so that it is representative of COD levels in this study. The solutions were stirred at 180 rpm in a shaker for a sufficient period of time (~ 24 hours) required to reach equilibrium. Each experiment was replicated four times under identical conditions. The amount of COD adsorbed onto the CNTs at time *t* was determined by mass balance relationsip equation as follows:

$$q_t = C_0 - C_t \; x\frac{V}{m} \qquad (5.3)$$

where q_t is the amount of COD adsorbed onto CNTs (mg/g); C_0 is the initial concentration of COD (mg/L) in the liquid phase; C_t is the concentration of COD at time t (mg/L) in the liquid phase; V is the initial volume of solution (L); and m is the mass of the CNTs (g) added to the solution.

As stated above the Langmuir and the Freundlich models were used to determine the nature of the adsorption mechanism. Langmuir adsorption isotherm is based on the assumption that the molecules of the adsorbate form a monolayer on the surface of the adsorbent (Toor and Jin, 2012). Adjacent adsorbed molecules do not interact, i.e., the adsorption of adsorbate at a particular site is independent whether or not the neighboring sites are adsorbed (Toor and Jin, 2012). Equation (5.4) is a non-linear expression for the Langmuir isotherm, while the linearized expression for the Langmuir isotherm is represented as Equation (5.5).

$$q_e = \frac{q_m K_L C_e}{1 + K_L C_e} \tag{5.4}$$

$$\frac{1}{q_e} = \frac{1}{q_m} + \left(\frac{1}{K_L q_m} \right) \frac{1}{C_e} \tag{5.5}$$

where q_e is the amount of COD adsorbed per unit mass of CNT at equilibrium (mg/g); C_e is the equilibrium concentration of COD in aqeous phase after adsorption has taken place (mg/L); q_m is the maximum amount of COD adsorbed per unit mass of CNT for the formation of complete monolayer on the surface of CNT (mg/g); K_L is the Langmuir constant related to energy of adsorption (L/mg). The q_m and the Langmuir constant can be estimated from the linear plot of $1/q_e$ versus $1/C_e$ (Annadurai et al., 2008; Toor and Jin, 2012).

Freundlich isotherm is applicable to heterogeneous adsorption reactions and involves formation of multilayers (Annadurai et al., 2008; Toor and Jin, 2012). The Freundlich isotherm can be represented as Equation (5.6) or as a linearized Equation (5.7).

$$q_e = K_F C_e^{1/n} \tag{5.6}$$

$$\ln q_e = \ln K_F + \frac{1}{n} \ln C_e \tag{5.7}$$

where K_F and n are the Freundlich constants. The constant n indicates the bond energies between the adsorbate and the adsorbent, whereas K_F is related to bond strength (El-Ashtoukhy et al., 2008). The value of n and K_F can be obtained from the slope and intercept, respectively, of a linear plot of ln (q_e) versus ln (C_e).

The Langmuir constants q_m and K_L as determined from the intercept and slope, respectively, of the plot of $1/q_e$ versus $1/C_e$ (Figure 5.12) are tabulated in Table 5.3. The Freundlich constants obtained from a plot of ln (q_e) versus ln (C_e) (Figure 5.13) and the coefficients of determination (R^2) for the two isotherms are also tabulated in Table 5.3. For the discussion of Figures 5.12 and 5.13, reference should also be made to the experimental data in Appendix C (Table C8). The results in Table C8 are an average of the runs conducted under similar experimental conditions.

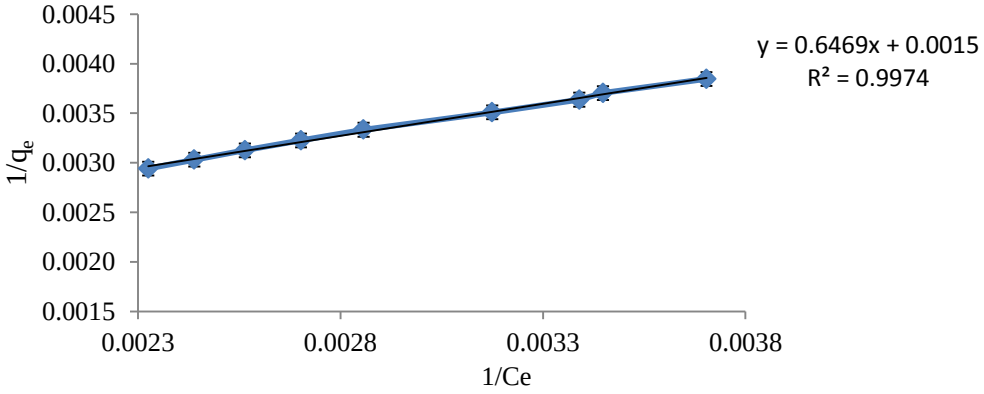


Figure 5.12. Langmuir isotherm plot for COD adsorption onto hydrochloric acid functionalised CNTs.

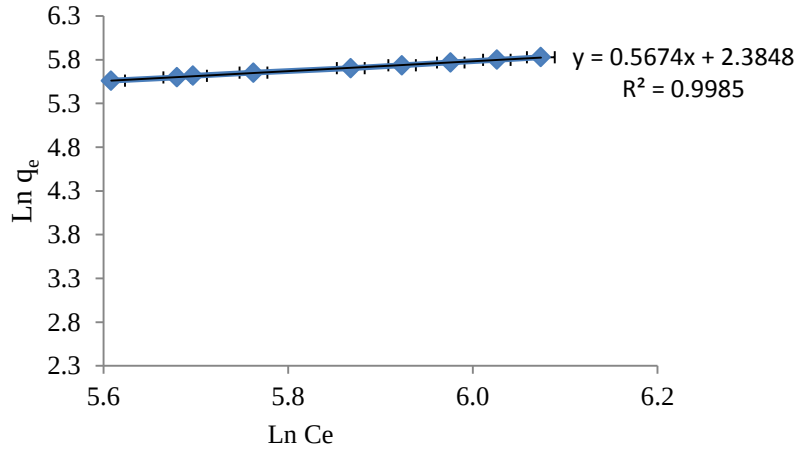


Figure 5.13. Freundlich isotherm plot for COD adsorption onto hydrochloric acid functionalised CNTs.

Table 5.3. Isotherm parameters for the adsorption of COD by functionalised CNTs.

Langmuir				**Freundlich**			
Correlation coefficient R^2	q_m (mg/g)	K_L(L/ mg)	F_{error}	Correlation coefficient R^2	n	K_F (mg/L)	F_{error}
0.9974	6.6667	0.0023	0.0919	0.9985	1.7624	10.8569	0.0034

The results in Table 5.3 (and Figures 5.12 and 5.13) show that the experimental data was better correlated with the Freundlich model than with the Langmuir model. As can be seen from this table, the graph (Figure 5.13) that was plotted from the Freundlich model yielded a straight line with the regression coefficient (R^2) of 0.9985. In contrast, the Langmuir isotherm model (Figure 5.12) was less precise, with lower R^2 value of 0.9974. The value of R^2 is regarded as a measure of the goodness-of-fit of experimental data on the isotherm models (El-Ashtoukhy et al., 2008). However, determination of R^2 alone is not the best way to judge the model's lack of fit (Montgomery, 2005). Therefore, the isotherm models were evaluated further by an error function given in Equation 5.8. It compares the differences in the mount of adsorbate uptaken by the adsorbent using the models to the actual uptake measured experimentally (Arenas et al., 2007).

$$\text{Error function, } F_{error} = \sqrt{\frac{\sum_{i=1}^{N}((q_{i\,model} - q_{i\,experimntal})/q_{i\,experimntal})^2}{N}} \quad (5.8)$$

where q_{imodel} is each value of q predicted by the fitted model and $q_{iexperimental}$ is each value of q measured experimentally, and N is the total number of experients performed.

The lower the error function, the better the fitted model. Thus, the data of COD adsorption on functionalised CNTs represented in Table 5.3 perfectly fit the Freundlich isotherm model because it had a lower error function of 0.0034 compared to that of Langumuir isotherm of 0.0919. This indicates that there is no formation of a COD monolayer on the hydrochloric acid functionalised CNTs. Instead, multilayers are formed due to the heterogeneity nature of the sites and the exponential distribution of sites and their energies (Oladoja et al., 2008). These results are a further confirmation that, indeed, heterogeneous coagulation is occurring between the colloidal particles in brewery wastewater and the hydrochloric acid functionalised CNTs. Moreover, heterogeneous adsorption is one of the two recognised features of interactions between organic compounds and CNTs (Pan and Xing, 2008; Ren et al., 2011). Furthermore, Freundlich isotherm is widely applied in heterogeneous systems especially of organic compounds and highly interactive species on activated carbon and molecular sieves (Ng et al., 2003).

5.3. Challenges and Future Prospects

A lot of challenges arise in attempting to use CNTs in their present state as coagulants or flocculants. Firstly, the CNTs lack dispersion and solubility properties. In recent years, however, there have been several successful attempts to prepare water

soluble CNTs by various techniques (Zhang et al., 2009; Pei et al., 2008), and improvements in their dispersivity through functionalisation (Zhang et al., 2002). However, converting CNTs to complete water soluble form is not recommended since it poses practical difficulties of using them as adsorbent media (Upadhyayula et al., 2009). Nevertheless, dispersivity of CNTs is important because the benefit of water soluble CNTs can be exploited further in the fabrication of CNT composite membranes (Upadhyayula et al., 2009). On the other hand, semi dispersible and partially hydrophobic CNTs exhibit greater affinity towards bacteria than both completely dispersed or weakly dispersed CNTs (Upadhyayula et al., 2009). Secondly, CNTs are very expensive, thus they require to be regenerated after use. If the CNTs are applied in the form of slurry, an efficient separation process downstream such as membrane filtration is needed to retain and recycle the CNTs. Thirdly, and most importantly, CNTs have potential impacts on human health and ecosystems (Moore, 2006; Smart et al., 2006; Wiesner, 2006; Simate et al., 2012b). Whilst in use, CNTs may escape from the treatment system and enter the product water as residual CNTs. It is the residual CNTs that are of concern to human health. The residual CNTs can be ingested into the gastrointestinal tract to various organs through drinking water contaminated with CNTs. Some of the health effects associated with CNTs may include cancer, granulomas and, inflammation and fibrosis, etc (Lam et al., 2006; Simate et al., 2012b).

In view of the apparent human health effects of CNTs, it is important that their use is limited or measures are taken for their removal in water treatment operations. The CNTs may be removed from water using two methods (Simate et al., 2012b). The first method is called membrane filtration, i.e., it constrains the particles by a membrane and the liquid is allowed to flow freely through the membrane. In the second method called ultracentrifugation, the liquid is constrained in a rotating vessel, and the particles move freely within the liquid by an external field of acceleration caused by the ultra-centrifugal field. These methods have been used quite extensively

in the separation of macromolecules and molecules from liquids, and they are also presently becoming important in the separation of nanoparticles from liquids.

5.4 Summary and Conclusions

Research on CNTs has opened new avenues and applications in materials science. This study has demonstrated one other new application of CNTs – heterogeneous coagulation and/ or flocculation of colloidal particles from brewery wastewater. The results have categorically shown that both functionalised and unfunctionalised CNTs can coagulate colloidal particles from brewery wastewater. Previous studies have shown that CNTs are superior sorbents for various contaminants (Upadhyayula, 2009). On the other hand, as stated already, the results of this study have shown that colloidal particles can be removed from brewery wastewater through heterogeneous coagulation. Therefore, by applying positively charged CNTs to brewery wastewater, it is expected that soluble pollutants can be adsorbed as shown from previous studies; and at the same time, colloidal particles can be removed through heterogeneous coagulation, which results from surface charge neutralisation between CNTs and colloidal particles. Prior to surface charge neutralisation, the adsorption of colloidal particles onto hydrochloric acid functionalised CNTs is described better by the Freundlich isotherm.

For effective heterogeneous coagulation and flocculation of brewery wastewater, the pH of the hydrochloric acid functionalised CNTs is supposed to be below 7.3; the PZC. This is advantageous because there will be no residual CNTs dispersed in the treated brewery wastewater, thus preventing the apparent human health risks arising from ingesting CNTs.

The next Chapter deals with the integration of wastewater treatment systems and devices. The study was undertaken using a semi-continuous LSWTP.

References

Amuda, O. S., Alade, A., 2006. Coagulation/flocculation process in the treatment of abattoir wastewater. *Desalination* 196, 22-31.

Annadurai, G., Ling, L. Y., Lee, J. F., 2008. Adsorption of reactive dye from an aqueous solution by chitosan: isotherm, kinetic and thermodynamic analysis. *Journal of Hazardous Materials* 152, 337-346.

Arenas, L. T., Lima, E. C., dos Santos, A. A., Vaghetti, J. C. P., Costa, T. M. H., Benvenutti, E. V., 2007. Use of statistical design of experiments to evaluate the sorption capacity of 1,4-diazoniabicycle (2.2.2) octane/silica chloride for Cr (VI) adsorption. *Colloids and Surfaces* A: *Physicochemical and Engineering Aspects* 297, 240-248.

Assaad, E., Azzouz, A., Nistor, D., Ursu, A. V., Sajin, T., Miron, D. N., Monette, F., Niquette, P., Hausler, R., 2007. Metal removal through synergic coagulation-flocculation using an optimised chitosan-montrollonite system. *Applied Clay Science* 37, 258-274.

Bahr, J. L., Tour, J.M., 2001. Highly functionalized carbon nanotubes using in situ generated diazonium compounds. *Chemistry of Materials* 13, 3823-3824.

Barrera-Díaz, C., Linares-Hernández, I., Roa-Morales, G., Bilyeu, B., Balderas-Hernández, P., 2009. Removal of biorefractory compounds in industrial wastewater by chemical and electrochemical pretreatments. *Industrial and Engineering Chemistry Research* 48 (3), 1253-1258.

Boehm , H.P., 1966. Chemical identification of surface groups. In: Eley, D.D., Pines, H., Weisz, P. B. (Editors), Advances in Catalysis 16. Academic Press, New York, pp. 179-287.

Boehm, H. P, 1994. Some aspects of the surface chemistry of carbon blacks and other carbons. *Carbon* 32 (5), 759-769.

Brukh, R., Mitra, S., 2007. Kinetics of carbon nanotube oxidation. *Journal of Materials Chemistry* 17, 619-623.

Cheng, W. P., Chi, F. H., Yu, R. F., Lee, Y. C., 2005. Using chitosan as a coagulant in recovery of organic matters from the mash and lauter wastewater of brewery. *Journal of Polymers and the Environment* 13 (4), 383-388.

Childress, A.E., Vrijenhoek, E.M., Elimelech, M., Tanaka, T. S., Beuhler, M. D., 1999. Particulate and THM precursor removal with ferric chloride. *Journal of Environmental Engineering* 125 (11), 1054-1061.

Chuang, S.H., Chang, T.C., You, S.J., Ouyang, C.F., 2005. Evaluation of wastewater reclamation processes in a high-tech industrial park. *Desalination* 175, 143-152.

Derjaguin, B. V., Landau, L. D., 1941. Theory of the stability of strongly charged lyophobic sols and of the adhesion of strongly charged particles in solutions of electrolytes. *Acta Physicochimica URSS* 14, 633-662.

Ebeling, J. M., Sibrell, P. L., Ogden, S. R., Summerfelt, S. T., 2003. Evaluation of chemical coagulation-flocculation aids for the removal of suspended solids and phosphorus from intensive recirculating aquaculture effluent discharge. *Aquacultural Engineering* 29, 23-42.

El-Ashtoukhy, E. S. Z., Amin, N. K., Abdelwahab, O., 2008. Removal of lead (II) and copper (II) from aqueous solution using pomegranate peel as a new adsorbent. *Desalination* 223 (1-3), 162-173.

Graupner, R., 2007. Raman spectroscopy of covalently functionalized single-wall carbon nanotubes. *Journal of Raman Spectroscopy* 38 (6), 673-683.

Gregory. J., 2006. Particles in water: properties and processes. IWA Publishing/CRC Press, London.

Heister, E., Lamprecht, C., Neves, V., Tilmaciu, C., Datas, L., Flahaut, E., Soula, B., Hinterdorfer, P., Coley, H. M., Silva, S. R. P., McFadden, J., 2010. Higher dispersion efficacy of functionalised carbon nanotubes in chemical and biological environments. *Nano* 4 (5), 2615-2626.

Jorio, A., Pimenta, M. A., Filho, A.G.S., Saito, R., Dresselhaus, G., Dresselhaus, M.S., 2003. Characterizing carbon nanotube samples with resonance Raman scattering. *New Journal of Physics* 5, 139.1-139.17.

Kuo, C. Y., Lin, H. Y., 2009. Adsorption of aqueous cadmium (II) onto modified multi-walled carbon nanotubes following microwave/chemical treatment. *Desalination* 249, 792-796.

Lam, C.W., James, J.T., McCluskey, R., Arepalli, S., Hunter, R. L., 2006. A review of carbon nanotube toxicity and assessment of potential occupational and environmental health risks. *Critical Reviews in Toxicology* 36 (3), 189-217.

Leon, C. A., Solar, J. M., Calemma, V., Radovic, L. R., 1992. Evidence for the protonation of basal plane sites on carbon. *Carbon* 30 (5), 797-811.

Li, Y. H., Xu, C., Wei, B., Zhang, X., Zheng, M., Wu, D., Ajayan, P. M., 2002. Self-organized ribbons of aligned carbon nanotubes. *Chemistry of Materials* 14, 483-485.

Lin, D.Q., Brixius, P.J., Hubbuch, J.J., Thommes, J., Kula, M.R., 2003. Biomass/adsorbent electrostatic interactions in expanded bed adsorption: A zeta potential study. *Biotechnology and Bioengineering* 83 (2), 149-157.

Lu, C., Su, F., 2007. Adsorption of natural organic matter by carbon nanotubes. *Separation and Purification Technology* 58, 113-121.

Malvern Instruments Ltd (MIL), 2004. Zetasizer nano series user manual. Malvern Instruments Ltd, Worcestershire.

Mandzy, N., Grulke, E., Druffel, T., 2005. Breakage of TiO_2 agglomerates in electrostatically stabilized aqueous dispersions. *Powder Technology* 160, 121-126.

Montgomery, D. C., 2005. Design and Analysis of Experiments. John Wiley and Sons, Inc., New Jersey.

Montes-Moran, M. A., Suarez, D., Menendez, J. A., Fuente, E., 2004. On the nature of basic sites on carbon surfaces: an overview. *Carbon* 42, 1219-1225

Moore, M. N., 2006. Do nanoparticles present ecotoxicological risks for the health of the aquatic environment. *Environmental International* 32, 967-976.

Naseh, M.V., Khodadadi, A.A., Mortazavi, Y., Sahraei, O.A., Pourfayaz, F., Sedghi, S.M., 2009. Functionalisation of carbon nanotubes using nitric acid oxidation and DBD plasma. *World Academy of Science, Engineering and Technology* 49, 177-179.

Ng, J.C.Y., Cheung, W.H., McKay, G., 2003. Equilibrium studies for the sorption of lead from effluents using chitosan. *Chemosphere* 52, 1021-1030.

Oladoja, N. A., Aboluwoye, C. O., Oladimeji, Y. B., 2008. Kinetics and isotherm studies on methylene blue adsorption onto ground palm kernel coat. *Turkish Journal of Engineering and Environmental Sciences* 32, 303-312.

Osorio, A. G., Silveira, I. C. L., Bueno, V. L., Bergmann, C. P., 2008. H_2SO_4/HNO_3/HCl -functionalization and its effect on dispersion of carbon nanotubes in aqueous media. *Applied Surface Science* 255, 2485-2489.

Pan, B., Xing, B., 2008. Adsorption mechanisms of organic chemicals on carbon nanotubes. *Environmental Science and Technology* 42 (24), 9005-9013.

Pei, X., Hua, L., Liu, W., Hao, J., 2008. Synthesis of water-soluble carbon nanotubes via surface initiated redox polymerization and their tribological properties as water-based lubricant additive. *European Polymer Journal* 44, 2458-2464.

Pereira, M.F.R., Soares, S.F., Orfao, J.J.M., Figueiredo, J.L.,2003. Adsorption of dyes on activated carbons: influence of surface chemical groups. *Carbon* 41, 811-821.

Ramesh, B. P., Blau, W. J., Tyagi, P. K., Misra, D. S., Ali, N., Gracio, J., Cabral, G., Titus, E., 2006. Thermogravimetric analysis of cobalt-filled carbon nanotubes deposited by chemical vapour deposition. *Thin Solid Films* 494, 128-132.

Ren, X., Chen, C., Nagatsu, M., Wang, X., 2011. Carbon nanotubes as adsorbents in environmental pollution management: A review. *Chemical Engineering Journal* 170, 395-410.

Rodriguez-Santiago, V., Vidojkovic, S., Fedkin, M. V., Lvov, S. N., and Wesolowski, D. J., 2008. Zeta potential of deposit components at elevated temperatures. Available at http:// www.icpws15.de/papers/06_Electro-07_rodriguez-santiago.pdf. [Accessed: October 2011]

Roussy, J., van Vooren, M., Guibal, E., 2004. Chitosan for the coagulation and flocculation of mineral colloids. *Journal of Dispersion Science and Technology* 25 (5), 663-677.

Rurlle, B., Peeterbroeck, S., Gouttebaron, R.., Godfroid, T., Monteverde, F., Dauchot, J., Alexandre, M., Hecq, M., Dubois, P., 2007. Functionalization of carbon nanotubes by atomic nitrogen formed in a microwave plasma $Ar+N_2$ and subsequent poly(ε-caprolactone) grafting. *Journal of Materials Chemistry* 17, 157-159.

Seo, G. T., Suzuki, Y., Ohgaki, S., 1996. Biological powdered activated carbon (BPAC) microfiltration for wastewater reclamation and reuse. *Desalination* 106, 39-45.

Shieh, Y. T., Wu, H. M., Twu, Y. K., Chung, Y. C., 2010. An investigation on dispersion of carbon nanotubes in chitosan aqueous solutions. *Colloid and Polymer Science* 288, 377-385.

Simate, G. S., Cluett, J., Iyuke, S. E., Musapatika, E. T., Ndlovu, S., Walubita, L. F., Alvarez, A. E., 2011. The treatment of brewery wastewater for reuse: state of the art. *Desalination* 273, 235-247.

Singh, P., Campidelli, S., Giordani, S., Bonifazi, D., Bianco, A., Prato ,M., 2009. Organic functionalisation and characterisation of single-walled carbon nanotubes. *Chemical Society Reviews* 38, 2214-2230.

Simate, G. S., Iyuke, S. E., Ndlovu, S., Heydenrych, M., 2012a. The heterogeneous coagulation and flocculation of brewery wastewater using carbon nanotubes. *Water Research* 46 (4), 1185-1197.

Simate, G. S., Iyuke, S. E., Ndlovu, S., Heydenrych, M., Walubita, L. F., 2012b. Human health effects of residual carbon nanotubes and traditional water

treatment chemicals in drinking water. *Environment International* 39 (1), 38-49.

Smart, S.K.., Cassady, A. I., Lu, G. Q., Martin, D.J., 2006. The biocompatibility of carbon nanotubes. *Carbon* 44, 1034-1047.

Su, F., Lu, C., Hu, S., 2010. Adsorption of benzene, toluene, ethylbenzene and p-xylene by NaOCl-oxidized carbon nanotubes. Colloids and Surfaces A: *Physicochemical and Engineering Aspects* 353, 83-91.

Toor, M., Jin, B., 2012. Adsorption characteristics, isotherm, kinetics, and diffusion of modified natural bentonite for removing diazo dye. *Chemical Engineering Journal* 187, 79-88.

Tripathy, T., Ranjan De, B., 2006. Flocculation: A new way to treat the waste water. *Journal of Physical Sciences* 10, 93-127.

Upadhyayula, V. K. K., Deng, S., Mitchell, M. C., Smith, G. B., 2009. Application of carbon nanotube technology for removal of contaminants in drinking water: a review. *Science of the Total Environment* 408, 1-13.

Verwey, E. J. W., Overbeek, J. T. G., 1948. Theory of the stability of lyophobic colloids. *Journal of Physical Chemistry* 51, 631-636.

Wiesner, M. R., Lowry, G. V., Alvarez, P., Dionysiou, D., Biswas, P., 2006. Assessing the risks of manufactured nanomaterials. *Environmental Science and Technology* 40 (14), 4336-4337.

Zhang, N, Xie, J., Varadan, V. K., 2002. Functionalisation of carbon nanotubes by potassium permanganate assisted with phase transfer catalyst. *Smart Materials and Structures* 11, 962-965.

Zhang, L., Ni, Q-Q., Fu, Y., Natsuki, T., 2009. One-step preparation of water-soluble single-walled carbon nanotubes. *Applied Surface Science* 255, 7095-7099.

Zhou, Y., Franks, G.V., 2006. Flocculation mechanism induced by cationic polymers investigated by light scattering. *Langmuir* 22, 6775-6786.

CHAPTER SIX

TREATMENT OF BREWERY WASTEWATER THROUGH A SEMI-CONTINUOUS LABORATORY SCALE WATER TREATMENT PLANT

"*Theory guides, experiment decides*".

- I. M. Kolthoff

6.1 Introduction

In spite of the size of the brewery plant, the main challenges faced include, (1) the treatment of brewery wastewater efficiently and economically to meet local discharge requirements and/ or in some cases to meet the stringent requirements for reuse, and (2) minimizing their net water consumption during the beer brewing process. These challenges may be addressed by improving and integration of existing processes. Therefore, this Chapter investigates the prospects of treating brewery wastewater by integrating coagulation/flocculation and sedimentation processes with CNTs adsorption in a granular filter bed using a semi-continuous LSWTP. In fact, previous studies have shown that combinations of physico-chemical treatments may be able to remove some organic and inorganic contaminants, including turbidity, COD, arsenic, asbestos fibres, cadmium, chromium, lead, phosphorus, and selenium, etc (Dobias, 1993; Xie et al., 1994; Wickramasinghe et al., 2004; Harrelkas et al., 2009). This Chapter is also aligned with Objective III of this study which assesses the efficacy of using CNTs as adsorptive filter media in granular filtration.

The details of the equipment, experimental setup and procedures followed are outlined in sub-section 3.3.3. The analytical techniques outlined in sub-section 3.4.1 were used to analyse the quality of raw and treated water samples.

6.2. Results and Discussion

This section discusses the results of the various treatment schemes that were adopted during the operation of the semi-continuous LSWTP. In particular, it discusses the following modes of operation:

(i) *Conventional filtration*, which includes addition of coagulants (rapid mixing), flocculation (slow mixing), sedimentation, and filtration;

(ii) *Direct filtration,* in which the sedimentation step is omitted;
(iii) *In-line filtration,* in which both flocculation and sedimentation steps are omitted.

6.2.1. Determination of the optimum dose of ferric chloride coagulant

The optimum dosage of ferric chloride and CNTs were previously determined following the jar tests (Simate et al., 2012). In summary, the following procedure was followed. Exactly 100-mL of brewery waste water was measured into each jar test beaker. The pH was adjusted accordingly using 0.1N HCl or 0.1N NaOH before addition of various dosages of ferric chloride and CNT coagulants. The mixture was then rapidly mixed at 150 rpm for 3 minutes followed by slow mixing at 60 rpm for 20 minutes. Finally it was allowed to settle for 30 minutes. The supernatant (or a filtrate) was then collected and analysed for turbidity and COD.

The results showed that 20 mg/L of ferric chloride was optimum for removal of both turbidity and COD. In the case of CNTs, about 40 - 50 mg/L of CNTs was found to be optimum. However, a mixture of the two (ferric chloride and CNTs) at a constant dosage of 2 mg/L of ferric chloride did not show any significant synergic effect (Simate et al., 2012).

6.2.2. Determination of the optimum loading rate

The loading rate (flowrate normalized by filter cross sectional area) is a significant factor in the control of both the slow and the rapid sand filtration processes (Williams et al., 2007; Tyagi et al., 2009). At the moment, the typical values for loading rates that are used in the design of rapid filters for drinking water lie between 5.0 and 25.0 m^3/m^2 hr inclusive (AWWA and ASCE, 2005). For the treatment of surface water in slow sand filters, filtration rate of 0.1 to 0.32 m^3/m^2 hr is generally recommended.

However, rates of up to 0.6 m^3/m^2 hr have been reported in the literature (Tyagi et al., 2009). The head loss readings (as cm of water) together with the evolution of the outlet hydraulic loading rate through the filter were used to optimise the loading rate to the filter. These two parameters were evaluated in an in-line filtration scheme. Head loss in a filter bed is a valuable indicator of filter bed condition and may be used to automatically activate filter washing (AWWA and ASCE, 2005). Head loss developments were calculated using Equation 6.1.

$$H_L = H_2 - H_1 \quad (6.1)$$

where H_L = head loss (cm), H_1 = first manometer level (cm), and H_2 = second manometer level (cm).

For the purpose of optimisation, the filter was operated at three different loading rates of 5, 7.5, 10 m^3/m^2 hr, i.e., flow rates of 0.03, 0.04, and 0.06 m^3/hr, respectively.

Figures 6.1 shows the effect of the initial hydraulic loading rate to the filter on head loss development over a period of time. For the discussion of Figure 6.1, reference should also be made to the experimental data in Appendix D (Table D1). The results in Table D1 are an average of the runs conducted under similar experimental conditions.

As can be seen from Figure 6.1, head loss development was observed earlier for higher initial flow rates. The trend is as follows in terms of head loss development time: 10 m^3/m^2 hr < 7.5 m^3/m^2 hr < 5 m^3/m^2 hr. Furthermore, head losses increased proportionally with the square of the flow rate as was also observed by Farizoglu et al. (2003) in their studies. The *p*-value of 0.0055 (Table D1) which is less than the significance level of 0.05 suggests the null hypothesis should be rejected. This is an indication that there were statistical differences in at least two of the hydraulic

loading rates, thus confirming the trend in Figure 6.1. As expected, Figure 6.1 also shows that head losses increase with time of operation of the filter. This is because of the progressive reduction in the filter effective surface area as the particulates are deposited onto the filter surface or lodged into the spaces between sand grains (filter *pores*).

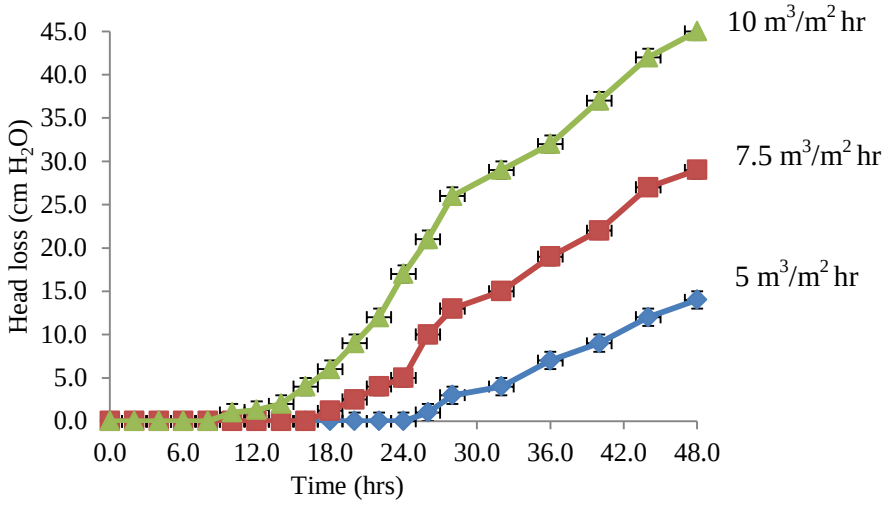


Figure 6.1. Head loss development under various hydraulic loading rates (flow rates). P-value = 0.0055 at the significance level of 0.05.

Figure 6.2 is a picture of a filter *pore*. The filter pore spaces in the media are the most important features of granular media rather than the grain particles (Emerick et al., 1997). Essentially, the treatment of wastewater occurs in the pores where suspended solids are trapped, microorganisms grow, and air and water flow (Emerick et al., 1997). As is the case for rapid sand filters, it can be seen from Figure 6.2 that the particles to be removed are far smaller than the *pores*.

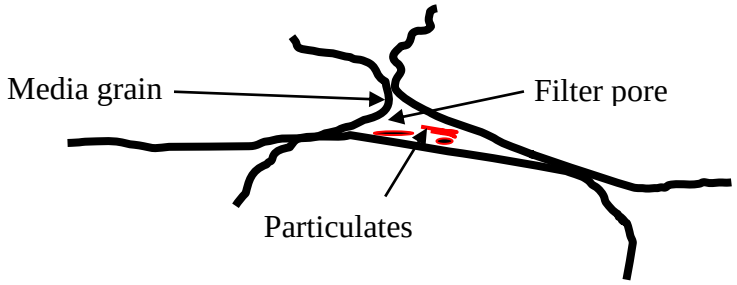


Figure 6.2. Diagram of a granular filter pore showing particles to be filtered.

Figure 6.3 illustrates the effect of the initial hydraulic loading rate to the filter on the outlet hydraulic loading rate over a period of time. For the discussion of Figure 6.3, reference should also be made to the experimental data in Appendix D (Table D2). The results in Table D2 are an average of the runs conducted under similar experimental conditions.

Figure 6.3 shows that the rate of reduction of outlet hydraulic load is more for the higher initial flow rates as can be seen from the slopes of evolution of hydraulic loading rate versus time. This is in agreement with Figure 6.1, which shows that a higher inlet hydraulic loading rate results in a higher head loss hence less outlet hydraulic rate. Furthermore, the ANOVA results in Table D2 show that the differences shown in Figure 6.3 are statistically highly significant (*p*-value of 2.09×10^{-8}) in at least two hydraulic loading rates.

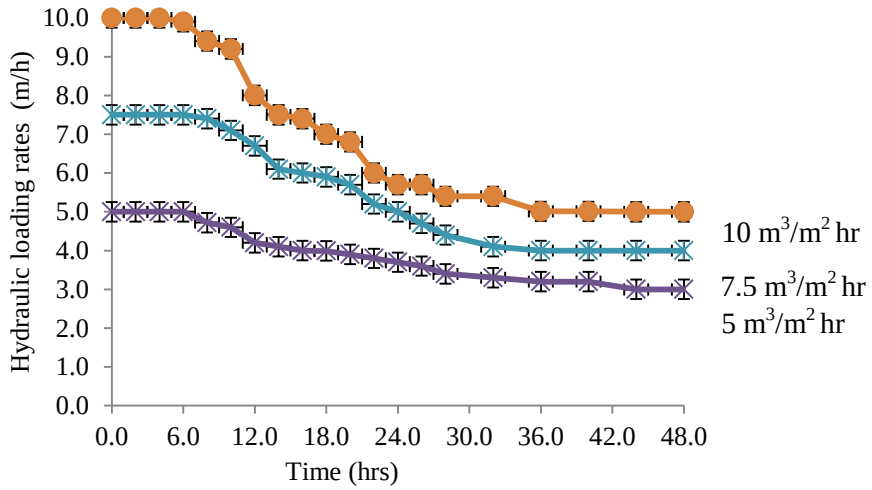


Figure 6.3. The evolution of outlet hydraulic loading rates over time. P-value = 2.09×10^{-8} at the significance level of 0.05.

At the higher initial flow rate, the amount of particles arriving on the filter per unit area (i.e., concentration of particles) is high, thus overloading the filter quickly. These

materials accumulate in the upper layer of filter media and gradually fill the *pores*, thus reducing the permeability. In other words, the impurities on the upper layers and in the *pores* cause surface sealing (or cake formation) and *pore* clogging, respectively. Clogging is considered as the gradual blocking of the pores (or interstices) of the filter media. Clogging reduces the effective area available for water movement, thus increasing the average water retention time in the filter. As a result, clogging and/or surface sealing increases the head losses (Figure 6.1) and reduces the flow of filtrate or the evolution of the outlet hydraulic loading rate (Figure 6.3). These trends have also been observed from other similar studies by other researchers (Tyagi et al., 2009; Achak et al., 2009), thus supporting the results of this study.

Therefore, the lower hydraulic loading rate of 5 m^3/m^2 hr was chosen as an optimum rate because it had the longer running period for the filter due to minimal clogging that resulted into low head losses.

6.2.3. Comparison of different modes of filtration

This sub-section compares the performance of different modes of filtration (conventional filtration, direct filtration and in-line filtration). Turbidity and COD removal including head losses (or outlet hydraulic loading rates) were investigated, and used to assess the performance of the filtration modes. All the filtration modes were operated at the already determined optimum filtration rate of 5 m^3/m^2 hr, and, where applicable, with a ferric chloride dosage of 20 mg/L.

Development of head loss

Figure 6.4 is a plot of the development of the head loss against the time of operation for different modes of the filter at a hydraulic loading rate of 5 m^3/m^2 hr. For the discussion of Figure 6.4, reference should also be made to the experimental data in

Appendix D (Table D3). The results in Table D3 are an average of the runs conducted under similar experimental conditions. From Figure 6.4, it can be seen that head loss development is observed earlier in the direct filtration than in the conventional filtration. The head loss is also found to be higher for direct filtration than for the conventional filtration. In-line filtration had the longest head loss initiation time and the lowest head loss.

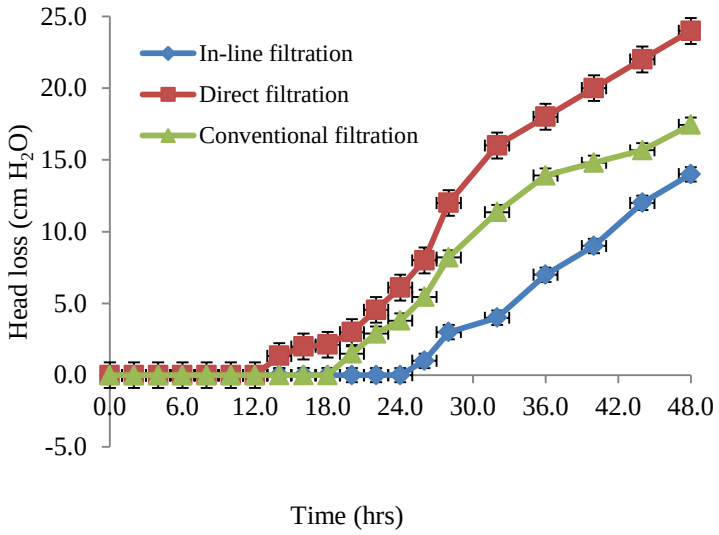


Figure 6.4. Head loss development under various modes of filtration. P-value = 0.1076 at the significance level of 0.05.

The head loss develops early and is higher in magnitude in the direct filtration (flocculated and non-sedimentated) than in the in-line filtration (non-flocculated and non-sedimentated) as a result of large particulates that are produced by coagulation/flocculation, thus enhancing the rate of deposition of the particles onto and within the filter bed. As discussed earlier (see sub-section 6.2.2), the particulate matter lodged in the *pores* lead to size reduction of the *pores* of a filter. Thus, the resistance of the filter bed to the flow of water increases due to the size reduction of the *pores*. Increasing resistance with time increases the head losses. The same effect

is observed when the filter surface is caked with coagulated particulate matter. The small-sized particulates in the non-flocculated and non-sedimentated in-line filtration quickly passed through the filter media with low rate of deposition and retention in the filter *pores*; leading to less head loss. In other words, in the in-line filtration, only a few of the smaller particles are captured in the filter leading to very little head loss during the operation.

As for conventional filtration (flocculated and sedimentated), most of the large flocculated particles settle in the sedimentation basin resulting in less pore clogging or cake layer formation. Therefore, it takes longer time for head loss to develop and also lower head loss is observed than in direct filtration. The order of the initiation time of head loss is as follows: direct filtration < conventional filtration < in-line filtration; and head loss is in the following order: direct filtration > conventional filtration > in-line filtration.

The ANOVA results of the experimental data ploted in Figure 6.4 are shown in Table D3. The value of the test statistic ($F = 2.319$) and its *p*-value of 0.1076 indicate that there was enough evidence to show that non-significant differences exist amongst the modes of filtration. Such values resulted possibly from shorter filter running time. As discussed earlier (sub-section 6.2.2) head losses increase with time of operation of the filter. However, as would be seen in the preeding sub-sections, there was some statistical significance in at least two modes of filtration with respect to turbidity and COD.

Turbidity removal

Turbidity is an important parameter in the water industry that is used in assessing the effectiveness of the filtration process and the quality of drinking water. It is also believed that turbidity serves as a carrier for nutrients and pathogens, which can result

in biological activity (Tyagi et al., 2009). In the brewery industry the major source of turbidity in the brewery wastewater is the cleaning processes.

Figure 6.5 is a plot of the turbidity of the filtrate against the time of operation for various filtration schemes. For the discussion of Figure 6.5, reference should also be made to the experimental data in Appendix D (Table D4). The results in Table D4 are an average of the runs conducted under similar experimental conditions. Initially, the bed was filled (or rinsed) with clean water to minimise channeling. Therefore, for all the filtration modes, Figure 6.5 shows that there was very low turbidity at the beginning of the filtration process. However, as the brewery wastewater pass through the clean bed, its low capability for capturing particles caused the turbidity to reach a maximum rapidly. This observation concurs well with that of Chuang and Li (1997) who found low turbidity at the start of direct filtration, and subsequent maximum turbidity followed. During the filtration of bacteriophages out of tap water by rapid sand filtration the same trend was also observed by Aronino et al. (2009).

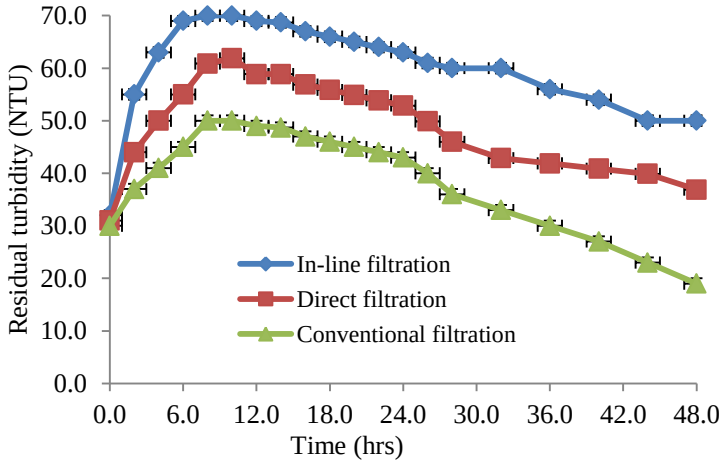


Figure 6.5. Effect of the mode of filtration on removal of turbidity. P-value = 4.58×10^{-9} at the significance level of 0.05.

Figure 6.5 also shows that higher turbidity removal efficiencies were achieved in a conventional filtration (84.2%) mode than in the direct filtration (69.3%). The in-line filtration mode had the lowest turbidity removal efficiency (58.3%). Stastical analysis

also supports the results in Figure 6.5. As can be seen from Table D4 (p-value = $4.58x10^{-9}$), there was enough evidence to infer that there were high significant differences amongst the modes of filtration.

The role of coagulation/flocculation and sedimentation processes in the removal of turbidity may be explained as follows. During coagulation and flocculation, insoluble particles and/or dissolved organic matter interact to form larger and denser particles or flocs. These larger and denser aggregates are then removed by allowing them to settle out of the water naturally under the force of gravity in the subsequent sedimentation stage. Therefore, coagulation/flocculation step followed by sedimentation enhanced the removal of colloidal particulates and other suspensions that cause turbidity.

In the granular filter itself, the removal of particles occurs by two main processes. Firstly, physical straining (or size exclusion) by trapping the particulates matter between the grains of filter media as illustrated in Figure 6.6 (a). Secondly, adsorption, when particulates in the wastewater attach themselves to the filter media or to previously retained particles (Figure 6.6 (b)). The destabilisation of particulates by coagulation and flocculation also enables particles to be attached to the filter media more readily. This is because, almost universally, coagulants carry positive charges and part of their action is undoubtedly the increasing of the particle-grain attachment efficiency by Coulombic attractive forces (Graham, 1988).

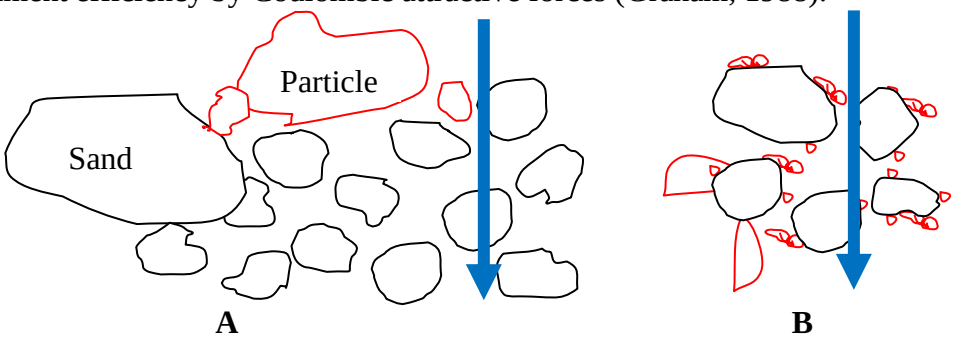


Figure 6.6. Mechanisms of filtration. (a) straining, and (b) adsorption.

The difference in performance between the conventional and the direct filtration processes is due to the fact that the conventional filtration processes use sedimentation to allow particulates to settle out of water for removal, whereas the direct filtration eliminates this step and allows the filter material itself to do the work. However, in the direct filtration some sedimentation will take place on top of the filter, while the main reduction occurs within the filter, thus increasing the filter resistance or head loss as observed in sub-section 6.2.3. Therefore, because all the particles are removed by filtration, the direct filtration is not as efficient as the conventional filtration process.

In the in-line filtration, the brewery wastewater was filtered with no coagulation/ flocculation and sedimentation steps; the resulting filtrate had the highest turbidity compared to the other two modes which provides evidence that without the coagulation/flocculation and sedimentation stages, only little of the fine particles passing through the filter bed can be removed. In other words, because there is no coagulation/flocculation and/or sedimentation stage and that all the particles are removed by filtration, the in-line filtration is not as efficient as the conventional or the direct filtration method.

Chemical oxygen demand removal

Typically, the brewery wastewater has high COD values originating from organic components such as sugars, soluble starch, ethanol, volatile fatty acids, etc, (Goldammer, 2008). The disposal of such wastewater, if untreated (or partially treated), into water bodies can constitute potential or severe pollution problems to the water bodies since the effluents contain organic compounds that require oxygen for degradation (Sarfo-Afriye, 1999; Simate et al., 2011). For example, if water of high organic content value flows into a river, the bacteria in the river will oxidize the organic matter, thus consuming oxygen from the water faster than the oxygen

dissolving back into the river from the air. Brewery wastewater must, therefore, be treated prior to disposal.

The COD of the filtrate from different filtration modes as a function of operation time is given in Figure 6.7. For the discussion of Figure 6.7, reference should also be made to the experimental data in Appendix D (Table D5). The results in Table D5 are an average of the runs conducted under similar experimental conditions. A similar trend to turbidity removal (Figure 6.5) was also observed for the COD removal. Just like turbidity, which is also a physico-chemical parameter, the removal of COD in the filter-bed is believed to occur through the processes of straining (minor) and adsorption (major) by/to filter media and previously removed particulates (Achak et al., 2009; Tyagi et al., 2009).

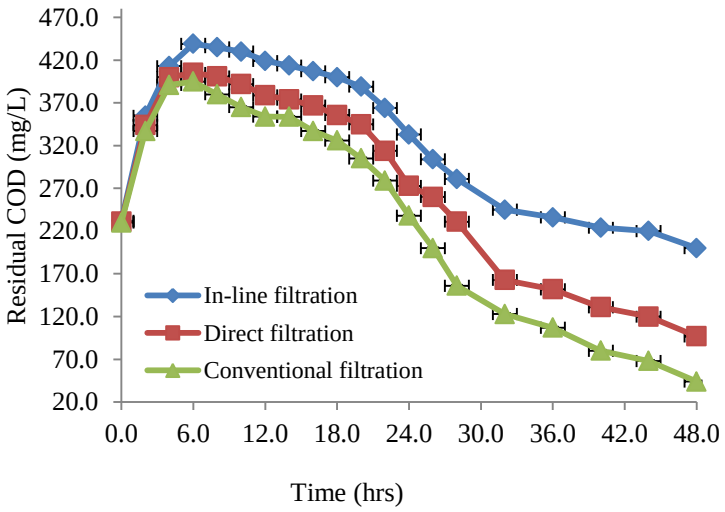


Figure 6.7. Effect of the mode of filtration on removal of COD. P-value = 0.0467 at the significance level of 0.05.

Conventional filtration was found to be the most effective (91.7%) as it removed most of the COD. This is attributed to both the coagulation/flocculation of COD and its subsequent removal in the sedimentation step. As for the in-line filtration, both the

coagulation/flocculation and sedimentation steps are missing, therefore, the removal of the small-size particulates of COD only happens in the filter-bed; hence the least COD removal efficiency (66.7%) observed in the in-line filtration mode. Fisher's *F*-test (F = 3.24) in Table D5 and its *p*-value of 0.0467 show that the data in Figure 6.7 is statistically significant in at least two filtration modes.

6.2.4. Effects of carbon nanotubes

The previous sub-sections have shown that conventional filtration is superior to the other two types (the direct filtration and the in-line filtration) in terms of turbidity and COD removal. Therefore, the effects of CNTs in the subsequent sub-sections will only be applied to conventional filtration operated using the already determined optimum filtration rate of 5 m^3/m^2 hr. As discussed in section 2.4, many unique properties possessed by CNTs make them potential candidates in many applications. In water treatment, functionalised CNTs have been found to have superior adsorption capabilities for various organic and inorganic substances (Upadhyayula et al., 2009), and more recently as heterogeneous coagulants and flocculants (Simate et al., 2012).

This sub-section discusses the results of the addition of CNTs to either the coagulation/flocculation tanks or the filter bed, or to both. For the purpose of this study the treatment schemes are denoted as follows:

(i) scheme A = CNTs added to both the coagulation/flocculation tanks and the filter bed;
(ii) scheme B = CNTs added to the coagulation/flocculation tanks only;
(iii) scheme C = CNTs added to the filter bed only;
(iv) scheme D = no CNTs added.

Development of head loss

Figure 6.8 shows the evolution of head loss in various treatment schemes. For the discussion of Figure 6.8, reference should also be made to the experimental data in Appendix D (Table D6). The results in Table D6 are an average of the runs conducted under similar experimental conditions.

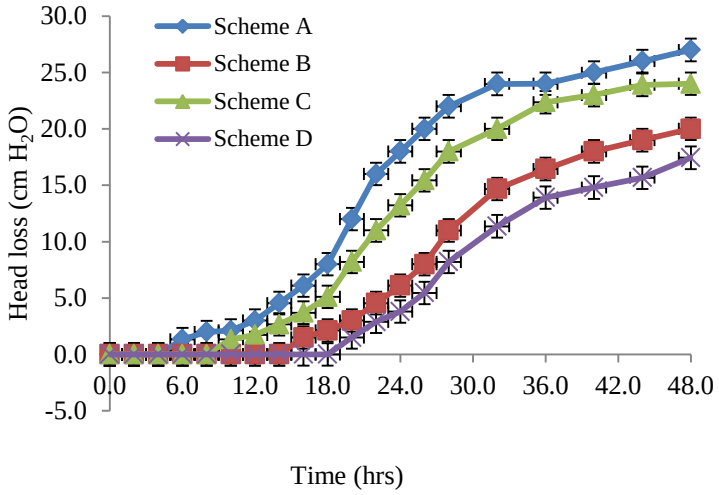


Figure 6.8. Head loss development under various treatment schemes with CNTs. P-value = 0.0350 at the significance level of 0.05.

It can be seen from Figure 6.8 that head loss developed early in treatment scheme A, where CNTs were applied to both the coagulation/flocculation tanks, and the filter bed. This mode also achieved the highest head loss. The CNTs are poorly dispersed in water (see sub-section 5.2.3); therefore, they were carried over from the coagulation/flocculation tanks via the sedimentation basin to the sand filter, where they behaved as solid particulates; covered the filter bed surface, and lodged and reduced filter pores. Thus, the presence of CNTs in the sand grain pores and filter surface together with particulate matter in the brewery wastewater led to an increase in head loss. In addition, the minute pores of a 'sandwiched' bed of CNTs in the filter

were also easily clogged by particulate matter. Head loss for all the four treatment schemes were found to be in the following order; scheme A > scheme C > scheme B > scheme D.

The ANOVA results tabulated in Table D6 (p-value = 0.0350) shows that there was significant difference in at least two of the filtration schemes. This agrees very well with Figure 6.8 which shows different head losses for all the four filtration schemes.

Turbidity removal

The results of the residual turbidity in the filtrate as a function of operation time for various treatment schemes are shown in Figure 6.9. For the discussion of Figure 6.9, reference should also be made to the experimental data in Appendix D (Table D7). The results in Table D7 are an average of the runs conducted under similar experimental conditions.

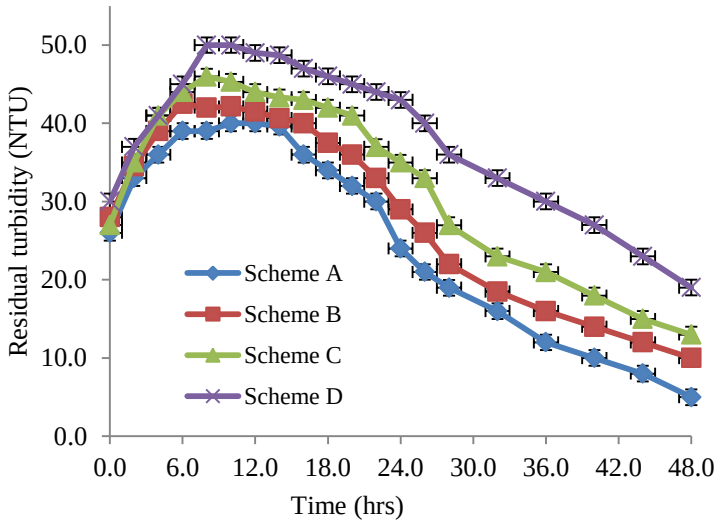


Figure 6.9. Turbidity removal under various treatment schemes with CNTs. P-value = 0.0051 at the significance level of 0.05.

Figure 6.9 shows that the highest turbidity removed is observed in scheme A followed by scheme B. In scheme A, the addition of CNTs to both the coagulation/flocculation tanks and the filter bed enhanced turbidity removal. Comparing schemes B and C, it can be seen that agitation of CNTs and brewery wastewater in the coagulation/flocculation tanks enhanced the removal of particulate matter by the CNTs; hence, the turbidity removal efficiency in scheme B was higher than that in scheme C. This is attributed to effective mixing of CNTs and brewery wastewater that enhanced mass transfer of particulates to the surface of CNTs for adsorption thus leading to an increase in the removal of particulates. Moreover, the addition of CNTs in the coagulation/flocculation tanks acted not only as adsorbents for turbidity, but also as heterogeneous coagulants (Simate et al., 2012). Furthermore, the CNTs in scheme B that escaped onto the filter bed also assisted in further particulate adsorption and straining.

In the filter-bed, the presence of fine particles of CNTs was desirable because of the adsorptive capabilities and the relatively large surface area per unit volume that the fine particle of CNTs provided for particulate matter adhesion. Therefore, the CNTs were instrumental in particulate removal leading to the achievement of low turbidity in the filtrate. The turbidity removal efficiency occurred in the following order; scheme A > scheme B > scheme C > scheme D.

Table D7 is the ANOVA for the data used in Figure 6.9. From the analysis of the table (p-value = 0.0051), it is apparent that the observations in Figure 6.9 are statistically and physically significant in at least two of the filtration schemes.

Chemical oxygen demand removal

Figure 6.10 shows the concentration of COD versus the time of operation of the system. For the discussion of Figure 6.10, reference should also be made to the

experimental data in Appendix D (Table D8). The results in Table D8 are an average of the runs conducted under similar experimental conditions.

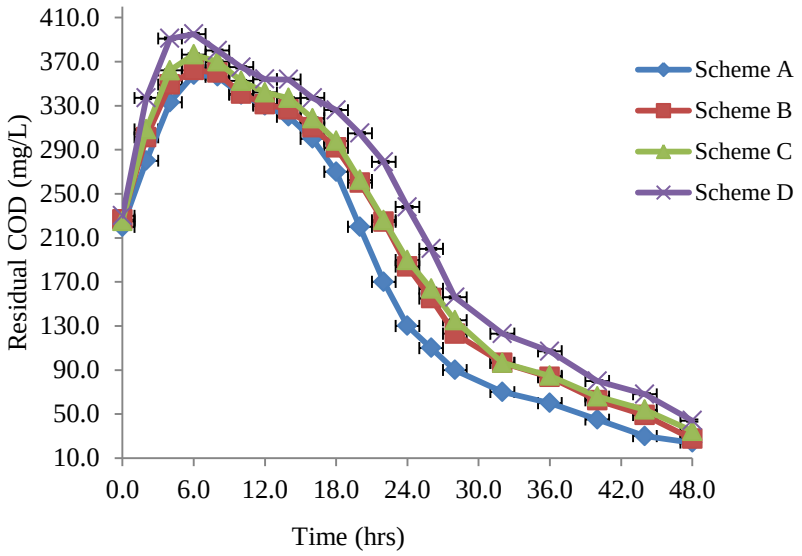


Figure 6.10. COD removal under various treatment schemes with CNTs. P-value = 0.6269 at the significance level of 0.05.

The trend of Figure 6.10 is similar to that of turbidity removal (Figure 6.9). Similarly, the following order of efficiency was observed for the COD removal; scheme A > scheme B > scheme C > scheme D. Comparing turbidity and COD removal efficiencies, it can be concluded that similar mechanisms governed their removal. However, it must be noted that in the coagulation/flocculation tanks, CNTs acted as heterogeneous coagulants (Simate et al., 2011; Simate et al., 2012) and as adsorbents (Upadhyayula et al., 2009). In that case, colloidal matter including organics was removed by heterogeneous coagulation, which results from surface charge neutralisation between CNTs and colloidal particles, whereas soluble components were adsorbed onto CNTs (Suzuki and Chihara, 1988; Simate et al., 2011; Simate et al., 2012).

According to the ANOVA results in Table D8 (p-value = 0.6269), there were no significant differences amongst the filtration modes which is in contrast to the turbidity results shown in Table D7. This can be attributed to high individual COD variations between runs.

6.2.5. Backwashing studies

Backwashing is an important process in the operation of a granular filter; during which the unit is taken off-line, solids removed, and then returned to service. In other words, when the filter's pores become clogged such that there is an increase in pressure, they need to be cleaned. The need for backwashing may be determined using various criteria – a terminal head loss, a fixed time interval, or a breakthrough of solids (when solids begin to pass out with the effluent) (LeChevallier and Au, 2004). In this study, the filter was backwashed using a time interval of 24 hrs of filter operation. Backwashing studies were conducted using scheme D in which conventional filtration was adopted without the use of CNTs.

Head loss development

Figure 6.11 shows the development of head loss before and after backwashing. For the discussion of Figure 6.11, reference should also be made to the experimental data in Appendix D (Table D9). The results in Table D9 are an average of the runs conducted under similar experimental conditions. It can be seen from Figure 6.11 that there was a reduction in head loss after backwashing. This is because of the removal of accumulated solids within the filter bed that created a resistance to flow. The figure also shows that after backwashing, head loss development was gradual implying that backwashing was able to remove particulates within the filter and on the surface of the filter. However, if the particulate removal occurred at the surface only, the head

loss development could have been quite rapid after backwashing (Schuler et al., 1991).

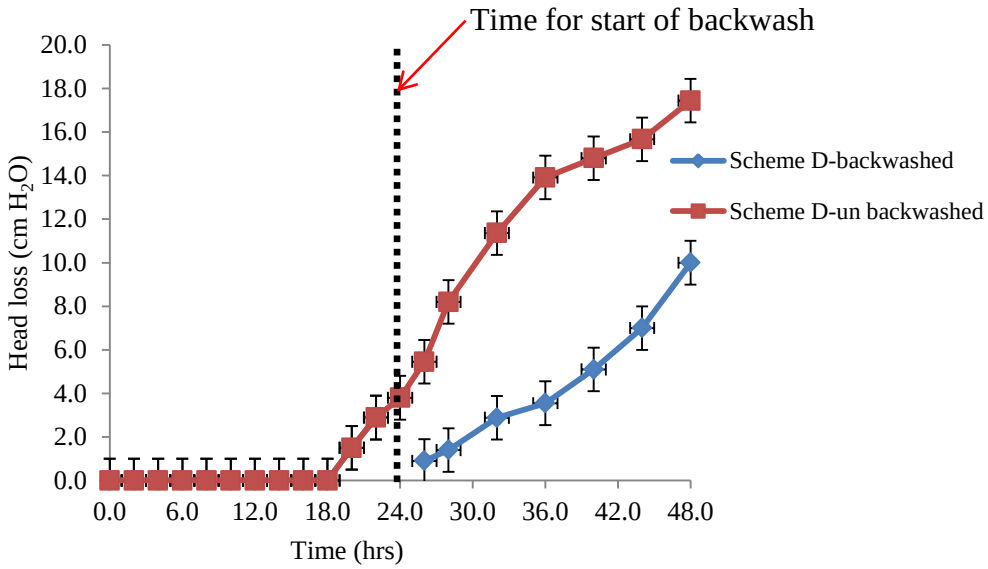


Figure 6.11. Head loss development in backwashed and un-backwashed conventional filtration. P-value = 0.0031 at the significance level of 0.05.

The Student's t-test was used to analyse the experimental data used to plot Figure 6.11. The value of the test statistic (t = 3.08) and its *p*-value (0.0031) in Table D9-2 shows that there is enough evidence to infer that backwashing minimises head losses.

Removal of turbidity and chemical oxygen demand

The percentage of turbidity and COD removed before and after backwashing are shown in Figures 6.12 and 6.13, respectively. For the discussion of Figures 6.12 and 6.13, reference should also be made to the experimental data in Appendix D (Table D10 and D11, respectively). The results in Table D10 and D11 are averages of the runs conducted under similar experimental conditions.

Figures 6.12 and 6.13 show that the removal trends before and after backwashing are similar. However, after backwashing the initial removal for both cases (turbidity and COD) are not as high as that at the start of filtration. This is because the presence of some particulates that remained after backwashing reduced the maturation or 'ripening' period of the granular filter.

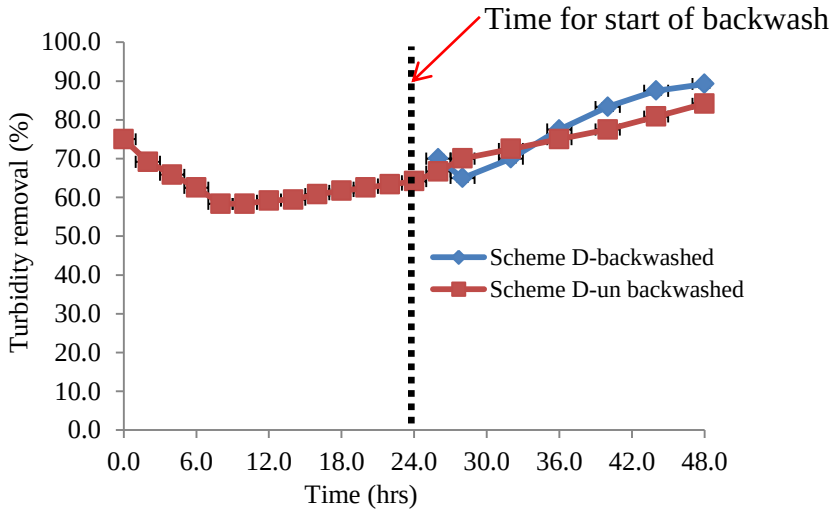


Figure 6.12. Turbidity removal in backwashed and un-backwashed conventional filtration. P-value = 0.1029 at the significance level of 0.05.

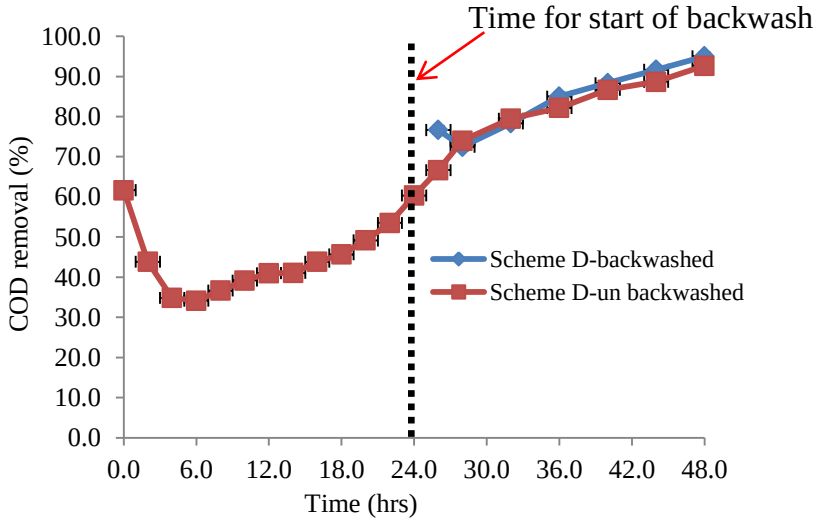


Figure 6.13. COD removal in backwashed and un-backwashed conventional filtration. P-value = 0.0669 at the significance level of 0.05.

From Figures 6.12 and 6.13 it can be seen that an increase in the removal of turbidity and COD were achieved after backwashing the filter, i.e., 5.1% increment and 2.3% increment for turbidity and COD removal, respectively.

Tables D10-2 and D11-2 show ANOVA results for testing the statistical significance of experimental data used to plot Figures 6.12 and 6.13, respectively. As illustrated in the two tables, the ANOVA infers that neither experimental data is statistically significant. This may be attributed to ineffective backwashing as can be seen from the small increments of turbidity (5.1%) and COD (2.3%) removals achieved. As a result there were no significant differences between the residual turbidity or residual COD for un-backwashed and backwashed processes.

6.2.6. Determination of entrained carbon nanotubes in the filtrate

It is possible that during filtration, the CNTs 'sandwiched' in the granular filter may be entrained in the filtrate and, thus pose human health risks as will be discussed in Chapter 7 (Objective IV). It is, therefore, important to monitor and ascertain the amount of CNTs that might escape from the granular filter over time.

To evaluate the amount of the entrained CNTs, the granular filter filtrate was analysed under the UV-Visible double beam spectrophotometer (Unico spectrophotometer model 4802) at 600 nm. Unlike the bundled CNTs that are not active in the UV-visible region, the individual CNT tubes absorb ultraviolet and visible radiation in this region (Rastogi et al., 2008). Therefore, the UV-Visible absorption spectroscopy was appropriately chosen to characterise any entrained functionalised CNTs. This study was conducted using scheme A, i.e., CNTs were added to both the coagulation/flocculation tanks and the granular filter bed.

The methodology used here for determining the concentration of CNTs in filtrate is an extension of the one already described in sub-section 3.4.2 (determination of

dispersion stability of CNTs). Initially, several different concentrations of CNTs in 'clear filtrate' ranging from 0 to 50 mg/L in steps of 5 mg/L were prepared by stirring with a magnetic stirrer. For each sample, the absorption spectrum was measured against 'clear filtrate' as a reference. The concentrations (in mg/L) of CNTs in conjunction with the absorbance at 600 nm allowed preparation of the plot shown in Figure 6.14. Therefore, Figure 6.14 shows the Beer-Lambert dependence of absorption at 600 nm on the concentration of CNTs. For the discussion of Figure 6.14, reference should also be made to the experimental data in Appendix D (Table D12). The results in Table D12 are an average of the runs conducted under similar experimental conditions. Subsequently, Figure 6.14 was used to determine the concentrations of entrained CNTs in the filtrate from the granular filter 'sandwiched' with CNTs over a period of time.

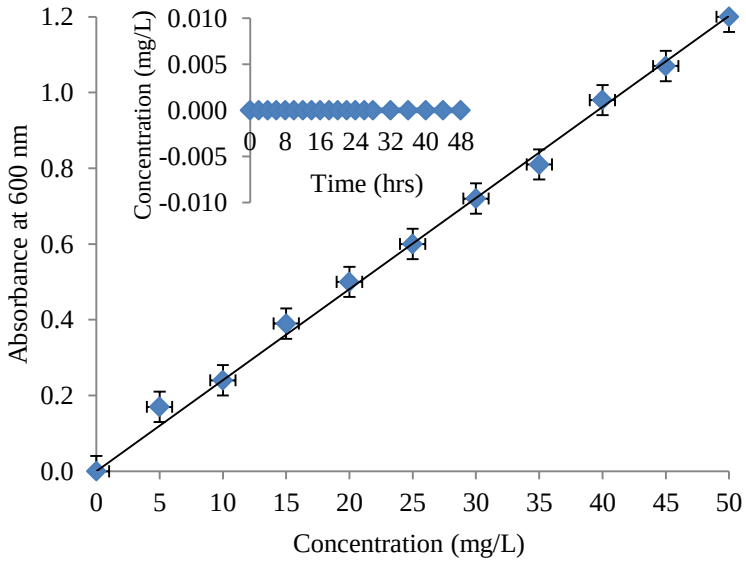


Figure 6.14. Optical density at 600 nm as a function of the concentration of CNTs.

The results of the concentration of entrained CNTs in filtrate as a function of operation time are shown in the insert to Figure 6.14. For the discussion of Figure

6.14 insert, reference should also be made to the experimental data in Appendix D (Table D13). The results in Table D13 are an average of the runs conducted under similar experimental conditions. As can be seen from Figure 6.14 insert, during the 48 hours period in which the granular filter was operated, there were no CNTs detected in the filtrate. This is attributed to, (1) CNTs's lack of dispersion, and (2) 'sandwiching' of CNTs in the filter bed. The lack of dispersion means that the CNTs that escaped from the coagulation/flocculation tanks were easily strained by the filter bed. Furthermore, the 'sandwiching' of CNTs in between two layers of sand also meant that CNTs could not escape from the filter bed.

These results are a good assurance that the filtrate from the semi-continuous LSWTP is safe because of the absence of entrained CNTs. However, as meantioned above, a discussion of the apparent human health riks of CNTs in drinking water is presented in Chapter 7. In particular, Chapter 7 uses available literature to give a qualitative comparison of the human health effects of residual CNTs and traditional water treatment chemicals.

6.3. Summary of Results

Table 6.1 is a summary of the results of the studies conducted after 48 hours, showing the treatment schemes, their makeup, and a range of turbidity and COD reductions obtained. From the table, it can be seen that coagulation/flocculation and sedimentation steps play an important role in the removal of turbidity and COD. It can also be seen that the presence of CNTs enhances the removal of turbidity and COD; and the stage at which CNTs are added to the water treatment process is also paramount.

Table 6.1. Summary of results of different treatment schemes.

Treatment schemes	Reductions (%)	
	Turbidity	COD
In-line filtration	58.3	66.7
Direct filtration	69.3	83.9
Conventional filtration only	84.2	92.7
Conventional filtration only (backwashed)	89.3	95.0
Conventional filtration with carbon nanotubes 'sandwiched' in filter bed	89.2	94.2
Conventional filtration with carbon nanotubes in coagulation/flocculation tanks	91.7	95.4
Conventional filtration with carbon nanotubes in coagulation/flocculation tanks and 'sandwiched' in filter bed	95.9	96.0

6.4. Summary and Conclusions

This study developed and applied a series of experimental procedures to investigate the effectiveness of integrating coagulation/flocculation, sedimentation and granular filtration for turbidity and COD removal from brewery wastewater. Several treatment schemes were evaluated, and the major findings of this study are summarised as follows:-

(1) The presence of coagulation/flocculation and sedimentation steps improved the efficiency of the granular filter as observed from reduction in the head loss, residual turbidity and residual COD.

(2) The addition of CNTs in the coagulation/flocculation tanks resulted in better turbidity and COD removal than 'sandwiched' CNTs in the filter bed. This is attributed to effective mixing of CNTs and brewery wastewater that enhanced mass transfer of particulates to the surface of CNTs for adsorption thus leading to an increase in the removal of particulates. Moreover, the addition of CNTs in the coagulation/flocculation tanks acted not only as adsorbents for turbidity and COD, but also as heterogeneous coagulants.

(3) The results of the study have demonstrated that treatment scheme in which CNTs are added to both the coagulation/flocculation tanks and the filter bed is the best option for the treatment of brewery wastewater.

(4) No entrained CNTs were detected in the filtrate which gives a good assurance that the filtrate from the semi-continuous LSWTP is safe.

The next Chapter is a review of the available literature and qualitatively compares the the human health effects of residual CNTs to traditional water treatment chemicals.

References

Achak, M., Mandi, L., Ouazzani, N., 2009. Removal of organic pollutants and nutrients from olive mill wastewater by a sand filter. *Journal of Environmental Management* 90, 2771-2779.

American Water Works Association (AWWA) and American Society of Civil Engineers (ASCE), 1998. Water Treatment Plant Design. McGraw-Hill, New York.

Aronino, R., Dlugy, C., Arkhangelsky, E., Shandolov, S., Oron, G., Brenner, A., Gitis, V., 2009. Removal of viruses from surface water and secondary effluents by sand filtration. *Water Research* 43, 87-96.

Chuang, C. J., Li, K. Y., 1997. Effect of coagulant dosage and grain size on the performance of direct filtration. *Separation and Purification Technology* 12, 229-241.

Dobias, B., 1993. Coagulation and flocculation. Marcel Dekker, New York

Emerick, R. W., Test, R. M., Tchobanoglous, G., Darby, J., 1997. Shallow intermittent sand filtration: performance evaluation. *Small Flows Journal* 3 (1), 12-22.

Farizoglu, B., Nuhoglu, A., Yildiz, E., Keskinler, B., 2003. The performance of pumice as a filter bed material under rapid filtration conditions. *Filtration and Separation* 40 (3), 41-47.

Goldammer, T., 2008. The Brewers' Handbook, 2nd edition. Apex Publishers, Clifton.

Graham, N. J. D., 1988. Filter pore flocculation as a mechanism in rapid filtration. *Water Research* 22 (10), 1229-1238.

Harrelkas, F., Azizi, A., Yaacoubi, A., Benhammou, A. Pons, M. N., 2009. Treatment of textile dye effluents using coagulation-flocculation coupled with membrane processes or adsorption on powdered activated carbon. *Desalination* 235, 330-339.

LeChevallier, M. W., Au, K. K., 2004. Water treatment and pathogen control: process efficiency in achieving safe drinking water. IWA Publishing, London.

Rastogi, R., Kaushal, R., Tripathi, S. K., Sharma, A. L., Kaur, I., Bharadwaj, L. M., 2008. Comparative study of carbon nanotube dispersion using surfactants. *Journal of Colloid and Interface Science* 328, 421-428.

Sarfo-Afriye, Y., 1999. A Study of Industrial Waste Management in Kumasi (Case Study), Kumasi Breweries Limited, The Coca-Cola Bottling Company of Ghana.

Schuler, P. F., Ghosh, M. M., Gopalan, P., 1991. Slow sand and diatomaceous earth filtration of cysts and other particulates. *Water Research* 25 (8), 995-1005.

Simate, G. S., Cluett, J., Iyuke, S. E., Musapatika, E. T., Ndlovu, S., Walubita, L. F., Alvarez, A. E., 2011. The treatment of brewery wastewater for reuse: state of the art. *Desalination* 273, 235-247.

Simate, G. S., Iyuke, S. E., Ndlovu, S., Heydenrych, M., 2012. The heterogeneous coagulation and flocculation of brewery wastewater using carbon nanotubes. *Water Research* 46 (4), 1185-1197.

Suzuki, M., Chihara, K., 1988. Heterogeneous coagulation of organic colloid and powdered activated carbon. *Water Research* 22 (5), 627-633.

Tyagi, V. K., Khan, A. A., Kazmi, A. A., Mehrotra, I., Chopra, A.K., 2009. Slow sand filtration of UASB reactor effluent: A promising post treatment technique. *Desalination* 249, 571-576.

Upadhyayula, V. K. K., Deng, S., Mitchell, M. C. & Smith, G. B., 2009. Application of carbon nanotube technology for removal of contaminants in drinking water: a review. *Science of the Total Environment* 408, 1-13.

Williams, G. J., Sheikh, B., Holden, R. B., Kouretas, T. J., Nelson, K. L.., 2007. The impact of increased loading rate on granular media, rapid depth filtration of wastewater. *Water Research* 41, 4535-4545.

Xie, W., Kondo, M., Naito, Y., 1994. Study of phosphorus removal using a new coagulation system. *Water Science and Technology* 30, 257-262.

CHAPTER SEVEN

COMPARISON OF HUMAN HEALTH EFFECTS OF CARBON NANOTUBES AND TRADITIONAL WATER TREATMENT CHEMICALS

"*There are known knowns. These are things we know that we know. There are known unknowns. That is to say, there are things that we know we don't know. But there are also unknown unknowns. These are things we do not know we don't know".*

- Donald Rumsfeld (former USA Secretary of Defence on the war against terrorism)

7.1. Introduction

The production of clean and safe drinking water is vital for the whole society. This is because water of poor quality impacts adversely on human health. It is, therefore, recommended that any chemical used in, on, or near drinking water sources, or used during the treatment of drinking water should, (1) not present a public health concern, and (2) not result in the chemical, its by-products, or any contaminants exceeding drinking water guideline values as provided by the WHO (NHMRC-NRMMC, 2011; Simate et al., 2012).

This Chapter brings together data derived from a number of distinct studies, and critically analyses and compares the human health effects of CNTs to those of traditional water treatment chemicals – alum, ferric chloride, chlorine, copper sulphate, and fluoride. The Chapter provides answers to the questions raised by Objective IV of this thesis.

7.2 Discussion of Literature Reviewed

7.2.1 Human health effects of residual carbon nanotubes

The industrial production and rapidly emerging potential applications of CNTs in many fields including water treatment and purification are a welcome discovery. However, this may be offset by the concern that CNTs are toxic and may become a new class of hazardous pollutants that threaten public health if accidentally or incidentally released to the environment including drinking water. Therefore, understanding the human health effects of CNTs is of paramount importance.

To start with, biologically relevant effects of CNTs and other engineered nanomaterials (ENMs) can only occur if, firstly, they can enter the body or a

biological system, and secondly, at a sufficient level (Som et al., 2011). Thirdly, they have to have the potential to influence biochemical/cell biology processes and to have a direct or indirect effect on the biological system (Som et al., 2011).

Research has shown that CNTs are able to enter the body through the skin, respiratory tract or gastrointestinal tract, depositing themselves in several organs within the body and may thus cause many adverse biological effects (Davoren et al., 2007; Hoet et al., 2004; Lam et al., 2004; Oberdörster et al., 2005; Warheit et al., 2004). Of particular interest in this study is the gastrointestinal route. This is because any ingested CNTs would pass through the intestinal tract. Ingestion can occur from unintentional hand to mouth transfer of materials or as a consequence of swallowing inhaled material following mucociliary clearance (Aschberger et al., 2011; Simkó et al., 2010). The CNTs can also be ingested into the gastrointestinal tract through drinking water contaminated with CNTs (Simate et al., 2012). This later method in which CNTs may be ingested into the gastrointestinal tract by drinking contaminated water is a focus of this study. Though there is limited research in this area, analogues can be drawn from other portal routes and from the studies of other ENMs.

Gastrointestinal exposure

Following ingestion and as shown in Figure 7.1, four different pathways by which particles such as CNTs can translocate into and across the gastrointestinal mucosa include the following: (1) endocytosis through ‘regular’ epithelial cells, (2) M-cell-uptake (transcytosis) at the surface of intestinal lymphoid aggregates, (3) persorption, and (4) putative paracellular uptake (Powell et al., 2010).

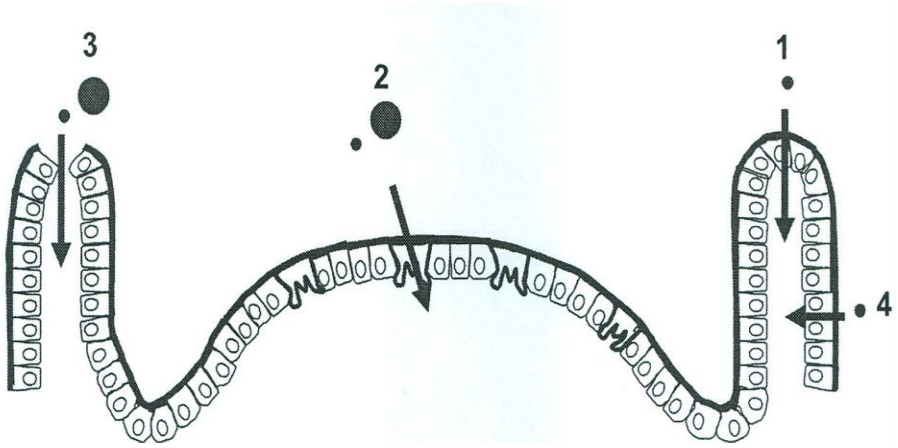


Figure 7.1. Summary of particles translocation across the gastrointestinal tract (Powell et al., 2010).

Endocytosis. Although the main function of the regular epithelial cells (enterocytes) is to absorb and transport nutrients for systemic dissemination and optimal cell function, there are some data showing that they can also take up material in the nano-range via endocytosis (Powell et al., 2010).

Transcellular route. This is the most documented and common route of uptake for both nano- and micro-particles (Powell et al., 2010). This route describes the process by which particles are taken up at the apical side of the intestinal epithelium (by endocytosis), are transported through the M-cells in the Peyer's Patches (small intestinal lymphoid aggregates) and/or the enterocytes and subsequently released at the basolateral side of the intestinal epithelium (Bouwmeeste et al 2009). The M-cells are specialised, differentiated epithelial cells, which have an avid appetite for the transcytosis of macromolecules and particles (Powell et al., 2010), and are able to pass intact material from the lumen to abutting/interlocking mononuclear cells. Specific CNTs characteristics, such as particle size, the surface charge of particles, attachment of ligands or coating with surfactants, may influence the transcellular uptake of particles in the gastrointestinal tract (Bouwmeeste et al 2009). If the

encapsulates or CNTs are protected/ prevented from local degradation or metabolism due to the modification, they will enter both the blood and lymphoid circulation intact (Bouwmeeste et al 2009) and can be further distributed in the body thus affecting human health.

Persorption. This is a third possible route for translocation of particles, which has been widely described by Volkheimer (Volkenheimer and Schulz, 1968; Volkheimer, 1974; Volkheimer, 1993). Persorption is the term used to describe the passage of particles from the intestinal lumen through gaps in the mucosa and into the general circulation (Freedman, 1991). However, persorption is unlikely to be highly efficient (Powel et al., 2010) because it is limited to materials with diameters of less than 0.005 µm (5nm) (Weiner, 1988). As already stated in section 2.4, the sizes of CNTs range from 1-100 nm.

Paracellular route. This is the final possible route where nanoparticles pass between the cells. It is possible that under certain conditions, very small nanoparticles can gain access to the gastrointestinal tissue via paracellular transcytosis across tight junctions of the epithelial cell layer (Powell et al., 2010). In other words, though cells of the gastrointestinal epithelium are tightly connected to each other by means of tight junctions, the permeability of the tight junctions can be modulated, for instance, by specific functional groups on the CNTs (e.g., polymers). These polymers can act as expanders for the tight junctions, thereby introducing a port of entry for many particles including toxins, bacteria, and immunogens (Salamat-Miller and Johnston, 2005). Therefore, passage of CNTs (and nanoparticles in general) via tight junctions cannot be excluded beforehand; they should be considered by risk assessors (Bouwmeeste et al 2009). In fact, there is a body of evidence which indicates that the intestinal epithelium is permeable to large proteins and polypeptides (Bouwmeeste et al 2009).

General toxicological effects of CNTs

Current studies on the toxicological and environmental effects of nanomaterial are still scarce (Jia et al., 2005). Contradictory reports on cytotoxicity of CNTs often appear in the literature and a mechanistic explanation of the reported toxicity remains obscure (Kang et al., 2008; Hussain et al., 2009). Some of these contradictions are attributed to the use of CNTs with different purities and functional groups, different cell culture media, and a variety of cell types (Kang et al., 2008). Furthermore, the other major and recurring problem encountered by researchers in the investigation of CNT toxicity and biocompatibility is the tendency of CNT to aggregate in large bundles and ropes, i.e., lack of dispersion (Smart et al., 2006). Indeed, it is very likely that a large portion of the discrepancies in toxicity and biocompatibility data are due to differences in CNT dispersion, the factor that ultimately dictates the presentation of CNT to the cells (Smart et al., 2006). The CNTs dispersion depends upon a number of factors, such as the type of CNTs, their geometry, the presence of surface chemical state as well as the type of surfactants (Fraczek-Szczypta et al., 2011).

However, there are three generally accepted factors, which determine the potential of a particle to cause harm (Smart et al., 2006): Firstly, the surface area/mass ratio of the particle - a large surface area gives the particle(s) a greater area of contact with the cellular membrane, as well as a greater capacity for absorption and transportation of toxic substances. For example, according to Auffan et al (2008), nanosize particles have an elevated surface/volume ratio of approximately 35-40% of atoms localized at the surface of a 10 nm nanoparticles compared with less than 20% for particles larger than 30 nm. Secondly, the particle retention time - the longer the particle stays in contact with the cellular membrane the greater the chance for damage. This factor also incorporates the concept of particle mobility, either through clearance or migration to the surrounding tissues. Thirdly, the reactivity or inherent toxicity of the chemical(s) contained within the particle. For example, untreated CNTs contain the

nanoparticles of transition metals such as iron and nickel, which are used as catalysts in the synthesis of CNTs. These nickel-containing CNTs have been reported to be toxic (Lam et al., 2004).

Irrefutably, CNTs have been shown to be toxic to cells when used as a suspension in cell culture media in any given experiment, while they appear as nontoxic if immobilized to a matrix or to a culture dish (Hussain et al., 2009; Chigumbu, 2011; Iyuke et al., 2012). However, the bottom line is that CNTs may cause adverse human or environmental health effects; therefore, further studies are necessary to determine their impact. In fact, the properties that make CNTs attractive for numerous applications may also make them a potential health risk concern. Recent studies have actually shown that the biopersistence of CNTs may limit their potential usage in systems having a direct impact on public health such as drinking water treatment (Upadhyayula et al., 2009).

As alluded to earlier, once CNTs enter the body either through the gastrointestinal tract or any other route, they can deposit themselves in several organs within the body and may thus cause many adverse biological effects. Some of the health effects associated with CNTs may include cancer, granulomas, inflammation and fibrosis, etc (Lam et al., 2006; Simate et al., 2012).

Given below are results of specific cytotoxicity and genotoxicity studies of CNTs.

***Cytotoxicity*.** The accurate study of cytotoxicity, the degree to which an agent possesses a specific destructive action on certain cells, is very important. Recent research has shown that CNTs have multiple effects on mammalian cell systems (Upadhyayula et al., 2009). It is also found that the toxicity of CNTs on mammalian cells is greater than quartz (Dreher, 2004; Jia et al., 2005) and asbestos (Wick et al., 2007). In general, the cytotoxicity effects of CNTs depend on inherent physical and

chemical properties, such as their structure, length and size distribution, aspects ratio, surface area, shape, degree of dispersion and aggregation, agglomeration state, presence of amorphous impurities, extent of oxidation, bound functional group, method of manufacturing, metal impurities, coating, concentration and dose, immobilization, cellular uptake or internalization and cytotoxic response of different cell types to CNTs as well, among others (Helland et al., 2007; Auffan et al., 2008; Hussain et al., 2009; Upadhyayula et al., 2009; Simkó et al., 2010; Stellaa, 2011). For example, small and round particles appear to be taken up easily and penetrate the tissues easily compared to long and fibre-like particles (Som et al., 2011), and well-dispersed SWCNTs were less cytotoxic than micrometer-size agglomerates of SWCNTs (Wick et al., 2007).

Experiments with well-characterized SWCNTs and MWCNTs demonstrated that SWCNTs are much more toxic to bacteria than MWCNTs (Kang et al., 2008). The enhanced bacterial toxicity of SWCNTs may be attributed to the following (Kang et al., 2008), (1) a smaller nanotube diameter that facilitates the partitioning and partial penetration of nanotubes into the cell wall, (2) a larger surface area for contact and interaction with the cell surface, and/or (3) unique chemical and electronic properties conveying greater chemical reactivity. In pulmonary cytotoxicity studies, Jia et al. (2005) showed that the cytotoxicity apparently follows SWCNTs > MWCNTs > quartz > fullerenes. Wang and co-workers reported that MWCNTs of smaller diameters showed less cytotoxicity than the larger ones at the same dosage (Wang et al., 2009). These results, therefore, indicate that MWCNTs of different diameters exhibit quite different cytotoxicity.

***Genotoxicity*.** In genetics, genotoxicity refers to the destructive action on a cell's genetic material (DNA, RNA) thus affecting its integrity. At present, only a few studies on the genotoxicity of CNTs have been published. A few studies using intraperitoneal and intrascrotal exposure showed that long straight MWCNTs (>5

μm) could behave in a similar manner to asbestos and have the potential to induce mesotheliomas in mice and rats (Aschberger et al., 2011). No carcinogenic effects were observed following intraperitoneal injection of short MWCNTs (<5 μm) (Muller et al., 2009; Aschberger et al., 2011), which could be explained by the ability of phagocytes to ingest them and a mechanism of particle clearance from the pleura, which may fail for long fibres (Donaldson et al., 2010; Aschberger et al., 2011).

Patlolla et al. (2010) investigated the toxicity of purified MWCNTs in normal human dermal fibroblast cells using cell viability, DNA damage and apoptosis as the toxicological endpoints. The results obtained indicated a significant increase in cytotoxicity, genotoxicity and apoptosis in the normal human dermal fibroblast cell line, due to exposure to MWCNTs. Zhu et al. (2007) assessed the DNA damage response to MWCNTs in mouse embryonic stem cells. They found that MWCNTs can accumulate and induce apoptosis in mouse embryonic stem cells and activate the tumor suppressor protein. A mutagenesis study using an endogenous molecular marker, adenine phosphoribosyltransferase, showed that MWCNTs increased the mutation frequency by 2-fold compared with the spontaneous mutation frequency in mouse embryonic stem cells (Zhu et al., 2007). The CNTs which were predominantly single-walled were found to be genotoxic in human bronchial epithelial cell line exhibiting an epithelial phenotype, as measured by the alkaline comet assay and the micronucleus assay (Lindberg et al., 2009).

Several hypotheses have been suggested to account for the genotoxic effects of MWCNTs, including the formation of adduct and/or damage at the level of DNA or chromosomes (Patlolla et al., 2010). A direct interaction between the particles and the genetic material should also be considered (Zhu et al., 2007; Patlolla et al., 2010). This possibility is supported by the data reported by Li et al (2005) suggesting that CNT are efficient in interacting with biomolecules with similar dimensions such as DNA.

7.2.2 Human health effects of residual traditional water treatment chemicals

In the production of drinking water, a number of different chemicals may be added to the water for various purposes during the treatment process. Table 7.1 shows some common traditional chemicals that are used in the treatment of drinking water. The uses of some of these chemicals have already been discussed in sub-section 2.3.4.

Table 7.1. Some common traditional chemicals recommended for use in the treatment of drinking water (NHMRC-NRMMC, 2011; Simate et al., 2012).

Treatment chemical	**Formula**	**Uses**
Aluminium sulphate (alum)	Al_2SO_4	coagulation
Ferric chloride	Fe_2Cl_3	coagulation
Chlorine	Cl_2	Disinfection/oxidation
Copper sulphate	$CuSO_4$	Algicide, fungicide
Fluoride	F^-	Fluoridation

The sub-sections below provide a description of the chemicals listed in Table 7.1, along with their human health effects.

Alum

Alum (or aluminium constituents) is one of the common traditional coagulants. In particular, aluminium is the third most abundant element in the earth's crust (Imandel et al., 1994), and the most abundant metal (Simate et al., 2012). However, it is not an essential trace element for mammals (Bondy, 2010). It occurs naturally and may be present in water due to natural leaching of the soil and rocks. It can also be present as a residual from the use of alum and other derivatives that are widely used as traditional coagulants and /or flocculants in water treatment. It is present in drinking water in a low molecular mass form that is labile (i.e., chemically reactive) (Nieboer et al., 1995).

In order for aluminum to have health effects it has to be absorbed into the human body. However, aluminium is very poorly absorbed in the gastrointestinal tract, though the possibility that some aluminium fractions present in drinking water may be particularly bioavailable cannot be dismissed (Flaten, 2001).

Nevertheless, previous and current research has associated high dosages of residual aluminium salts in water with the Alzheimer's disease (AD) – the most common form of dementia (McLachlan, 1995; Ndabigengesere and Narasiah, 1998; Simate et al., 2012). Dementia (brain disorder) is a general term for memory loss and other intellectual abilities (e.g., thinking, disorientation, confusion, trouble expressing thoughts, etc) serious enough to interfere with daily life (Thompson, 2009). There is also evidence that aluminum exposure may promote the onset of Parkinson's disease (PD) (Bondy, 2010). The PD is a disorder increasingly recognized as involving inflammatory events, microglial activation and increased levels of proinflammatory cytokines (Bondy, 2010). In addition, aluminum is a proven potent neurotoxicant (Flaten, 2001)

Although there is still ongoing debate about the human health effects of aluminum, particularly its link to AD and PD, it is appropriate that the right treatment processes are used to limit the concentration of aluminum in treated water. In fact, if the treatment process is functioning optimally, the addition of aluminum may actually result in lower aluminium values in the treated water than in the raw water (Flaten, 2001).

Ferric chloride

Just like alum, ferric chloride has been used to improve water quality for a long time. At this point, it is important to stress that there is general lack of information on the possible toxicity of ferric compounds. Iron salts are thought to have low acute

toxicity because of their rapid oxidation to insoluble forms (Sotero-Santos et al., 2007). Iron itself, is an essential trace element for the growth, development, and long-term survival of most organisms (Chandrasekaran et al., 2010). In fact, ferric chloride ($FeCI_3.6H_2O$) is used throughout the world as a food additive to modified milk powder, as well as a haemostatic or treatment for hypochromic anaemia (Sato et al., 1992).

However, despite the importance of iron, it is reported that concentration of iron exceeding 200 mg/day are considered toxic to the human body (Bowen, 1979). For example, water soluble binary iron compounds such as ferrous chloride and iron sulphate may cause toxic effects upon concentrations exceeding 200 mg, and are lethal for adults upon doses of 10-50 g (CSIR, 2010).

Furthermore, epidemiological studies and clinical observations have shown that increased levels of iron in the body are associated with an increased risk of cancer, vascular diseases, and neurological disorder conditions (Weinberg, 1984; Stevens et al., 1988; Sato et al., 1992; Berg et al., 2001; Siah et al., 2005; Chandrasekaran et al., 2010). It has also been shown that exposure to ferric chloride significantly induces high levels of aberrations and damage chromosome of the human lymphocyte cells (Poddar et al., 2004). Recent study has also raised an important public health issue; using iron precipitates to remove arsenic from water may cause oxidative hepatic damage in humans (Chandrasekaran et al., 2010).

Chlorine

For many years chlorine has been the popular drinking water disinfectant due to its higher oxidising power, provision of a minimum level of residual chlorine throughout the distribution system and protection against microbial recontamination (Sadiq and Rodrssiguez, 2004; Gopal et al., 2007). Despite its popularity, its main drawback is the production of unwanted by-products commonly called disinfection by-products

(DBPs) or chlorination by-products (CBPs) which have impact on human health. The DBPs are produced upon chlorination only if the water contains DBPs precursors such as natural organic matter (NOM) (Mesdaghinia et al., 2005). Furthermore, the disinfectant still present in drinking water can react with saliva and the stomach contents to form DBPs similar to those produced in water (GreenFacts, 2004). Table 7.2 is a summary of the chlorination by-products and their health effects (Gopal et al., 2007).

Despite the development of methods for removing DBPS, the formation of these by-products in drinking water has actually motivated the need for exploring alternative disinfectants and new treatment technologies. Amongst the most promising chemical alternatives are chlorine dioxide and ozone (Simate et al., 2012).

Table 7.2. Chlorination by-products and their health effects (Gopal et al., 2007).

Class of disinfection by-products	Compounds	Health effects
Trihalomethanes (THM)	Chloroform	Cancer, liver, kidney and reproductive effects
	Dibromochloromethane	Nervous system, liver, kidney and reproductive effects
	Bromodichloromethane	Cancer, liver, kidney and reproductive effects
	Bromoform	Cancer, liver, kidney and reproductive effects
Haloacetonitrile (HAN)	Trichloroacetonitrile	Cancer, mutagenic and clastogenic effects
Halogenated aldehydes/ketones	Formaldehyde	Mutagenic
Halophenol	2-Chlorophenol	Cancer and tumor promoter
Haloacetic acids (HAA)	Dichloroacetic acid	Cancer and reproductive and developmental effects
	Trichloroacetic acid	Liver, kidney, spleen and developmental effects

Copper sulphate

Amongst the common copper compounds, copper sulphate has been used as a water treatment chemical, and is regarded as the algicide of choice because it is cheap, effective, relatively safe, and easy to apply (Elder and Horne, 1978; McKnight et al., 1983). Though copper is also an essential micronutrient involved in a variety of biological processes indispensable to sustain human life, it can be toxic when present in excess (de Romaña et al., 2011). The most noticeable chronic effect is liver damage commonly called Wilson disease (de Romaña et al., 2011). Indian Childhood Cirrhosis (ICC) and Idiopathic Chronic Toxicosis (ICT) represent other examples of chronic copper toxicity (de Romaña et al., 2011; ATSDR, 2004). The former has been related to a high copper exposure due to consumption of animal milk stored or heated in copper or copper alloy containers (de Romaña et al., 2011). The ICT is believed to be caused by an autosomal-recessive inherited defect in copper metabolism and excess dietary copper (Wijmenga, 2002; ATSDR, 2004).

The other most commonly reported adverse health effect of copper is gastrointestinal distress (Araya et al., 2001; Gotteland et al., 2001; ATSDR, 2004). Nausea, vomiting, diarrhea, and/or abdominal pain have been reported, usually occurring shortly after drinking a copper sulphate solution, beverages that were stored in a copper or un-tinned brass container, or first draw water (water that sat in the pipe overnight) (ATSDR, 2004). However, these observed effects are not usually persistent and gastrointestinal effects have not been linked with other health effects (ATSDR, 2004).

At the moment, the carcinogenicity of copper has not been adequately studied, at least based on the author' review of the existing literature – weather ingested or inhaled. However, an increase in cancer risk has been found among copper smelters; though the increased risk has been attributed to concomitant exposure to arsenic (ATSDR, 2004). Increased lung and stomach cancer risks have also been found in copper miners (ATSDR, 2004).

As a result of several available evidence on acute adverse effects of copper, WHO has set the safe level for human consumption of copper in drinking water at 2 mg of copper per litre. However, it is believed that copper sulphate will not exhibit toxicity until a dosage of 375 mg for a 150-pound (~ 68 kg) person (Mooney, 2004).

On the other hand, severe deficiency of copper also leads to Menkes disease (or Menkes syndrome or Kinky hair disease) with the primary outcome usually being death (de Romaña et al., 2011). Menkes syndrome is characterized by sparse, kinky hair; failure to gain weight and grow at the expected rate (failure to thrive); and deterioration of the nervous system (Menkes. 1999). Additional signs and symptoms include weak muscle tone (hypotonia), sagging facial features, seizures, developmental delay, and intellectual disability (Menkes, 1999).

Fluoride

Though fluoridation of water may not be considered as a water treatment process, it is a public health measure. Thus, the addition of fluoride to drinking water has, for long time now, been found to be effective in reducing the incidences of dental caries (also known as tooth decay or a cavity). Compared to alternative methods, fluoridation is cheaper, has consistent exposure, has equal distribution to all socioeconomic groups, is simple, and is considered safe (Harrison, 2005).

In some areas, fluoride occurs naturally in drinking water. In areas where the drinking water supply is artificially fluoridated, the process is generally undertaken after clarification and chlorination of the water, because fluoride ions may adsorb onto the surface of suspended matter in the water and be subsequently removed through these processes (NHMRC-NRMMC, 2011). Fluoridation is generally achieved by adding a slurry of sodium fluorosilicate, a solution of hydrofluorosilicic acid, or (less commonly) a saturated solution of sodium fluoride (NHMRC-NRMMC, 2011).

Correction of pH may need to be carried out after fluoride addition (NHMRC-NRMMC, 2011).

Although a moderate intake of fluoride is the effective way of reducing dental caries among children and adult, high concentration of fluoride has toxic effects in both humans and animals, causing disorders such as endemic fluorosis and industrial fluorosis (Xiong et al., 2007). Endemic fluorosis is related to the high concentration of fluoride present in the drinking water, while industrial fluorosis is mainly due to air pollution of fluoride in the working environment (Xiong et al., 2007).

Due to its strong electronegativity, fluoride is attracted by positively charged calcium ions in teeth and bones (Singh et al., 2007). It displaces hydroxide ions from hydroxyapatite, $Ca_5(PO_4)_3OH$, the principal mineral constituent of teeth (in particular the enamel) and bones, to form the harder and tougher fluoroapatite, $Ca_5(PO_4)_3F$ (Mohapatra et al., 2009). Up to a small level this strengthens the enamel. However, fluoroapatite is an order of magnitude less soluble than hydroxyapatite, and at high fluoride concentration the conversion of a large amount of the hydroxyapatite into fluoroapatite makes the teeth and (after prolonged exposure) the bones denser, harder and more brittle (Mohapatra et al., 2009). In the teeth this causes mottling and embrittlement, a condition known as dental fluorosis (Mohapatra et al., 2009). With prolonged exposure at higher fluoride concentrations dental fluorosis progresses to skeletal fluorosis.

7.3 Summary and Conclusions

This Chapter covered the human health impacts of different residual water treatment chemicals; including CNTs in drinking water. The Chapter has shown that despite an explosion of research into potential applications of CNTs, human health effects of CNTs is still a subject of intense research. In fact, at present, there are no well-defined global agreements about the risks (including concentrations) of CNTs on

human health and in particular on their transformation capacity (Stellaa, 2011). On the other hand, there is a vast amount of information concerning the human health effects of traditional water treatment chemicals. Table 7.3 is a comparative summation of the human health effects of various water treatment chemicals and includes CNTs, alum, ferric chloride, chlorine, copper sulphate and fluoride. The notable characteristic in Table 7.3 is that most of the chemicals including CNTs pose the risk of cancer. Therefore, it is important to exercise caution about which chemical to utilize for drinking water treatment.

Table 7.3. Summary of human health effects of various water treatment chemicals.

Chemical	**Methods of entry into human body**	**Methods of removal from drinking water**	**Health effects**
CNTs	skin, lungs, digestive system	membrane filtration; ultracentrifugation;	inflammation and fibrosis; granulomas; cancer
Alum	digestive system	cation exchange resin; chelating; reverse osmosis and electrodialysis; adsorption using carbon nanotubes; coagulation and flocculation	Alzheimer's disease; neurotoxicant; Parkinson's disease; cancer
Ferric chloride	digestive system	adsorption using carbon nanotubes; coagulation and flocculation followed by filtration; oxidation followed by filtration; ion exchange	cancer; vascular diseases; hepatic damage; neurological disorder, aberrations; damage chromosome of lymphocyte
Chlorine	digestive system	adsorption using carbon nanotubes, and/or activated carbon	Cancer; liver; kidney; spleen; mutagenic; reproductive and developmental effects
Copper sulphate	digestive system	chemical precipitation; ion exchange	hepatic damage; liver damage; nausea; vomiting; abdominal pains
Fluoride	digestive system	membrane filtration and adsorption	liver; kidney; brain; spinal cord; parathyroid; reproductive system; DNA damage; dental and skeletal fluoroses

References

Araya, M., McGoldrick, M. C., Klevay, L. M., Strain, J. J., Robson, P., Nielsen, F., Olivares, M., Pizzaro, F., Johnson, L., Poirier, K. A., 2001. Determination of an acute no-observed-adverse effect level (NOAEL) for copper in water. *Regulatory Toxicology and Pharmacology* 34 (2), 137-148.

Aschberger, K., Micheletti, C., Sokull-Klüttgen, B., Christensen, F.M., 2011. Analysis of currently available data for characterising the risk of engineered nanomaterials to the environment and human health - lessons learned from four case studies. *Environment International* 37 (6), 1143-1156.

ATSRD, 2004. Toxicological profile for copper. Agency for Toxic Substances and Disease Registry, Atlanta

Auffan, M., Achouak, W., Rose, J., Chane, C., Waite, D. T., Masion, A., Woicik, .J, Wiesner, M. R., Bottero, J. Y., 2008. Relation between the redox state of iron based nanoparticles and their cytotoxicity towards Escherichia coli. *Environmental Science and Technology* 42 (17), 6730–6735.

Berg, D., Gerlach, M., Youdim, M.B., Double, K.L., Zecca, L., Riederer, P., Becker, G., 2001. Brain iron pathways and their relevance to Parkinson's disease. *Journal of Neurochemistry* 79, 225-236.

Bondy, S.C., 2010. The neurotoxicity of environmental aluminum is still an issue. *Neuro Toxicology* 31, 575–581.

Bouwmeeste, H., Dekkers, S., Noordam, M. Y., Hagens, W. I., Bulder, A., S., de Heer, C., ten Voorde, S. E. C. G., Wijnhoven, S. W. P., Marvin, H. J. P., Sips, A. J. A. M., 2009. Review of health safety aspects of nanotechnologies in food production. *Regulatory Toxicology and Pharmacology* 53, 52-62

Bowen, H. J. M., 1979. Environmental chemistry of elements. Academic Press, New York/London.

Chandrasekaran, V. R. M., Muthaiya, I., Huang, P-C., Liu, M-Y., 2010. Using iron precipitants to remove arsenic from water: Is it safe? *Water Research* 44, 5823-5827

Chigumbu, N., 2011. The invitro evaluation of the physiochemical effects of drug loaded carbon nanotubes on toxicity. MSc Dissertation, University of the Witwatersrand, Johannesburg, South Africa.

CSIR, 2010. Household iron removal plant - CSIR - NEERI technology. Available at: http://technology.ezinemark.com/household-iron-removal-plant-csir-neeri-technology-170667c52d9.html. [Accessed: July 2011]

Davoren, M., Herzog, E., Casey, A., Benjamin, C., Gordon, C., Hugh, J. B., Fiona, M. L., 2007. In vitro toxicity evaluation of single walled carbon nanotubes on human A549 lung cells. *Toxicology in Vitro* 21, 438-448.

de Romaña, D. L., Olivares, M., Uauy, R., Araya, M., 2011. Risks and benefits of copper in light of new insights of copper homeostasis. *Journal of Trace Elements in Medicine and Biology* 25, 3-13.

Donaldson, K., Murphy, F., Duffin, R., Poland, C. R., 2010. Asbestos, carbon nanotubes and the pleural mesothelium: a review of the hypothesis regarding the role of long fibre retention in the parietal pleura, inflammation and mesothelioma. *Particle and Fibre Toxicology* 7, 5.

Dreher, K. L., 2004. Health and environmental impact of nanotechnology: toxicological assessment of manufactured nanoparticles. *Toxicological Sciences* 77, 3–5.

Elder, J. F., Horne, A. J., 1978. Copper cycles and $CuSO_4$ algicidal capacity in two California lakes. *Environmental Management* 2 (1), 17-30.

Flaten, T. P., 2001. Aluminium as a risk factor in Alzheimer's disease, with emphasis on drinking water. *Brain Research Bulletin* 55 (2), 187–196.

Fraczek-Szczypta, A., Menaszek, E., Blazewicz, S., 2011. Some observations on carbon nanotubes susceptibility to cell phagocytosis. J*ournal of Nanomaterials*, doi:10.1155/2011/473516.

Freedman, B. J., 1991. Persorption of raw starch: a cause of senile dementia? *Medical Hypotheses* 35, 85-87.

Gopal, K., Tripathy, S. S., Bersillon, J. L., Dubey, S. P., 2007. Chlorination byproducts, their toxicodynamics and removal from drinking water. *Journal of Hazardous Materials* 140, 1-6.

Gotteland, M., Araya ,M., Pizarro, F., Olivares, M., 2001. Effect of acute copper exposure on gastrointestinal permeability in healthy volunteers. *Digestive Diseases and Sciences* 46 (9), 1909-1914.

Harrison, P. T. C., 2005. Fluoride in water: A UK perspective. *Journal of Fluorine Chemistry* 126, 1448–1456.

Helland, A., Wick, P., Koehler, A., Schmid, K., Som, C., 2007. Reviewing the environmental and health knowledge base of carbon nanotubes. *Environmental Health Perspectives* 115 (8), 1125-1131.

Hoet, P. H., Brüske-Hohlfeld, I. B. H., Salata, O. V., 2004. Nanoparticles - known and unknown health risks. *Journal of Nanobiotechnology* 2, 12.

Hussain, M. A., Kabir, M. A., Sood, A. K., 2009. On the cytotoxicity of carbon nanotubes. *Current Science* 96 (5), 664-673.

Imandel, K., Farhud, D. D., Derakhtian, A., 1994. The occurrence of aluminium in municipal treated water supply of Bushehr and Borazjan area of Iran. *Iranian Journal of Public Health* 23 (1-4), 34-40.

Iyuke, S., Chigumbu, N., Pillay, V., Ndlovu, S., 2012. Invitro evaluation of the physiochemical effects of drug loaded carbon nanotubes on toxicity. In: International Conference and Exhibition on Nanotechnology and Nanomedicine, Omaha, USA, March 12-14.

Jia, G., Wang, H., Yan, L., Wang, X., Pei, R., Yan, T., Zhao, Y., Guo, X., 2005. Cytotoxicity of carbon nanomaterials: single-wall nanotube, multi-wall nanotube and fullerene. *Environmental Science and Technology* 39, 1378-1383.

Kang, S., Herzberg, M., Rodrigues, D. F., Elimelech, M., 2008. Antibacterial effects of carbon nanotubes: size does matter! *Langmuir* 24, 6409-6413.

Lam, C.W., James, J.T., McCluskey, R., Hunter, R. L., 2004. Pulmonary toxicity of single-wall carbon nanotubes in mice 7 and 90 days after intratracheal instillation. *Toxicological Sciences* 77, 126-134.

Lam, C.W., James, J.T., McCluskey, R., Arepalli, S., Hunter, R. L., 2006. A review of carbon nanotube toxicity and assessment of potential occupational and environmental health risks. *Critical Reviews in Toxicology* 36 (3), 189-217.

Li, S., He, P., Dong, J., Guo, Z., Dai, L., 2005. DNA-directed of carbon self-assembling nanotubes. *Journal of American Chemical Society* 127, 14-15.

Lindberg, H. K., Falck, G. C. M., Suhonen, S., Vippola, M., Vanhala, E., Catalán, J., Savolainen, K., Norppa, H., 2009. Genotoxicity of nanomaterials: DNA damage and micronuclei induced by carbon nanotubes and graphite nanofibres in human bronchial epithelial cells in vitro. *Toxicological Letters* 186, 166-173.

McKnight, D.M., Chisholm, S.W., Harleman, D.R.F., 1983. $CuSO_4$ treatment of nuisance algal blooms in drinking water reservoirs. *Environmental Management* 7 (4), 311-320.

McLachlan, D.R.C., 1995. Aluminum and the risk for Alzheimer's disease, *Environmetrics* 6, 233-275.

Menkes, J. H., 1999. Menkes disease and Wilson disease: two sides of the same copper coin. *European Journal of Paediatric Neurology* 3 (4), 147-l58.

Mesdaghinia, A., Rafiee, M. T., Vaezi, F., Mahvi, A. H., 2005. Evaluation of ferric chloride and alum efficiencies in enhanced coagulation for TOC removal and related residual metal concentrations. *Iranian Journal of Environmental Health, Science and Engineering* 2 (3), 189-194.

Mohapatra, M., Anand, S., Mishra, B. K., Giles, D. E., Singh, P., 2009. Review of fluoride removal from drinking water. *Journal of Environmental Management* 91, 67 – 77.

Mooney, M., 2004. Supernutrition's facts versus fiction. Available at http:// www.supernutritionusa.com/images/pdfs/CopperSulfate.pdf. [Accessed: July 2011]

Muller, J., Delos, M., Panin, N., Rabolli, V., Huaux, F., Lison, D., 2009. Absence of carcinogenic response to multiwall carbon nanotubes in a 2-year bioassay in the peritoneal cavity of the rat. *Toxicological Sciences* 110 (2), 442-448.

NHMRC-NRMMC, 2011. Australian Drinking Water Guidelines Paper 6 National Water Quality Management Strategy. National Health and Medical Research Council, National Resource Management Ministerial Council, Commonwealth of Australia, Canberra.

Nieboer, E., Gibson, B.L., Oxman, A. D., Kramer, J.R., 1995. Health effects of aluminum: a critical review with emphasis on aluminum in drinking water. *Environmental Reviews* 3, 29-81.

Ndabigengesere, A., Narasiah, K. S., 1998. Quality of water treated by coagulation using Moringa oleifera seeds. *Water Research* 32, 781-791.

Oberdörster, G., Oberdörster, E., Oberdörster, J., 2005. Nanotoxicology: an emerging discipline evolving from studies of ultrafine particles. *Environmental Health Perspectives* 113 (7), 823-839.

Patlolla, A., Knighten, B., Tchounwou, P., 2010. Multi-walled carbon nanotubes induce cytotoxicity, genotoxicity and apoptosis in normal human dermal fibroblast cells. *Ethnicity and Disease* 20, S1-65-72.

Poddar, S., Talukder, G., Sharma, A., 2004. Chromosome damaged induced by ferric chloride in human peripheral lymphocytes. *International Journal of Human Genetics* 4 (4): 261-264.

Powell, J. J., Faria, N., Thomas-Mckay, E., Pele, L. C., 2010. Origin and fate of diatery nanoparticles and microparticles in the gastrointestinal tract. *Journal of Autoimmunity* 34, J226-J233.

Sadiq, R., Rodrssiguez, M.J.,2004. Disinfection byproducts (DBPs) in drinking water and predictive models for their occurrence: a review. *Science of the Total Environment* 321, 21-46.

Salamat-Miller, N., Johnston, T.P., 2005. Current strategies used to enhance the paracellular transport of therapeutic polypeptides across the intestinal epithelium. *International Journal of Pharmaceutics* 294 (1–2), 201–216.

Sato, M., Furukawa, F., Toyoda, K., Mitsumori, K., Nishikawa, A., Takahashi, M., 1992. Lack of carcinogenicity of ferric chloride in F344 rats. *Food and Chemical Toxicology* 30 (10), 837-842.

Siah, C.W., Trinder, D., Olynyk, J.K., 2005. Iron overload. *Clinica Chimica Acta* 358, 24-36.

Simate, G. S., Iyuke, S. E., Ndlovu, S., Heydenrych, M., Walubita, L. F., 2012. Human health effects of residual carbon nanotubes and traditional water treatment chemicals in drinking water. *Environment International* 39, 38-49.

Simkó, M., Nentwich, M., Gazsó, A., Fiedeler, U., 2010. How nanoparticles enter the human body and their effects there. Nano Trust-Dossier No. 003en, November 2010: epub.oeaw.ac.at/ita/ nanotrust-dossiers/dossier003en.pdf. [Accessed: January 2012]

Singh, B., Gaur, S., Garg, V. K., 2007. Fluoride in drinking water and human urine in Southern Haryana, India. *Journal of Hazardous Materials* 144, 147–151.

Smart, S.K.., Cassady, A. I., Lu, G. Q., Martin, D.J., 2006. The biocompatibility of carbon nanotubes. *Carbon* 44, 1034 – 1047.

Som, C., Wick, P., Krug, H., Nowack, B., 2011. Environmental and health effects of nanomaterials in nanotextiles and façade coatings. *Environment International* 37 (6), 1131-1142.

Sotero-Santos, R. B., Rocha, O., Povinelli, J., 2007. Environmental and health effects of nanomaterials in nanotextiles and façade coatings. *Chemosphere* 68, 628-636.

Stellaa, G. M., 2011. Carbon nanotubes and pleural damage: perspectives of nanosafety in the light of asbestos experience. *Biointerphases* 6 (2), P1-P17.

Stevens, R. G., Jones, Y., Micozzi, M. S., Taylor, P. R., 1988. Body iron stores and the risk of cancer. The New England Journal of Medicine 319, 1047-1052.

Weinberg, E. D., 1984. Iron withholding: a defense against infection and neoplasia. *Physiological Reviews* 64, 65-102.

Wijmenga, C., 2002. Non-Indian childhood cirrhosis - using a founder population to identify the underlying genetic defect. In: Massaro, E. J. (Editor), Handbook of copper pharmacology and toxicology. Humana Press, New Jersey, pp. 369-382.

Thompson, S., 2009. Alzheimer's disease. Available at: http://www.bami.us/Neuro /Alzheimers2. html. [Accessed: July 2011]

Upadhyayula, V. K. K., Deng, S., Mitchell, M. C., Smith, G. B., 2009. Application of carbon nanotube technology for removal of contaminants in drinking water: a review. *Science of the Total Environment* 408, 1-13.

Volkenheimer, G., Schulz, F.H., 1968. The phenomenon of persorption. *Digestion* 1, 213-218.

Volkheimer, G., 1974. Passage of particles through the wall of the gastrointestinal tract. *Environmental Health Perspectives* 9, 215-225.

Volkheimer, G., 1993. Persorption of microparticles. *Pathologe* 14 (5), 247-252.

Wang, X., Jia, G., Wang, H., Nie, H., Yan, L., Deng, X.Y., Wang, S., 2009. Diameter effects on cytotoxicity of multi-walled carbon nanotubes. J*ournal of Nanoscience and Nanotechnology* 9 (5), 3025-3033.

Warheit, D. B., Laurence, B. R., Reed, K. L., Roach, D. H., Reynolds, G. A. M., Webb, T. R., 2004. Comparative pulmonary toxicity assessment of single-wall carbon nanotubes in rats. *Toxicological Sciences* 77, 117-125.

Weiner, M. L., 1988. Intestinal transport of some macromolecules in food. *Food and Chemical Toxicology* 26 (10), 867-880.

Wick, P., Manser, P., Limbach, L. K., Weglikowska, U.D., Krumeich, F., Roth, S., Stark, W. J., Bruinink, A., 2007. The degree and kind of agglomeration affect carbon nanotube cytotoxicity. *Toxicology Letters* 168, 121-131.

Xiong, X.Z., Liu, J.L., He, W.H., Xia, T., He, P., Chen, X.M., Yang, K.D., Wang, A.G., 2007. Dose-effect relationship between drinking water fluoride levels and damage to liver and kidney functions in children. *Environmental Research* 103, 112-116.

Zhu, L., Chang, D. W., Dai, L., Hong, Y., 2007. DNA damage induced by multiwalled carbon nanotubes in mouse embryogenic stem cells. *Nano Letters* 7 (12), 3592-3597.

CHAPTER EIGHT

CONCLUSIONS AND RECOMMENDATIONS

"I wanted a perfect ending. Now I have learned the hard way that some poems don't rhyme and some stories don't have a clear beginning, middle or end".

- Radner Gilda

8.1 Conclusions

8.1.1 Introduction

A review of the existing literature has shown that the ability of CNTs to remove organic and inorganic impurities from wastewaters is based on the principle of adsorption. Therefore, the main objective of this work was to exploit this principle to investigate the possibility of using CNTs as heterogeneous coagulants/flocculants, and/ or granular media filter in the treatment of brewery wastewater.

In order to investigate this possibility, the objectives of this study were defined as:

I. To synthesize CNTs from CO_2 using existing chemical vapour deposition (CVD) techniques.
II. To evaluate the feasibility of using CNTs in the treatment of brewery wastewater, by comparing their coagulation/flocculation capabilities with traditionally used water treatment chemicals.
III. To assess the possibility of using CNTs as adsorptive filter media in granular filtration.
IV. To use available literature and give a qualitative comparison of the human health impact (if any) of residual CNTs with traditional water treatment chemicals.

8.1.2 Synthesis of carbon nanotubes from carbon dioxide

A review of literature has shown that although the pyrolysis of hydrocarbon precursors for synthesizing CNTs are very useful and are used widely, there are some disadvantages with these carbon sources. For example, most hydrocarbons are hazardous chemicals, and for most cases, the pyrolysis temperatures are around

1000°C, which are impractical for large scale industrial production. The use of hydrocarbons also leads to greenhouse gas emissions. These problems can be solved by the use of CO_2 which is a cheap, non-toxic, low-energy, and abundant molecule on the earth. Therefore, different techniques used for the production of CNTs from CO_2 were theoretically and analytically evaluated. This was aimed at selecting a suitable synthesis technique with great potential for production of low cost, but high quality CNTs for brewery wastewater treatment. The commonest method produced CNTs using $scCO_2$ in autoclaves or sealed quartz tubes. The use of $scCO_2$ generates abnormally high pressure, thus this method was not found to be practical. As for metal bearing ferrites, their application is limited to the conditions where reduction of the catalyst is possible. Therefore, the CVD methodology was found to be the most suitable for the production of CNTs from CO_2.

While CNT literature is full of recipes, growth results and application potential, the detailed study of the effects of reactor temperature as well as the concentration and flow rate of CO_2 using CVD techniques is almost nonexistent. Nevertheless, these studies are useful as they guide the development and optimisation of CNT synthesis. Therefore, in Chapter 4, the effects of these critical parameters on the production of CNTs from CO_2 were studied and analysed.

High concentration and high flow rates of CO_2 were found to impact negatively on the production rates of CNTs. At higher carbon concentrations, the rate of formation of adsorbed surface carbon exceeds the diffusion rate leading to formation of a monolayer or multiple layers of carbon on the catalyst particles, thus reducing CNT synthesis. On the other hand, a higher volumetric flow rate lessens the residence time for the reaction, leading to the production of a lower number of carbon atoms during the reaction. These results demonstrate the importance of controlling the concentration and flow rate of the carbon source.

Temperature is also another parameter that played a vital role in the production of CNTs from CO_2. As explained in Chapter 4, the CNT synthesis occurs via the Boudouard reaction, which involves the disproportionation of CO arising from the initial stage in the splitting of CO_2. Up to about 800°C, CNT production increased with temperature and then reduced as the temperature increased. These results supported the two main limitations of the CO disproportionation – kinetics and thermodynamics. At lower temperatures the reaction is limited kinetically, and at higher temperatures it is limited thermodynamically.

8.1.3 Evaluation of carbon nanotubes as heterogeneous coagulants/flocculants for brewery wastewater

If CNTs can adsorb onto particle surfaces, then charge neutralisation or near zero net charge can occur. In Chapter 5 this theory was tested in the heterogeneous coagulation and flocculation of brewery wastewater. A series of experiments were conducted in which the efficiencies of pristine and functionalised CNTs were compared with the efficiency of traditional ferric chloride.

The results showed that both pristine and hydrochloric acid functionalised CNTs have the ability to coagulate colloidal particles in the brewery wastewater. Overall, ferric chloride was found to be a more effective coagulant than both the pristine and functionalised CNTs. The hydrochloric acid functionalised CNTs were more effective than pristine CNTs, thus confirming that hydrochloric acid functionalised CNTs possessed basic (or positively charged) functional groups. The basic sites were responsible for adsorbing the negatively charged colloidal particles that were present in brewery wastewater. The results also showed that concentrated hydrochloric acid rendered the surfaces of CNTs basic in nature.

Charge neutralisation was found to be the main mechanism for the heterogeneous coagulation of colloidal particles in brewery wastewater by hydrochloric acid functionalised CNTs. This is because there was an increase in zeta potential, and a reduction in residual turbidity and COD as CNT dosage increased. Zeta potential results also showed that the hydrochloric acid functionalised CNTs did not form a stable dispersion. This is advantageous because there will be no residual CNTs dispersed in the treated brewery wastewater. In addition, CNTs can easily be retained and separated from treated water using membrane filtration and ultracentrifugation, thus preventing the apparent human health risks of residual CNTs in treated water.

8.1.4 The treatment of brewery wastewater in a semi-continuous laboratory scale water treatment plant

For industrial application, the heterogeneous coagulation and flocculation of colloidal particles using CNTs should be integrated to other water treatment processes. For this purpose, a semi-continuous LSWTP was used. Several treatment schemes were evaluated in the semi-continuous LSWTP.

The results obtained showed that higher hydraulic loading rates induced rapid clogging of granular filter pores due to the high amount of particles arriving on the filter per unit area. Thus leading to a higher head loss and reduced outlet hydraulic rate. It was also observed that coagulation and flocculation of particulates increased head loss in the direct filtration process because large particulates that are produced enhanced the rate of deposition of the particles onto and within the granular filter bed.

Higher turbidity and COD removal efficiencies were achieved in a conventional filtration process than in either the direct filtration or the in-line filtration systems. The difference in performance between the conventional and the direct filtration processes is due to the fact that the conventional filtration processes use

sedimentation stage that allowed particulates to settle out of water for removal, whereas the direct filtration mode eliminated this step and allowed the filter material itself to do the work. As for the in-line filtration system that has no coagulation/flocculation and sedimentation stages, only a small amount of the fine particles passing through the filter bed could be removed. Consequently, the in-line filtration is not as efficient as the conventional or the direct filtration methods.

The addition of CNTs to the coagulation/flocculation tanks resulted in better turbidity and COD removal than 'sandwiched' CNTs in the filter bed. This is attributed to effective mixing of CNTs and brewery wastewater leading to good mass transfer that increased the removal of the particulates. Moreover, the addition of CNTs in the coagulation/flocculation tanks acted not only as adsorbents for turbidity and COD, but also as heterogeneous coagulants.

The analyses of the results also showed that during the period in which the granular filter was operated, there were no CNTs detected in the filtrate. This is attributed to, (1) CNTs's lack of dispersion, and (2) 'sandwiching' of CNTs in the filter bed. The lack of dispersion means that the CNTs that escaped from the coagulation/flocculation tanks were easily strained by the filter bed. In addition, the 'sandwiching' of CNTs in between two layers of sand also meant that CNTs could not escape from the filter bed. These results are a good assurance that the filtrate from the semi-continuous LSWTP is safe because of the absence of entrained CNTs.

8.1.5 Comparison of human health effects of residual carbon nanotubes and traditional water treatment chemicals in drinking water

The effects of residual CNTs and traditional water treatment chemicals in drinking water were reviewed from available literature. The review showed that despite an explosion of research into potential devices and applications of CNTs, it is only

recently that information on their toxicity is becoming available. Furthermore, this study illustrates that there is still much work to be done in establishing the toxicity of CNTs as far as drinking water is concerned. However, once the CNTs escape from the water treatment system and enter the drinking water as residual CNTs, it can be ingested into the gastrointestinal tract to various organs of the body, thus triggering several biological effects. Some of the health effects associated with CNTs may include cancer, granulomas, inflammation and fibrosis, etc.

On the other hand, there is a vast amount of information concerning the human health effects of traditional water treatment chemicals. For example, the various DBPs that are formed during the chlorination process are known to cause cancer. Whether or not aluminum causes AD, the fact is that it is a neurotoxicant. Aluminum exposure may also promote the onset of PD. Both "copper deficiency" and "excess copper" induce adverse health effects. For example, Menkes syndrome and Wilson disease are conditions associated with severe copper deficiency and severe copper toxicity, respectively. Increased levels of iron in the body that may come from drinking water can also increase the risk of a variety of diseases such as cancer, vascular diseases, and neurological disorder conditions.

The notable characteristic observed in this study is that most of the chemicals including CNTs used in water treatment pose the risk of cancer. Therefore, it is important to exercise caution about which chemical to utilize for drinking water treatment. Furthermore, in view of several human health effects of various water treatment chemicals including CNTs, it is important that their use is limited or measures are taken for their removal in water treatment operations.

8.1.6 Potential application in industry

This whole study has opened up new avenues for the application of CNTs. As heterogeneous coagulants and flocculants, CNTs can be combined with several other

processes such as sedimentation; dissolved air flotation; rapid filtration; and membrane filtration. In fact this study has demonstrated that CNTs can be used as heterogeneous coagulants/flocculants and as granular filter media in a complete integrated water treatment system (semi-continuous LSWTP) that comprised coagulation/flocculation, sedimentation, and granular filtration processes.

8.2 Recommendations

With the knowledge that has been gathered from this work, the following recommendations for further studies are proposed.

8.2.1 Use of water-dispersible carbon nanotubes

This study evaluated the feasibility of employing CNTs as heterogeneous coagulants. Due to lack of dispersion or solubility by CNTs it was practically difficult to measure residual turbidity and COD of the treated brewery wastewater without filtration. It is thus recommended that the use of water-dispersible CNTs be investigated. However, in dispersible state, CNTs are likely to bring a number of challenges. As already discussed in Chapter 7, there are concerns over the risks associated with CNTs and their behaviour in the human body. Therefore, the recovery system for residual CNTs would also need to be thoroughly investigated.

8.2.2 Extension of monitoring parameters

The initial evaluation of the coagulation process was determined by analysis of residual turbidity and COD. Though these parameters are very important as primary indicators or measures of water quality, further research needs to be carried out to investigate the effect of CNTs on other impurities.

8.2.3 Functionalisation of carbon nanotubes

This study has shown that by introducing basic (or positively charged) functional groups using concentrated hydrochloric acid, CNTs can coagulate and flocculate brewery wastewater heterogeneously. Future studies in this area may entail the use of other chemicals for imparting basic functional groups onto CNTs. This should enable the determination of the most suitable chemical to functionalise CNTs.

8.2.4 Economic analysis of using carbon nanotubes

The potential for using CNTs both as heterogeneous coagulants/flocullants and as granular filter media has been established in this study. However, it is agreed by researchers that one of the major obstacles to using CNTs is production cost. Therefore, further studies should thoroughly investigate the cost benefits (if any) of using CNTs as coagulants/flocculants and/or as granular filter media.

APPENDICES

"The things taught in colleges and schools are not an education, but the means of education".

-Ralph Waldo Emerson

APPENDIX A

ABSTRACTS OF PUBLISHED/SUBMITTED PAPERS

"Experience does not err; it is only your judgement that errs in promising itself results which are caused by your experiments".

-Leonard Da Vinci

ABSTRACT FOR PAPER I

Titile: The treatment of brewery wastewater for reuse: State of the art

Authors: Simate, G. S.., Cluett, J., Iyuke, S. E., Musapatika, E. T., Ndlovu, S., Walubita, L. F., Alvarez, A. E.

The beer brewing process often generates large amounts of wastewater effluent and solid wastes that must be disposed off or treated in the least costly and safest way so as to meet the strict discharge regulations that are set by government entities to protect life (both human and animal) and the environment. It is widely estimated that for every one liter of beer that is brewed, close to ten liters of water is used; mostly for the brewing, rinsing, and cooling processes. Thereafter, this water must be disposed off or safely treated for reuse, which is often costly and problematic for most breweries. As a result, many brewers are today searching for: (1) ways to cut down on this water usage during the beer brewing process, and/or (2) means to cost effectively and safely treat the brewery wastewater for reuse. Based on the available documented literature, this paper provides a review assessment of the current status of the brewery wastewater treatment processes including potential applications for reuse. Key challenges for both brewery wastewater treatment and reuse are also discussed in the paper and include recommendations for future developments.

Keywords: Brewery wastewater; Biological oxygen demand; Chemical oxygen demand; Pretreatment; Treatment; Reuse

ABSTRACT FOR PAPER II

Titile: The production of carbon nanotubes from carbon dioxide: Challenges and opportunities

Authors: Simate, G. S., Iyuke, S.E., Ndlovu, S., Yah, C., Walubita, L. F.

Recent advances in the production of carbon nanotubes (CNTs) are reviewed with an emphasis on the use of carbon dioxide (CO_2) as a sole source of carbon. Compared to the most widely used carbon precursors such as graphite, methane, acetylene, ethanol, ethylene, and coal-derived hydrocarbons, CO_2 is competitively cheaper with relatively high carbon yield content. However, CNT synthesis from CO_2 is a newly emerging technology, and hence it needs to be explored further. A theoretical and analytical comparison of the currently existing CNT-CO_2 synthesis techniques is given including a review of some of the process parameters (i.e., temperature, pressure, catalyst, etc.) that affect the CO_2 reduction rate. Such analysis indicates that there is still a fundamental need to further explore the following aspects so as to realize the full potential of CO_2 based CNT technology: (1) the CNT-CO_2 synthesis and formation mechanism, (2) catalytic effects of transitional metals and mechanisms, (3) utilization of metallocenes in the CNT-CO_2 reactions, (4) applicability of ferrite-organometallic compounds in the CNT-CO_2 synthesis reactions, and (5) the effects of process parameters such as temperature, etc.

***Key words*:** supercritical CO_2; CO_2 reduction; chemical vapour decomposition (CVD); carbon nanotubes; ferrite catalysts

ABSTRACT FOR PAPER III

Titile: The production of carbon nanotubes from carbon dioxide in a 'modified' swirled floating catalytic chemical vapour deposition reactor

Authors: Simate, G. S., Iyuke, S. E., Heydenrych, M., Ndlovu, S., Moothi, K.

One possible approach for mitigating the effects of global warming arising from greenhouse gases such as carbon dioxide (CO_2) is to use nanotechnology. Therefore, the capture and transformation of some of the billions of tons of CO_2 produced annually by burning fossil fuels into useful products such as carbon nanotubes (CNTs) is one of the methods being pursued in current research activities. Whilst CNT literature is full of recipes, growth results and application potential, the detailed study of the effects of reactor temperature as well as the concentration and flow rate of CO_2 using chemical vapour deposition (CVD) techniques is almost non-existent. Thus, a series of experiments were conducted in the 'modified' swirled floating catalytic CVD (SFCCVD) reactor in which the effect of reactor temperature, concentration and flow rate of the CO_2 were investigated. The CNTs were analysed using the transmission electron microscopy (TEM) and the Raman spectroscopy. The results showed that the production of CNTs was only possible between 750-840°C, with the optimum growth rate achieved at about 800°C. This is in agreement with the two main limitations of the carbon monoxide (CO) disproportionation reaction. The results also showed that very high concentration and flow rates of CO_2 negatively affected the CNT growth rates.

Keywords: carbon dioxide; carbon monoxide; disproportionation; carbon nanotubes; modified swirled floating catalytic CVD

ABSTRACT FOR PAPER IV

Titile: The heterogeneous coagulation and flocculation of brewery wastewater using carbon nanotubes

Authors: Simate, G. S., Iyuke, S. E., Ndlovu, S., Heydenrych, M.

Coagulation and flocculation treatment processes play a central role in the way wastewater effluents are managed. Their primary function is particle removal that can impart colour to a water source, create turbidity, and/or retain bacterial and viral organisms. This study was carried out to investigate whether carbon nanotubes (CNTs) can be used as heterogeneous coagulants and/or flocculants in the pretreatment of brewery wastewater. A series of experiments were conducted in which the efficiencies of pristine and functionalised CNTs were compared with the efficiency of traditional ferric chloride in a coagulation/flocculation process. Turbidity and chemical oxygen demand (COD), including the zeta potential were used to monitor the progress of the coagulation/flocculation process. Both pristine and functionalised CNTs demonstrated the ability to successfully coagulate colloidal particles in the brewery wastewater. Overall, ferric chloride was found to be a more effective coagulant than both the pristine and functionalised CNTs.

Keywords: Brewery wastewater treatment; Carbon nanotubes; Heterogeneous coagulation and flocculation; Turbidity; Chemical oxygen demand; Zeta potential

ABSTRACT FOR PAPER V

Titile: The treatment of brewery wastewater for reuse: Integration of coagulation/flocculation and sedimentation with carbon nanotubes 'sandwiched' in a granular filter bed

Authors: Simate, G. S., Iyuke, S. E., Ndlovu, S., Heydenrych, M.

The unavailability of adequate fresh and clean water is a major driver to finding new effective methods for treating wastewater for reuse. For example, the brewery industry is one industry that requires the use of large volumes of clean water in its beer production. However, a large amount of effluent generated during the brewing process is largely polluted by both organic and chemical impurities. Therefore, there is need to purify brewery wastewater from an environmental perspective when wastewater is discharged back into the environment and from an economic standpoint where a lot of water go into the production process. This study deals with the integration of treatment systems and devices for reducing turbidity and chemical oxygen demand (COD) in brewery wastewater for re-use. For this purpose, a semi-continuous laboratory scale water treatment plant (semi-continuous LSWTP) was used. Several treatment schemes were evaluated in the semi-continuous LSWTP. As expected, the presence of coagulation/flocculation and sedimentation steps was found to improve the efficiency of the semi-continuous LSWTP. Particularly, the treatment scheme in which carbon nanotubes (CNTs) were added to both the coagulation/flocculation tanks and the filter bed was found to be the best option for the treatment of brewery wastewater. This treatment removed 96.0% of COD and residual turbidity of only 5 NTU remained in the effluent.

Keywords: brewery wastewater treatment; carbon nanotubes; coagulation and flocculation; sedimentation; rapid sand filtration; chemical oxygen demand and turbidity

ABSTRACT FOR PAPER VI

Titile: Human health effects of residual carbon nanotubes and traditional water treatment chemicals in drinking water
Authors: Simate, G. S., Iyuke, S. E., Ndlovu, S., Heydenrych, M., Walubita, L. F.

The volume of industrial and domestic wastewater is increasing significantly year by year with the change in the lifestyle based on mass consumption and mass disposal brought about by the dramatic development of economies and industries. Therefore, effective advanced wastewater treatment is required because wastewater contains a variety of constituents such as particles, organic materials, and emulsion depending on the resource. However, residual chemicals that remain during the treatment of wastewaters form a variety of known and unknown by products through reactions between the chemicals and some pollutants. Chronic exposure to these by-products or residual chemicals through the ingestion of drinking water, inhalation and dermal contact during regular indoor activities (e.g., showering, bathing, cooking) may pose cancer and non-cancer risks to human health. For example, residual aluminium salts in treated water may cause Alzheimer's disease (AD). As for carbon nanotubes (CNTs), despite their potential impacts on human health and the environment having been receiving more and more attention in the recent past, existing information on the toxicity of CNTs in drinking water is limited with many open questions. Furthermore, though general topics on the human health impacts of traditional water treatment chemicals have been studied, no comparative analysis has been done. Therefore, a qualitative comparison of the human health effects of both residual CNTs and traditional water treatment chemicals is given in this paper. In addition, it is also important to cover and compare the human health effects of CNTs to those of traditional water treatment chemicals together in one review because they are both used for water treatment and purification.

Keywords: Water treatment; Drinking water; Carbon nanotubes; Disinfection by-products; Toxicity; Human health

APPENDIX B

DATA FOR CHAPTER 4

"There's plenty of room at the bottom".

-Richard Feynman

Table B1. Effect of temperature on production of carbon nanotubes

Conditions: carbon dioxide flow rate: 400 ml/min; time of operation: 45 minutes

Temperature (°C)	740	750	780	800	830	840	850
[1]Weight of CNTs produced (mg)	0	232	702	810	675	270	0
Production rate (mg/s)	0.00	0.09	0.26	0.30	0.25	0.10	0.00

[1]the results are an average of four replicate runs conducted under similar experimental conditions

Table B2. Effect of carbon dioxide concentration on production of carbon nanotubes

Conditions: reactor temperature: 800°C; time of operation: 45 minutes

Concentration (ppm)	1000	2000	3000	4000	5000	6000
[1]Weight of CNTs produced (mg)	243	567	864	1174	1472	1662
Actual production rate (mg/s)	0.09	0.21	0.32	0.43	0.55	0.62
Simulated production rate (mg/s)	0.10	0.21	0.35	0.49	0.63	0.76

[1]the results are an average of four replicate runs conducted under similar experimental conditions

Table B3. Effect of flow rate on production of carbon nanotubes

Conditions: reactor temperature: 800°C; time of operation: 45 minutes

Flow rate (ml/min)	50	100	150	200	250	300	350
[1]Weight of CNTs produced (mg)	81	267	432	567	643	686	700
Production rate (mg/s)	0.03	0.10	0.16	0.21	0.24	0.25	0.26

[1]the results are an average of four replicate runs conducted under similar experimental conditions

APPENDIX C

DATA FOR CHAPTER 5

"Failure is instructive. The person who really thinks learns quite as much from his failures as from his successes".

- John Dewey

Table C1. pH of solution of different masses of carbon nanotubes

Conditions: Running time: 24 hours

	[1]Final pH		
Mass %	**Initial pH=3.0**	**Initial pH=6.0**	**Initial pH=11.0**
0	3.0	6.0	11.0
0.05	4.0	6.5	10.0
0.10	5.0	6.8	9.0
0.5	5.6	6.9	8.1
1.0	6.2	7.2	8.0
5.0	6.7	7.2	7.9
10.0	6.8	7.2	7.9

[1]the results are an average of four replicate runs conducted under similar experimental conditions

Table C2. Effect of CNT dosage on turbidity removal using various carbon nanotubes and ferric chloride

Conditions: initial turbidity: mean = 84.75 NTU, range = 79-94 NTU ; flash mixing speed of 150 rpm for 3 minutes; slow mixing speed of 60 rpm for 20 minutes

	[1]Residual turbidity (NTU)		
Dosage	**Pristine CNTs**	**Functionalised CNTs**	**Ferric chloride**
0	84.75	84.75	84.75
10	73.20	66.90	51.70
20	68.20	54.35	33.38
30	65.90	47.28	24.85
40	63.60	41.22	17.25
50	61.45	36.47	14.00
60	61.10	35.31	17.00

[1]the results are an average of four replicate runs conducted under similar experimental conditions

Analysis of variance; H_0: ($\mu_1 = \mu_2 = \mu_3$, etc) or H_1: At least two means differ

Source of Variation	**SS**	**Df**	**MS**	**F**	**P-value**	**F crit**
Between Groups	3956.8121	2	1978.4060	5.64	0.0126	3.55
Within Groups	6318.1999	18	351.0111			
Total	10275.0120	20				

Table C3. Effect of pH on zeta potential of carbon nanotubes

Conditions: temperature = 25°C; solvent = water

	[1]Zeta potential (mV)	
pH	**Pristine CNTs**	**Functionalised CNTs**
2.0	-2.74	22.05
5.4	-16.25	12.8
7.0	-22.80	0.45
8.3	-29.05	-13.25
10.0	-31.05	-25.23
13.0	-43.00	-38.00

[1]the results are an average of four replicate runs conducted under similar experimental conditions

Student's *t*-test of paired two samples for means; one tail hypothesis - H_0: $(\mu_1-\mu_2) = 0$ or H_1: $(\mu_1-\mu_2) > 0$

	Pristine	**Hydrochloric acid functionalised CNTs**
Mean	-24.15	-6.86
Variance	189.91	524.75
Observations	6	6
Pearson Correlation	0.97	
Hypothesized Mean Difference	0	
Df	5	
t Stat	-4.17	
P(T<=t) one-tail	0.0044	
t Critical one-tail	2.02	
P(T<=t) two-tail	0.0087	
t Critical two-tail	2.57	

Table C4. Effect of pH on turbidity and COD removal by functionalised carbon nanotubes

Conditions: initial turbidity: mean = 84.75 NTU, range = 79-94 NTU ; initial COD: mean = 597.27 mg/L , range = 454-673 mg/L; flash mixing speed of 150 rpm for 3 minutes; slow mixing speed of 60 rpm for 20 minutes

pH	[1]Residual turbidity (NTU)	[1]Residual COD (mg/L)
2.0	17.25	343.54
5.4	27.95	389.00
7.0	31.63	396.69
8.3	34.95	409.23
10.0	38.85	412.06
13.0	41.53	445.92

[1]the results are an average of four replicate runs conducted under similar experimental conditions

Table C5. Effect of CNT dosage on turbidity and COD removal using functionalised carbon nanotubes

Conditions: initial turbidity: mean = 84.75 NTU, range = 79-94 NTU ; initial COD: mean = 597.27 mg/L , range = 454-673 mg/L; flash mixing speed of 150 rpm for 3 minutes; slow mixing speed of 60 rpm for 20 minutes

	[1]Turbidity		[1]COD	
Dosage	Residual	% removal	Residual	% removal
0	84.75	0	597.27	0
10	66.90	21.06	420.00	29.68
20	54.35	35.87	293.67	54.18
30	47.28	44.21	263.40	55.90
40	41.22	51.36	249.26	58.27
50	36.47	56.97	238.87	60.01
60	35.30	58.34	261.00	56.30

[1]the results are an average of four replicate runs conducted under similar experimental conditions

Table C6. Effect of CNT dosage on turbidity removal using functionalised carbon nanotubes, and a mixture of ferric chloride and functionalised carbon nanotubes

Conditions: initial turbidity: mean = 84.75 NTU, range = 79-94 NTU ; flash mixing speed of 150 rpm for 3 minutes; slow mixing speed of 60 rpm for 20 minutes; ferric chloride dosage = 2 mg/L; initial pH of brewery wastewater = 6.5

	[1]Residual turbidity (NTU)	
Dosage	**Functionalised CNTs**	**Mixture of functionalised CNTs and ferric chloride**
0	84.75	84.75
10	66.90	62.90
20	54.35	50.35
30	47.28	42.28
40	41.22	39.22
50	36.47	33.47
60	35.30	31.30

[1]the results are an average of four replicate runs conducted under similar experimental conditions

Student's t-test of paired two samples for means; one tail hypothesis - H_0: $(\mu_1-\mu_2) = 0$ or H_1: $(\mu_1-\mu_2) > 0$

	Hydrochloric acid functionalised CNTs	**Mixture**
Mean	52.32	49.18
Variance	326.32	361.36
Observations	7	7
Pearson Correlation	1.00	
Hypothesized Mean Difference	0	
df	6	
t Stat	4.96	
P(T<=t) one-tail	0.0013	
t Critical one-tail	1.94	
P(T<=t) two-tail	0.0026	
t Critical two-tail	2.45	

Table C7. Effect of CNT dosage on evolution of zeta potential of brewery wastewater

Conditions: initial turbidity: mean = 84.75 NTU, range = 79-94 NTU ; initial COD: mean = 597.27 mg/L , range = 454-673 mg/L; flash mixing speed of 150 rpm for 3 minutes; slow mixing speed of 60 rpm for 20 minutes; initial pH of brewery wastewater = 6.5

Dosage	[1]Zeta potential (mV)
0	-25.50
5	-21.30
10	-18.00
15	-12.10
20	-5.00
25	-1.00
30	5.00
35	7.00
40	9.00
45	10.00
50	11.00
60	12.00

[1]the results are an average of four replicate runs conducted under similar experimental conditions

Table C8. Effect of initial COD concentration on adsorbed COD at constant mass of CNTs

Conditions: Mass of CNTs added = 50 mg; volume of brewery wastewater = 100 mL; initial pH of brewery wastewater = 6.5; speed of shaker = 180 rpm; duration = 24 hrs

Initial COD (C_0), mg/L	Final COD (C_e), mg/L	Adsorbed COD (q_e), mg/g
400	270	260
425	290	270
450	295	275
475	315	285
500	350	300
525	370	310
550	390	320
575	410	330
600	430	340

[1]the results are an average of four replicate runs conducted under similar experimental conditions

APPENDIX D

DATA FOR CHAPTER 6

"If you don't learn from mistakes, there is no need making them".

-Herbert V. Prochnow

Table D1. Effect of inlet hydraulic loading rate on head loss

Conditions: total running time = 48 hrs; filtration mode = in-line filtration; coagulant used = ferric chloride

	[1]Head loss (cm Water)		
Running time (hrs)	**5 m^3/m^2 hr**	**7.5 m^3/m^2 hr**	**10 m^3/m^2 hr**
0	0	0	0
2	0	0	0
4	0	0	0
6	0	0	0
8	0	0	0
10	0	0	1.00
12	0	0	1.30
14	0	0	2.00
16	0	0	4.00
18	0	1.20	6.00
20	0	2.50	9.00
22	0	4.00	12.00
24	0	5.00	17.00
26	1.00	10.00	21.00
28	3.00	13.00	26.00
32	4.00	15.00	29.00
36	7.00	19.00	32.00
40	9.00	22.00	37.00
44	12.00	27.00	42.00
48	14.00	29.00	45.00

[1]the results are an average of four replicate runs conducted under similar experimental conditions

Analysis of variance; H_0: ($\mu_1 = \mu_2 = \mu_3$, etc) or H_A: at least two means differ; $\alpha = 0.05$

Source of Variation	**SS**	**Df**	**MS**	**F**	**P-value**	**F crit**
Between Groups	1385.0223	2	692.5112	5.71	0.0055	3.16
Within Groups	6909.2910	57	121.2156			
Total	8294.3133	59				

Table D2. Effect of inlet hydraulic loading rate on outlet hydraulic loading rates

Conditions: total running time = 48 hrs; filtration mode = in-line filtration; coagulant used = ferric chloride

	[1]Outlet hydraulic loading rate (m/hr)		
Running time (hrs)	**5 m^3/m^2 hr**	**7.5 m^3/m^2 hr**	**10 m^3/m^2 hr**
0	5.00	7.50	10.00
2	5.00	7.50	10.00
4	5.00	7.50	10.00
6	5.00	7.50	9.90
8	4.72	7.40	9.40
10	4.60	7.10	9.20
12	4.20	6.70	8.00
14	4.10	6.10	7.50
16	4.00	6.00	7.40
18	3.99	5.90	7.00
20	3.90	5.70	6.80
22	3.80	5.20	6.00
24	3.70	5.00	5.70
26	3.60	4.70	5.70
28	3.40	4.40	5.40
32	3.30	4.10	5.40
36	3.20	4.00	5.01
40	3.20	4.00	5.01
44	3.00	4.00	5.00
48	3.00	4.00	5.00

[1]the results are an average of four replicate runs conducted under similar experimental conditions

Analysis of variance; H_0: ($\mu_1 = \mu_2 = \mu_3$, etc) or H_A: at least two means differ; $\alpha = 0.05$

Source of Variation	**SS**	**df**	**MS**	**F**	**P-value**	**F crit**
Between Groups	101.7234	2	50.8617	24.51	2.09×10^{-8}	3.16
Within Groups	118.2952	57	2.0754			
Total	220.0186	59				

Table D3. Head loss development under various modes of filtration

Conditions: total running time = 48 hrs; hydraulic loading rate = 5 m^3/m^2 hr

	[1]Head loss (cm Water)		
Running time (hrs)	**In-line filtration**	**Direct filtration**	**Conventional filtration**
0	0	0	0
2	0	0	0
4	0	0	0
6	0	0	0
8	0	0	0
10	0	0	0
12	0	0	0
14	0	1.34	0
16	0	1.99	0
18	0	2.12	0
20	0	3.00	1.50
22	0	4.55	2.89
24	0	6.10	3.80
26	1.00	8.00	5.45
28	3.00	12.00	8.20
32	4.00	16.00	11.36
36	7.00	18.00	13.91
40	9.00	20.00	14.80
44	12.00	22.00	15.67
48	14.00	23.99	17.44

[1]the results are an average of four replicate runs conducted under similar experimental conditions

Analysis of variance; H_0: ($\mu_1 = \mu_2 = \mu_3$, etc) or H_A: at least two means differ; $\alpha = 0.05$

Source of Variation	**SS**	**df**	**MS**	**F**	**P-value**	**F crit**
Between Groups	202.9369	2	101.4684	2.319	0.1076	3.159
Within Groups	2494.1561	57	43.7571			
Total	2697.0930	59				

Table D4. Effect of the mode of filtration on removal of turbidity

Conditions: total running time = 48 hrs; hydraulic loading rate = 5 m^3/m^2 hr; initial turbidity: mean = 84.75 NTU, range = 79-94 NTU

	[1]Residual turbidity (NTU)		
Running time (hrs)	**In-line filtration**	**Direct filtration**	**Conventional filtration**
0	32.00	31.00	30.00
2	55.00	44.00	37.00
4	63.00	50.00	41.00
6	69.00	55.00	45.00
8	70.00	60.88	50.00
10	70.00	61.89	50.00
12	69.00	59.01	49.00
14	68.00	59.00	48.70
16	67.00	56.78	47.00
18	66.00	56.04	46.00
20	65.00	55.00	45.00
22	64.00	54.76	44.00
24	63.00	53.15	43.00
26	61.00	49.90	40.00
28	60.00	46.00	36.00
32	60.00	43.06	33.00
36	56.00	41.83	30.00
40	54.00	41.00	27.00
44	50.00	40.00	23.00
48	50.00	36.87	19.00

[1]the results are an average of four replicate runs conducted under similar experimental conditions

Analysis of variance; H_0: ($\mu_1 = \mu_2 = \mu_3$, etc) or H_A: At least two means differ; $\alpha = 0.05$

Source of Variation	**SS**	**df**	**MS**	**F**	**P-value**	**F crit**
Between Groups	4586.2617	2	2293.1308	27.41	4.58×10^{-9}	3.16
Within Groups	4769.3152	57	83.6722			
Total	9355.5768	59				

Table D5. Effect of the mode of filtration on removal of COD

Conditions: total running time = 48 hrs; hydraulic loading rate = 5 m^3/m^2 hr; initial COD: mean = 597.27 mg/L, range = 454-673 mg/L

	[1]Residual COD (mg/L)		
Running time (hrs)	**In-line filtration**	**Direct filtration**	**Conventional filtration**
0	232.00	231.00	230.00
2	355.00	344.00	337.00
4	413.00	400.00	391.00
6	439.00	405.00	395.00
8	435.00	400.88	380.00
10	430.00	391.88	365.00
12	419.00	378.90	354.00
14	413.70	374.00	353.00
16	407.00	366.77	337.00
18	400.00	356.00	326.00
20	389.00	344.98	305.00
22	364.00	318.87	279.00
24	333.00	272.80	238.00
26	304.00	260.00	200.00
28	281.00	231.00	156.00
32	245.00	162.88	123.00
36	236.00	152.00	107.00
40	224.00	131.00	80.00
44	220.00	120.07	68.00
48	200.00	97.05	44.00

[1]the results are an average of four replicate runs conducted under similar experimental conditions

Analysis of variance; H_0: ($\mu_1 = \mu_2 = \mu_3$, etc) or H_A: at least two means differ; $\alpha = 0.05$

Source of Variation	**SS**	**df**	**MS**	**F**	**P-value**	**F crit**
Between Groups	70769.4940	2	35384.7470	3.24	0.0467	3.16
Within Groups	623289.3940	57	10934.9016			
Total	694058.8880	59				

Table D6. Head loss development under various treatment schemes with carbon nanotubes

Conditions: total running time = 48 hrs; hydraulic loading rate = 5 m^3/m^2 hr; scheme A = CNTs added to both the coagulation/flocculation tanks and the filter bed; scheme B = CNTs added to the coagulation/flocculation tanks only; scheme C = CNTs added to the filter bed only; scheme D = no CNTs added

	[1]Head loss (cm water)			
Running time (hrs)	**Scheme A**	**Scheme B**	**Scheme C**	**Scheme D**
0	0	0	0	0
2	0	0	0	0
4	0	0	0	0
6	1.34	0	0	0
8	1.99	0	0	0
10	2.12	0	1.34	0
12	3.00	0	1.73	0
14	4.55	0	2.66	0
16	6.10	1.50	3.70	0
18	8.00	2.12	5.10	0
20	12.00	3.00	8.20	1.50
22	16.00	4.55	11.00	2.89
24	18.00	6.10	13.22	3.80
26	20.00	8.00	15.44	5.45
28	22.00	10.99	18.00	8.20
32	23.99	14.67	20.00	11.36
36	24.00	16.44	22.36	13.91
40	24.99	18.00	23.00	14.80
44	26.00	19.00	23.90	15.67
48	27.00	20.00	24.00	17.44

[1]the results are an average of four replicate runs conducted under similar experimental conditions

Analysis of variance; H_0: ($\mu_1 = \mu_2 = \mu_3$, etc) or H_1: At least two means differ

Source of Variation	**SS**	**df**	**MS**	**F**	**P-value**	**F crit**
Between Groups	657.4171	3	219.1390	3.02	0.0350	2.72
Within Groups	5519.6835	76	72.6274			
Total	6177.1006	79				

Table D7. Turbidity removal under various treatment schemes with carbon nanotubes

Conditions: total running time = 48 hrs; hydraulic loading rate = 5 m^3/m^2 hr; initial turbidity: mean = 84.75 NTU, range = 79-94 NTU; scheme A = CNTs added to both the coagulation/flocculation tanks and the filter bed; scheme B = CNTs added to the coagulation/flocculation tanks only; scheme C = CNTs added to the filter bed only; scheme D = no CNTs added

	[1]Residual turbidity (NTU)			
Running time (hrs)	**Scheme A**	**Scheme B**	**Scheme C**	**Scheme D**
0	26.00	28.00	27.00	30.00
2	33.00	34.50	34.99	37.00
4	36.00	39.00	40.99	41.00
6	39.00	42.50	43.99	45.00
8	39.00	42.00	45.99	50.00
10	40.00	42.16	45.30	50.00
12	40.00	41.50	43.99	49.00
14	39.60	40.67	43.33	48.70
16	36.00	40.00	42.89	47.00
18	34.00	37.50	42.00	46.00
20	32.00	36.00	41.08	45.00
22	30.00	33.00	36.90	44.00
24	24.00	29.00	35.00	43.00
26	21.00	26.00	32.74	40.00
28	18.99	22.00	27.10	36.00
32	16.00	18.50	23.22	33.00
36	12.00	16.00	20.98	30.00
40	10.00	14.00	18.00	27.00
44	8.00	12.00	15.00	23.00
48	5.00	10.00	12.93	19.00

[1]the results are an average of four replicate runs conducted under similar experimental conditions

Analysis of variance; H_0: ($\mu_1 = \mu_2 = \mu_3$, etc) or H_A: at least two means differ; $\alpha = 0.05$

Source of Variation	**SS**	**Df**	**MS**	**F**	**P-value**	**F crit**
Between Groups	1635.0017	3	545.0006	4.61	0.0051	2.72
Within Groups	8975.5586	76	118.0995			
Total	10610.5603	79				

Table D8. COD removal under various treatment schemes with carbon nanotubes

Conditions: total running time = 48 hrs; hydraulic loading rate = 5 m^3/m^2 hr; initial COD: mean = 597.27 mg/L, range = 454-673 mg/L; scheme A = CNTs added to both the coagulation/flocculation tanks and the filter bed; scheme B = CNTs added to the coagulation/flocculation tanks only; scheme C = CNTs added to the filter bed only; scheme D = no CNTs added

	[1]Residual COD (mg/L)			
Running time (hrs)	**Scheme A**	**Scheme B**	**Scheme C**	**Scheme D**
0	220.00	226.49	225.00	230.00
2	280.00	301.27	308.50	337.00
4	333.00	349.18	362.00	391.00
6	358.00	362.16	376.50	395.00
8	356.00	360.00	370.00	380.00
10	340.00	340.67	352.50	365.00
12	330.00	331.27	342.00	354.00
14	320.00	326.66	336.85	353.70
16	300.00	310.22	318.50	337.00
18	270.00	291.87	298.00	326.00
20	220.00	260.07	262.50	305.00
22	170.00	224.50	226.04	279.00
24	130.00	184.00	189.78	238.00
26	110.00	155.00	163.81	200.00
28	90.00	123.00	135.15	156.00
32	70.00	96.50	96.42	123.00
36	60.00	53.50	84.78	107.00
40	40.00	62.50	65.97	80.00
44	44.00	49.00	53.88	68.00
48	48.00	27.50	34.63	44.00

[1]the results are an average of four replicate runs conducted under similar experimental conditions

Analysis of variance; H_0: ($\mu_1 = \mu_2 = \mu_3$, etc) or H_A: at least two means differ; $\alpha = 0.05$

Source of Variation	**SS**	**Df**	**MS**	**F**	**P-value**	**F crit**
Between Groups	24874.8826	3	8291.6275	0.58	0.6269	2.72
Within Groups	1077724.1709	76	14180.5812			
Total	1102599.0535	79				

Table D9-1. Head loss development in backwashed and un-backwashed conventional filtration

Conditions: total running time = 48 hrs; hydraulic loading rate = 5 m^3/m^2 hr; scheme D in which conventional filtration was adopted without the use of CNTs

	[1]Head loss (cm water)	
Running time (hrs)	**Un-backwashed**	**Backwashed**
0	0	0
2	0	0
4	0	0
6	0	0
8	0	0
10	0	0
12	0	0
14	0	0
16	0	0
18	0	0
20	1.50	1.50
22	2.89	2.89
24*	3.80	3.80
26	5.45	0.90
28	8.20	1.40
32	11.36	2.88
36	13.91	3.55
40	14.80	5.10
44	15.67	7.00
48	17.44	10.00

[1]the results are an average of four replicate runs conducted under similar experimental conditions; * time for start of backwashing

Table D9-2. ANOVA for head loss development in backwashed and un-backwashed conventional filtration

Student's t-test of paired two samples for means; one tail hypothesis - H_0: $(\mu_1-\mu_2) = 0$ or H_A: $(\mu_1-\mu_2) > 0$; $\alpha = 0.05$

	Un-backwashed	Backwashed
Mean	4.75	1.95
Variance	40.10	7.77
Observations	20	20
Pearson Correlation	0.89	
Hypothesized Mean Difference	0	
df	19	
t Stat	3.08	
P(T<=t) one-tail	0.0031	
t Critical one-tail	1.73	
P(T<=t) two-tail	0.0062	
t Critical two-tail	2.09	

Table D10-1. Turbidity removal in backwashed and un-backwashed conventional filtration

Conditions: total running time = 48 hrs; hydraulic loading rate = 5 m^3/m^2 hr; initial turbidity: mean = 84.75 NTU, range = 79-94 NTU; scheme D in which conventional filtration was adopted without the use of CNTs

	[1]Residual turbidity (NTU)	
Running time (hrs)	**Un-backwashed**	**Backwashed**
0	30.00	30.00
2	37.00	37.00
4	41.00	41.00
6	45.00	45.00
8	50.00	50.00
10	50.00	50.00
12	49.00	49.00
14	48.70	48.70
16	47.00	47.00
18	46.00	46.00
20	45.00	45.00
22	44.00	44.00
24*	43.00	43.00
26	40.00	36.00
28	36.00	42.00
32	33.00	36.00
36	30.00	27.00
40	27.00	20.00
44	23.00	15.00
48	19.00	12.89

[1]the results are an average of four replicate runs conducted under similar experimental conditions; * time for start of backwashing

Table D10-2. ANOVA for turbidity removal in backwashed and un-backwashed conventional filtration

Student's t-test of paired two samples for means; one tail hypothesis - H_0: $(\mu_1-\mu_2) = 0$ or H_A: $(\mu_1-\mu_2) > 0$; $\alpha = 0.05$

	Un-backwashed	Backwashed
Mean	39.19	38.23
Variance	88.28	133.10
Observations	20	20
Pearson Correlation	0.97	
Hypothesized Mean Difference	0	
Df	19	
t Stat	1.31	
P(T<=t) one-tail	0.1029	
t Critical one-tail	1.73	
P(T<=t) two-tail	0.2057	
t Critical two-tail	2.09	

Table D11-1. COD removal in backwashed and un-backwashed conventional filtration

Conditions: total running time = 48 hrs; hydraulic loading rate = 5 m^3/m^2 hr; initial COD: mean = 597.27 mg/L, range = 454-673 mg/L; scheme D in which conventional filtration was adopted without the use of CNTs

	[1]COD (mg/L)	
Running time (hrs)	**Un-backwashed**	**Backwashed**
0	230.00	230.00
2	337.00	337.00
4	391.00	391.00
6	395.00	395.00
8	380.00	380.00
10	365.00	365.00
12	354.00	354.00
14	353.70	353.70
16	337.00	337.00
18	326.00	326.00
20	305.00	305.00
22	279.00	279.00
24*	238.00	238.00
26	200.00	140.00
28	156.00	165.00
32	123.00	130.00
36	107.00	90.00
40	80.00	70.00
44	68.00	50.00
48	44.00	30.00

[1]the results are an average of four replicate runs conducted under similar experimental conditions; * time for start of backwashing

Table D11-2. ANOVA for COD removal in backwashed and un-backwashed conventional filtration

Student's t-test of paired two samples for means; one tail hypothesis - H_0: $(\mu_1-\mu_2) = 0$ or H_A: $(\mu_1-\mu_2) > 0$; $\alpha = 0.05$

	Un-backwashed	Backwashed
Mean	253.44	248.29
Variance	14213.83	15683.73
Observations	20	20
Pearson Correlation	0.99	
Hypothesized Mean Difference	0	
Df	19	
t Stat	1.57	
P(T<=t) one-tail	0.0669	
t Critical one-tail	1.73	
P(T<=t) two-tail	0.1338	
t Critical two-tail	2.09	

Table D12. Optical density of carbon nanotubes at 600 nm in 'clear filtrate'

Conditions: wave length = 600 nm; solution = 'clear filtrate' from the semi-continuous LSWTP

[1]CNT concentration (mg/L)	[1]Absorbance
0	0.00
5	0.17
10	0.24
15	0.39
20	0.50
25	0.60
30	0.72
35	0.81
40	0.98
45	1.07
50	1.20

[1]the results are an average of four replicate runs conducted under similar experimental conditions

Table D13. Optical density of filtrate from the semi-continuous LSWTP at 600 nm over time

Conditions: wave length = 600 nm; total running time = 48 hrs

Running time (hrs)	[1]Absorbance
0	0.00
2	0.00
4	0.00
6	0.00
8	0.00
10	0.00
12	0.00
14	0.00
16	0.00
18	0.00
20	0.00
22	0.00
24	0.00
26	0.00
28	0.00
32	0.00
36	0.00
40	0.00
44	0.00
48	0.00

[1]the results are an average of four replicate runs conducted under similar experimental conditions

APPENDIX E

STATISTICAL VALIDATION OF EQUIPMENT AND REPRODUCIBILITY OF EXPERIMENTAL DATA

"*If your experiment needs statistics, then you ought to have done a better experiment*".

-Ernest Rutherford (Nobel Prize for Chemistry 1908)

Determination of the accuracy of 744 Metrohm model pH meter analysis

The accuracy of the 744 Metrohm model pH meter for estimating pH was tested by comparing the mean of the ten standards having the same known pH of 4.00.

Table E1. Determination of the accuracy of the pH meter

Sample number	Measured pH
1	4.01
2	4.01
4	4.00
5	3.99
6	4.01
7	4.00
8	3.99
9	3.99
10	4.00

$t_{calculated}$ is computed from equation G1 and compared with t_{table}. If $t_{calculated}$ is greater than t_{table} at the 99% confidence level, then the two results are considered to be different.

$$t_{calculated} = \frac{|\bar{x} - \text{known value}|}{s}\sqrt{n} \qquad \textbf{(E1)}$$

Known pH	4.00	
Mean, $\bar{x}$		4.00
Standard deviation, *s*		0.009
Number of observations, *n*		10
Degree of freedom, *n-1*		9

$$t_{calculated} = \frac{|4.00 - 4.00|}{0.008660}\sqrt{10} = 0.00$$

For α =0.001, the t_{table} = 4.781.

The $t_{calculated}$ is smaller than the t_{table}, therefore, the mean is a good estimate of the pH. At 99% confidence level, therefore, the 744 Metrohm model pH meter can be used to measure the pH of the samples with minimum error.

Reproducibility of turbidity experimental data obtained from Hatch 2100N turbidimeter

The reproducibility of turbidity experimental data was tested using the analysis of variance for four replicates. The significance level (α) was 0.01. The hypotheses for the analysis of variance are as follows:

(1) The null hypothesis states that 'all means are equal'
H_0: $\mu_1 = \mu_2 = \ldots = \mu_k$

(2) The alternative hypothesis states that 'at least one of the means differs from all of the other'
H_A: Not $\mu_1 = \mu_2 = \ldots = \mu_k$ or the means are not all equal

The most common decision rule is to reject the null hypothesis if the probability value (*p*-value) is less than or equal to α and to retain it otherwise. The statistical significance (*p*-value) of a result is the probability that the observed relationship (e.g., between variables) or a difference (e.g., between means) in a sample occurred by pure chance ("luck of the draw"), and that in the population from which the sample was drawn, no such relationship or differences exist.

The experimental results of the four replicate runs are given below in Table E2-1.

Table E2-1. Effect of CNT dosage on turbidity removal using hydrochloric acid functionalised CNTs

Conditions: initial turbidity: mean = 84.75 NTU, range = 79-94 NTU ; flash mixing speed of 150 rpm for 3 minutes; slow mixing speed of 60 rpm for 20 minutes

	[1]Residual turbidity (NTU)				
Dosage	**Run 1**	**Run 2**	**Run 3**	**Run 4**	**Average**
0	86.25	85.05	83.68	84.02	84.75
10	67.99	65.81	67.57	66.23	66.90
20	56.22	55.34	52.48	53.36	54.35
30	48.49	46.06	47.20	47.36	47.28
40	41.57	40.88	42.77	39.68	41.22
50	35.46	36.71	36.15	37.57	36.47
60	36.29	34.90	34.17	35.87	35.30

[1]Results of four replicate runs conducted under similar experimental conditions

Table E2-2 shows the results of ANOVA used for evaluating the reproducibility of experimental data obtained from Hatch 2100N turbidimeter. As can be seen from the ANOVA results, the *p*-value at 0.9992 is far much greater than α (0.01). Therefore, the results infer that the reproducibility of experiemental data when using the Hatch 2100N turbidimeter is guaranteed.

Table E2-2. Single factor ANOVA results for effect of CNT dosage on turbidity removal using hydrochloric acid functionalised CNTs

SUMMARY

Groups	Count	Sum	Average	Variance
Run 1	7	372.26	53.18	346.42
Run 2	7	364.75	52.11	329.89
Run 3	7	364.02	52.00	320.67
Run 4	7	364.07	52.01	311.92

ANOVA

Source of Variation	SS	df	MS	F	P-value	F crit
Between Groups	6.8762	3	2.2921	0.01	0.9992	4.72
Within Groups	7853.4242	24	327.2260			
Total	7860.3004	27				

Reproducibility of COD experimental data obtained from Shimadzu UV-1601 spectrophotometer

The reproducibility of COD experimental data was tested using the analysis of variance for four replicates. The significance level (α) was 0.01. The hypotheses for the analysis of variance are as follows:

(3) The null hypothesis states that 'all means are equal'
H_0: $\mu_1 = \mu_2 = \ldots = \mu_k$

(4) The alternative hypothesis states that 'at least one of the means differs from all of the other'
H_A: Not $\mu_1 = \mu_2 = \ldots = \mu_k$ or the means are not all equal

The most common decision rule is to reject the null hypothesis if the probability value (*p*-value) is less than or equal to α and to retain it otherwise. The statistical significance (*p*-value) of a result is the probability that the observed relationship (e.g., between variables) or a difference (e.g., between means) in a sample occurred by pure chance ("luck of the draw"), and that in the population from which the sample was drawn, no such relationship or differences exist.

The experimental results of the four replicate runs are given below in Table E3-1.

Table E3-1. Effect of CNT dosage on COD removal using hydrochloric acid functionalised CNTs

Conditions: initial COD: mean = 597.27 mg/L , range = 454-673 mg/L; flash mixing speed of 150 rpm for 3 minutes; slow mixing speed of 60 rpm for 20 minutes

	[1]COD (mg/L)				
Dosage	**Run 1**	**Run 2**	**Run 3**	**Run 4**	**Average**
0	596.50	597.20	598.27	597.11	597.27
10	421.04	418.96	419.45	420.55	420.00
20	292.64	294.67	294.80	292.57	293.67
30	262.50	264.33	263.54	263.21	263.40
40	248.27	249.48	250.25	249.04	249.26
50	239.50	239.89	238.24	237.85	238.87
60	262.33	259.67	261.44	260.56	261.00

[1]Results of four replicate runs conducted under similar experimental conditions

Table E3-2 shows the results of ANOVA used for evaluating the reproducibility of experimental data obtained from Shimadzu UV-1601 spectrophotometer. As can be seen from the ANOVA results, the p-value at 1.00 is far much greater than α (0.01). Therefore, the results infer that the reproducibility of experiemental data when using the Shimadzu UV-1601 spectrophotometer is guaranteed.

Table E3-2. Single factor ANOVA results for effect of CNT dosage on turbidity removal using hydrochloric acid functionalised CNTs

SUMMARY

Groups	Count	Sum	Average	Variance
Run 1	7	2322.78	331.83	17448.08
Run 2	7	2324.20	332.03	17398.54
Run 3	7	2325.99	332.28	17511.66
Run 4	7	2320.89	331.56	17543.35

ANOVA

Source of Variation	SS	df	MS	F	P-value	F crit
Between Groups	2.0022	3	0.6674	3.82×10^{-5}	1.0000	4.72
Within Groups	419409.8100	24	17475.4088			
Total	419411.8122	27				

Reproducibility of zeta potential experimental data obtained from Zetasizer Nanoseries Nano ZS

The reproducibility of zeta potential experimental data was tested using the analysis of variance for four replicates. The significance level (α) was 0.01. The hypotheses for the analysis of variance are as follows:

(1) The null hypothesis states that 'all means are equal'
H_0: $\mu_1 = \mu_2 = \ldots = \mu_k$

(2) The alternative hypothesis states that 'at least one of the means differs from all of the other'
H_A: Not $\mu_1 = \mu_2 = \ldots = \mu_k$ or the means are not all equal

The most common decision rule is to reject the null hypothesis if the probability value (*p*-value) is less than or equal to α and to retain it otherwise. The statistical significance (*p*-value) of a result is the probability that the observed relationship (e.g., between variables) or a difference (e.g., between means) in a sample occurred by pure chance ("luck of the draw"), and that in the population from which the sample was drawn, no such relationship or differences exist.

The experimental results of the four replicate runs are given below in Table E4-1.

Table E4-1. Effect of CNT dosage on evolution of zeta potential of brewery wastewater

Conditions: flash mixing speed of 150 rpm for 3 minutes; slow mixing speed of 60 rpm for 20 minutes

	Zeta potential (mV)				
Dosage	**Run 1**	**Run 2**	**Run 3**	**Run 4**	**Average**
0	-25.20	-26.40	-24.90	-25.50	-25.50
5	-21.31	-20.53	-22.39	-20.97	-21.30
10	-17.20	-18.80	-18.10	-19.50	-18.40
15	-13.12	-11.08	-12.98	-11.22	-12.10
20	-4.91	-5.19	-5.20	-4.70	-5.00
25	-0.97	-1.05	-0.97	-1.02	-1.00
30	5.49	4.20	4.65	5.66	5.00
35	7.00	6.92	7.01	7.06	7.00
40	9.07	8.92	9.02	8.97	9.00
45	9.97	10.01	10.10	9.93	10.00
50	11.89	10.91	10.09	11.11	11.00
60	10.99	13.01	12.45	11.54	12.00

[1]Results are an average of four replicate runs conducted under similar experimental conditions

Table E4-2 shows the results of ANOVA used for evaluating the reproducibility of experimental data obtained from Zetasizer Nanoseries Nano ZS. As can be seen from the ANOVA results, the p-value at 1.00 is far much greater than α (0.01). Therefore, the results infer that that the reproducibility of experiemental data when using the Zetasizer Nanoseries Nano ZS is guaranteed.

Table E4-2. Single factor ANOVA results for effect of CNT dosage on turbidity removal using hydrochloric acid functionalised CNTs

SUMMARY

Groups	Count	Sum	Average	Variance
Run 1	12	-28.31	-2.36	185.29
Run 2	12	-29.09	-2.42	189.61
Run 3	12	-31.22	-2.60	188.65
Run 4	12	-28.64	-2.39	188.05

ANOVA

Source of Variation	SS	Df	MS	F	P-value	F crit
Between Groups	0.4292	3	0.1431	0.0008	1.0000	4.26
Within Groups	8267.5252	44	187.8983			
Total	8267.9544	47				

APPENDIX F

DERIVATION OF THE SIMPLE KINETIC MODEL FOR THE PRODUCTION OF CARBON NANOTUBES FROM CARBON DIOXIDE

"*Great is the art of beginning, but greater is the art of ending".*

- Henry Wadsworth Longfellow (1807-1882), Elegiac Verse

F.1 Kinetic model formulation

Several models have been suggested for the growth of CNTs using catalysts, viz, the scooter model (Thess et al., 1996; Lee et al., 1997), metal-particle model (Yudasaka et al., 1999), fullerene-cap model (Kataura et al., 2000), etc. However, the vapor–liquid–solid (VLS) growth model is the most popular model used to explain the growth of CNTs using catalysts (Saito, 1995). In this model, the liquid catalyst particle acts as follows, (i) as a catalyst for the decomposition or reduction of the carbon feedstock (e.g., carbon monoxide (CO), CO_2, methane (CH_4) or alcohols), (ii) as a solvent for the carbon atoms that are released from the feedstock, and (iii) as a template for the nucleation and growth of the CNTs. According to the VLS growth model, the carbon feed stock is initially in the vapour phase before dissolving into the metal catalyst to form a liquid metal-carbide particle (Raji et al., 2011). When this particle is carbon-saturated, the solid phase CNTs begin to grow (Raji et al., 2011).

For many years, it was generally assumed that carbon diffusion through the catalyst bulk or over the catalyst nanoparticle was the only rate limiting step in the CNT growth process (Wirth et al., 2009). However, in the CVD, CNT growth rate can be limited by several other steps such as diffusion and mass transfer in the gas phase, surface reactions on the catalyst, carbon diffusion through the catalyst bulk or over the catalyst surface as shown schematically in Figure F.1 (Hofmann et al., 2005; Wirth et al., 2009).

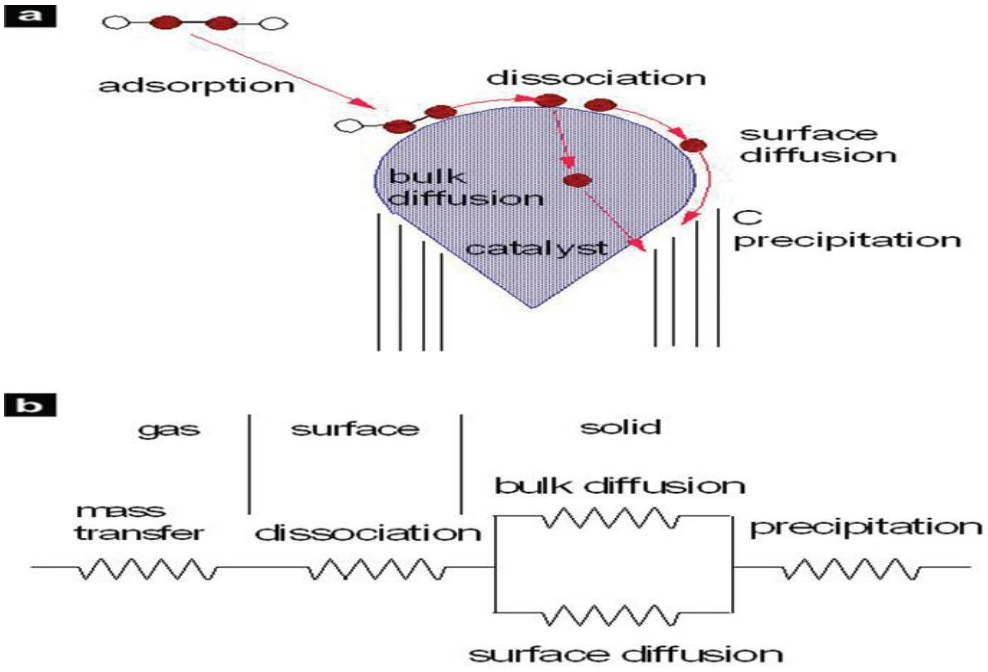


Figure F.1. Schematics of carbon nanotubes growth. (a) CNT growth process, (b) possible rate-limiting processes (Hofmann et al., 2005; Wirth et al., 2009).

Furthermore, the growth rate may also be dependent on many other factors including the gas-phase decomposition reactions. Therefore, in order to understand the chemical mechanism that takes place during CNT growth from CO_2, the thermal decomposition of CO_2 should also be analysed and fully understood. In fact, the understanding of the thermal and kinetic aspects of gas phase decomposition reactions is imperative in many fundamental and applied fields, including the environmental sciences, combustion and explosions, catalysis, matter under extreme condition, and planetary sciences (Sharia and Kuklja, 2010). However, the thermal and kinetic aspects of gas-phase decomposition reactions can be extremely complex due to a large number of variables, a variety of possible intermediates, and an overlap in thermal decomposition traces (Sharia and Kuklja, 2010). Nevertheless, calculations

intended to provide an interpretation of the experiment are often of little help if they ignore the kinetics of the decomposition process (Sharia and Kuklja, 2010).

Therefore, in this study, it is proposed that the decomposition or reduction of the CO_2 into the required chemical species is an important step that needs to be incorporated into the rate equation for the production of CNTs.

For several decades, many researchers have studied the benefits of the decomposition or reduction of CO_2 and several other gaseous oxides such as H_2O over metal substrates for industrial processes and pollution control (Copperthwaite et al., 1988; Tamaura and Tabata, 1990; Kato et al., 1994; Chun-lei et al., 1995; Chunlei et al., 1996). In particular, the decomposition and/or conversion of CO_2 gas has been mostly studied using catalytic processes. It has been postulated that the catalysed or un-catalysed thermal splitting of CO_2 involves the following overall reaction (Rayne, 2008):

$$CO_2 \rightarrow C + O_2 \qquad \text{(F.1)}$$

However, the initial stage in the splitting of CO_2 produces CO and oxygen (Shin et al., 2001; Xu and Huang, 2007; Rayne, 2008) as shown in reaction (F.2).

$$2CO_2 \rightarrow 2CO + O_2 \qquad \text{(F.2)}$$

After reaction (F.2), the two reactions which merit consideration as possible means for the complete splitting process are either the Boudouard reaction, which involves the disproportionation of CO to carbon and CO_2 (see reaction (F.3)) or direct splitting of CO to carbon and oxygen as given by reaction (F.4).

$$2CO \rightarrow C + CO_2 \qquad \text{(F.3)}$$

$$CO \rightarrow C + \tfrac{1}{2}O_2 \quad \text{(F.4)}$$

However, the reaction represented by Equation F.4 can be ruled out because it is only likely to occur at extremely high temperatures (Rayne, 2008). Therefore, reaction F.3 (CO disproportionation) is assumed to take place in this study. The reaction of CO disproportionation on iron catalyst has long been known to produce filamentous carbon (Monthioux and Kuznetsov, 2006), and such filaments having a tubular graphic structure later came to be called CNTs (Iijima, 1991). In fact, CO has now become one of the most common carbon sources for the production of CNTs (Franklin, 2001; Nasibulin et al., 2003; Moisala et al., 2006; Nasibulin et al., 2006; Jiang, 2007), due to the reasonable temperature range for CO disproportionation and the good CNT yield (Lanzani et al., 2009).

It is known that there are a number of possible elementary reaction processes occurring before the production of CNTs. Therefore, it is assumed here that, initially, CO_2 adsorbs on the catalyst surface (Jin et al., 2008),

$$CO_{2\,(gas)} \rightleftharpoons CO_{2\,(ads)} \quad \text{(F.5)}$$

and then dissociates reversibly into two adsorbed fragments of CO and oxygen as shown in reaction (F.6) (Jin et al., 2008):

$$CO_{2\,(ads)} \rightleftharpoons CO_{(ads)} + O_{\,(ads)} \quad \text{(F.6)}$$

The reaction rates for reaction (F.6) can be calculated for the forward and reverse reactions as,

$$R_{forward} = k_1[CO_{2(ads)}] \quad \text{(F.7)}$$

$$R_{reverse} = k_{-1}[CO_{(ads)}][O_{(ad)}] \quad \text{(F.8)}$$

The adsorbed CO in reaction (F.6) first dissociates into carbon and oxygen, and then, the adsorbed oxygen reacts with the undissociated CO to form surface or adsorbed CO_2 (Lanzani et al., 2009), which desorbs to gaseous CO_2 as shown in reactions F.9, F.10, and F.11, respectively.

$$CO_{(ads)} \rightleftharpoons C_{(ads)} + O_{(ads)} \quad \text{(F.9)}$$

$$CO_{(ads)} + O_{(ads)} \rightleftharpoons CO_{2(ads)} \quad \text{(F.10)}$$

$$CO_{2(ads)} \rightleftharpoons CO_{2(gas)} \quad \text{(F.11)}$$

In order to obtain the rate equation for the Boudouard reaction, reactions (F.9) and (F.10) are first combined as overall reaction (F.12),

$$2CO_{(ads)} \rightleftharpoons C_{(ads)} + CO_{2(ads)} \quad \text{(F.12)}$$

The rate constants for the forward and reverse reaction (F.12) of the equilibrium are given as k_2 and k_{-2} in Equation (F.13) and (F.14), respectively,

$$R_{forward} = k_2[CO_{(ads)}]^2 \quad \text{(F.13)}$$

$$R_{reverse} = k_{-2}[C_{(ads)}][CO_{2(ads)}] \quad \text{(F.14)}$$

As shown in Figure F.1, the carbon species produced in reaction (F.12) diffuse in or on the catalyst surfaces; nucleate and segregate to the surface forming the graphene networks of CNTs,

$$C_{(ads)} \rightarrow CNT \quad \text{(F.15)}$$

which is given by the following CNT growth rate:

$$\frac{d[CNT]}{dt} = k_3[C(ads)] \quad \text{(F.16)}$$

In Equation (F.16), k_3 is the rate constant proportional to the diffusion coefficient (or rate) of carbons in the metal catalyst nanoparticles (Kim et al., 2005).

If the rates of formation of the intermediate products and their decay back into reactants were much faster than the rate of formation of CNTs ($k_1 \gg k_3$; $k_2 \gg k_3$), then rate-determining step of CNT growth would follow a slower reaction (F.15). In other words reactions (F.5), (F.6), (F.9) and (F.10) are fast reactions followed by a slower reaction of carbon diffusing through or over the catalyst and precipitating to form the nanotubes. Since it is assumed that the reactants are in equilibrium with the intermediate products, the equilibrium constants, K_1 and K_2, are then defined as follows:

$$K_1 = \frac{k_1}{k_{-1}} = \frac{[CO_{(ads)}][O_{(ads)}]}{[CO_{2(ads)}]} \quad \text{(F.17)}$$

$$K_2 = \frac{k_2}{k_{-2}} = \frac{[C_{(ads)}][CO_{2(ads)}]}{[CO_{(ads)}]^2} \quad \text{(F.18)}$$

Therefore, the growth rate of CNTs is given as follows:

$$\frac{d[CNT]}{dt} = k_3[C(ads)] = K[CO_2] \quad \text{(F.19)}$$

where K is the rate constant that incorporates [O], k_3, K_1, and K_2. The overall rate as shown in Equation (F.19) is proportional to the concentration of adsorbed carbon

atoms, [$C_{(ads)}$], or it is proportional to the concentration of CO_2, [CO_2], raised to the power one.

Therefore, Equation (F.19) is a simple kinetic model equation for predicting the rate of CNT production from CO_2 in the modified SFCCVD reactor. The rate constant, K, is proportional to the diffusion coefficient of carbon (Kim et al., 2005). Therefore, in this study, the activation energy (E_a) of the rate constant is taken as the diffusion energy of carbon into the bulk iron metal (γ–Fe), i.e., 35 kcal/mol (Baker, 1989; Brandes and Book, 1992).

In this work, H_2 was used together with CO_2. Nasibulin and colleagues (Nasibulin et al., 2006) have already demonstrated the important role of H_2 in the CVD process. However, the following need to be noted. Firstly, the H_2 is believed to prevent the oxidation of the nanosized catalyst iron particles, thus maintaining the catalyst in their reduced state (Bahome et al., 2005; Nasibulin et al., 2006; Lanzani et al., 2009). In fact, Moisala et al. (2003) thermodynamically showed that only non-oxide metal particles behave as catalysts in the CNT formation, thus metal oxide particles must be reduced. Secondly, the H_2 limit or alleviate the carbon poisoning of the metal catalysts (Kim et al., 1991). Thirdly, it is also reported that adsorbed H_2 on the catalyst surfaces catalyses the disproportionation of CO (Zheng et al., 2002). Fourthly, though not related to this study, H_2 reduces the rate of dehydrogenation of the CH_x intermediates, which form the precursor soot involved in the formation of multi-walled CNTs (Reilly and Whitten, 2006). Lastly, at the studied furnace temperature, H_2 can provide additional carbon atoms for the CNT synthesis from its reaction with CO_2 as shown in Equation F.20 (Xu and Huang, 2007; Lanzani et al., 2009),

$$CO_2 + 2H_2 \rightleftharpoons 2H_2O + C \qquad \text{(F.20)}$$

However, the reaction with CNTs and hydrogen, as given by reaction (F.21),

$$2C + 4H_2 \rightleftharpoons 2CH_4 \qquad (F.21)$$

also occurs in the reactor, where CNTs are reduced to methane (Nasibulin et al., 2006). This reaction is assumed to counter the effect of CNT produced due to the presence of H_2 (reaction F.20). Therefore, this study assumed that only the first, second, and third roles of H_2 are applicable, i.e., H_2 does not need to be included in the simple kinetic equation (F.19).

F.2 References

Baker, R.T.K.,1989. Catalytic growth of carbon filaments. *Carbon* 27 (3), 315-323.

Bahome, M. C., Jewell, L.L., Hildebrandt D., Glasser, D., Coville, N. J., 2005. Fischer-Tropsch synthesis over iron catalysts supported on carbon nanotubes. *Applied Catalysis* A: General 287, 60-67.

Brandes, E.A., Book, G. B (Editors).,1992. Smithells's Metals Reference Book, 7th edition., Butterworth-Heinemann Limited, London.

Chunlei, Z., Zhi-qiang, L., Tong-hao, W., Hong-mao, Y., Yu-zi, J., Shao-yi, P., 1995. Complete reduction of carbon dioxide to carbon and indirect conversion to O2 using cation-excess magnetite. *Materials Science and Physics* 44, 194-198.

Chunlei, Z., Lijun, W., Tonghao, W., Hongmao, Y., Yuzi, J., Shaoyi, P., 1996. Preparation of magnetite and its decomposition of water. *Science in China* B 39 (1), 95-104.

Copperthwaite, R.G., Davies, P.R., Morris, M.A., Roberts, M.W., Ryder, R.A., 1988. The reactive chemisorption of carbon dioxide at magnesium and copper surfaces at low temperature. *Catalysis Letters* 1, 11-20.

Franklin, N. R., Li, Y., Chen, R. J., Javey, A., Dai. H., 2001. Patterned growth of single-walled carbon nanotubes on full 4-inch wafers. *Applied Physics Letters* 79, 4571-4573.

Hofmann, S., Csányi, G., Ferrari, A. C., Payne, M. C., Robertson, J., 2005. Surface diffusion: The low activation energy path for nanotube growth. *Physical Review Letters* 95, 036101-1-036101-4

Iijima, S., 1991. Helical microtubules of graphitic carbon. *Nature* 354, 56-58.

Jiang, H., Nasibulin, A. G., Brown, D. P., Kauppinen, E. I., 2007. Unambiguous atomic structural determination of singlewalled carbon nanotubes by electron diffraction. *Carbon* 45, 662-667.

Jin, W., Zhang, C., Chang, X., Fan, Y., Xing, W., Xu, N., 2008. Efficient catalytic decomposition of CO2 to CO and O2 over Pd/mixed-conducting oxide catalyst in an oxygen-permeable membrane reactor. *Environmental Science and Technology* 42 (8), 3064-3068.

Kato, H., Kodama, T., Tsuji, M., Tamaura, Y., 1994. Decomposition of carbon dioxide to carbon by hydrogen-reduced Ni(II)-bearing ferrite. *Journal of Materials Science* 29, 5689-5692.

Kataura, H., Kumazawa, Y., Maniwa, Y., Ohtsuka, Y., Sen, R., Suzuki, S., Achiba, Y., 2000. Diameter control of single-walled carbon nanotubes. *Carbon* 38 (11-12), 1691-1697.

Kim, M. S., Rodriguez, N. M., Baker, R. T. K., 1991. The interaction of hydrocarbons with copper-nickel and nickel in the formation of carbon filaments. *Journal of Catalysis* 131, 60-73.

Kim, K. E., Kim, K. J., Jung, W. S., Bae, S. Y., Park, J., Choi, J., Choo, J., 2005. Investigation on the temperature-dependent growth rate of carbon nanotubes using chemical vapor deposition of ferrocene and acetylene. *Chemical Physics Letters* 401, 459-464.

Lanzani, G., Nasibulin, A. G., Laasonen, K., Kauppinen, E. I., 2009. CO dissociation and CO+O reactions on a nanosized iron cluster. *Nano Research* 2, 660-670.

Lee, Y.H., Kim, S.G., Tománek, D., 1997. Catalytic growth of single-wall carbon nanotubes: an ab initio study. *Physical Review Letters* 78, 2393-2396.

Moisala A., Nasibulin A.G., Kauppinen E.I., 2003. The role of metal nanoparticles in the catalytic production of singlewalled carbon nanotubes – A review. *Journal of Physics: Condensed Matter* 15 (42), S3011-S3035.

Moisala, A., Nasibulin, A. G., Brown, D. P., Jiang, H., Khriachtchev, L., Kauppinen, E. I., 2006. Single-walled carbon nanotube synthesis using ferrocene and iron pentacarbonyl in a laminar flow reactor. *Chemical Engineering Scie*nce. 61, 4393-4402.

Monthioux, M., Kuznetsov, V. L., 2006. Who should be given the credit for the discovery of carbon nanotubes? *Carbon* 44: 1621-1623.

Nasibulin, A. G., Moisala, A., Brown, D. P., Kauppinen, E.I., 2003. Carbon nanotubes and onions from carbon monoxide using Ni(acac)2 and Cu(acac)2 as catalyst precursors. *Carbon* 41, 2711-2724.

Nasibulin, A. G., Queipo, P., Shandakov, S. D., Brown, D. P., Jiang, H., Pikhitsa, P. V., Tolochko, O. V., Kauppinen. E. I., 2006. Studies on mechanism of single-walled carbon nanotube formation. *Journal of Nanoscience and Nanotechnology* 6, 1233-1246.

Raji, K., Thomas, S., Sobhan, C. B., 2011. A chemical kinetic model for chemical vapor deposition of carbon nanotubes. *Applied Surface Science* 257 (24), 10562-10570.

Rayne, S., 2008. Nature Precedings, Doi:10.1038/npre.2008.1741.2.

Reilly, P. T. A., Whitten, W. B., 2006. The role of free radical condensates in the production of carbon nanotubes during the hydrocarbon CVD process. *Carbon* 44, 1653-1660.

Saito, Y., 1995. Nanoparticles and filled nanocapsules. *Carbon* 33, 979–988.

Sharia, O., Kuklja, M. M., 2010. Ab initio kinetics of gas phase decomposition reactions. *Journal of Physical Chemistry* A 114, 12656-12661.

Shin H C, Choi S C, Jung K D, Han S H, 2001. Mechanism of M ferrites (M = Cu and Ni) in the CO_2 decomposition reaction. *Chemistry of Materials*, 13: 1238-1242.

Tamaura, W., Tabata, M., 1990. Complete reduction of carbon dioxide to carbon using cation-excess magnetite. *Nature* 346, 255-256.

Thess, A., Lee, R., Nikolaev, P., Dai, H., Petit, P., Robert, J., Xu, C., Lee, Y.H., Kim, S.G., Rinzler, A. G., Colbert, D. T., Scuseria, G. E., Tománek, D., Fischer, J. E., Smalley, R. E.,1996. Crystalline ropes of metallic carbon nanotubes. *Science* 273, 483-487.

Wirth, C. T., Zhang, C., Zhong, G., Hofmann, S., Robertson, J., 2009. Diffusion-and reaction-limited growth of carbon nanotube forests. *Nano* 3 (11), 3560-3566.

Xu, X.J., Huang, S. M., 2007. Carbon dioxide as a carbon source for synthesis of carbon nanotubes by chemical vapour deposition. *Materials Letters* 61, 4235-4237.

Yudasaka, M., Yamada, R., Sensui, N., Wilkins, T., Ichihashi, T., Iijima, S., 1999. Mechanism of the effect of NiCo, Ni and Co catalysts on the yield of single-wall carbon nanotubes formed by pulsed Nd:YAG laser ablation. *Journal of Physical Chemistry* B 103, 6224-6229.

Zheng, B., Lu, C., Gu, G., Makarovski, A., Finkelstein, G., Liu, J., 2002. Efficient CVD growth of single-walled carbon nanotubes on surfaces using carbon monoxide precursor. *Nano Letters* 2(8), 895-898.